UTS UNIVERSITY OF TECHNOLOGY SYDNEY

Improving Remote Sensing of Vehicle Emissions through Monitoring Data, Vehicle Fault Analysis and Tailpipe Temperature Setting

by Bruce Douglas Organ

Thesis submitted in fulfilment of the requirements for the degree of

Doctor of Philosophy

Under the supervision of Prof John Zhou, A/Prof Guang Hong and Dr Yuhan Huang

University of Technology Sydney

Faculty of Engineering and Information Technology

January 2022

CERTIFICATE OF ORIGINAL AUTHORSHIP

I, Bruce Douglas Organ declare that this thesis is submitted in fulfilment of the requirements for the reward of Doctor of Philosophy, in the School of Civil and Environmental Engineering / Faculty of Engineering and Information Technology at the University of Technology Sydney.

This thesis is wholly my own work unless otherwise referenced or acknowledged. In addition, I certify that all information sources and literature used are indicated in the thesis.

This document has not been submitted for qualifications at any other academic institution.

This research is supported by the Australian Government Research Training Program.

Signature: Production Note:
Signature removed prior to publication.

Date: 12th January 2022

Acknowledgements

This undertaking or journey to study a doctoral degree is a long one and demanding one I could not undertake without the support and encouragement of some exceptional people.

Firstly, I would like to thank my principal supervisor Professor John Zhou who without his support and direction this could not have proceeded. He invested time and gave direction supervising and helped guide my research choices. The research experience I've gained from him is greatly appreciated. I would also like to thank my co-supervisors Associate Professor Guang Hong and Dr. Yuhan Huang for their support, Guang in the early stages to help with getting started on research writing and analysis. I thank Yuhan for his positive outlook, guidance, enthusiasm and on-going support throughout my studies. His guidance and suggestions have been key in delivering each of the research stages of my work.

I also appreciate the support of Senior Environmental Protection Officer Mr. Yam Yat-Shing from the Hong Kong Environmental Protection Department (HKEPD) for providing their RS data for analysis and being the key supporter helping to arrange RS testing sessions with their equipment many times over the years of my studies. I really appreciate the support of Mr. Casey K.C. Lee also from HKEPD for his support with testing and discussing new development concepts. I wish to thank my manager when I began my studies, Mr Eddy Chan, for getting the support to undertake this and my current manager Dr. Joe K.W. LO for his support to complete my studies. Thanks to Elvin C.Y. Ng, Oscar H.H. Tang, Leo Chan, Chan Ka Chun and Chan Sui from JCEC in helping to arrange and support testing. Mr Jackson Chan from Green Environmental Emissions Consultants for providing the RS measurement systems and raw data for analysis.

I would like to acknowledge the support and belief of my friend Dr Heiko Rudolf, who, although is no longer with us, with his faith in me and this undertaking he was one of the key people to help me start this journey.

Most importantly, I would like to thank my wife Carmon Organ whose support, drive, motivation and love have gotten me through the times when I needed support the most. She's been the constant beside me who has walked this journey with me and helped me realise it. I would also like to thank my parents and children for their love and support.

List of Publications

Journal articles derived from this PhD:

Organ B, Huang Y, Zhou JL, Surawski NC, Yam Y-S, Mok W-C, et al. A remote sensing emissions monitoring programme reduces emissions of gasoline and LPG vehicles. *Environmental Research* 2019; 177: 108614.

Organ B, Huang Y, Zhou JL, Yam Y-S, Mok W-C, Chan EFC. Simulation of engine faults and their impact on emissions and vehicle performance for a liquefied petroleum gas taxi. *Science of The Total Environment* 2020; 716: 137066.

Organ B, Huang Y, Zhou JL. Determination of exhaust plume temperature profiles for remote sensing applications. Under preparation 2022.

Conference proceedings from this PhD:

Organ B, Huang Y, Zhou JL, Hong G, Yam YS, Chan EFC. Emission Performance of LPG Vehicles by RS Technique in Hong Kong. *SAE*, Heidelberg, Germany, 2018, *SAE Technical Paper 2018-01-1820*.

Other related journal articles:

Huang Y, Organ B, Zhou JL, Surawski NC, Hong G, Chan EFC, et al. Emission measurement of diesel vehicles in Hong Kong through on-road RS: Performance review and identification of high-emitters. *Environmental Pollution* 2018; 237: 133-142.

Huang Y, Organ B, Zhou JL, Surawski NC, Hong G, Chan EFC, et al. Remote sensing of on-road vehicle emissions: Mechanism, applications and a case study from Hong Kong. *Atmospheric Environment* 2018; 182: 58-74.

Huang Y, Yam YS, Lee CKC, Organ B, Zhou JL, Surawski NC, et al. Tackling nitric oxide emissions from dominant diesel vehicle models using on-road remote sensing technology. *Environmental Pollution* 2018; 243: 1177-1185.

Huang Y, Ng ECY, Yam Y-s, Lee CKC, Surawski NC, Mok W-C, Organ B, Zhou JL, et al. Impact of potential engine malfunctions on fuel consumption and gaseous emissions of a Euro VI diesel truck. *Energy Conversion and Management* 2019; 184: 521-529.

Huang Y, Organ B, Zhou JL, Surawski NC, Yam Y-S, Chan EFC. Characterisation of diesel vehicle emissions and determination of remote sensing cutpoints for diesel high-emitters. *Environmental Pollution* 2019; 252: 31-38.

Huang Y, Surawski NC, Organ B, Zhou JL, Tang OHH, Chan EFC. Fuel consumption and emissions performance under real driving: Comparison between hybrid and conventional vehicles. *Science of The Total Environment* 2019; 659: 275-282.

Wang B, Lau Y-S, Huang Y, Organ B, Lee S-C, Ho K-F. Investigation of factors affecting the gaseous and particulate matter emissions from diesel vehicles. *Air Quality, Atmosphere & Health* 2019

Huang Y, Mok W-C, Yam Y-S, Zhou JL, Surawski NC, Organ B, et al. Evaluating in-use vehicle emissions using air quality monitoring stations and on-road remote sensing systems. *Science of The Total Environment* 2020; 740: 139868.

Huang Y, Ng ECY, Surawski NC, Yam Y-S, Mok W-C, Liu C-H, et al. Large eddy simulation of vehicle emissions dispersion: Implications for on-road remote sensing measurements. *Environmental Pollution* 2020; 259: 113974.

Huang Y, Surawski NC, Yam Y-S, Lee CKC, Zhou JL, Organ B, et al. Re-evaluating effectiveness of vehicle emission control programmes targeting high-emitters. *Nature Sustainability* 2020; 3: 904-907.

Huang Y, Yu Y, Yam Y-s, Zhou JL, Lei C, Organ B, et al. Statistical evaluation of on-road vehicle emissions measurement using a dual remote sensing technique. *Environmental Pollution* 2020; 267: 115456.

Wang B, Lau Y-S, Huang Y, Organ B, Chuang H-C, Ho SSH, et al. Chemical and toxicological characterization of particulate emissions from diesel vehicles. *Journal of Hazardous Materials* 2021; 405: 124613.

Huang Y, Lee CKC, Yam YS, Mok WC, Zhou JL, Zhuang Y, Surawski NC, Organ B, Chan EFC. Rapid detection of high-emitting vehicles by on-road remote sensing technology improves urban air quality. *Science Advances* 2022; 8: eabl7575.

Abstract

Air pollution is a serious public health issue around the globe that needs to be addressed. The World Health Organisation (WHO) estimates there are 7 million deaths annually resulting from air pollution, with an estimated 4.2 million of these resulting from ambient air pollution. Pollution from vehicle transport emissions is a significant component of this problem worldwide and pollution control programmes utilising ambient monitoring, annualised vehicle checks for licensing, random testing and so forth conducted by government or commercial organisations have not been able to satisfactorily control and reduce this issue. Traditional detection and testing methods alone are not sufficient to reduce vehicle emissions without the addition of non-intrusive wide spread vehicle fleet monitoring. To deliver such non-intrusive monitoring, Remote Sensing (RS) of vehicle emissions can be utilised. Since September 2014, RS has been deployed by the Hong Kong Environmental Protection Department (HKEPD) to identify Gasoline and Liquified Petroleum Gas (LPG) fuelled vehicles excessively emitting pollutants. Analysis and assessment of the effectiveness of this HKEPD RS system application by investigating the data from the enforcement programme has been undertaken. This allowed assessment of areas of uncertainty from RS measurements or the available programme knowledge to be identified for potential improvements. Furthermore, this permitted study of RS variability under controlled experimental conditions and also the determination of common engine faults generating high emissions. The knowledge and benefits from these studies are able to be utilised to develop technology and facilitate improvements into the RS programme.

To understand how effective the emissions control programme using RS was, an investigation was undertaken to assess RS data for Gasoline and LPG vehicles collected by the HKEPD from 6th January 2012 to 30th December 2016. This encompassed a large dataset of 2,144,422 records. The analysis of the data showed the highest Emissions Factors (EFs) for the first two measurement years. This was followed by significant improvements in the LPG vehicle fleet after a maintenance programme in 2013 then followed by further improvements with the influence of RS based enforcement and subsequent effective repairs of high emitting vehicles in 2015 and 2016. The analysis allowed identification of individual vehicles, makes and models of vehicles and years of manufacture where high emitters and problematic models could be assessed and targeted for follow up maintenance and verification testing. The results showed by 2016 that there

were significant EFs reductions of 40.5% HC, 45.3% CO and 29.6% NO for gasoline vehicles. Furthermore, EF reductions of 48.4% HC, 41.1% CO and 58.7% NO were achieved for LPG vehicles. This analysis highlighted the capability this unique emissions enforcement programme utilising RS to effectively reduce vehicle emissions and in turn improve air quality.

Upon implementation of RS enforcement by the HKEPD, it was apparent that there was a significant lack of knowledge in the automotive repair industry's capability to identify various emissions problems and how to implement repairs to pass the mandatory short duration chassis dynamometer emissions test. To help address this, I undertook research for the HKEPD to develop a Toyota Crown Comfort Taxi with relevant engine hardware which could simulate 15 different faults that could impact emissions. Testing of these simulated fault conditions showed they could increase emissions by up to 317%, 782% and 282% for THC, CO and NO_x respectively. The knowledge developed from this was used to educate the repair industry on the largest emissions fault sources so effective repairs could be performed on high emitting vehicles to return them to an optimum performance condition.

The analysis of the RS programme data showed the technique is mainly effective for identifying gross emitters for earlier emissions standard vehicles (Pre Euro to Euro 5). To improve this situation, testing and calibration devices were built and experiments conducted to assess potential sources of measurement variability. As the experiments with the devices were refined and control improved, they identified that the temperature of exhaust gas being measured impacted the RS measurements. A measured ΔT of 14.6°C resulted in 2.6% variation in the RS data for the same CO_2 concentration. As gas temperature variation across a plume could be significantly higher, the RS percentage variation would increase in proportion to the temperature. This could impact every RS measurement, further experiments were developed and confirmed the influence of exhaust gas temperature. Utilising this information, a vehicle-based experiment was designed to determine exhaust plume temperature profiles using a chassis dynamometer with gasoline and diesel test vehicles. From the experimental data, a speed temperature profile was determined. To improve RS reliability, such measurements should occur 50 cm away from the exhaust tailpipe which helps reduce temperature related variability. Applying this will help to improve RS measurement accuracy, with an aim to make RS effective for all types of vehicles regardless of fuel or their size.

Contents

Figures

Tables

Definitions and Abbreviations

Acronyms

AFR	Air Fuel Ratio
AQO	Air Quality Objectives
BAR	California Bureau of Automotive Repair
BC	Black Carbon
CARB	California Air Resources Board
CFR	Code of Federal Regulations (US)
CN_x	China National Emission Regulation (x = UNECE regulation level)
CO	Carbon monoxide
CLA	Chemiluminescence Analyser
CO_2	Carbon dioxide
conc.	Concentration
CVS	Constant Volume Sampler
DU	University of Denver
ECU	Engine Control Unit
EET	Exhaust Emission Temperature
EF	Emission Factor
EGR	Exhaust Gas Recirculation
EMS	Engine Management System
ETN	Emissions Test Notice
FEAT	Fuel Efficiency Automobile Test

FID	Flame Ionisation Detector
FSP	Fine Suspended Particles
GDI	Gasoline Direct Injection
GEEC	Green Environmental Emission Consultant Ltd.
GMRL	General Motors Research Laboratories
HC	Hydrocarbons
HKEPD	Hong Kong Environmental Protection Department
HKTET	Hong Kong Transient Emissions Test
HP	Horsepower
IDI	Indirect Injection
I/M	Inspection Maintenance
IM240	Inspection Maintenance 240 second chassis dynamometer emissions test
IVE	Institute of Vocational Education
JCEC	Jockey Club Emissions Centre
kW	Kilowatts
LPG	Liquified Petroleum Gas
MPV	Multi-Purpose Vehicle
Nd:YAG	Neodymium-doped yttrium aluminium garnet
NDIR	Non-Dispersive Infra-Red
NEDC	New European Drive Cycle
NMHC	Non-Methane Hydrocarbons
NG	Natural Gas (Methane – CH_4)
Nm	Newton metres

NO	Nitrogen monoxide
NO_2	Nitrogen dioxide
NO_x	Total Oxides of Nitrogen
O_3	Ozone
OBD	On Board Diagnostics
PEMS	Portable Emissions Measurement System
PLB	Public Light Bus (minibus)
PMR	Power to Mass Ratio
$PM_{2.5}$	Particulate Matter of 2.5 micrometer or less
Q_P	Concentration ratio of pollutant P over CO_2
rpm	Revolutions per minute
RDE	Real Driving Emissions
RS	Remote Sensing
RSP	Respirable Suspended Particles
TC	Particulate Carbon
THC	Total Hydrocarbons
TWC	Three Way Catalytic converter
UFP	Ultra-Fine Particles
UNECE	United Nations Economic Commission for Europe
USEPA	United States Environmental Protection Department
UV	Ultra Violet
VW	Volkswagen

Symbols

Vol_{CVS}	CVS Test volume of dilute gas
K_V	Venturi Calibration co-efficient
$Temp_{CVS}$	CVS Test Ambient Temperature
$Press_{CVS}$	CVS Barometric Pressure
P_R	Barometric Pressure
V_R	Volume of dilute gas for test
T_R	Ambient Temperature for test
P_C	Regulation Barometric Pressure
V_C	Corrected volume of dilute gas for test
T_C	Regulation Ambient Temperature
M_i	Pollutant mass emission i
V_C	Corrected volume of diluted exhaust gas
Q_i	Pollutant density 'i'
K_H	Humidity correction factor for oxides of nitrogen only
C_i	Corrected concentration of pollutant in diluted exhaust gas (in ppm)
d	Test cycle distance
C_i	Corrected concentration of pollutant i in diluted exhaust gas
C_e	Measured pollutant concentration i in exhaust sample
C_d	Pollutant concentration i in air
DF	Dilution Factor
C_{CO}	Gas concentration of CO in sample bag
C_{H2O}	Gas concentration of H_2O in sample bag

C_{H2O-DA}	Concentration of H_2O in dilution air
C_{H2}	Concentration of H_2 in sampling bag
C_{NMHC}	Corrected concentration of NMHC (carbon equivalent)
C_{THC}	Corrected concentration of THC (carbon equivalent)
C_{CH4}	Corrected concentration of CH_4 (carbon equivalent)
Rf_{CH4}	FID response factor to CH_4
H	Absolute Humidity
R_a	Relative Humidity
P_d	Saturation Vapour Pressure at Ambient Temperature
P_B	Barometric Pressure
T	Test Temperature
$\int_{t_1}^{t_2} C_{HC} \cdot dt$	integral of recording for heated FID for test.
C_e	HC concentration of Ci is substituted for CHC in equations.
M_p	Particulate emission
V_{mix}	Corrected volume of diluted exhaust gas
V_{ep}	Volume of exhaust flow through particulate filter
P_e	Particulate mass on filter(s)
P_R	Barometric Pressure
V_R	Gas volume flow through filters
T_R	Test Ambient Temperature
P_C	Regulation Barometric Pressure
V_C	Corrected gas volume flow through filters
T_C	Regulation Ambient Temperature

m_{corr}	Corrected PM mass for buoyancy
m_{uncorr}	Uncorrected PM mass for buoyancy
ρ_{air}	Air density
ρ_{weight}	Calibration weight density for span balance
ρ_{media}	PM sample medium density (filter)
P_{abs}	Absolute pressure in balance chamber
M_{mix}	Molar mass of air in balance chamber (28.836 g/mol)
R	Molar gas constant (8.314 g/mol)
T_{amb}	Absolute ambient temperature in balance chamber.
ΔT	Temperature difference
N	particulate number emissions
V	Corrected volume of the diluted exhaust gas
K	calibration factor for correction of particulate number counter measurements.
$\bar{C}_s$	Corrected concentration of particulates of diluted exhaust gas.
$\bar{f}_r$	mean particulate concentration reduction factor

Chapter One

1. Introduction

1.1 Research background and motivation

Gaseous pollution from man-made sources has a long-recorded history. It has been suggested it dates back to the beginning of the industrial revolution in the 1750s, but this is far too recent. In 1306 King Edward I of England proclaimed a ban on burning sea coal in London to reduce major smoke and soot pollution. In the days of Ancient Rome they called the city's smoke pollution clouds gravioris caeli ("heavy heaven") and infamis aer ("infamous air"). The Roman empire tried in 535 AD under Emperor Justinian to proclaim the importance of clean air as a birthright, this was an early attempt to regulate for clean air.

The impact of modern life and technology on the environments which we live in at both local and global levels is significant and measurable. In particular, the impact of air pollution in major cities and urban areas from road transportation has increased dramatically in the last few decades. As economic development has improved the income and living conditions of millions of people in numerous countries, a portion of the wealth generated has translated into increased vehicle ownership rates globally. This combined with factors such as rapid urbanisation and significant population growth in cities has led to high vehicle emissions from increased traffic and road congestion becoming a serious daily issue in major cities.

The increasing pollution from motor vehicles has a daily impact on the lives of people who are living and working in built up areas. In city centres, concentrated traffic flows occur in densely populated areas, high rise buildings create urban canyons (Li et al., 2021; Rakowska et al., 2014). These emissions collect and become concentrated with limited airflow. From early morning when the daily commute to work begins, the concentrations of vehicle pollutants (i.e., hydrocarbons (HCs), volatile organic compounds (VOCs), carbon monoxide (CO), oxides of nitrogen (NO_x) and carbon dioxide (CO_2)) steadily

increase and with heavy traffic flows lasting well beyond the morning peak time, the levels of these gases remain much higher than would normally occur outside of these areas. As the day progresses and the sun rises the ultraviolet radiation levels increase resulting in increased photochemical processing of NO_x emissions which can produce high levels of ozone at street level which is known to have both acute and chronic effects on both healthy people and those with health conditions. The impact on the community in all age groups is significant, including more visits to hospitals and medical costs, economic costs relating to absence from work and the impact on children with absence from schools impacting education, their health and families.

The awareness of pollution from vehicle emissions has been long established. In the years after the second world war, economies grew and boomed. Countries like the U.S.A. experienced rapid urbanisation and the cities grew outwards beyond the reach of existing mass transit systems. Subsequently, vehicle ownership increased rapidly, road and highways systems developed and mass commuting in personal vehicles became the norm. In conjunction with this growth the occurrence of haze in areas previously known for clear skies became a daily event. Air pollution controls became a priority in areas such as Los Angeles, California where legislation for the first air pollution control district was introduced in 1946 and established in 1947 (Bay Area Air District, 2021; California Air Resources Board, 2021). Initial efforts focused on visible emissions from industrial plants and factories. This action reduced the amount of smoke, dust and sulphurous compounds emitted significantly. Whilst significant measurable improvements were made, the haze and smog remained with growing health impacts on the wider community. Investigations identified emissions of HC, CO and NO_x from gasoline fuelled motor vehicles to be the primary source of these pollutants.

The impact of air pollution from industrial and automotive sources lead to government action to establish laws, Air Pollution Control Act 1955 (US Public Law, 1955), to recognise the dangers of air pollution to public health and welfare, its potential to damage and cause deterioration to property and the natural environment we depend upon to support our survival. Organisations such as the California Air Resources Board (CARB, 1967) and later the United States Environment Protection Agency (USEPA, 1970) were established to consolidate government resources and take the responsibility to introduce policies to address and abate the impact of air pollution.

Policies began to be introduced from the mid-1940s through the 50s and 60s at city and state levels and which then were later applied across various states and countries such as the USA, Germany, France, the United Kingdom and other developed European nations. In the 1970s the USEPA established a nationwide set of regulations for automotive manufacturers. This was the minimum standard required for all vehicles to meet. Furthermore, states like California, which had longer established pollution controls, set their own higher standards through CARB. Regulations in Europe progressed with major economies like Germany, France and the UK setting standards to address automotive air pollution. In 1992, under the United Nations Economic Commission for Europe (UNECE) the 'Euro standards' were implemented harmonising the automotive vehicle emissions requirements within the member states of the European Union (EU) for the manufacture and in-service performance for the industry.

Since the establishment of regulations for emissions controls, regulators and governments have regularly and progressively enacted lower emissions limits and vehicle manufacturers have developed technologies to meet these requirements. This delivers an outcome where all new vehicles sold meet these requirements. Vehicle manufacturers are further required to ensure their vehicle models can meet minimum mileage accumulation requirements of 100,000 miles or 160,000 km with all emissions equipment still functioning and passing when tested against emissions limits. This is only practical to check against reference vehicles which are maintained and kept by manufacturers. Once vehicles are sold and in service/on the road the ability of governments and local authorities to enforce compliance with emissions regulations have been limited as measurement of emissions gases has required specialist laboratory equipment. The systems and equipment used by vehicle manufacturers to test for compliance are expensive, require significant infrastructure and are ill suited to be applied to on-road large scale vehicle fleet measurements.

The identification of high emitting vehicles from the on-road fleet initially utilised a couple of mechanisms. Visual smoke emissions spotting (by police and environmental protection officers) and garage based roadworthy CO and CO_2 checks were implemented early on and effective on all generations of vehicles which could produce high emissions. As regulations and control technology developed these tools were only effective for detection of seriously faulty vehicles or gross emitters. Inspection and Maintenance (I/M) testing programmes were established by amendments to the Clean Air Act in the USA in

1977 and progressively implemented in the 1980s by various states. These involved establishing testing stations utilising an enhanced 240 second transient/dynamic driven test on a chassis dynamometer with high grade emissions analysers and flow measurement systems to identify those vehicles which were high emitters. High emitters being those vehicles which exceed an assigned emissions threshold for one or more nominated pollutant gases. Implementation was required in areas where air quality failed to reach federal standards and this led to partial implementation covering only some cities, regions and states. This proved effective in areas where implemented, but did not provide comprehensive coverage.

During the 1980s vehicle technology developed affordable electronic control and monitoring systems. The industry adopted a standard to implement 'On Board Diagnostic' (OBD) systems to monitor critical emissions controls systems. The intent of OBD was to detect any faulty equipment so the driver could be notified by a 'Malfunction Indication Lamp' (MIL) on the dashboard and undertake repairs to rectify the fault(s). With OBD becoming a standardised feature in vehicles, during the mid-1990's the USEPA expanded the I/M protocol to include plugin OBD test system monitoring which could be implemented in lieu of I/M testing. It was envisioned that this would provide an effective alternative to capture high emitters in areas where I/M programmes were not implemented. Whilst OBD systems proved effective, it became evident they were best at identifying serious faults and major deterioration. The majority of owners/drivers will pay attention to the MIL and follow up with required service and maintenance. Unfortunately, there will still be a minority who do not follow up to undertake regular servicing/maintenance or repairs to keep vehicles in optimal condition. Being those who can do so, but make the conscious decision not to or those whose socioeconomic position limits their ability to do so at all. Furthermore, the systems only trigger when a pre-set condition (or OBD limit) is met. In the meantime, before these limits are met the vehicle systems will be deteriorating and slowly increasing the amount of regulated emissions being released when operating. Many vehicles can be operating in this deterioration range with owners, drivers and mechanics being unaware of the growing emissions impact occurring whilst vehicles appear to be running well. It is also becoming evident there is a small portion who are aware and may be tampering as well with emissions control systems to avoid triggering OBE conditions and limits too.

Serious efforts have been made to address this as the need for good monitoring and management is more important than ever. This has led to additional technologies being developed and implemented to enhance identification of high emitters. These include ambient and tunnel air quality monitoring stations, plume chasing, portable emissions measurement systems (PEMS) and remote sensing (RS). Ambient air quality monitoring and tunnel air quality monitoring systems are effective and can provide real-time data at specific locations and can be combined to provide a regional air quality map. They effectively identify the magnitude of fleet impacts, but are not able to identify individual high emitting vehicles. Plume chasing utilises a monitoring vehicle to follow target vehicles on-road and take a series of exhaust plume samples to provide an individual emissions analysis. This is effective to provide an accurate short series of measurements for a vehicle, but it is limited as it can only target a small number of the population of vehicles being used daily during an on-road measurement shift. The use of PEMS has become popular over the last decade as a means to provide emissions measurements which are much more comparable to those from laboratory grade analysers in the on-road environment. Whilst providing higher accuracy measurements, it is noted that the on-road measurement environment is much more variable and PEMS analysers can experience greater drift and a larger measurement uncertainty than would be expected in a laboratory. Providing a real-time result for the vehicle under test and delivering a high level of measurement accuracy requires a significant amount of preparation, a longer duration of on-road testing and quality assurance measures to be taken. The amount of time required for this effectively limits the number of vehicle tests that can be performed using PEMS.

Each of these techniques provides data that can be used to deliver results for either a fleet level approach or a small number of individual vehicle measurements. None delivers the magnitude of data required to individually identify the high emitting vehicles in a fleet. This lead to the development of RS technology which involves setting up equipment at a fixed point such as on a ramp to a major/busy roadway where significant amounts of vehicles are driving by frequently. The RS equipment utilises light sources and detectors to determine the concentration ratios of emissions gases in comparison to CO_2 in the exhaust plumes of passing vehicles. This provides a non-intrusive real-time emissions measurement of vehicles without the need to disrupt traffic flows or the driving plans of commuters. It has been effective in survey applications to determine the emissions profile/characteristics of the on-road vehicle fleet in particular cities and regions, but has

not had its full potential realised for identifying individual high emitting vehicles except in a few cities or areas.

A unique enforcement programme implemented in Hong Kong has proven to be one of the leading examples of RS being applied to identify high emitting vehicles successfully, but it has been limited to part of the on-road fleet, i.e., gasoline and liquified petroleum gas (LPG) fuelled vehicles. Further research into the characteristics of RS is required for successful application to the broader vehicle fleet i.e., the diesel fuelled vehicle segment and to newer emission standards such as Euro 5 and 6 for gasoline and LPG vehicles.

1.2 Research methodology and objectives

The goal of my research was to investigate RS techniques to develop a better understanding of the nature and functionality of the measurement and its results, so RS could be further utilised to allow improved measurement of lower level emissions from gasoline (spark ignition) vehicles and work towards solving the problems that have effectively excluded diesel (compression ignition) fuelled vehicles from accurate measurement characterisation. The application of RS technology is regularly used (Borken-Kleefeld and Dallmann, 2018; Chen and Borken-Kleefeld, 2014; Collins, 2018; Vescio, 2019) for emissions survey purposes to provide a reliable measurement of on-road fleet emissions in heavily trafficked areas. Whilst it is a strong tool for fleet measurements, it has been considered more limited when being applied to measurement of individual vehicles to determine if they are high emitting vehicles exceeding their respective emissions limit due to the brief snapshot measurement it takes when compared to conventional emissions testing techniques.

The unique enforcement programme utilising RS in Hong Kong developed by the Hong Kong Environmental Protection Department (HKEPD) conducted extensive testing programmes over a period of more than a decade collecting data to characterise gasoline and LPG emissions from RS and chassis dynamometer testing. The database established from this has provided a baseline means for identifying gross emitters for older emissions standards (such as pre-Euro and Euro 1 to 4) of gasoline and LPG vehicles. The research undertaken in this PhD aims to investigate the existing database to determine effectiveness of RS, identify weaknesses of the current technique and to determine what

new knowledge or modification can help improve the RS programme process to broaden its application and improve its accuracy. The detailed objectives of this project are described as follows:

1) To analyse and assess the effectiveness of existing RS system applications by investigating the characteristics of RS data from the HKEPD enforcement programme
2) To investigate and simulate a range of commonly occurring faults for an LPG spark ignition engine vehicle to determine those faults which have the greatest impact upon emissions to highlight those items whose repair will lead to vehicles passing emissions monitoring by RS measurement.
3) To determine measurement variability by investigating characteristics of RS measurements under controlled emissions conditions for gasoline and diesel engines.
4) To experimentally verify ideas for determining the optimal measurement window for RS based on the understanding achieved through the investigative steps.

1.3 Thesis outline

Figure 1.1 illustrates the structure of this thesis and the inter-connections between chapters. The contents of the following chapters of this thesis are as follows.

Chapter One introduces the research background, aims, and thesis framework.

Chapter Two is literature review of air pollution from vehicle emissions, emissions measurement methods, vehicle emission control, how RS has developed and challenges and knowledge gaps existing for its utilisation.

Chapter Three introduces the materials used, laboratory experiments undertaken and RS monitoring methodology.

Chapter Four presents and discusses the results from analysing five years RS emissions measurements taken in Hong Kong and the impact of the unique emissions control programme.

Chapter Five presents and identifies the need for specialised emissions repair knowledge in the automotive industry and discusses the analysis of simulated of engine faults and

their impact on emissions and vehicle performance for an LPG taxi and how this was used to develop specialised industry training.

Chapter Six presents and discusses the experimental studies undertaken and focussing on the effect of the varying temperature of exhaust gases on RS sensitivity for vehicle engine emissions.

Chapter Seven concludes this thesis by summarising the outcomes of each chapter and recommending future work.

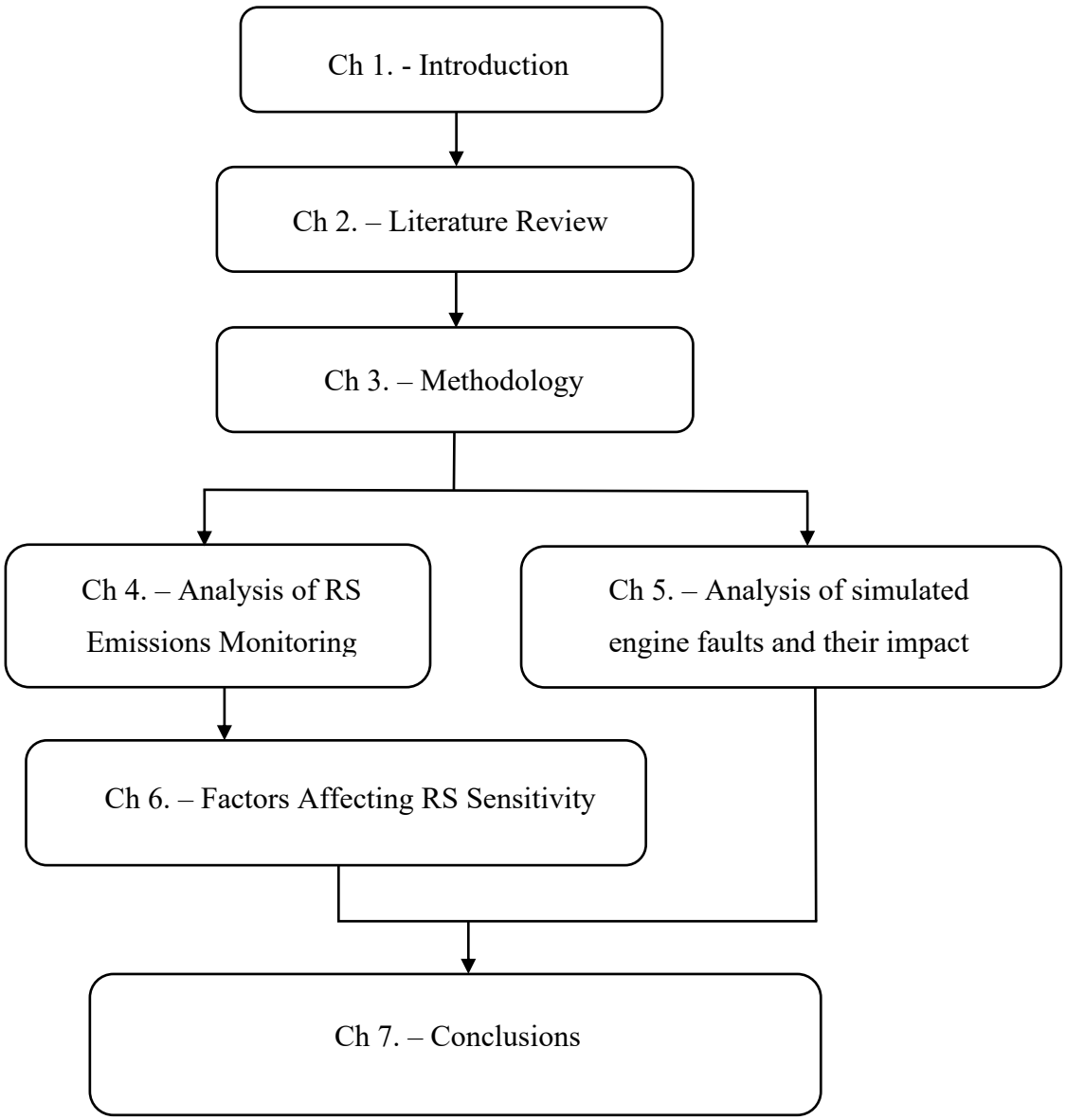

Figure 1.1: Thesis structure and inter-connections between chapters.

Chapter Two

2. Literature Review

2.1 Air pollution from vehicle emissions

Air pollution is unfortunately not a new phenomenon. The air pollution created from human activities has been with us for centuries from various sources. From the impact of burning of wood or coal in cities for heating and cooking over the millennia's to the onset of the industrial revolution and the rapid exploitation of these resources and mineral oil in the second half of the 19th century (EKT Interactive, 2022). These natural and fossil fuels were used to run the machines of industry which boosted and accelerated industrial productivity and in turn the uncontrolled pollution of the environment.

The air pollution impacts were initially restricted to the cities and areas where industry and factories were located. This changed with the development and growth of automobiles with internal combustion engines in the 20th century. Initially the use and ownership of vehicles was low due to the limited supply and their expense. But with the advent of the moving production line being implemented in Ford factories in 1913 (Hounshell, 1984) and the wide availability of affordable petroleum brought the reality of vehicle ownership to the mass market. Beginning in the US and then in Europe manufacturers began to accelerate the rate of motor vehicle production and in turn its proliferation into the fabric of society. The advent of widely available motorised transportation allowed airborne pollution to spread into the wider environment beyond cities and industrial locations.

After the second world war when major economies began to boom and a significant portion of manufacturing capacity, some newly developed for the war effort and that previously existing that had been repurposed, returned to producing motor vehicles (Huddle, 1945). Demand for vehicles was high and communities began to change. Rapid urbanisation followed, cities started spreading and with this expansion the reach of air pollution grew as well. In communities which had previously lived in areas with clear

skies began to experience deterioration in air quality due to urban smog occurring, in the worst cases on a daily basis. Before the advent of affordable and rapid personal transportation it was more common for people to live in the same area as they worked in. With the new reality of affordable transport, people also began commuting greater distances en masse in private vehicles for work. In turn the concentration of uncontrolled motor vehicle emissions spread even further and became one of the major contributors to deteriorating air quality. With reduced air quality increasing significantly and occurring in numerous cities and regions the problem could no longer be ignored and needed to be addressed by governments.

2.2 Vehicle emissions testing – the journey begins

With the establishment of the first air pollution control districts across California in 1947 which acknowledged the problem of urban air pollution, such as photochemical smog, visible pollution sources were the first to be addressed with controls and legislation. As progress was made in managing these sources, shutting some polluting plants down and reducing emissions from others the problem of smog did not abate. It became apparent that these sources were only a part of the overall problem. Further investigations identified that impact of the automotive sector and transport industry was much greater than earlier anticipated (Haagen-Smit, 1952).

As fossil fuel consumption increased across the country, the problem of air pollution and smog became more apparent across other cities and regions. The US Federal government established the Air Pollution Control act in 1955 and provided a mechanism for federal services and financial aid to be able to assist state and local governments agencies to develop methods to abate this pollution. In 1963 the Clean Air Act (US Public Law, 1963) was passed; it was an extension to the Air Pollution Control act which now contained direct references to ‘automotive vehicle and fuel pollution’. This was further amended specifically with relation to vehicle emissions and was called the Motor Vehicle Air Pollution Control Act in 1965 (US Public Law, 1965). This set the standards for HC and CO emissions to be met by 1968 for light duty vehicle (LDV) models. These national standards were the same as those set earlier by California for their 1966 LDV models to meet. These standards were reductions from 1963 emissions: 72% reduction for HC to

6.3 g/mile, 56% reduction for CO to 51.0 g/mile, and 100% reduction for crankcase HCs (The Health Effects Institute, 1988).

Similar to the US standards, regulation limits for automotive vehicle emissions were also being established in western European countries such as Germany (in 1968) and France (in 1969). These regulations were the fore runners to the establishment of the common European Directive 70/220/EEC in March 1970 (European Economic Community, 1970). This directive came into force on 1 August 1970 as UN-ECE regulation No. 15, with an urban driving cycle (UDC, also known as ECE-15) and was progressively introduced across the countries of the EU. It remained in place until superseded by UN ECE Regulation 101 in 1990 which added a highspeed motorway/extra urban driving cycle (EUDC) to the test.

In principle, the US standards and the European standards that were developed for emissions testing used similar analytical processes and types equipment to assess the emissions performance of vehicles. They differed though in the early years of their evolution in what they focussed on. Following the experience of poor air quality in numerous cities in the US during the 1950s and 1960s, this led to a primary focus on improving air quality by regulating and reducing pollutant emissions, HC, CO and later NO_x as the primary targets of regulations. It was later in the 1970s that fuel economy became a focus of attention as well when oil prices spiked a number of times. The response to this was for legislation to be introduced to require vehicle manufacturers to improve the corporate average fuel economy (CAFÉ) figures by roughly double between 1975 to 1985.

In Europe, this process occurred somewhat in the reverse order. During the 1950s, some cities in Germany and France were also beginning to experience smog issues like those experienced in the USA. They were encouraged by the work undertaken already in California to reduce emissions from exhaust emissions and following this lead Germany and France began research programmes working together focussed on reducing exhaust emissions as well which led to the implementation of the aforementioned European Directive 70/20/EEC. When the EU countries experienced the spike in oil prices in the 1970s, they then began to focus on reducing fuel consumption as a methodology to reduce vehicle emissions and to also try to reduce dependency on imported fossil fuels. The approach used to implement this was by increasing government taxation on fuel, in particular gasoline, as a means to reduce consumption (Klier and Linn, 2016). This policy

approach resulted in the trend of much higher fuel prices being established in the EU in comparison to lower fuel prices in the USA.

Automotive manufacturers in the EU responded to this by focussing on smaller and more fuel-efficient vehicles with smaller engines sizes to meet targets for fuel economy and reduced emissions set by legislators. This delivered a 50% reduction between 1970 to 1982 for the HC, CO and NO_x emissions (Smith and Davies, 1996).

A further difference that occurred at this time in emissions control approaches was the technology focus and setting of emissions limits. In the USA, CARB and the USEPA developed plans in consultation with the industry to eliminate toxic pollutants by phasing out leaded gasoline and introducing catalytic converters with the combined goal to reduce amount of airborne lead exposure to the community and to introduce an effective means that could potentially eliminate almost all HC, CO and NO_x emissions over time from motor vehicles. With respect to emissions limits, legislation was progressively revised to set ambitious reduction targets. Between 1968 and 1989 emission limits reduced by 93% for HC and CO, and 90% for NO_x.

The European approach differed in that they considered the assessment of emission control technologies with respect to both economic and environmental costs. It was determined that setting absolute limits for each pollutant would be difficult and instead decided it would be better to set emissions limits that were desirable and achievable. With regard to the emissions control technologies available, research on their effectiveness and the cost benefit analysis of each that could be utilised as emissions control measures was conducted. They decided to apply a combination of lean burn technology, multi-point fuel injection combined with an oxidation catalyst. It was considered this was the most promising combination of technology for lowering fuel consumption and emissions. This was in contrast to the CARB and USEPA approach (in the USA) to use three-way catalysts which was considered more costly and unproven in European conditions at that time.

This divergence of ideologies led to the regulations in the USA progressing further and leading the world on emissions reductions during the 1970s and 1980s. This began to change when press reports in Germany (Gregory et al., 1996; Grennfelt et al., 2020) began to highlight the damage occurring to forests which was attributed to pollution from vehicle exhaust emissions. The public outcry pressured the German government to act,

which responded by announcing it would implement emissions standards similar to those in the USA. This decision by Germany placed pressure upon the European Commission (EC) which responded by developing updated regulations to maintain legislative harmony among the member states. This reaction resulted in the introduction of unleaded gasoline and three-way catalytic converters into the European market being introduced by the directive 91/441/EEC (European Economic Community, 1991). These actions ushered in the beginning of the now familiar Euro series of regulations in the 1990s. What followed in Europe was the subsequent catch up needed for the Euro emissions standards to become comparable to those in the USA.

2.3 Vehicle emissions laboratory testing and techniques

As identification of the toxic pollutants had been accomplished by dedicated researchers, the need for effective, quantifiable, reliable and fast emissions measurement equipment became a necessity. The development of transistor and microprocessor technologies developed and emerged during this time. Equipment manufacturers were able to develop and realise smaller, faster and more reliable electronically controlled equipment to measure emissions gases. Development of testing procedures for motor vehicles by manufacturers had focussed on the reliability and drivability performance prior to this time so new testing methods were required to acquire meaningful emissions measurements.

The first of these test procedures was developed after the California Department of Public Health established prescribed concentration limits for HC of 275 ppm and for CO of 1.5% in motor vehicle exhaust gases (Maga and Hass, 1960). The Motor Vehicle Pollution Control Board (MVPCB) was contracted to derive the test procedure which it did with support of four engineers from the Automobile Manufacturers Association (AMA) and a consultant from The Standard Oil Company. Information had been gathered by the AMA from traffic pattern surveys which allowed identification of 11 driving modes, consisting of various idle, cruise, acceleration and deceleration events, which were representative of urban driving usage. These formed the basis to derive potential driving cycles that could be used to test vehicles and evaluate the effectiveness of any pollution control devices fitted to the vehicle. Further assessment of the traffic survey data identified that

significant amount of urban driving consists of short trips. During the period after the vehicle starts and is warming up, (in the first minutes of driving) the fuelling is initially rich (producing high HC and CO emissions) and many of the potential emissions control components were not effective until the engine reached a stablished operating temperature. Furthermore, the identification of short trips to be significant in urban driving led to the need to ensure there was a cold start element included in the design of the test procedures.

To develop the most realistic test procedure, it was thought driving on a test track road would provide the most normalised temperatures, engine loading and cooling conditions. That considered, the practicality of having transportable instrumentation, exhaust to analyser sample conditioning and finding a level, unobstructed track for unobstructed driving with no wind made this choice problematic. These problems lead to the choice of a chassis dynamometer being utilised for development of the test procedure. After consideration of numerous potential driving cycles, two testing modes were developed and used together. The first was a 7 mode warmup cycle of 137s duration and the second was a 11 mode hot test of approximately 300 s duration (Hass and Brubache, 1962). A complete test consisted of six warm up cycles and one hot cycle. The driving cycles for this test are shown in Figure 2.1 (a) and (b).

The measurements of emissions gases utilised four Non-Dispersive Infrared (NDIR) type gas analysers. They measured HC low range, HC high range, CO and CO_2. To optimise measurement results, they utilised high flow rates and short sample lines to avoid HC hang up issues due its potential adsorption onto the walls of the sampling lines. For best measurement sensitivity there was also a switching mechanism to allow the low range HC analyser to bypass the input sample gas when emissions loading was higher.

Driving the vehicle on the chassis dynamometer required the correct selection of inertia weights to simulate a targeted vehicle loading. It was noted that if not carefully controlled the loading could significantly impact weighted results from the test modes. Other elements that were found to impact results were the temperature of the engine and air at the start of a test, operation of a vehicles' automatic choke, variations in fuel quality and potential heat build-up during testing. Overall, the test procedure proved to provide reasonable repeatability (around ±10%) on consecutive tests. After review and critique the test procedure was approved for use on the 19th of May 1961 by the MVPCB of California. This was one of the first formalised procedures in the development of vehicle

emissions testing using chassis dynamometer-based driving cycles which would become the foundation in the years ahead for determining compliance of new vehicle models and individual vehicles with emissions standards.

Whilst this initial procedure proved valuable, it was noted that there were areas where the test performance varied from real-world conditions and it was determined that further research was required. For some pollution control devices, the driving cycle could create conditions where they were either not active or their functionality could be shutdown. Test temperatures were also higher than would normally occur whilst driving on-road. Moving ahead from these outcomes, research was undertaken focussing further on vehicle performance and when control systems were operational, the driving styles of drivers and the study of various driving routes traffic, distance and speed profiles.

Driving cycles and emissions testing developed further with research during the 1960s, but it was with passing of the Clean Air Act of 1970 (USEPA, 2022) and the establishment of the USEPA shortly after that there was a legal authority that existed which was able to regulate pollution from vehicles across the USA. There could now be national regulatory programmes with specific requirements that could be federally enforced.

A new baseline driving cycle/test for the USEPA was developed, it was called the urban driving dynamometer schedule, (UDDS or also known as Federal Test Procedure 72, FTP-72) (USEPA, 1972) and was able to be used for verifying emissions after a cold start and was also suitable for determination of vehicle fuel economy. This cycle was based on measurements of real word driving, representing an urban route being driven with frequent stops. The cycle consists of two phases, the first being a cold start phase of 505s, over a distance of 5.78 km (3.59 mi) followed by a second transient phase of 864s over a distance of (3.86 mi). The total test time was 1379s and 12.0 km (7.45 mi). The FTP-72 driving cycle is shown in Figure 2.1 c.

Combined with this new driving cycle were the emissions testing techniques which had also been developed through the 1960s with flow measurement techniques progressing from determining the instantaneous concentration of emissions only to being able to determine of the mass emissions factors in g/mi (or g/km) of pollutant gases from the vehicles. These combined with improved vehicle chassis dynamometer equipment able to provide more consistent loading control established the foundation for a standard testing methodology which would become the dominant choice for light duty vehicle

emissions measurements. The USEPA mandatory testing requirement produced a significant amount of data being generated by the automotive industry and regulators. It was soon determined that the UDDS needed to evolve further. Whilst the UDDS covered cold start and transient driving emissions, it was noted from driving pattern studies that usage regularly involved vehicles stopping for a short period of before being restarted and driven again. To adapt the UDDS to cover this a hot start phase was added to the driving cycle. This revised test became commonly known as the FTP-75 drive cycle (USEPA, 1975). It consists of the UDDS followed by a hot soak period of 10 minutes where the vehicle is turned off. After 10 minutes the vehicle is restarted and repeats the first 505s of the UDDS drive cycle effectively emulating a hot start phase of the test. This revised version of the UDDS has been utilised since mid-1970s and is still in current use supplemented by additional testing procedures that have been developed over the years.

The cycle consists of three phases, the first is a cold start phase of 505s, over a distance of 5.78 km (3.59 mi) followed by a second transient phase of 864s over a distance of (3.86 mi), followed by the third hot start phase of 505s, the same as the first phase. The total test time was 1874s and 17.8 km (11.04 mi). The EPA75/FTP-75 driving cycle is shown in Figure 2.1(d).

Such catalyst effectively needed a lean fuel environment to achieve the oxidation reactions. Whilst good for HC and CO, they were not effective in reducing NO_x emissions. Up to 1978, NO_x reduction was primarily achieved through the use of exhaust gas recirculation (EGR). To achieve the NO_x emissions reduction targets set in 1978 a new type of catalyst was required, one which would also accommodate a reduction reaction to minimise NO_x levels.

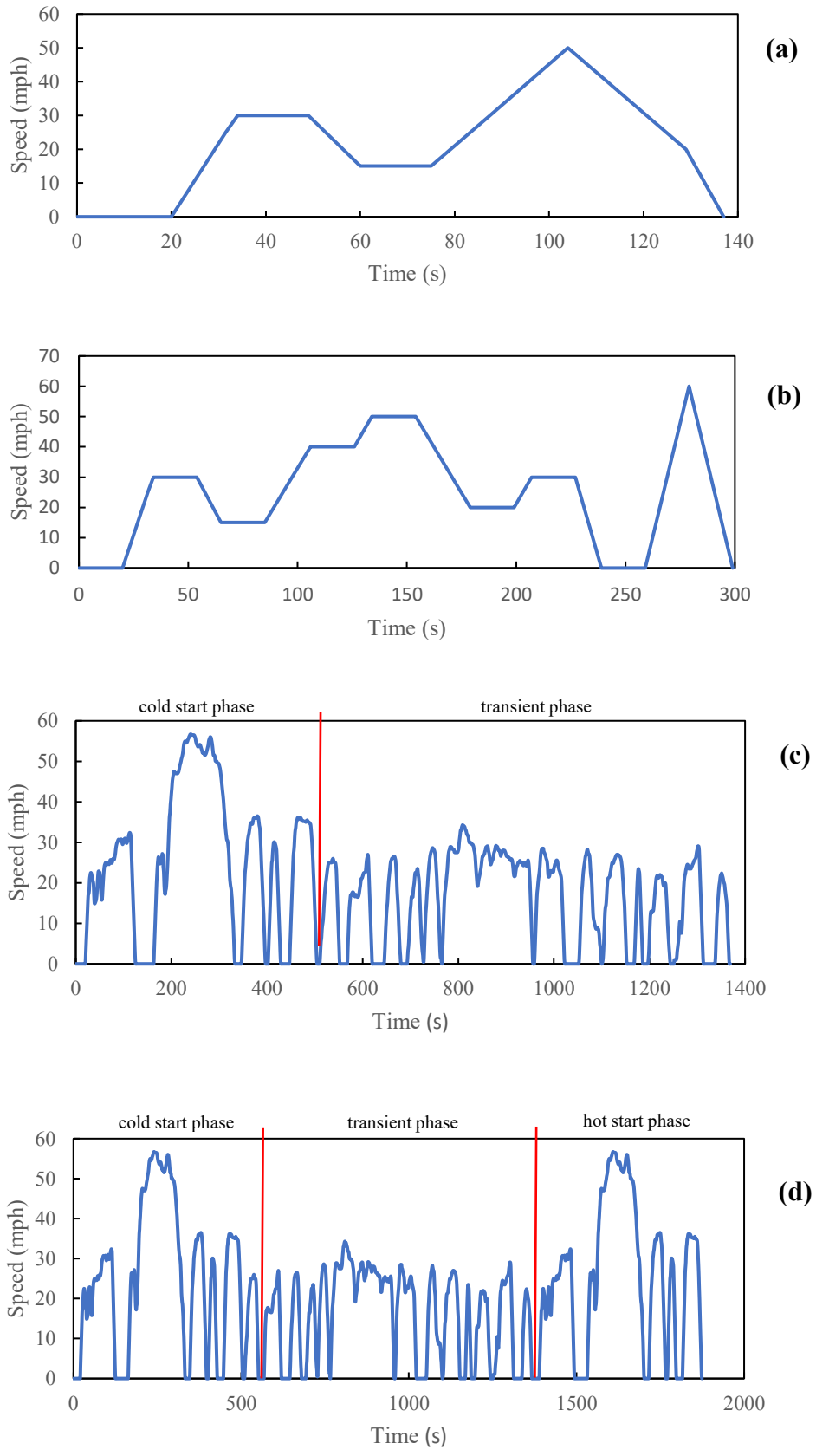

Figure 2.1: US Emissions testing drive cycles. a) 7 Mode warm up cycle, b) 11 Mode hot cycle, c) EPA Urban Dynamometer Driving Schedule FTP-72 and d) EPA Federal Test Procedure 75 FTP-75/EPA75

This new type of catalyst able to do this was called a three-way catalyst (TWC) and was introduced into the US market in 1981, effectively replacing the older two-way catalyst technology. A TWC operates with two main reaction types. Oxidation reactions, already utilised in the two-way catalyst and now with reduction reactions to eliminate NOx via a NO reduction strategy. The stoichiometric reactions for this are shown below (Kašpar et al., 2003; Turner, 1984):

$$2\mathrm{CO} + \mathrm{O}_2 = 2\mathrm{CO}_2 \tag{2.1}$$

$$\mathrm{HCs} + \mathrm{O}_2 \rightarrow \mathrm{xCO}_2 + (\mathrm{x}+1)\mathrm{H}_2\mathrm{0} \tag{2.2}$$

$$2H_2 + O_2 \rightarrow 2H_2O \tag{2.3}$$

$$2NO + 2CO \rightarrow N_2 + CO_2 \tag{2.4}$$

$$2NO + 2H_2 \rightarrow N_2 + H_2O \tag{2.5}$$

$$HCs + NO \rightarrow N_2 + H_2O + CO_2 \tag{2.6}$$

$$2NO + 5H_2 \rightarrow NH_3 + H_2O \tag{2.7}$$

$$CO + H_2O \rightarrow CO_2 + H_2 \tag{2.8}$$

$$HCs + H_2O \rightarrow CO + CO_2 + H_2 \tag{2.9}$$

The ideal stoichiometric air fuel ratio (AFR) in gasoline engines is 14.7 parts air to 1 part fuel (SAE, 2015). In theory, this mixture can allow for complete combustion of the fuel and produce CO_2 and H_2O without toxic pollutants or excess air. In an internal combustion engine, combustion is not 100% effective at converting all gases to the desired compounds and will produce pollutants HC and CO or NO_x depending if the AFR is rich or lean respectively. It is necessary then to be able to reduce pollutants with a TWC, to be able to control the AFR and have it oscillating in the range of 14.6 to 14.8 (rich/lean) continuously. This switching between rich and lean provides conditions which suit both oxidation and reduction reactions. This was enabled by the introduction of computerised engine management systems (EMS) with closed loop feedback control of fuel injection and ignition systems. Feedback is provided by oxygen sensors fitted before and after the TWC to monitor the oxygen content in the exhaust gas to determine if the AFR mixture is rich or lean. The EMS is then able to adjust the amount of fuel injected and the spark/ignition timing to alternate the AFR mixture as needed to allow the TWC to clean up the toxic pollutants.

Since its introduction, electronic EMS have been improved progressively using newer and faster processors with expanded storage capabilities and sensor technologies. These systems have made it possible to push subsequent generations of vehicles to comply with more stringent emissions regulations from the 1980s to the present day.

The evolution of emissions regulations in the European Union progressed differently based on the alternate path taken in the early years. The first European emissions test cycle was the urban driving cycle ECE-15. It was devised to represent city driving conditions, i.e., such as in Rome or Paris. It reflects low driving speed, low engine load and low exhaust gas temperature. It has a duration of 195s over a distance of 0.9941 km, which is considered one cycle. It begins with a cold start and is repeated 4 times to make up a test duration of 780s with a total distance of 3.9764 km. The UDC/ECE-15 driving cycle is shown in Figure 2.2 (a).

This cycle was first introduced in March 1970 and was utilised up until the development of the Euro emissions levels were introduced with UNECE regulation 83. The Euro 1 regulation came into force for all new spark ignition and compression ignition vehicles up to a maximum gross vehicle weight of 3,500 kg from the 31st December 1992. The updated emissions test now consisted of 2 phases. The first part, being the same as before the UDC/ECE-15 cycle repeated 4 times over 780 seconds. The second part, added an extra urban drive cycle (EUDC) to account for more aggressive high-speed driving. It has a duration of 400s over a distance of 6.9549 km. When combined with part 1 it makes up a measured test duration of 1180s with a total distance of 10.9314 km. This cycle is called ECE-15 + EUDC or the New European Driving Cycle (NEDC) and is shown in Figure 2.2 (b).

For the Euro 1 and 2 emissions regulations there was an additional period of 40 s at the start of the drive cycle for the engine and TWC to warm up before the first part of testing began. The emissions gases were not collected during the warm up. When the test is used in this format and at an ambient temperature of 20 – 30 °C, it is referred to as the Type I test in the regulations. When the Euro 3 regulations were introduced in 2000, a change was introduced to the Type I test and the 40s warm up was removed from the test. Now all vehicle emissions were collected from the beginning of the test, as soon as the engine started. Further development at this time was the addition of a new low temperature test conducted at -7°C and utilising the first part of the NEDC of 780 s was introduced to assess low temperature emissions performance, it is referred to as the Type VI test.

The NEDC, in its entirety and in its parts was utilised for the Euro regulations from Euro 1 through to Euro 5. For Euro 6 a new series of drive cycles was introduced from the World harmonised Light vehicles Test Procedures (WLTP) (European Economic Community, 2007; 2008). These were developed as global harmonised means to determine passenger car emissions and CO_2 emissions/fuel consumption across different regions with values that would be comparable. Furthermore, it is based on real word driving data and can better match on-road performance of vehicles. They are called the Worldwide harmonized Light vehicles Test Cycles (WLTC) (United Nations Economic Commission for Europe, 2014). There are four drive cycles for various test classes, 1, 2, 3a and 3b. This moves away from the single cycle for all vehicle tests and applies a power to mass ratio (PMR) to select the appropriate cycle and for class 3 vehicles there is also a high-speed selection criterion applied as well. Table 2.1 shows the summary of the WLTC classes.

Table 2.1: Summary of WLTC test cycles.

Category	PMR (W/kg)	v_max (kph)	Speed Phase Sequence
Class 3b	PMR > 34	v_max ≥ 120	Low 3 + Medium 3-2 + High 3-2 + Extra High 3
Class 3a		v_max < 120	Low 3 + Medium 3-1 + High 3-1 + Extra High 3
Class 2	34 ≥ PMR > 22	-	Low 2 + Medium 2 + High 2 + Extra High 2
Class 1	PMR ≤ 22	-	Low 1 + Medium 1 + Low 1

Figure 2.2 c shows the WLTC for class 3b vehicles which is one of the four drive cycle variants in use for Euro 6 regulations. Drive cycles are the dynamic vehicle component of emissions testing. The other major component of vehicle emissions testing is the laboratory equipment and set up. The systems and equipment utilised between the USEPA/CARB and Euro regulations for testing are very similar and use the same technologies to determine the emissions factors results of pollutants, in g/km or g/mile pending the regulation or rules. As the most widely utilised regulation globally are the Euro regulations, the following outlines the equipment and calculation methodology needed to determine emissions factors.

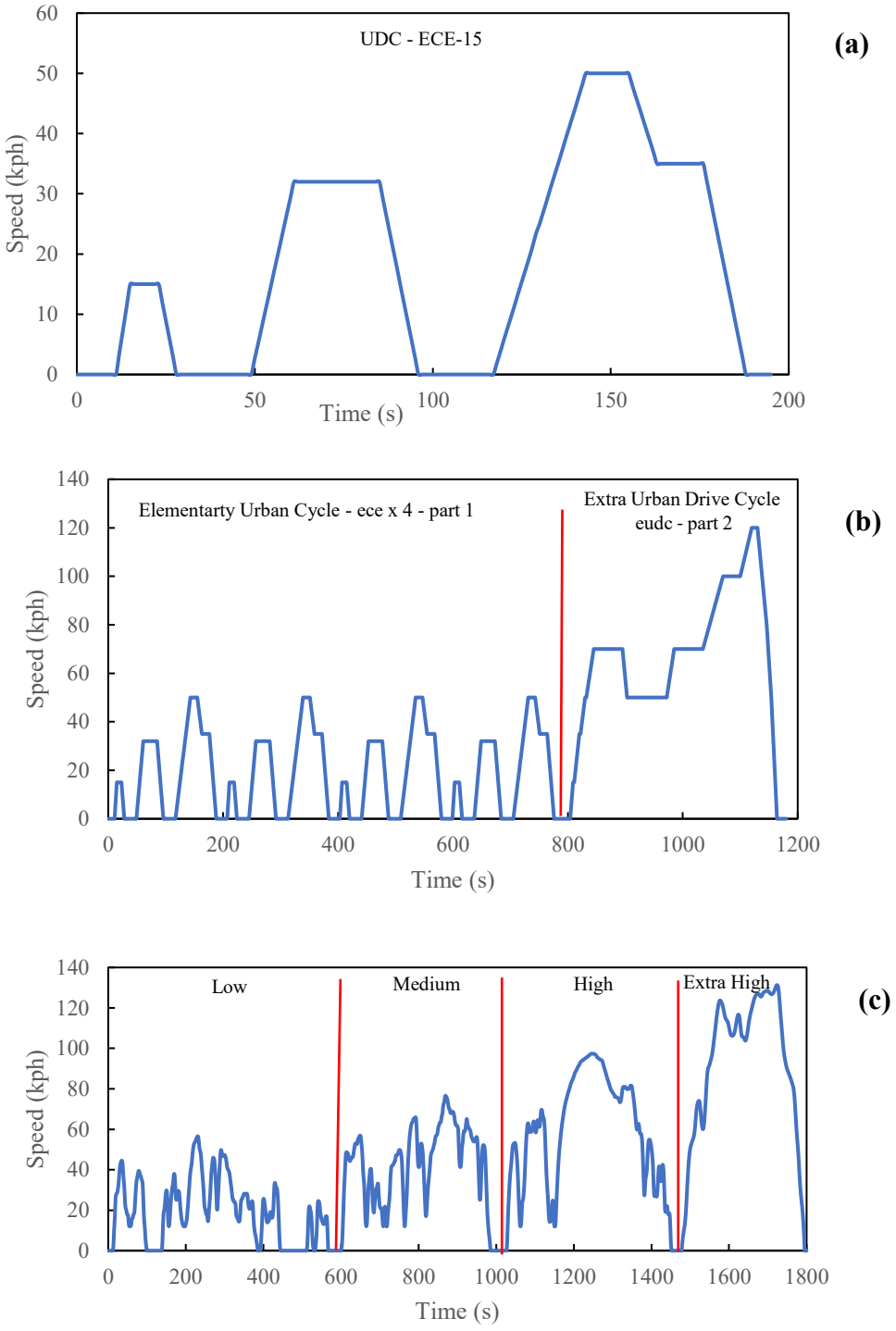

Figure 2.2: European emissions testing drive cycles. a) UNECE Regulation 15 - Urban Drive Cycle, b) UNECE Regulation 83 - New European Drive Cycle and c) WLTC for Class 3b vehicles

An emissions testing laboratory will consist of a number of systems operating together to provide a controlled environment, vehicle loading and gaseous measurement systems. A schematic representation of an emissions laboratory is shown in Figure 2.3.

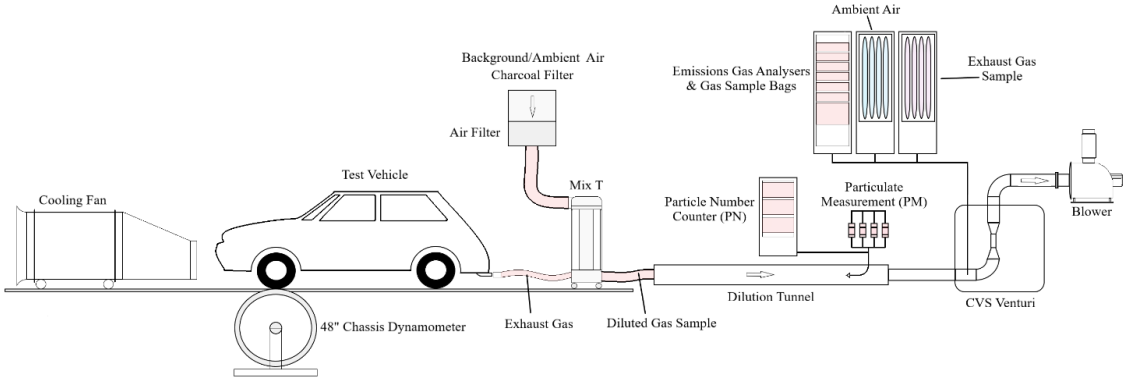

Figure 2.3: Emissions testing laboratory setup.

In this schematic the test vehicle is set up to be driven on the chassis dynamometer rollers. At the beginning of the test the driver starts the car and shortly afterwards begins to drive the vehicle following the selected drive cycle speed trace as it progresses second by second. A sample hose is connected to the exhaust pipe on the vehicle and this collects the all the exhaust gas emissions from the vehicle. The exhaust gas is drawn into the system to a point called the Mix T, where the exhaust gas emissions are mixed with ambient back ground air and diluted. This diluted sample then travels further through the system through the dilution tunnel where Particulate Matter (PM) and Particle Number (PN) are measured then to the constant volume sampler (CVS) venturi(s). At the CVS the combination of the selected venturi and the blower fan at the end of the system controls the volume flow through the system at a constant rate. At the venturi, the temperature and pressure are continuously measured and recorded so the flow rate can be calculated. It is also at this point that a gas sample is continuously collected and transferred into a sample bag for analysis after each part of the test is complete or measured second by second for research analysis. In addition to the diluted exhaust gas sample, another ambient air sample is collected in parallel so the background levels of any pollutant can be quantified and later removed from the final calculated emissions factors.

2.3.1 Calculation of vehicle emissions factors

This section is based on paraphrasing the following references: UNECE Regulation No. 83 for the emission of pollutants, 2015 and UNECE Regulation No. 101 for the measurement of the emission of carbon dioxide and fuel consumption, 2013. The absence of references hereafter implies that these information sources are being relied upon.

Gaseous emissions

The gas samples are collected in a pair of sample bags (one for the gas sample, and one for ambient air) throughout each part of the test. For the NEDC test there are two parts, in the FTP-75 test there 3 parts. As the first part of a test finishes and the second begins, valves shut on the first pair of bags and then open on a second pair of sample bags which begins to be filled. The gas sample already collected from the first part is then transferred from the sample bags to the gas analysers. For emissions measurements, three main analyser types are used for measurement.

- THC and CH_4 measurements utilise flame ionisation detectors (FID).
- NO/NO_x measurements utilise Chemiluminescent analysers.
- CO and CO_2 measurements utilise non dispersive infrared (NDIR) analysers.

The gas samples from the bags are all required to be measured within 20 minutes of the end of an emissions test. All dilute exhaust gas samples and ambient air sample concentrations are recorded from the measurements. The data collected and recorded from the emissions test is processed as follows to determine the emission factor results for each test.

Determination of the volume of gas that has flowed through the CVS system critical flow venturi is required. 1 Hz data for the temperature and pressure at the venturi are recorded for the duration of the test cycle. The equation/formula to calculate the volume is:

$$Vol_{CVS} = \left(\frac{K_V \times Press_{CVS}}{\sqrt{Temp_{CVS}+273.15}}\right) \times \frac{1000}{60} \qquad (2.10)$$

where

Table 2.2: CVS Volume flow parameters.

Vol_{CVS}	CVS Test volume of dilute gas	(l)
K_V	Venturi Calibration co-efficient	(-)
$Temp_{CVS}$	CVS Test Ambient Temperature	(K)
$Press_{CVS}$	CVS Barometric Pressure	(kPa)

This calculation, using the parameters outlined in Table 2.2, is performed for each second of the test. As all testing needs to be standardised and comparable, the volume flow is next corrected to standard conditions. The combined gas law/general gas equation is used for calculation of the corrected test volume:

$$\frac{P_R V_R}{T_R} = \frac{P_C V_C}{T_C}$$

$$V_C = \frac{P_R V_R T_C}{P_C T_R} \tag{2.11}$$

where P_R, V_R, T_R, P_C, V_C and T_C are: Barometric Pressure (kPa), Volume of dilute gas (l), Ambient temperature (K), Regulation Barometric Pressure (103.3, kPa), Corrected volume of dilute gas (l) and Regulation Ambient Temperature (273.2, K) respectively. When the volume has been corrected, the results are summed up for each second to determine the total volume of dilute gas which flowed through the CVS during the test.

To determine the total mass of pollutants that are emitted during the test, the densities of the various pollutants at the above-mentioned reference conditions are needed. The following standardised densities (Table 2.3) are used for the calculations:

Table 2.3: Standardised density values of different gases.

Pollutant	**Q_i (g/l)**
Q_{CO}	1.25
Q_{CO2}	1.964
Q_{NOx}	2.05
For HC, the density depends on the reference fuel being used	
HC Fuel type	**Q_{THC} (g/l)**
Gasoline (E5) ($C_1H_{1.89}O_{0.016}$)	0.631
Gasoline (E10) ($C_1H_{1.93}O_{0.033}$)	0.631
Diesel (B5) ($C_1H_{1.86O0.005}$)	0.622
Diesel (B10) ($C_1H_{1.86O0.007}$)	0.623
LPG ($C_1H_{2.525}$)	0.649
NG/biomethane (C_1H_4)	0.714
Ethanol (E85) ($C_1H_{2.74}O_{0.385}$)	0.932
Ethanol (E75) ($C_1H_{2.61}O_{0.329}$)	0.866

The mass emissions of pollutants will be calculated using the following equation:

$$M_i = \frac{V_C \cdot Q_i \cdot K_H \cdot C_i \cdot 10^{-5}}{d} \tag{2.12}$$

where

Table 2.4: Mass emissions calculation parameters.

M_i	Pollutant mass emission *i*	(g/km)
V_C	Corrected volume of diluted exhaust gas	(l)
Q_i	Pollutant density '*i*'	(g/l)
K_H	Humidity correction factor for oxides of nitrogen only	(-)
C_i	Corrected concentration of pollutant in diluted exhaust gas	(ppm)
d	Test cycle distance	(km)
i	Pollutant mass emission *i*	(-)

The following equations are needed to calculate the remaining factors listed in Table 2.5 for the mass emissions calculation.

To ensure the effect of background emissions gas concentrations are accounted for the measured emissions concentrations need to be corrected. The corrected concentration is calculated as follows:

$$C_i = C_e - C_d \cdot \left(1 - \frac{1}{DF}\right) \tag{2.13}$$

Where

Table 2.5: Corrected emissions calculations parameters

C_i	Corrected concentration of pollutant i in diluted exhaust gas	(ppm)
C_e	Measured pollutant concentration i in exhaust sample	(ppm)
C_d	Pollutant concentration i in air	(ppm)
DF	Dilution Factor	(-)

DF calculation is dependent upon the fuel type used for the testing. Per the regulation the following fuels have reference calculations: Gasoline (E5 and E10), Diesel (B5 and B7), LPG, NG/Biomethane, Ethanol (E85 and E75) and Hydrogen.

For each reference fuel, except hydrogen, DF is calculated as follows:

$$DF = \frac{X}{CO_2 + (C_{HC} + C_{CO}) \cdot 10^{-4}} \tag{2.14}$$

For a fuel composition of CxHyOz, the general formula is:

$$X = 100 \cdot \frac{x}{x + \frac{y}{2} + 3.76 \cdot \left(x + \frac{y}{4} - \frac{z}{2}\right)} \tag{2.15}$$

DF values for the reference fuels covered by this regulation are listed in Table 2.6:

Table 2.6: Dilution factor regulation parameters.

Fuel type	X
Gasoline (E5)	13.4
Gasoline (E10)	13.4
Diesel (B5)	13.5
Diesel (B7)	13.5
LPG	11.9
NG/Biomethane	9.5
Ethanol (E85)	12.5
Ethanol (E75)	12.7

In the case of hydrogen, the DF is calculated by eq. 2.16:

$$DF = \frac{35.03}{C_{H2O} - C_{H2O-DA} + C_{H2} \cdot 10^{-4}} \quad (2.16)$$

Where C_{CO}, C_{H2O}, C_{H2} and $C_{H2O\text{-}DA}$ are the gas concentrations of CO, H_2O and H_2 in the sample bag and the gas concentration of H_2O in the dilution air.

In the case of non-methane hydrocarbons (NMHC), concentration is calculated as follows:

$$C_{NMHC} = C_{THC} - (Rf_{CH4} \cdot C_{CH4}) \quad (2.17)$$

where C_{NMHC}, C_{THC}, C_{CH4} and Rf_{CH4} are the corrected concentrations of NMHC, THC, CH_4 carbon equivalents and the FID response factor for CH_4.

The next parameter needed is the NO humidity correction factor. This is required to adjust for the influence of humidity on the measurement of oxide of nitrogen. The following calculation is applied:

$$K_h = \frac{1}{1 - 0.0329 \cdot (H - 10.71)} \quad (2.18)$$

where K_h, H are the NO humidity correction factor and the Absolute Humidity (g H_2O /kg Air).

H is calculated as follows:

$$H = \frac{6.211.R_a.P_d}{P_B - P_d.R_a.10^{-2}} \tag{2.19}$$

where R_a, P_d, P_B are Relative Humidity, Saturation Vapour Pressure at ambient temperature and Barometric Pressure.

For the calculation of absolute humidity, saturation vapour pressure is calculated as follows:

$$P_d = 6.112.e^{(17.62T/(243.12+T)} \tag{2.20}$$

Where P_d, T are Saturation Vapour Pressure at ambient temperature and the Test temperature.

When performing a 'diesel fuel' or 'compression ignition' vehicle emissions test, the calculation of HC does not utilise the diluted exhaust gas collected in the sample bag. This requires a heated FID HC emissions analyser (operating at 190°C +/-10°C) to be connected to the dilution tunnel. The sample is measured continuously and the exhaust gas from the analyser returned to the dilution tunnel to ensure gas flow is consistent and no compensation calculation is needed.

To calculate HC-mass emission for compression-ignition engines, the average HC concentration is calculated as follows:

$$C_e = \frac{\int_{t_1}^{t_2} C_{HC} \cdot dt}{t_2 - t_1} \tag{2.21}$$

where C_e , $\int_{t_1}^{t_2} C_{HC} \cdot dt$ are the HC concentration of Ci and the integral of recording for the heated FID.

Particle emissions – particulate matter and particle number

Particle emissions have been associated with diesel fuelled vehicles since the beginning of vehicle pollution control and emissions measurement. The early diesel fuel systems, with indirect injection (IDI) did not have controls for particle emissions. The Euro 1 regulations beginning in 1992 pushed the wide scale enforcement of PM emissions limits in the EU and in turn other countries which utilised these regulations. Diesel combustion control improved, electronic controlled direct injection (DI) was implemented and PM emissions became far less visible. Whilst there was a visual improvement, PM remained, but the size of the particles had reduced significantly. This led to changes in the PM filters utilised for emissions testing. They were initially a diameter of 90 mm, which was subsequently reduced to 70 mm and then to 47 mm. The size of the filter for each generation of these systems were reduced to keep pace with the changing nature of PM emissions. The construction of a PM filter can vary, a common style utilised for these regulations is to use a Teflon (Polytetrafluoroethylene, PTFE) coated glass fibre construction (Pall Life Sciences, 2021)which is one of the suggested filters that can be used by the USEPA and the Euro regulations.

It was not until the Euro 5 regulations that gasoline vehicles also became subject to PM measurement requirements. This was to cover the introduction of gasoline direct injection (GDI) engines which were prone to PM emissions that earlier gasoline engines typically were not. This is due in part to the nature of the direct fuel injection into the cylinder that is utilised in GDI engines. With the fuel having less time to mix with the air and vapourise (La Rocca et al., 2015), soot formation can become an issue whereas it is not the case with gasoline engines using manifold port fuel injection as the fuel and air can mix effectively before entering the cylinder.

The calculation of PM emissions can be performed using equation 2.22, when exhaust gases from the system are returned to the emissions tunnel after PM sampling.

$$M_p = \frac{V_{mix} \cdot P_e}{V_{ep} . d} \tag{2.22}$$

where M_p, V_{mix}, V_{ep}, P_e , d are the Particulate emission (g/km), corrected volume of dilute exhaust gas (l), volume flow through particulate filter (l), particle mass on filter (g) and test cycle distance (km).

Using the combined gas law and general gas equation for calculating the corrected test volume following through the filters:

$$\frac{P_R V_R}{T_R} = \frac{P_C V_C}{T_C}$$

$$V_C = \frac{P_R V_R T_C}{P_C T_R} \tag{2.23}$$

$$V_C = V_{ep}$$

where P_R, V_R, T_R, P_C, V_C (V_{ep}) and T_C are Barometric Pressure (kPa), Volume of gas through filters (l), Test Ambient temperature (K), Regulation Barometric Pressure (103.3, kPa), Corrected volume flow through filters (l) and Regulation Ambient Temperature (273.2, K) respectively.

As the mass of PM on the filters for Euro 5 and 6 vehicles is only slight compared to the overall filter weight, it is necessary to account for the buoyancy effect of the filter in the air. To correct for this, it is necessary to know the density of the filter medium and the density of the air pending the humidity, temperature and ambient barometric pressure. The correction of buoyancy is done per the following calculation.

$$m_{coor} = m_{uncorr} \cdot \left(\left(1 - \left(\rho_{air}/\rho_{weight}\right)\right) / \left(1 - \left(\rho_{air}/\rho_{media}\right)\right) \right) \tag{2.24}$$

where m_{corr}, m_{uncorr}, ρ_{air}, ρ_{weight}, ρ_{media} are the Corrected PM mass for buoyancy (mg), Uncorrected PM mas for buoyancy (mg), Air density (kg/m^3), Calibration weight density for span balance (kg/m^3) and PM sample medium density (filter) (kg/m^3).
The density of the media and weight are obtained from manufacturer data. The density of the air needs to be calculated per the environmental measurements. It is calculated as follows.

$$\rho_{air} = \frac{P_{abs} \cdot M_{mix}}{R \cdot T_{amb}} \tag{2.25}$$

where P_{abs}, M_{mix}, R, T are Absolute Pressure in balance chamber (kPa), molar mass of air in balance chamber (28.836, g/mol), Molar gas constant (8.314, g/mol) and Absolute temperature in balance chamber (K).

When these factors have been calculated and applied, any buoyancy effect is negated and the mass of PM on the filter is obtained for calculation by subtracting the buoyancy effect.

The emissions calculations methodology described above has been the foundation for determining for PM for each of the Euro regulations since introduction. As the emissions regulations have progressed, the levels of discernible PM emissions, (measurable mass and visual stain on PM filters) has reduced. The requirement for vehicle emissions is to utilise a filter to capture coarse particles. This requires a filter which meets a PM_{10} specification. The PM filters can capture material that is larger than rating of the filter chosen for use (i.e., PM_{10}, $PM_{2.5}$ or $PM_{1.0}$. that is the filter is suitable for collecting particles in the size range of 10, 2.5 or 1 micron). Smaller particles than this exist in the vehicle exhaust and can range in measurable size from 1 micron down to 1 nanometre (Kittelson, 1998). Whilst it is impractical to attempt to measure the mass of these, it is possible to measure the number of fine and ultrafine particulates (UPFs) generated by both diesel and gasoline emissions. Currently these particles are measured down to a cut point of 23 nanometres in size with the this potentially being reduced to 10 nanometres for the next generations of emissions regulations(Giechaskiel et al., 2021).

Measurement of UFPs in the Euro emissions regulations is referred to as determination of the PN result for the vehicle being tested. Introduction of PN measurement or counting has provided a means to determine if newer generation emissions equipment such as Diesel Particle Filters (DPFs) are functioning as required. This is crucial as the use of DPFs has been a key factor in achieving the reduction of the amount of PM generated by a vehicle. Furthermore, smaller particles have also been the focus of health studies as due to their minute size they can enter the bloodstream after inhalation and cause health effects in secondary organs and can have serious impacts on individuals' health (Kassel et al., 2013; Ristovski et al., 2012). Measurement of PN has been addressed by regulations since the introduction of Euro 5.

To determine PN results, emission gases need to be fed into a dilution tunnel where a suitable sampling probe has been inserted into. This provides a feed to the PN equipment nearby. The gas is fed into a separator to remove any larger particles before being conditioned to ensure the sample is maintained in an aerosol form and having any volatile particles removed prior to entering the particle number counter.

The calculation of the PN result is obtained by equation 2.26:

$$N = \frac{V.k.\overline{C_s \cdot f_r}}{d} \tag{2.26}$$

Where N, V, K, $\overline{C_s}$, $\overline{f_r}$, d are particulate number emissions (particulates/km), Corrected volume of the diluted exhaust gas (litres), calibration factor for correction of particulate number counter measurements, Corrected concentration of particulates of diluted exhaust gas (particulates/cm^3), mean particulate concentration reduction factor and Test cycle distance (km).

Using equation 2.26, PN emissions can be determined for a vehicle under test. It should be noted further that the equipment utilised for PN counting can be set up to instantaneously calculate the parameters mentioned above and provide the number of particles each second. This enables the results for total number of particles per km to be simply calculated after each test.

The current regulations require PN measurement systems accurately measure particles of 23 nm in size and greater. The benefits of this are substantial, but unfortunately this currently does not reflect the reality that a significant number of smaller particles being generated from vehicle exhaust which can impact health are not measured. In future as new measurement techniques are able to implement measurements that reduce the uncertainty of current PN measurement systems for particle under 23 nm in size. It is anticipated that PN measurement system will continuously develop to provide further improvements in future to meet measurement needs to reduce health impacts.

These sections covering the calculation of vehicle emissions factors and particle emissions outline the accepted global practices that have been established and improved upon since the 1960s when the first laboratory-based chassis dynamometer vehicle emissions testing took place. There are testing facilities around the globe which are capable of conducting these types of tests. This type of testing was effectively the reference standard for which other types of vehicle emissions testing are compared to. As a reference standard, it utilises a significant investment in time and resources to run and maintain facilities like this. It is also limited in the amount of testing it can be used to conduct in a given period. Considering the vast size of on-road vehicle fleets in various countries, it is only possible to consider using this kind of laboratory setup for testing a

small percentage of any on-road vehicle fleet. It is for this reason that methodologies to passively monitor vehicles travelling en masse effectively are needed so the small portion of high emitting vehicles are identified, repaired and checked at a vehicle emissions laboratory test centre. This leads to the field of optical spectrometry, its development and application for this purpose.

2.3.2 Real driving emissions

As emissions standards progressed and were tightened to reduce pollutant emissions, the need to confirm the on-road performance of vehicle emissions control systems was apparent. In the 1990's the UK Environmental Research Programme and in the US the USEPA started to develop this type of technology. In 1995 the USEPA invented the Real-time On-road Vehicle Emissions Reporter (ROVER) (Johnson, 2002). This provided real-time emissions data for various types of combustion engine in vehicles and various other applications. Commercial products began to appear in 1999 with a system being released by Clean Air Technologies International (CATI) called OEM2100. It was at this time the term PEMS was first utilised as well. The first units of these OEM2100 were purchased and utilised by the university of South Carolina (Frey et al., 2003). This was followed by the next evolution of the product by CATI being the CATI Montana system and from Sensors Inc., the SEMTECH series of analysers in 2002 (Miller, 2018). Significant road testing of all sizes and types of vehicles proceeded starting with New York city buses, testing of vehicles before and after maintenance, emissions from non-road sources, trains and ferries as well. Universities, government agencies and research groups utilised PEMS to collect data for determining real-world emissions and developing models to represent the emissions generated by most every type of internal combustion engine.

The compilation of data from these PEMS measurements, some by government funded research projects allowed the USEPA to develop a framework with industry for determining the variation of real-world emissions from the laboratory emissions measurements. For heavy duty vehicle engines, it provided a means to determine if these vehicles complied with Not To Exceed (NTE) emissions standards set by the USEPA. Beyond the regulatory usage, PEMS provided a new means of testing if improvements made to engine hardware, sensors, ECUs and fuels performed as claimed under in use

conditions. The use of PEMS was incorporated into the Code of Federal Regulations 40 part 1065 (CFR 1065) (US Government, 2005) which is used to govern engine emissions in the US. This CFR provided the foundations for emissions measurement methodology, the calculations to be used and allowed the results to be comparable to known and accepted test methods. It raised the performance level for PEMS so it now performed to standards with traceability and certainty.

The use of PEMS continued and it became adopted for collecting data for emissions factor modelling used to support transport impacts as part of environmental impact assessments in regions like California and Hong Kong. For these applications the real-world data emissions factors supplemented or replaced assumptions made previously based on the volume of fuel sales and calculated emissions factors.

It was when the Volkswagen (VW) diesel vehicle emissions cheating scandal (Franco et al., 2014) came to light PEMS was utilised widely to verify the high NO_x emissions from many of the VW vehicles having software defeat devices installed to cheat the emissions regulations. This event pushed the usage of PEMS forward beyond just verification of on-road fuel consumption and performance to be now be required for Real-world Driving Emissions (RDE) measurements which were made part of the Euro 6 regulations in addition to the laboratory-based testing which it had previously been based on so any defeat devices or cheating of this type could not happen in future. As PEMS became a requirement for certification purposes, large Tier 1 emissions equipment suppliers, Horiba and AVL also further developed their own existing PEMS equipment systems, OBS-One and M.O.V.E. series respectively to meet these RDE requirements pushing the equipment from research applications into the mainstream of vehicle development and certification.

PEMS has proven valuable in verifying the actual vehicle emissions of perceived problems in various studies and quantifying previously unknown vehicle usage emissions performance(O'Driscoll et al., 2018). Whilst this value is significant, it is also limited as performing PEMS testing is one of the most time consuming and expensive choice of those available for emissions testing. It can only be used to test a small selection of vehicles when compared to other testing techniques, which effectively rules it out as a choice for large scale testing.

2.3.3 Comparison of different emissions measurement techniques

A comparison of emissions measurement techniques is necessary to ensure and validate the appropriate choice is made to enhance an I/M programme and in turn help to achieve the desired emissions reduction outcomes. To do this, each methodology needs to be considered for its advantages and disadvantages. A comparison of the positive and negative aspects of various emissions testing techniques is summarised in Table 2.7.

When considering the test advantages and disadvantages listed in Table 2.7, the following desired aspects have been identified which would assist in improving emissions enforcement programmes:

Tests which would allow the most measurements:

- 'I/M stationary vehicle idle and 2000 rpm test' (potentially 12 to 15 cars per hour)
- 'RS' (potentially hundreds of cars per hour).

Tests which are non-intrusive without inconveniencing a vehicle owner/driver:

- 'Ambient Air Monitoring'
- 'Tunnel Air monitoring'
- Plume chasing and
- 'RS'.

Tests which have the lowest operating costs:

- 'I/M stationary vehicle idle and 2000 rpm test'
- 'Ambient Air Monitoring'
- 'Tunnel Air monitoring' and
- 'RS'.

Table 2.7: Comparison of different emissions measurement testing techniques

Test Description (Pollutants measured)	Advantages	Disadvantages
I/M stationary vehicle–- Idle & 2000 rpm test. (HC, CO)	Very fast, simple to implement, very low cost	This test is not highly relevant for modern vehicles. It can only find seriously faulty/gross emitting vehicles.
I/M chassis dynamometer test HKTET/IM240. . (HC, CO, CO_2, NO, NO_x)	Moderately time consuming, accurate, repeatable.	High costs, limited daily capacity, it can only focus on a small portion of the vehicle fleet.
Laboratory engine dynamometer test ESC/ETC/ELR/WHSC/WHTC/FTP Transient. (HC, CH_4, CO, CO_2, NO, NO_x, O_2, PM, PN)	Can test full engine capability, accurate, repeatable,	Very high costs, lengthy preparations required (weeks), only tests engine. Not real-world testing.
Laboratory vehicle chassis dynamometer NEDC/WLTP/FTP75. (HC, CH_4, CO, CO_2, NO, NO_x, PM, PN)	Accurate, repeatable, tests complete vehicle	Very high costs, slow & time consuming for certification preparations (days), not real-world testing.
Ambient Air Monitoring (NO, NO_2, NO_x, O_3, CO, FSP, RSP, $PM_{2.5}$, SO_2)	Provides continuous long-term data, real-world, moderate costs.	Cannot identify individual vehicles.
Tunnel Air monitoring (NO_x, CO, NMHC, EC, TC,)	Provides continuous long-term data, real-world, moderate costs.	Cannot identify individual vehicles. Interference from non-vehicle sources.
Plume chasing (CO2, NO, NO_2, NO_x, UFP, $PM_{2.5}$, BC, O_3)	Provides accurate real-world data, measures individual vehicles. Specifically isolates vehicle-related pollution.	Limited to a series of measurements per vehicle, time consuming (30s ~ 2 minutes per vehicle) , moderate costs, limited measurement capacity.
PEMS (RDE- Real Driving Emissions) (HC, CH_4, NO, NO_2, NO_x, CO, CO_2, O_2, PM, PN)	Highly accurate, real-world representative, accurate	High costs, single vehicle result per test limit, slow & time consuming,
RS (remote sensing) (HC, CO, CO_2, NO, NO_2, NO_x, PM, O_2, NH_3, Smoke)	Low cost per measurement, non-invasive, does not require driver co-operation, can obtain large sample size	Snapshot emissions measurement only. Larger measurement uncertainty compared to other emissions analysers for a single result.

Considering the above, the one technique that combined each of these aspects favourability for measurement is ‘RS’.

These factors combined indicate using RS to passively monitor vehicles travelling en masse effectively has the potential to identify and allowing regulators to target the small portion of high emitting vehicles, which inventory information suggests is around 10 percent (Beaton et al., 1995; McClintock, 2007) that are driven on-road so they can be repaired and checked to pass emissions standards at a vehicle emissions laboratory test centre.

This assessment leads the literature review to the field of optical spectrometry and RS, its development and its application for emissions measuring purposes. To gain a deeper insight it is necessary to review RS to further understand how it works, what are its limits and what knowledge gaps exist that need to be examined.

2.4 Optical spectrometry and RS

2.4.1 The development of optical spectrometry and RS

RS has its origins in the development of spectroscopy, optics and photography. One of the most familiar aspects of ‘optical’ spectroscopy which was described in 1672, was the description of the fundamental observations on how sunlight is dispersed (or refracted) when it passes through a small hole then into a prism as published by Isaac Newton in 1672 (Newton, 1672). Newton in this work described how sunlight is dispersed in colours, the phrase he coined to describe this was ‘spectrum’. It was 80 years later in 1752 that further observations of distinctive patterns of colour generated when salts were added to an alcohol based flame had been observed and recorded in by studies undertaken by Thomas Melvill (Melvill, 1752). This was what was described as a by eye ‘flame test’ and the basis of what would later become flame emission spectrometry. Work to describe the spectral features of light other than the colour were described by William Wollaston in 1802 who identified dark lines in the sun’s spectra or gaps which he speculated to be the natural boundaries between the colours in the spectrum (Wollaston, 1802). This suggestion was later ruled out by work undertaken by Joseph Fraunhofer. It was in 1817

that Joseph Fraunhofer whilst working to measure refractive indices with a spectroscope he had built made the first recorded independent precision observations of the dark lines (absorption lines, also called Fraunhofer lines) visible in the spectra (Fraunhofer, 1817). He systematically studied and measured the wavelengths where these features were observed. In all he mapped 574 of these dark lines in the spectra of sunlight. Review and analysis of the distribution of these absorption lines within colours allowed the boundary hypothesis of Wollaston to be ruled out. Fraunhofer also studied the light from bright stars and planets using a telescope combined with his spectroscope to collect the light from sources such as the moon, Venus, Betelgeuse and Sirius. The light spectra of these distant objects were similar yet had different dark lines to that of the sun. From these measurements he was able to determine these dark lines arise in nature from the source of the lights origin and indicate that the characteristic nature of the stars to be unique from one another. This work provided the foundation for stellar spectroscopy (Fraunhofer, 1815). Further research was also undertaken to systematically analyse salts using flame spectroscopy. The work was conducted by Herschel and Talbot in the 1820s and identified spectral characteristics of different materials (Herschel and Fredrick, 1823; Talbot and Fox, 1826).

Spectroscopy developed further over the next decades, it was determined that various metals could be identified by the bright lines made in the emission spectra of the sparks that they made (Wheatstone, 1835), thus introducing a new method to generate spectra without using a flame. In 1849 it was experimentally demonstrated by Jean Bernard Léon Foucault that absorption and emissions lines appearing at the same wavelength were directly related to the same material being subjected to the same type of light source working at different temperatures (Corbin et al., 1848). Similarly, a few years later Swedish physicist Anders Jonas Ångström presented complimentary observations and theories regarding gas emission spectra. His theory suggested that an incandescent gas emits luminous rays of the same wavelength as those it can absorb (Ångström, 1853). In each instance it had been established that it was possible to identify a particular material, be it solid, liquid or gas by measurement of its optical emissions or absorption spectra.

In 1859, the analytical research undertaken by Robert Bunsen and Gustav Kirchhoff was published that showed there was a connection between the of emissions spectral lines from flame spectrometry that could be matched to the Fraunhofer lines observed in laboratory light sources (Kirchhoff, 1859). Bunsen had developed the ‘Bunsen burner’

which produced a bright flame which did not interfere with the coloured flame produced by a test material being burnt in a flame test. Kirchhoff suggested to use a spectroscope to help differentiate the sometimes-similar coloured emission spectra given off by the flame They utilised the optical technique developed by Fraunhofer with the improved flame source developed by Bunsen to establish a systematic procedure to examine the spectra of chemical compounds. An image of their spectrascope is shown in Figure 2.4.

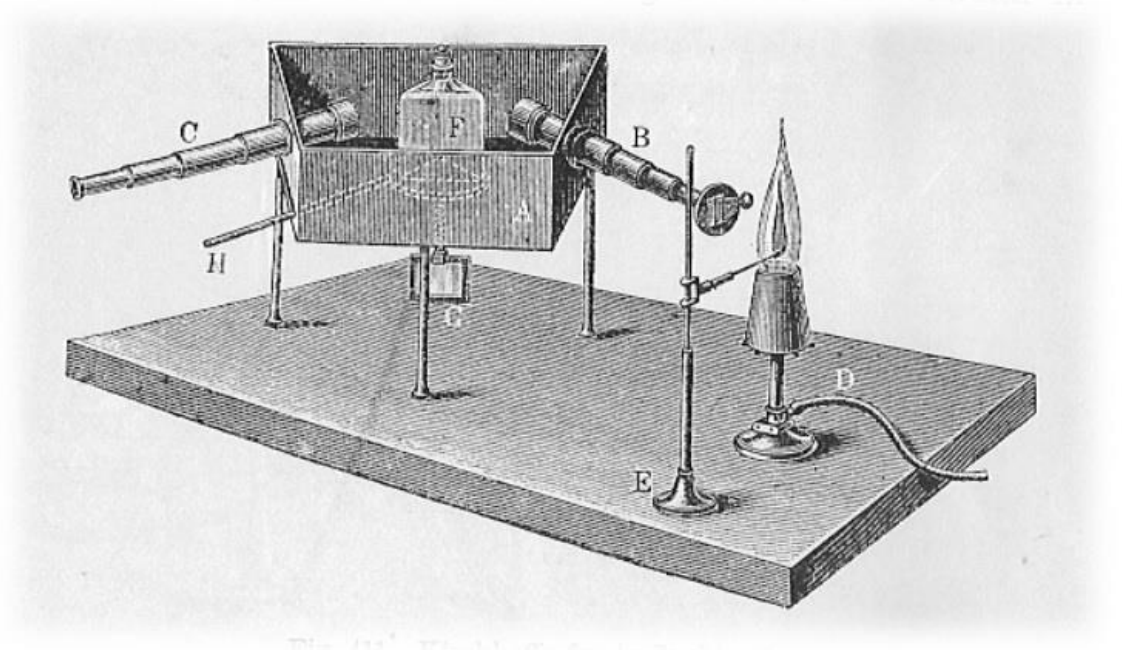

Figure 2.4: Kirchhoff and Bunsen's first spectrascope (Kirchhoff and Bunsen, 1860).

As the procedure was systematic and reliably repeatable, it enabled the linkage of individually unique spectral patterns to be connected to their elements. In effect they had developed a new technique that became known as analytical spectrometry (Kirchhoff and Bunsen, 1860). With this new technique they were able to discover new chemical elements, rubidium and caesium, that were previously unknown. One of their further discoveries made with their spectrascope equipment setup was to carefully align a beam of sunlight with a Bunsen burner flame burning a sodium compound to determine that the emission spectra from the flame and the absorption spectra from the sunlight showed the same absorption and emissions lines. This provided an effective proof that sodium was present in the burner flame and in the outer atmosphere of the sun. Thus, the spectrascope was effectively utilised for RS of the absorption spectra of sunlight and comparing it to the emission spectra of a known reference material allowed confirmation of what elements were present in its make-up composition. This discovery firmly established the

use of RS spectroscopy in astronomy and in the future in an array of new applications to sense different compounds from near or afar.

2.4.2 Photographic (optical) and satellite RS

The early uses of RS spectrometry emerged when flight developed with the first aerial photographs of a French village being taken from a tethered balloon in 1858 (PAPA International, 2021). The concept of aerial photography quickly developed and with advances in photographic equipment became simpler and were able to be fitted to kites, pigeons and rockets successfully. Shortly after the evolution of powered flight, the aircraft mounted photography, actually a motion picture, was taken by Wilbur Wright in 1909 in Italy when demonstrating the potential of his company's Wright Flyer Model A to the Italian government (Wright and Wright, 1909). Aircraft photography later became a tool used by the various militaries in the First World War to take photos of the front-line trench systems. Initially in limited locations and later effectively covering the whole of the front lines every day. After the war ended, the experience developed during this time provided the foundation for systematic development of aerial photography during the 20th century for commercial and military purposes reaching a high point during the cold war with specifically designed aircraft platforms like the U2 and SR71 reconnaissance aircraft (Britannica, 2021; Lockheed Martin, 2021) being used to collect photographic and other sensitive information. In doing so, this pushed the development of various types of cameras, radar instruments and electronic monitoring equipment to become suited to high attitude use which could show fine details of the areas being monitored 70,000 to 85,000 feet (21,000 to 24,000 m) below. During the 1960s the space race between the USA and the Soviet Union resulted in satellites being developed that could be used for orbital reconnaissance. This involved the further development of RS technologies (i.e., active types such as radar or microwave emitters and receivers. Or passive types with optical photography, infrared photography or measurement spectrometers) and techniques being able to be function in orbits at heights anywhere between 200 km to 35,000 km above the surface of the earth (Shimoda, 2013). The first civilian/commercial applications for satellite RS began in the 1970s with Landsat-1 in 1972 (Simonetti et al., 2014). Since this time, the field of satellite RS has had many new developments such as new higher spatial resolution optical and radar systems, hyperspectral sensors and digital elevation models

being implemented. The power of these tools has allowed for previously unimaginable research tasks to be undertaken on a regional or global scale. Furthermore, it has allowed daily measurements to be taken which can for example provide weather data for countries and localised regions enabling populations to plan activities or work for the day ahead. These capabilities have all been made possible through the work undertaken developing the fields of spectroscopy, optics, photography and their later adaption to aerial applications.

2.4.3 Near field emissions development for RS

As digital computing technologies developed in the 1970s progressively reducing the size of computing hardware and its cost while increasing processing speeds and the memory storage capability of instrumentation. It became possible to imagine that these technologies that had been developed and applied to aerial and satellite RS could also be applied in more compact nearer field applications. With the implementation of the Clean Air Act in 1970 and the subsequent establishment of the USEPA, the demand for new tools and instrumentation to address and quantify the impact of atmospheric emissions became constant request from regulators and in turn a new focus for researchers. A number of USEPA funded research projects were established to look into the potential applications of this technique. Initially Ford Aeronutronic built a Gas Filter Correlation (GFC) CO monitor which was used in a series of these USEPA sponsored research tests between 1974 to 1977 to measure rapid microscale variations in CO concentration in different situations (Chaney, 1979a). The primary test utilised the GFC technology and compared it to measurements taken from Gas chromatography instruments in a regional air monitoring station in St, Louis (Chaney, 1979b). In addition to this a long path laser for was setup side by side with the GFC as well to measure the same ambient air samples for comparing CO concentrations. The outcome of the comparison showed the GFC instrument successfully produced the same measurement results as the other instruments over a period of 24 hours. After this study was successfully completed, the University of Michigan investigated further various applications using the GFC to evaluate the technique in stationary (indoor and outdoor), mobile and aerial platforms completing these studies showing the system was capable and reporting on them in 1979. The next significant step was in 1983 when a research project studied the capability of the GFC

instrument to be utilised as system for taking CO emissions measurements of passing vehicles with its IR light source reflected across a roadway (Chaney, 1983). This concept proved successful in identifying individual vehicles with excessively high CO emissions. It was suggested in the conclusion of the report that this application if further developed could prove to be a useful tool in the identification of high emitting vehicles as part of a non-invasive and cost-effective inspection and maintenance to reduce emissions.

2.5 RS of vehicle emissions

2.5.1 CO optical measurement development

Based on the successful research and testing of the GFC technique for CO measurement undertaken in the 1970s and early 1980s, the value of developing an application using this for vehicle emissions measurement had been identified. Utilising the foundations of spectrometry, optics and remote photograph combined with the knowledge gained from the USEPA research. Significant steps to refine and develop a dedicated CO measurement system were undertaken at the University of Denver (DU) in the mid to late 1980s by the later Professor Donald H. Stedman. With newer instrumentation and electronics available, the RS system they developed to measure CO was smaller, lighter weight and transportable than the earlier GFC system so it could potentially be operated at any selected testing location (Bishop et al., 1989). The system consisted of three main components, a light source, a detector and a computer system to which was used to determine the levels of CO and CO_2 emitted by a passing vehicle. The detector schematic of the system is shown in Figure 2.5.

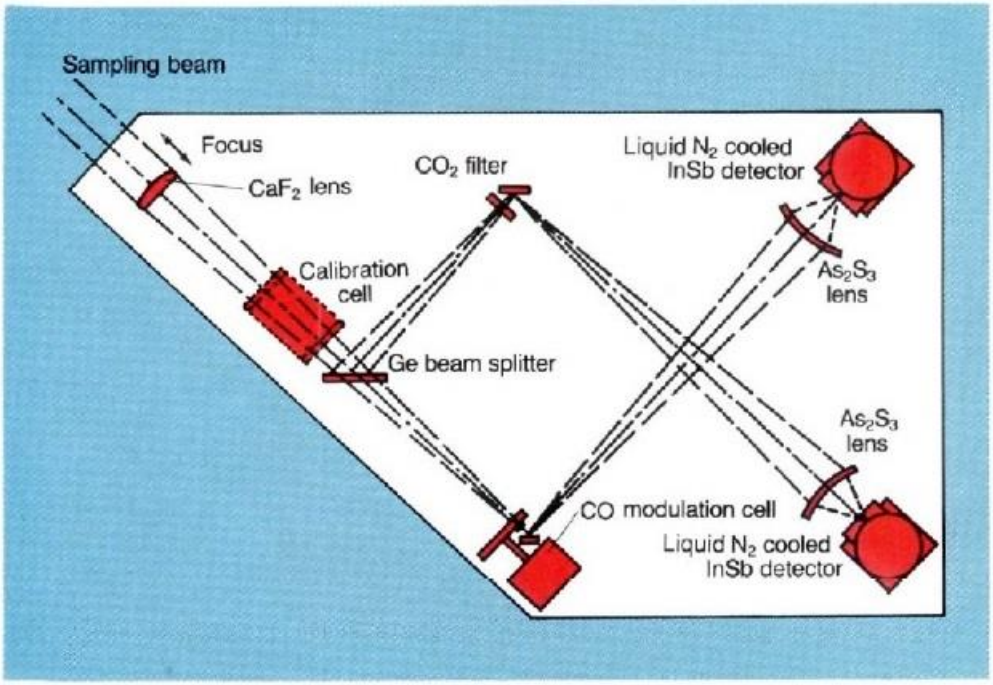

Figure 2.5: CO RS instrument detector schematic (Bishop et al., 1989).

The capability to measure CO_2 had been added to the instrument so it would be possible to provide an estimated emissions factor for an exhaust plume measurement. This had been absent from the earlier GFC instrument. The system was set up with an IR light source able to provide light with wavelengths of 4.3 μm and 4.6 μm wavelengths suitable for the identification of CO_2 and CO respectively. The light source was located on one side of roadway and the beam of light from it was focussed across the roadway at a height of 10 inches (25.4 cm) to the optics and detector. The detector splits the beams to a CO and CO_2 detector respectively. Rotating gas filter wheels for isolating CO an CO_2 wavelengths were fitted before the detectors (similar to those used in laboratory based NDIR instruments). This provided a reference channel and measurement channel signal from each of the detectors. The system was run through static testing with reference mixed gases, idle tests on vehicles, steady state driving speed tests and comparison tests with vehicles on chassis dynamometers. The data collected was utilised to develop calibration curves and a correlation curve for CO and CO_2 measurements. The DU RS instrument was also called the Fuel Efficiency Automobile Test or FEAT for short. This was due to it being able to find high CO emitters which could be tuned and /or repaired and achieve improved fuel economy result afterwards.

Further to this a two-week trial was run using FEAT collecting 20,725 vehicle measurements at a freeway onramp. Interestingly, this data showed 8.6% of the measured

vehicles accounted for half of the CO emissions. This trial showed the system capability for taking a large data set of measurements in a short amount of time was good. Whilst these first trials were promising, the system as tested did not have the capability to identify individual vehicles. This capability would be added as work continued on the FEAT RS system.

As the FEAT system continued its development, further functionality was added. To be able compare results from the system with emissions related data from other sources, a methodology to determine emissions factors from the measurements was developed. To ensure measuring accuracy of the RS instrument, an onsite instrument calibration check method was implemented with span gases and a video recording system to provide traceability of individual vehicles was integrated into the RS equipment (Stedman and Bishop, 1991). With this development the RS system now comprised of the IR source, detector system, computer for data processing and recording, calibration gases and a video recording system (Figure 2.6).

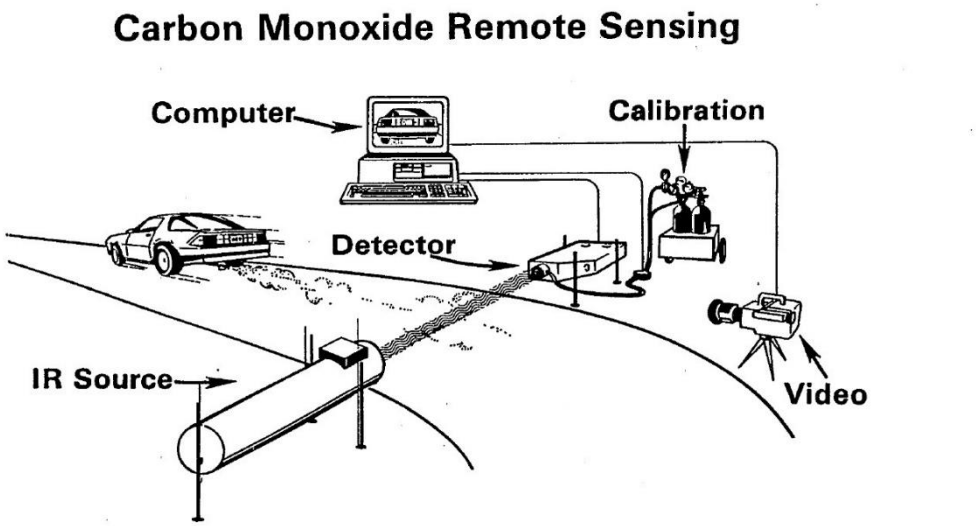

Figure 2.6: CO RS system schematic (Stedman and Bishop, 1991).

When a vehicle passes a RS system, it records the signals for CO and CO_2 then derives the CO/CO_2 ratio parameter which is called Q (note: this is a molar unit). Molar units are applied to simplify the chemical calculations. As Moles are identical to volume at constant temperature and pressure, therefore emissions percentage derived from Q are by volume. To compare Q to other emissions measurements a simplified by considering the

engine and catalyst system as one contained reaction. In this case the inputs are Fuel (CH_n) and Air and the output is the exhaust gas. The following combustion equation is derived.

$$CH_n + m(0.21O_2 + 0.79N_2) \rightarrow \frac{n}{2}(H_2O) + aCO + bCO_2 + 0.79mN_2 \qquad (2.26)$$

Figure 2.7 represents the combustion characteristics of fuel when burnt in a rich or lean mixture per the above combustion equation. When the mixture is rich the available oxygen is distributed to CO and CO_2 per the chart curves. If combustion is complete only H_2O and CO_2 are produced from the reaction. Further to this when the mixture is slightly lean and there are high combustion temperatures NO is produced during combustion (Popp et al., 1999).

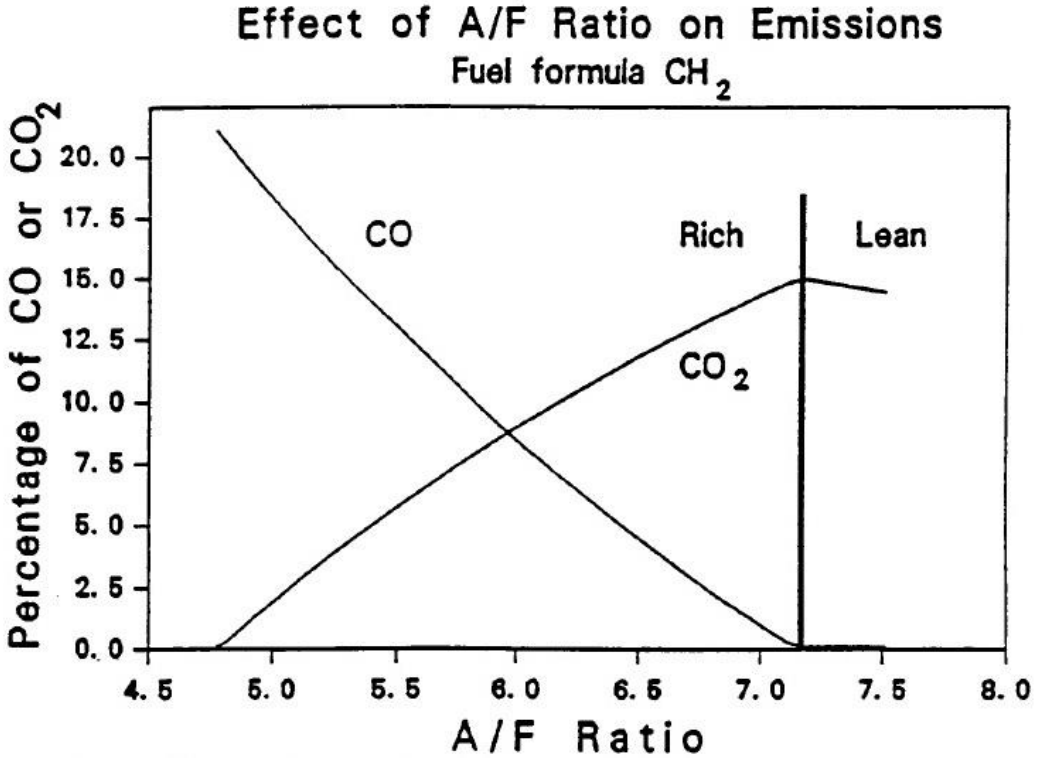

Figure 2.7: CH_2 combustion characteristics for CO and CO_2 (Stedman and Bishop, 1991)

The parameter Q is obtained when the efficiency of combustion deviates (rich or lean) from complete/stoichiometric combustion. In theory stoichiometric combustion would produce a Q value of 0 and not deliver a useable RS ratio result. In reality there are other known components in the exhaust such as unburnt HCs and oxides of nitrogen produced. Whilst they are important pollutants, in this first iteration of the RS system and with high

CO vehicle emissions during this time period, the considered effect of these gases did not have a major impact on the combustion equation for CO and CO_2.

To obtain concentration values for CO and CO_2 from the RS result, it is assumed that the air sample will be dry, undiluted and that all oxygen is consumed in the process. Whilst this is not exactly the case it allows for simple equations to be derived (Stedman and Bishop, 1991).

$$dry\ \%\ CO\ = \frac{42Q}{2.79+2Q} \tag{2.27}$$

$$dry\ \%\ CO_2\ = \frac{42}{2.79+2Q} \tag{2.28}$$

It will be noted that these calculations are based on a ratio of 1:2 for C/H. The C/H chemical nature of gasoline fuel is close to this, but not exactly this value. When analysis of all the saturated HCs contained within a sample is conducted that average value is determined to be 1:1.85 for C/H (Stedman and Bishop, 1991). It is possible to make corrections to the result, but the maximum potential error could be up to 8%. This does not significantly impact results when utilising RS to find high emitting vehicles.

With these concentration values it was also possible to determine the mass of CO emitted per gallon fuel. Using CO and CO_2 and solving the combustion equations the following approximate equation is determined when neglecting possible HC tailpipe emissions:

$$CO\ (gm)/gallon = \frac{5300Q}{1+Q} \tag{2.29}$$

In the research undertaken by DU they were able to determine a HC correction factor based on the correlation between measured tail pipe CO and HC. The resultant calculation equation is:

$$gmCO/gallon = \frac{5650Q}{1+1.08Q} \tag{2.30}$$

Whilst useful in the laboratory setting, applying the above equation to field RS measurements would involve accepting more assumptions for each measurement. To satisfactory address this in measurements would require the RS measurement of HC to become available.

Whilst DU first prepared and undertook this research, they were not alone in researching the capability of conducting CO measurement using RS techniques. General Motors

Research Laboratories also undertook development of a prototype CO and CO_2 RS measurement system in parallel (Stephens and Cadle, 1991). Their motivation was to further investigate CO emissions from vehicles under normal operating conditions so the information could be used to improve emissions modelling predications without the need to undertake time consuming emissions testing using the FTP-75 drive cycle to develop a larger database. When using the USEPA developed MOBILE4 emissions model, which was developed to predict fleet average emissions rates, some significant variations had been identified, such as roadside and tunnel studies measuring CO concentrations being a factor of two greater than those predicted by the MOBILE4 model. GMRL saw that the application of RS could deliver statistically a large sample of valid data which could be utilised for improving modelling. The concept of the GMRL designed system varied from the DU concept with separate detectors for each channel being measured. Figure 2.8 shows the GMRL RS equipment configuration.

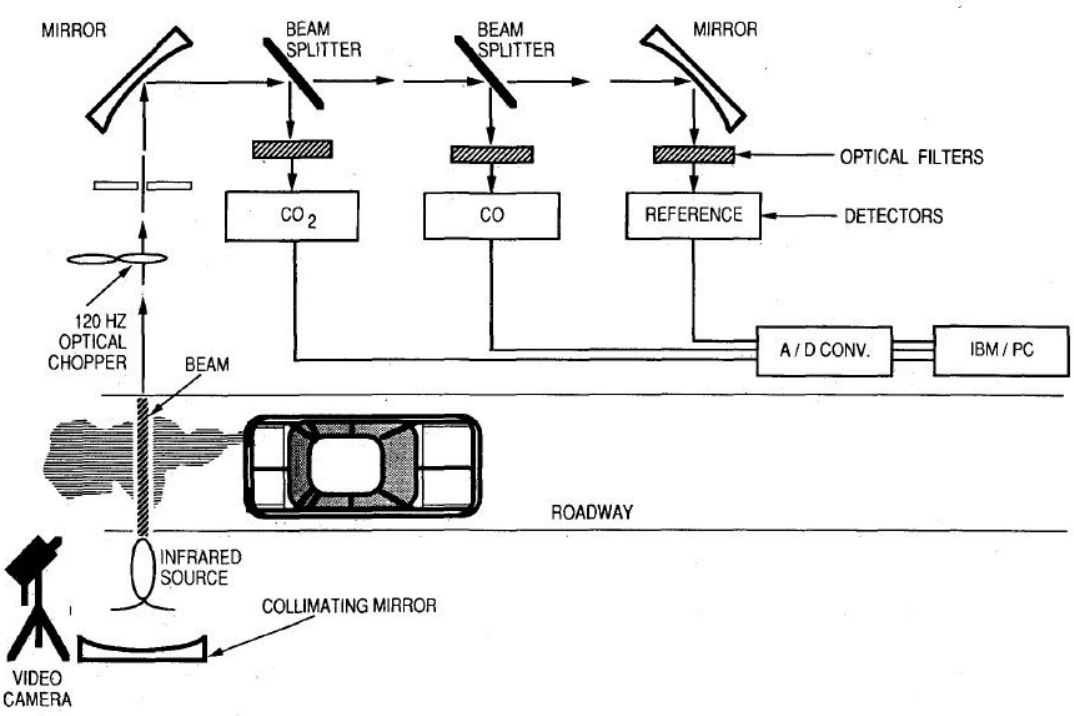

Figure 2.8: Concept of GMRL RS system configuration for CO measurement (Stephens and Cadle, 1991)

One perceived advantage GMRL claimed their instrument had was that each channel was able to take simultaneous measurements whereas the DU RS instrument had a spinning gas filter wheel which switched between the measurement channel and reference channel. Pending the rotational speed of the gas filter wheel the DU RS system could have a

noticeable delay between measurements. In January 1989 GMRL ran a comparison a week-long field test to compare their RS system and the DU RS system at the same arterial road exit ramp location in Denver Colorado. The comparison of CO/CO_2 ratio results showed a good agreement in measurements taken of the same vehicle. Each of these systems with their differences in measurement setup proved capable of providing comparable measurement results from the field study.

2.5.2 HC optical measurement development

Development of RS capability to measure HC followed shortly after the initial RS system developed by the DU for measuring CO had been implemented and was gaining exposure in field testing. Utilising the platform that had been developed for the CO/CO_2 system, the addition of a HC channel was implemented. The new HC channel also utilised a NDIR light source and a detector similar to the CO and CO_2 channels, but with a bandpass filter being applied to allow light with wavelengths of around 3.3 μm to be measured (Ashbaugh et al., 1992). This wavelength was selected as it is near to the setup that could be expected from a laboratory based NDIR system. This second-generation RS system was developed and tested with a variety of common HC compounds (including methane, propane, hexane and toluene) to assess its potential sensitivity. The testing proved feasible for measuring the physical concentrations of HCs in an exhaust plume even though their concentration could be factor of 10 or more lower than those measured for CO and CO_2. This new CO and HC instrument was constructed in a different manner compared to the original CO instrument. Instead of using lenses to focus the light, a 12 faceted polygon mirror spinning at 2400 Hz chops the light and across four focusing mirrors which then direct the light onto detectors. This allowed a sequential signal to be focussed on the detector for every measurement. Figure 2.9 shows the DU CO and HC analyser concept (Guenther et al., 1991).

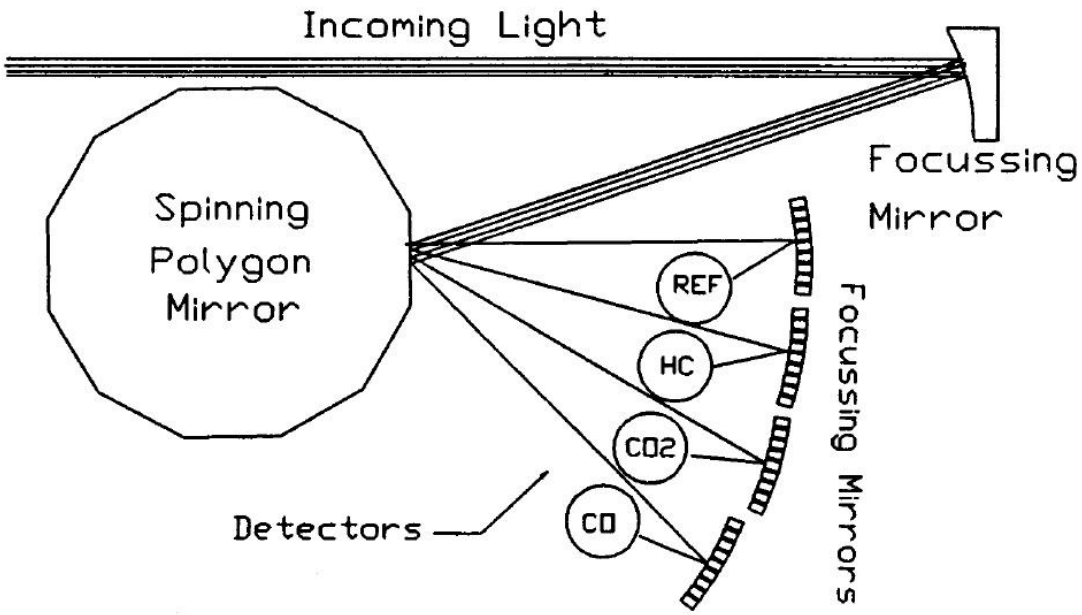

Figure 2.9: Concept of DU 2nd generation RS configuration for CO and HC measurement (Guenther et al., 1991).

A reading for each channel was produced from 24 signals being averaged from the detectors, then the background concentrations are subtracted and the signal is compared to the reference channel for any final correction. The data could then be utilised to determine ratios of CO/CO_2 and HC/CO_2. As before calibration of the instrument was performed with traceable reference gases. The CO measurement performance of this 2nd generation RS system was compared to the original and found to have very high correlation.

The new HC channel was noted to be subject to interference from water vapour at low emissions levels. As water vapour is often present in the exhaust plume an offset for its detection needed to be included in the calibration otherwise a zero measurement of HC would not be possible. Measurements determined that this interference could range up to 300 ppm. Once accounted for the noise levels for the HC channel were determined to be around 150 ppm HC using propane as the reference gas. From experimental measurements the majority of vehicles with nominally good emissions on-road at this time had levels of HC measurement in the range of 400-500 ppm when the emitted CO measurement was less than 1%. When on-road test data was collected and analysed those vehicles with high CO measurement above 4% had HC measurements in the range of 2700 ppm. Vehicle with CO measurements between 1% and 3% averaged HC

measurements around 1700 ppm. This data was able to be utilised to determine that half of the HC emissions were produced by 14% of the vehicles being measured, with HC emission being higher than 1000 ppm (Guenther et al., 1991). This showed that the HC measurement capabilities identified a similar percentage of high emitters as were identified from CO channel measurements. Combined the CO and HC channel measurements were able to complement each other to effectively identify high emitters.

GMRL also developed their RS system to include a HC measurement channel during this period. Comparison validation testing of the DU and GMLR RS systems was undertaken by CARB. A third system under development by Hughes Aircraft Company was assessed at the same time (utilising their satellite RS experience), but results were not published with the DU and GMRL data as the system was in the early stages of development. The testing undertaken compared 3 sets DU RS equipment against 1 set GMRL RS equipment. Using a test vehicle equipped with onboard emissions analysers and also with the capability to being able to adjust the air fuel ratio to deliver variable emissions. This provided a selected range of baseline data for comparison of the different RS systems. Both systems showed good correlation of CO results and HC compared well, but with more scatter than the CO results. The published accuracies of these systems were ±5% for CO and ±15% for HC. These reported outcomes provided a solid foundation for the broader acceptance and utilisation of the RS systems for pilot fleet measurement programmes during the 1990's.

2.5.3 NO optical measurement development

The integration of NO measurement into the DU RS followed the success of adding HC to the original CO and CO_2 RS measurement system. The measurement of NO required a new light source to be developed for the application. In vehicle emissions laboratory measurements of NO a chemiluminescence detector operates with a vacuum pump to measure the concentration of NO or NO_x. For RS this technique was not suitable as RS uses an absorption principle to determine the concentrations of pollutants, not chemiluminescence. It was therefore necessary to select the wavelength most suitable for NO absorption measurement. An Ultraviolet (UV) light source with a frequency of 227 nm was chosen as it avoided potential interference from water in the exhaust gases.

The new UV light source was integrated with the NDIR light source and would be setup across the road from the detectors. The detector unit was expanded to accommodate an additional detector for the NO channel. The beam was next reflected by a 12 sided mirror spinning at 12,000 rpm and then to a dichroic mirror which reflected the UV light and allowed the IR light to pass through and reach the NDIR detectors (Zhang et al., 1996a). Figure 2.10 shows the DU RS system with NO measurement concept added.

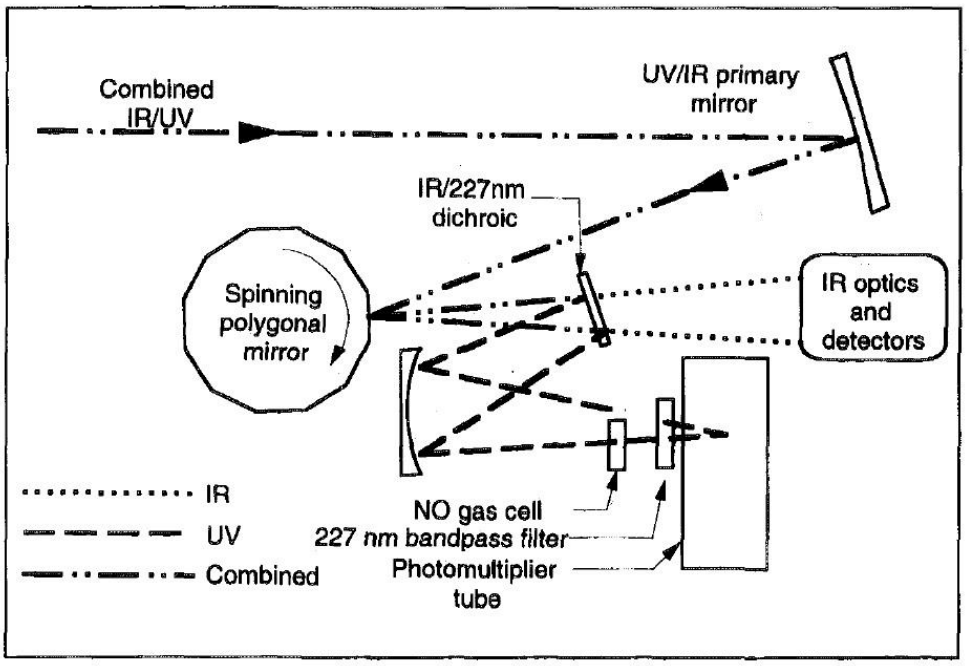

Figure 2.10: Concept of DU 3rd generation RS configuration for CO, HC and NO measurement (Zhang et al., 1996b)

The development and integration of measurement capabilities for CO, CO_2, HC and NO brought remote sensing to point where it could monitor each of the target pollutant gases proscribed under pollution control regulations. These and further major measurement developments of RS are shown in Table 2.8 tracking developments over time.

Table 2.8: Timeline of major RS testing developments

Year	RS Development
1989	CO & CO_2 measurement
1991	HC measurement
1996	NO measurement
1996/97	Feasibility RS Particulate measurement/On-road Opacity measurement
1999	High Speed UV spectrometer for NO measurement
2002	Opacity measurement enhancement for on-road RS
2004	Tuneable Near IR laser diode spectrometer
2004	PM measurement
2006	NO_2, SO_2, NH_3 measurement detectors
2014, 2017	EDAR/Differential Absorption LIDAR system developed and trialled

2.5.4 Further RS developments, inventories and research outcomes

Between 1989 and 1996 the foundations of the RS system for measurement of CO, CO_2, HC & NO gases were established with numerous field measurement projects undertaken to collect RS data in the US and in selected cities globally which laid the groundwork for future uptake of the methodology for widespread inventory purposes.

Further improvements for the NO channel were developed, tested and published in 1999. In the initial version of the RS system with NO measurement incorporated, the IR and UV detectors were arranged in the same assembly as shown in Figure 2.10. For the new system developed by DU (Popp et al., 1999) the IR and UV detectors were separated, then a beam splitter was utilised to provide a separate beam which was then routed and filtered through optic fibres before being transmitted to the UV receiver in an adjacent detector next to the IR system. This separation of the system for NO showed reduced noise levels delivering 10% lower average measurement values of NO and enabled confirmation of previously suspected HC interference on the NO measurement (which could now be quantified and accounted for) which effected the results taken by the earlier system. It was reported for measurements in controlled conditions, the new system had a detection limit of 54-24 ppm for NO pending the measurement conditions. Even though this technique was established, it appears to been limited in its use as the sensitivity of measurements on-road tended to have higher measurement detection limits.

In addition to the establishment of the RS measurement capability for the target emissions gases (CO, CO_2, HC & NO). Research investigating the feasibility of measuring opacity was undertaken at the University of Minnesota and reported in 1996 (Chen et al., 1996). The study results showed positive correlations with existing conventional measurement techniques and provided suggestions for on-road application. Development was also undertaken by DU to integrate PM measurement/opacity measurement into their RS system. They reported their measurements taken of on-road RS opacity from gasoline and diesel vehicles in 1997, (Stedman et al., 1997). This data reflected the patterns from IM240 chassis dynamometer testing results that diesel vehicles produced higher opacity emissions results when compared to those from gasoline vehicles. Although the magnitude of opacity measured by RS was twice that compared to the IM240 dynamometer testing.

Further development work on opacity measurement was reported in 2002 also by DU. Their initial development utilising an IR light source technique was found to have problems with IR extinction at the 3.9 μm wavelength being utilised and it was also determined that the particles being measured had no strong spectral features or tendency to scatter the IR light. Further to this, plumes with oil smoke from gasoline vehicles had trouble being detected at the source wavelength while opaque smoky plumes from diesel vehicles could lead to invalid measurements due to significant reductions in the source signal strength. These factors could lead to results with higher measured opacity values as noted earlier. To address these factors, a He/Ne visible laser was utilised to improve measurement capability (Stedman and Bishop, 2002). The inclusion of a laser in the application proved challenging as the fitment and combination of light and laser paths, reflector locations, beam splitters and focal points led to instances where sometime noise became a significant factor in the measurement. A solution for the application utilised the above-mentioned items along with three different laser light wavelengths combined with significant post processing software. The reported measurement results delivered a ±20% variation between the new laser technique and existing opacity measurement techniques. This result is an acceptable outcome considering all of the application variables and restrictions due to installation setup. With processing of the data PM measurement was able analysed pending the combination of results from each measurement channel as to whether an RS measurement should be considered excessively smoky or not. DU

considered this solution acceptable for integration into future RS measurement equipment.

Another PM measurement system was also developed beginning in 1999 by the Desert Research Institute in Reno, Nevada, USA. This was called Vehicle Emission Remote Sensing System, VERSS-PM, which utilised ultraviolet backscatter light detection and ranging (Lidar). The methodology it operated on was based on path-integrated particle backscatter and extinction measured fuel-based PM EFs (Mazzoleni et al., 2010; Mazzoleni et al., 2004). This PM system used a pulsed Nd:YAG laser as its light source. As described the VERSS PM uses a principle of operation similar to the DU RS visible laser system.

In 2004, work on the utilisation of near infrared tuneable diode lasers for RS measurement that had been conducted in the UK was published (Barrass et al., 2004). This application of a laser-based IR light source for use with testing looked to address some challenges experienced with RS systems existing at the time. The length of the measurement path had been limited to around 8 m which in effect restricted the measurement sites which could be selected for RS measurement. It was also desired to attempt to enhance the detection sensitivity as well. The gases of interest for measurement were CO and CO_2. Trials were conducted in laboratory conditions and in the field to evaluate this new RS system. The system showed potential as a compact unit having a relatively low cost and being tuneable for selective gas detection over long path lengths when compared to the existing type of systems. It also had the potential to measure different gas species such as NO, CH_4 and NH_3 and potentially Benzene, but was limited to preliminary tests and laboratory simulations.

Trials undertaken with this CO/CO_2 measurement system were successful, but it was determined that measurement sensitivity for the latest/cleanest vehicle models was an issue as the system was found to be insufficient to provide readings for low emitting vehicles. The application of laser-based IR light source provided successful trial results, but it also required further development to be to incorporate HC and NO measurements before it could be applied broadly for RS on-road measurements.

The next developments to broaden the measurement capabilities of RS were to measure NO_2, SO_2 and NH_3 pollutant gases. These gases were of interest as they are emissions precursor gases of secondary aerosols (Liu et al., 2019). DU undertook their development

and published their results in 2006 (Burgard et al., 2006b). Utilising their existing system which at this point consisted of an IR and UV source and a receiver to collect signal and split the IR and UV sources into separate analysers for measurement. To incorporate these additional molecular species in the measurement system required another separate UV spectrometer. Based upon the original UV spectrometer the measurement range needed to be expanded from the NO range at 227 nm down to 200 nm to be able to include SO2 and NH_3. Each of these gases produce their own unique emissions spectra, which in parts overlap. This required significant improvements which were made to the hardware to optimise the light sources, beam splitter, mirror utilised in the system for their target frequencies. Laboratory testing undertaken was able to verify performance of the new spectrometer and it was found to capably be able measure these gases from vehicles driving by at levels which would allow the determination of whether vehicles are potential high emitters or not. The DU FEAT RS system now had a range of measurement capabilities for CO, CO_2, HC, NO, PM/Opacity, NO_2, SO_2 and NH_3. This was the broadest range of gases measured by any RS system available at this time.

RS systems from this time forward remained similar to those described here with a range of manufacturers delivering systems for collecting emissions inventory data in regions with ambitious AQO's requiring significant vehicle fleet emissions data either for policy development or for targeting vehicles to improve their performance and reduce emissions.

In 2017, an evaluation paper was published outlining blind study results of an alternative measurement product that had been developed for RS. This product developed by Hager Environmental & Atmospheric Technologies (HEAT LLC) was called Emissions Detection And Reporting system, EDAR for short (Ropkins et al., 2017). There were a number of major innovations in this RS system the first being that the instrument utilised laser based differential spectrometry Light Detection and Ranging (LIDAR) instead of an IR or UV light source. Furthermore, the measurement is conducted with the equipment installed in a vertical orientation with the laser source being located above the road on a gantry pointed at a reflecting strip on the road to send the signals back to the detector located within the same unit as the source. See Figure 2.11 for details of EDAR concept setup. This system had been developed and utilised for data collections and studies various states in the US since 2014 and in a number of European countries since 2016 (Ghaffarpasand et al., 2020; Hager, 2021). It is based on the NASA Activity Sensing of CO_2 Emissions Nights, Days and Seasons (ASCENDS) satellite program (Abshire et al.,

2010). The system utilises an infrared laser which can be tuned for measuring conventional RS target gases and also individual HCs, NO_2 and PM. The first part of the reported trial comparison determined that measurements from EDAR for dry sample gases being emitted at regulated pressure from gas bottles i.e., NO, CO and CH_4 were all representative of in use vehicle emissions with detection limits of 50 to 100 ppm, 10 to30 ppm and 15 to 35 ppmC, respectively. The analysis of data indicated there was good linearity, low bias and speed dependence plus low measurement drift over a wide significant range of gas concentrations and subject vehicle speeds. The main consideration for these case study results was they were highly standardised as they released bottled reference gases at a fixed rate. The second part utilised real-world vehicle emissions measured by EDAR, PEMS and a Sniffer vehicle. These results showed reasonable correlation between EDAR, PEMS and the Sniffer vehicle, but for more reactive gases such as NO_2, which is subject to significant secondary chemistry, the comparisons showed non-linear characteristics due in part to atmospheric gas reactions, diffusion rates, the equipment sampling/measurement points and varying measurement speeds. From the assessment, real-world conditions indicate EDAR test performance results whilst good, diminish when compared to those obtained using simulated exhaust gases. This is not unexpected, and also reflects some of the varying aspects of the nature of RS measurement which is also experienced by other systems. The EDAR system shows satisfactory measurement performance for RS applications, but will benefit from more studies being conducted into its use to more fully realise its potential for RS applications.

With progressive development of RS systems with features and innovations mentioned here, there has been significant number of emissions inventory projects being conducted since the early 1990s continuing to the present day. The first effective RS measurement systems were developed and produced by DU in the 1990s and with these they worked to introduce RS measurement in the US and then around the world. DU conducted measurement trials with RS in the US in Denver (Bishop et al., 1992; Stedman and Bishop, 1989; Stephens and Cadle, 1991; Zhang et al., 1993), Los Angeles (Ashbaugh et al., 1992; Stedman et al., 1991a), Chicago (Stedman et al., 1991b). This was combined with studies abroad in Toronto (Peterson et al., 1991), Mexico (Beaton et al., 1992), Thessaloniki, Greece (Nikolao and Stedman, 1993), and culminating with a report on all the worldwide studies undertaken in 1995 (Zhang et al., 1995).

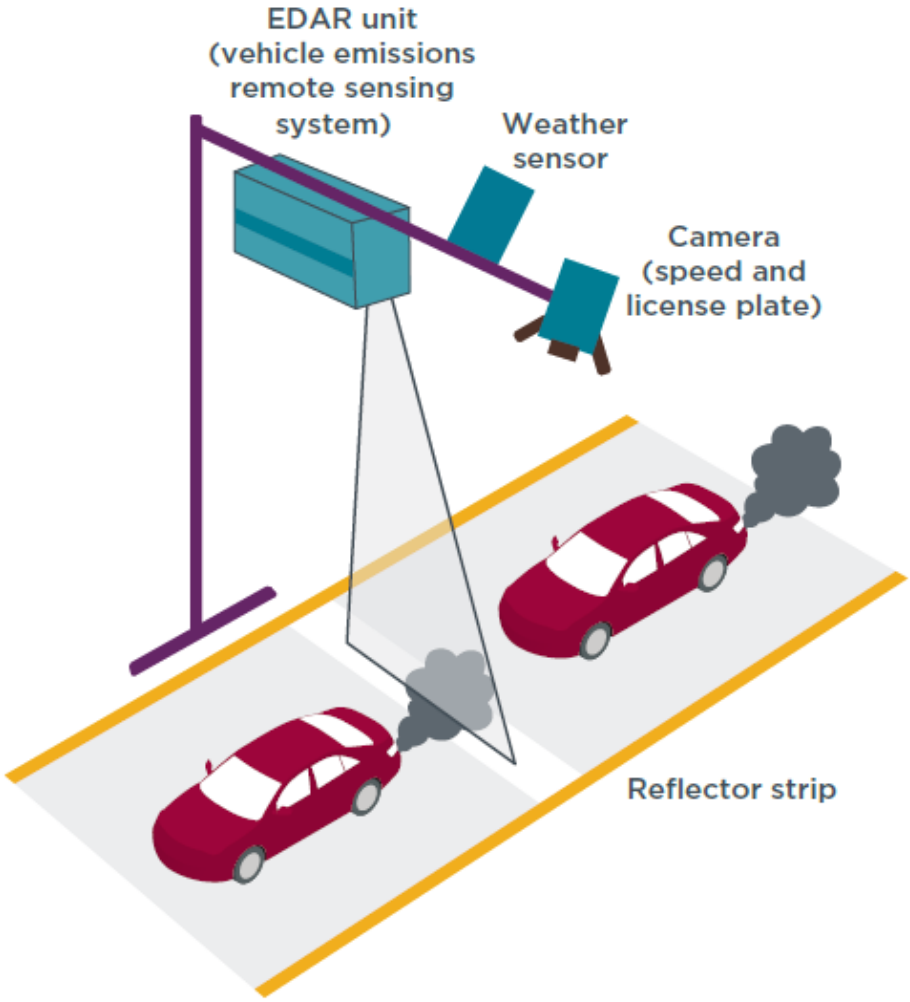

Figure 2.11: Concept of EDAR measurement configuration (Dallmann, 2018).

This work established RS as a reliable tool for collecting emissions inventory data for local vehicle fleet which could be used to check against other emissions inventory tools.

During this period other RS systems were developed in parallel to the DU FEAT system and a commercial product was produced in collaboration with DU and a company called Environmental Systems and Products Inc. These unit were marketed starting with the Accuscan RSD1000, followed by a series of upgrades, RSD-2000, RSD-3000, RSD-4000, (Vescio, 2019) incorporating new developments as they were proven by DUs research and development. These systems were sold and utilised in various regions and cities to measure and study local vehicle inventory conditions.

Studies continued to be published outlining the EFs and their implications for vehicle I/M programmes in different locations such as the UK (Sadler et al., 1996), Hong Kong (Chan and Ning, 2005; Chan et al., 2004; Ning and Chan, 2007), New Zealand (Xie et al., 2005),

China (Guo et al., 2007; Zhou et al., 2007). It was also applied to measurements beyond cars and trucks to snowmobiles, trains, aircraft and ships (Breuer and Burgard, 2019; Burgard et al., 2006a; Burgard and Bria, 2016; Burgard et al., 2011). There have been many more applications of RS to establish emissions inventories and determine EFs for vehicle fleets so the magnitude of local fleet issues can be determined up to the present day which have not been listed here to avoid unnecessary duplication of information.

Beyond building up emissions inventories, RS utilisation provided a mechanism for identifying and /or confirming the presence of other vehicle emissions related air pollution issues. A item of significant interest was the identification from inventory data of the trend of NOx emissions continuing to remain the same or increase from diesel vehicles in contrast to reducing regulation targets of the Euro 1 through 5 Regulations (Beevers et al., 2012; Carslaw et al., 2011; Carslaw and Rhys-Tyler, 2013; Chen and Borken-Kleefeld, 2014; Huang et al., 2018c). It has been able to provide confirmation of actual emissions system deterioration rates (Borken-Kleefeld and Chen, 2015), RDE profiles of vehicle fleets (Bernard et al., 2018; Pujadas et al., 2017). It has been utilised to propose suggested RS emissions measurement cut points for selecting high emitting diesel vehicles (Huang et al., 2019b) and also had proposed methods for conversion of its emission factors to g/km results for comparison to regulatory emissions targets (Bernard et al., 2018).

Further to the above in the US there are RS monitoring systems being utilised that identify vehicles as part of I/M rapid screening programmes in some states. For vehicles screened they have their emissions performance identified and are rated from a low to a high emitter. Clean vehicles with low emissions can then skip their next scheduled I/M emissions check. Vehicles identified as being high emitters must undergo testing and pass (Vescio, 2019).

The first emissions enforcement control programme to use RS to exclusively identify high emitting gasoline or LPG vehicles was established in Hong Kong and began in September 2014 (Hong Kong Government, 2014; Huang et al., 2018a; Organ et al., 2018). Under this emissions control programme, the HKEPD deployed mobile RS systems at roadsides to step up monitoring of excessive emissions from gasoline and LPG vehicles. Owners of vehicles found to have excessive emissions were notified by an emission testing notice (ETN) issued by the HKEPD. Their vehicles are then required to pass a dynamometer-based emission test (HKTET) at a designated vehicle emission testing centre within 12

working days to ensure the problem is rectified otherwise the vehicle cannot remain licensed and on-road.

Whilst this programme is effective, it is also limited by the fact that it is not including diesel-fuelled vehicles as part of the enforcement programme. It has been noted previously that diesel vehicles are major high emitters of NO_x and PM which are high contributors to daily air quality issues in many major cities and urban areas (Chen and Borken-Kleefeld, 2014; Landrigan et al., 2018; Saari et al., 2016; World Health Organisation, 2018; Zhang et al., 1996b). The nature of diesel combustion (The diesel cycle) which is a lean combustion process with variable CO_2 concentrations, unlike gasoline combustion (the Otto cycle) which maintains relatively constant CO_2 concentrations (by using a target AFR of 14.7) (SAE, 2015). This diesel combustion variability leads to the potential situation with RS of false positive/high emitter identification or false negative/low emitter identification (Huang et al., 2019b).

This is an area in which further investigation of the methodologies and techniques of RS measurement are needed to identify opportunities for technical development and areas in which improvement of the RS process is possible to enable inclusive identification of high emitters for emissions reduction enforcement programmes for all on-road vehicles fitted with internal combustion engines.

The literature highlights that RS is an effective tool for inventory monitoring purposes with results producing fleet analysis covering many types of vehicles and allowing for characterisation of EFs to quantify the emissions contributions being made by different segments of the vehicle population. Within the literature there are no reports available outlining the effectiveness of the emissions enforcement programmes and if they can make significant improvements in a short period of time. The programme established by the HKEPD in Hong Kong is a suitable candidate for this analysis and it is proposed to evaluate the effectiveness of the programme to determine its value and capability in reducing vehicle emissions and maintaining an improved on-road vehicle fleet emissions profile with lower EFs. As the first of its type of programme directly using RS to identify individual high emitters for enforcement actions, it is desirable to study its aspects for developing technical improvements to enhance RS measurement.

Furthermore, emissions inventory information suggests that the highest emissions are generated by the top 10 to 20% of vehicles on-road (Beaton et al., 1995; McClintock,

2007; Pujadas et al., 2017). This suggests a number of possibilities; there is a small potential of some faults occurring during vehicle production which impact emissions, perhaps they are either not being maintained or have been maintained but not effectively to minimise emissions or emissions control systems may have been tampered with to gain some perceived performance improvement at the cost of reducing or eliminating emissions control. Up until the introduction of the HKEPD RS emissions enforcement project there were limited studies that report on the effect of hardware failures in emissions control systems and their potential impacts (Chiang et al., 2008; Toma et al., 2019). Without comprehensive data outlining a broad range of regularly occurring faults in a vehicle with an emissions control system, the magnitude of emissions deterioration resulting from the fault could lead to incorrect maintenance choices being made and in turn having little or no benefit for air quality. This is a knowledge gap that needs to be addressed and can provide significant benefits to the repair industry and in turn air quality. Simulation of emissions faults and measuring the emissions impacts will provide much needed information currently unavailable on areas needing attention and repairs to return vehicles to their optimum performance condition.

Being able to assess and analyse RS data from the HKEPD emissions enforcement programme will show how it is performing and assist HKEPD and other environmental agencies to be well informed to develop effective policies and likewise it will help mechanics to gain knowledge on technical areas to target for potential improvements in repairing vehicles that is not at the expense of emissions.

Chapter Three

3. Methodology

The methodologies utilised in each of the research chapters cover the following three areas: Firstly, assessment of a large RS programme data set was conducted for identification of significant factors, performing statistical analysis followed by preparation and filtering of results in analytical formats.

Secondly, as identified from the literature review there is very little emissions repair study information available to help identify emissions failures. Described here is the undertaking of the investigation of vehicle engine and emissions systems failures to identify emissions magnitudes and fault mechanisms identified from industry input. This has been accomplished by developing a unique simulation vehicle able to quickly reproduce either good or a range of faulty characteristics for the purpose of quantifying emissions deterioration.

Finally, the assessment of the RS data indicated the need to investigate areas where RS testing could be improved. Development of RS testing and calibration devices with HKEPD has utilised emissions laboratory and data acquisition systems to collect data for characterising RS emissions measurements to improve calibration performance and identification of the area of the exhaust gas plume temperature effect on RS for possible development of improved measurement. This improved characterisation reviewed the influence of the exhaust plume temperature cooling with the potential response of exhaust gas absorbance response focussed on CO_2 in particular for this purpose. In the field, the exhaust gas plume temperature is dependent on the vehicle size, loading, how it is being driven and the RS field location. This results in a significant range of potential high gas temperatures at the exhaust pipe exit which if not accounted for creates greater uncertainty of measurements and potentially a false result. By studying the temperature characteristics of the exhaust plume in a laboratory, control over variables otherwise not possible in the field can be achieved. With the data collected and assessed, the results will provide improved understanding of temperature impacts from field measurements.

The vehicle emissions measurement technologies utilised range from high grade Inspection and Maintenance equipment to certification laboratory systems and PEMS. Each of these tools have been utilised where needed and coupled with experimental designs to assess conventional emissions and RS data to deliver improved information for each of the related aspect of RS development.

3.1 Remote sensing

3.1.1 Data collection

RS survey data has been collected using the dual RS techniques developed and employed by the HKEPD across 148 measurement sites (Figure 3.2) in the Hong Kong Special Administrative Region. The measurement sites encompass significant areas where heavy traffic conditions prevail and there are a sufficient number of passing vehicles available for measurement. The equipment used consists of 14 different units of the ETC-S420 RS system. Figure 3.1 shows an example of the remote sensing unit typically used.

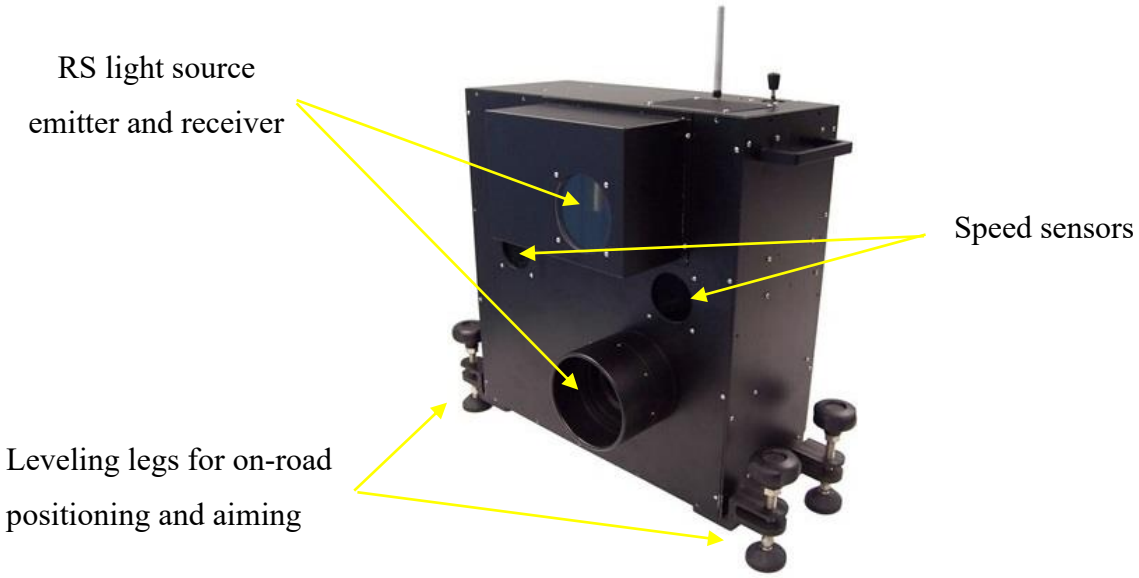

Figure 3.1: The ETC-S420 RS system.

It utilises specialised light sources to detect specific types of emissions gases. Non-dispersive infrared is used for detecting HC, CO and CO_2, whilst ultraviolet is used for NO detection. The RS equipment is set up with the unit containing all light sources on one side of the road. The light beams are directed across the road to a retro reflector which

reflects them back to the detectors in the RS unit. Figure 3.3 shows the setup of a typical RS measurement site. A measurement begins when a vehicle passes into the first light beam for speed and acceleration measurement. When the speed measurement system detects the vehicle has passed the RS unit the emissions gases are then recorded and photo of the vehicle license plate is taken. The vehicle emissions are recorded for approximately 0.5 s. The emissions data, speed, acceleration and license plate number are recorded in a database which is subsequently transmitted to the HKEPD survey database for assessment. For verification purposes vehicle data is made available to HKEPD from the Transport Department so that vehicle class, make, model, year of manufacture, engine size and fuel type are available to correctly identify the vehicle emissions limits that need to be applied per the appropriate UNECE emission regulations (Table 3.1).

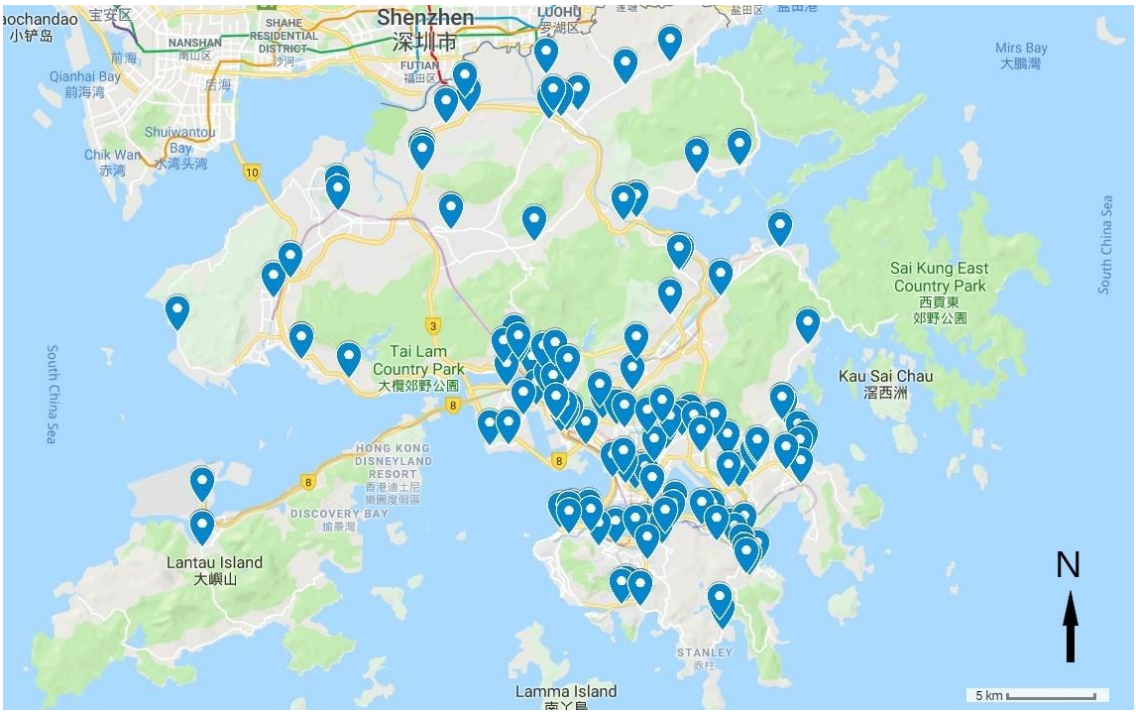

Figure 3.2: The locations of RS measurement sites in Hong Kong.

Table 3.1: European emissions standards and durability requirements.

	Euro 1	Euro 2	Euro 3	Euro 4	Euro 5b
THC (g/km)	-	-	0.200	0.100	0.100
NMHC (g/km)	-	-	-	-	0.068
NO (g/km)	-	-	0.150	0.080	0.060
HC+NO (g/km)	0.970	0.500	-	-	-
CO (g/km)	2.720	2.200	2.300	1.000	1.000
PM (mg/km)	-	-	-	-	4.5
Hong Kong implementation dates					
Gasoline	01/04/1995	01/04/1997	01/01/2001	01/01/2006	01/06/2012
LPG	-	01/08/2001	01/08/2001/	01/01/2006	01/06/2012
Durability requirements for maintaining emissions compliance					
Durability (km)	80,000	80,000	80,000	100,000	160,000

The selection of RS measurement site is determined by the HKEPD pending the vehicle makeup at each site and evaluation of the air quality. On any day up to 100 sites may be considered for selection. No prior notification to the public is made of daily RS measurement site section. The RS measurement sites have a 5-m wide single lane of traffic with a slight uphill gradient (2 to 5°), so vehicles are under load whilst driving. They are ideally located away from traffic lights or intersections to avoid off cycle emissions from hard acceleration or deceleration. Traffic volumes are significant, free flowing and the range of vehicle speeds for assessment need to be between 7 to 90 km/h for repeatability (Huang et al., 2018a). The site needs to allow for sufficient space to lay out the RS equipment including batteries, cameras and cabling. Staff and the support vehicle must also be safely stationed whilst undertaking the measurements. The two RS systems are to be setup so there is approximately one second travel distance between them. This distance between the units can range from 3 to 20 m pending on the average vehicle speeds for each individual site. The data from the 2nd RS unit is utilised to confirm the validity and repeatability of the measurement. This is necessary for quality assurance if the survey data is to be used for issuing an ETN to the vehicle owner. Equipment calibration for each RS unit is checked to be satisfactory onsite with a puff of High Range BAR-97 with NO span gas (3200 ppm HC, 8.0% CO, 12.0% CO_2 and 3000 ppm NO). After each hour of RS measurement, the system implements automated QA/QC testing to check if the data quality for the site is within the expected measurement ranges. The

QA/QC reference has been determined previously from thousands of RS measurements. If the data deviates beyond a specified tolerance for the site, the previous hour of data is considered unusable for enforcement purposes and the system must be checked and recalibrated before further measurement. Stable weather conditions are also desirable for consistency and quality of measurements. Temperature conditions in Hong Kong are relatively aseasonal with the difference in daily average high and low temperatures ranges being around 5°C (Hong Kong Observatory, 2019a). This stable temperature range combined with relatively low average wind speeds (Hong Kong Observatory, 2019b) allows for year round utilisation of the RS systems. The RS survey measurements are halted when there is either heavy rainfall or typhoon weather signals are raised. Measurements are conducted for a shift typically between 9:00am and 4:00pm. The measurements are taken at the site throughout the day, but the data during peak periods may not be used if the speed validity is poor (i.e., heavy traffic conditions). Since every site has different characteristics the number of RS measurements taken at each site varies as well. Information relating to the variations of number of measurements and make of vehicles at each site is included in Table A1.

Figure 3.3: Setup of a typical RS measurement site in Hong Kong, China.

3.1.2 Data analysis

Assessment of the RS data starts with the application of the methodology that was developed by the DU (Bishop et al., 1989; Bishop and Stedman, 2014; Burgard et al., 2006a; Huang et al., 2018b) to assess turbulent exhaust gas plumes. In every measurement the magnitude or volume of gas that will be measured varies. This combined with measurement uncertainties which are about ±15% (Huang et al., 2018c), requires some consideration on how to optimise the measurements. To mitigate this variability, the measured gas concentrations are used to determine ratios of individual pollutant gases in respect to the major exhaust gases in the plume i.e., CO_2. The resultant ratios of HC/CO_2, CO/CO_2 and NO/CO_2 are determined, which can be used to calculate the vehicle emissions factors (EFs, grams of pollutant/kg of fuel, with fuel type being identified from vehicle licensing records) and possibly identify a vehicle as a high emitter.

Using the principle of carbon balance, EFs can be calculated for each of the target pollutant gases using the method of Bishop and Stedman (1996, 2014) and Burgard et al. (2006). The emissions ratio of pollutant P relative to total carbon emitted C is given by.

$$\frac{moles\ P}{moles\ C} = \frac{P}{CO_2+CO+3HC} = \frac{Q_P}{1+Q_{CO}+3\times2\times Q_{HC}} \tag{3.1}$$

The EFs are calculated utilising equations (3.2-3.4) (Bishop and Stedman, 1996; Bishop and Stedman, 2014; Burgard et al., 2006a; Pokharel et al., 2001) where Q_P (P= pollutant) is the emission volume ratio of the target gas divided by CO_2:

$$EF_{HC} = \frac{2{\cdot}44}{0.014} \cdot \frac{Q_{HC}}{1+Q_{CO}+6Q_{HC}} \left[g/kg_{fuel}\right] \tag{3.2}$$

$$EF_{CO} = \frac{28}{0.014} \cdot \frac{Q_{CO}}{1+Q_{CO}+6Q_{HC}} \left[g/kg_{fuel}\right] \tag{3.3}$$

$$EF_{NO} = \frac{30}{0.014} \cdot \frac{Q_{NO}}{1+Q_{CO}+6Q_{HC}} \left[g/kg_{fuel}\right] \tag{3.4}$$

Prior to undertaking EF calculations, the RS survey data collected needs to be assessed for validity before it can be used for purposes such as general air quality impact assessments or identification of individual high emitting vehicles for the purpose of issuing ETNs. The following criteria (Huang et al., 2018c) have been utilised to filter and select data for analysis:

- Speed range between 7 to 90 km/h
- Acceleration range between -5.0 to 3.0 km/h/s
- Sufficient gas plume for measurement

The amount of CO_2 present in the measurement must be checked to ensure that a sufficient gas plume is available to determine quantitative emissions ratios of target gases to CO_2 (Borken-Kleefeld and Dallmann, 2018; Carslaw et al., 2011). The vehicle speed is checked to be valid for each individual measurement and between the two RS units used for the measurement. Additionally, the speed and acceleration ranges to be analysed are selected to match the actual ranges within the Hong Kong Transient Emissions Test (HKTET) used at designated emissions testing centres for providing vehicle emissions compliance certificates (Commissioner for Transport, 2012).

Only valid RS measurement data has been used for this assessment. Applying the criteria above, there were 937,660 out of the 2,144,422 records deemed to be invalid. Once the data has been filtered and calculations are completed the resultant EF values for each measurement can be used to characterise the on-road vehicle fleet.

3.2 Fault simulation in an LPG taxi

The deterioration of vehicle hardware results in reduced mechanical performance. The deterioration of the fuel system, engine components and the emissions control hardware in spark ignition engines results in high emitting vehicles creating serious air quality and pollution issues. By identifying the most commonly occurring of these faults, studying them and setting up a vehicle in which each can be reproduced as required, valuable lessons can learnt on the sources and magnitude of these emissions. The starting point for this fault simulation study was to identify a vehicle that many automotive repairers were familiar with and one that could easily be worked on by many workshops in Hong Kong. This led to the selection of the Toyota Crown Comfort LPG taxi (Figure 3.4 (a)) as the vehicle of choice for the demonstration programme. It was the dominant vehicle (>95% of 18,163 licensed taxis) of the local taxi fleet and thus was a common extensively utilised vehicle accumulating high mileage and likely to have emissions control systems that deteriorated quickly thus contributing to serious air quality problems in Hong Kong. It also contained the target emissions control technologies gasoline and LPG vehicles had in common.

Testing for this study was conducted at the Jockey Club Heavy Vehicle Emissions Testing and Research Centre of the Institute of Vocational Education (IVE) in Hong Kong. The

test vehicle specification is shown in Table 3.2. The Toyota Crown Comfort taxi had a kerb or unladen weight of 1400 kg and for testing a reference weight of 1470 kg was used in line with UNECE Regulation 83 simulated inertia and dyno loading requirements. It was equipped with a 1.988 L naturally aspirated LPG fuelled 4-cylinder engine. The specified maximum power and torque ratings for the engine are 58kW @ 4400 rpm and 160 Nm @ 2400 rpm respectively. This vehicle was built to meet the requirements of Euro 2 emissions standard and which at the time of testing was representative of 2/3 of the LPG taxis on-road in Hong Kong when the HKEPD began their 'Strengthened emissions control of gasoline and LPG vehicles' programme to identify high emitting gasoline and LPG vehicles. The vehicle had a TWC, oxygen sensor and EGR valve installed in the exhaust after treatment system to reduce emissions and meet the required standard.

Table 3.2: Specification of the vehicle used in this study.

Vehicle make	Toyota
Vehicle model	Crown Comfort – YXS10RAESBN
Manufacturing year	2000
Engine model	3Y-PE
Working Principle	Spark Ignition
Type of fuel used	Liquefied Petroleum Gas
Number of cylinders	4
Layout of cylinders	In line formation, Front Mounted Longitudinally
Bore (mm)	86.0 mm
Stroke (mm)	86.0 mm
Swept volume (litre)	1.998 litre
Compression ratio	10.5:1
Rated maximum power output	58 kW @ 4400 rpm
Rated maximum torque output	160 Nm @ 2400 rpm
Exhaust aftertreatment	TWC and EGR

The testing was conducted utilising a Euro 5 compliant and certified emissions chassis dynamometer, specifically a 48-inch 150 HP Mustang (Model: MIM48-150) single roller chassis dynamometer and Signal Maxsys900 emissions measurement system with a constant volume sampler (CVS). The emissions system was used to measure the

concentrations of THC, NO_x, CO and CO_2. THC was measured using a flame ionisation detector (FID), NO_x was measured by a chemiluminescence analyser (CLA), and CO and CO_2 were measured by NDIR analysers. The accuracy specification of these analysers is shown in Table B1. Modal emissions measurements were recorded at 1 Hz and emissions factors in g/km were calculated for each test cycle using the method defined in the Regulation 83 of the Economic Commission for Europe of the United Nations (UNECE, 2015). The fuel consumption rate was calculated in l/100km using the method defined in Regulation 101 of the Economic Commission for Europe of the United Nations (UNECE, 2013). The test cycle used to assess each simulated failure condition is the Hong Kong Transient Emissions Test (HKTET) cycle (Commissioner for Transport, 2012; Huang et al., 2019b). This test cycle is based on the TÜV Rheinland TUV-A short drive cycle (Samaras and Kitsopanidis, 2001; Samaras et al., 2001) which has been selected by the HKEPD as suitable for a short hot start I/M transient emissions test. As shown in Figure 3.3 (b), the test cycle has a duration of 200 s with a total distance of 1969 m and a maximum speed of 90.0 km/h.

It is to be noted that the HKTET test cycle is derived from the New European Drive Cycle (NEDC) which is used to determine compliance with the European standards for a vehicles' type approval (for pre Euro 6 vehicles). The HKTET is the I/M emissions certification test for Hong Kong's in-use vehicles which can be applied in a rapid, economic manner to a large number of vehicles that have been identified as high emitters. The results provide a reliable indication if a tested vehicle does or does not comply with its given European standard (for I/M emissions conformity, not type approval compliance).

The results of the testing for each malfunction/fault simulation have been collated, followed by the calculation of the average and standard deviation for each test malfunction simulation. The standard deviation results in the form of error bars show the range of variation.

(a)

(b)

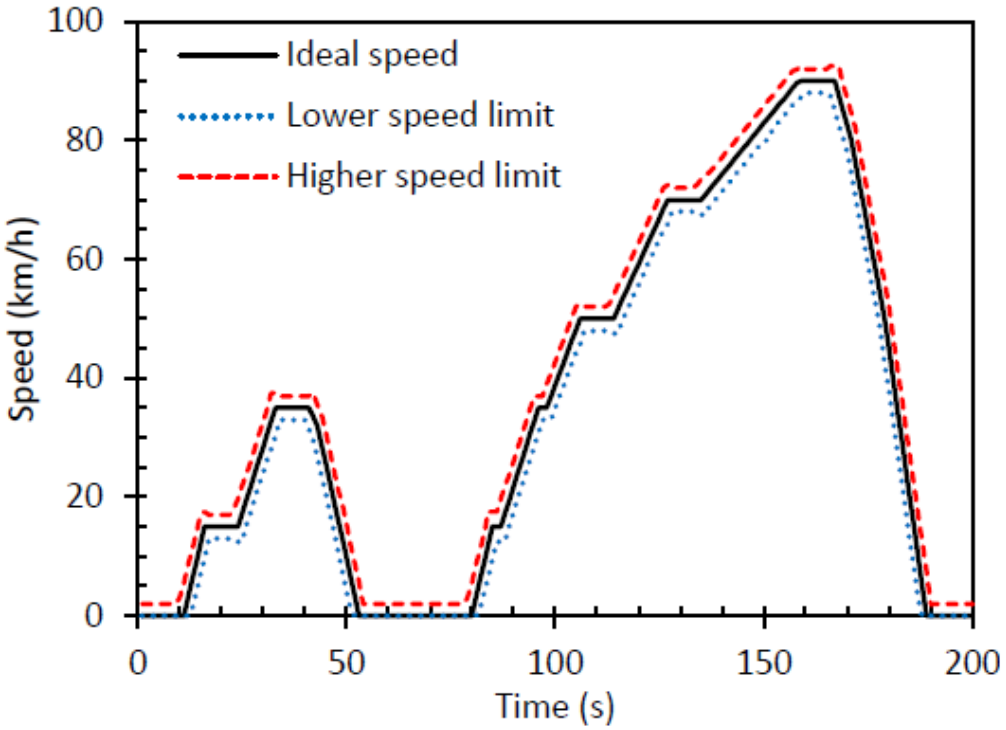

Figure 3.4: The study vehicle (a) and its HKTET speed chart (b).

3.2.1 Simulation of malfunctions

Before the testing began, the Toyota Crown Comfort taxi underwent significant maintenance work with the engine being rebuilt to as-new condition with machining of the engine block, the cylinders, replacement of pistons, bearings, machining of the cylinder head, valve replacement and all gaskets and seals. All filters, fluids and consumable parts were replaced. The transmission was serviced along with the drivetrain, suspension and new tyres were fitted. The emissions control hardware including the TWC and oxygen sensor were replaced with new components and the fuel system serviced with all degraded components being replaced. The vehicle was then independently checked by a third party to certify all work had been properly conducted and the vehicle was in a fully functional and roadworthy condition after completion of all work and before any testing was conducted. The vehicle was then tested with all hardware functioning properly on the chassis dynamometer, as shown in Figure 3.4(a), and this condition was utilised as the baseline for comparison with the simulated faults.

Following the baseline testing, each of the 15 simulated malfunctions was investigated, one by one, with all other system hardware being in good condition. These malfunctions covered the faults that could occur in the intake, fuel, ignition and exhaust after treatment systems. Malfunctions were simulated by either switching, disconnecting, mechanically disabling or electrically simulating an alternate output signal of the engine hardware or emissions system component. For each of these simulated malfunctions, there were a minimum of three test results collected for evaluation purposes.

It is noted that in the real-world environment wear and tear failures do not occur in isolation. Normally multiple systems can wear and have deteriorated performance in tandem. The goal of testing in isolation is to provide a foundation knowledge on the magnitude of the effect of a particular failure, which experienced automotive repair professionals can use to assess the likely combined emissions impact of deterioration of the systems and identify as faulty whilst conducting maintenance and repairs. Figures 3.5 to 3.8 show the components modified for testing.

3.2.2 Intake system

Worn shaft bushings in throttlebody butterfly valve

The butterfly valve in the throttlebody, Figure 3.5 (a), is used to control the airflow into the engine, pending the drivers speed/power demand via the throttle pedal. For efficient operation this must open and close smoothly at all times. The butterfly shaft runs on bushings and over time these can wear and the operation can become rough and the throttle plate can stick or jam in place which results in poor driveability for the vehicle. For simulation of the failure, the bearing bushings were lightly filed and scored so the butterfly shaft did not move smoothly and would momentarily stick in place when opening or closing.

Sticky mixture control valve in the fuel mixer

The mixture control valve (Figure 3.5 (b)) is installed in the throttlebody assembly of the vehicle and controls the flow of LPG into the inlet manifold. In normal operation, the mixture control valve moves smoothly and can deliver the fuel quickly as needed. To simulate failure, a used/worn mixture control valve which was sticking/not moving smoothly was installed in the throttlebody. The resultant impact on vehicle performance was a deterioration of the vehicle drivability, smoothness of acceleration and engine response.

Sticky idle control valve in the fuel mixer

The idle control valve (Figure 3.5 (c) in the throttlebody regulates the required fuel injection when the engine is idling, i.e., when the butterfly valve and the main fuel mixing valve are closed. To simulate a malfunction, an idle control valve which was sticking when operating to open or close was utilised. The sticky idle control valve impacts the engine idle stability resulting in poor/rough engine idling.

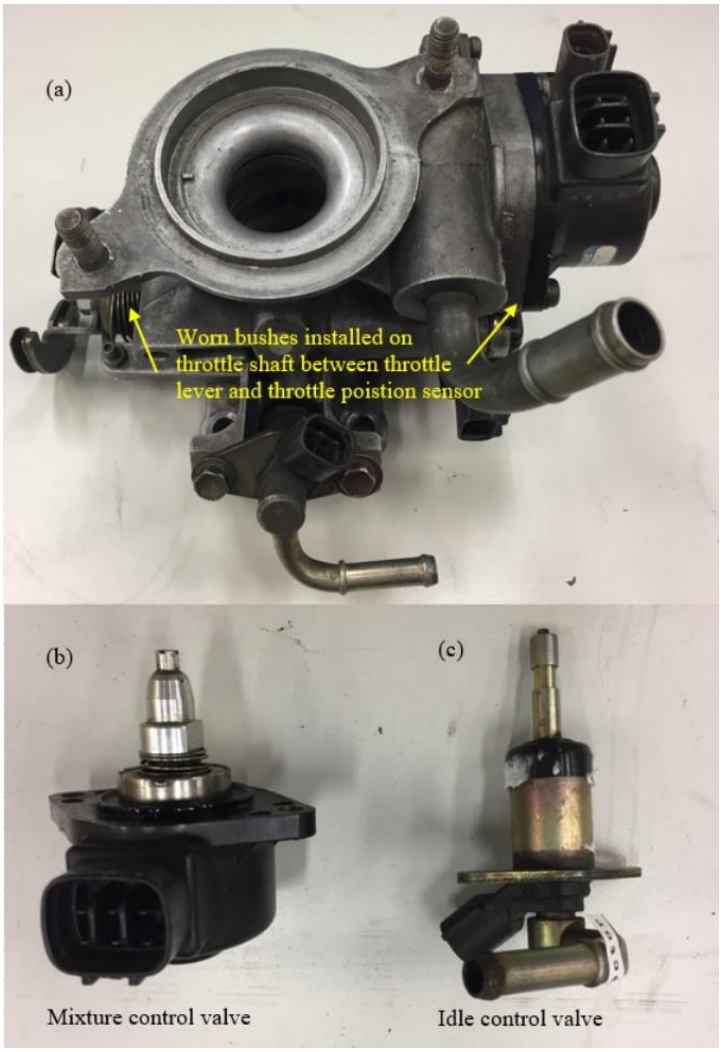

Figure 3.5: Modified Intake system hardware for experimental testing (a – c).

3.1.3 Fuel system

Overly rich/lean air-fuel ratio adjustment in vapouriser

The vapouriser (Figure 3.6 (a) is where the LPG is converted from liquid phase into a gas phase for mixing with the air into the intake manifold. The vapouriser has a diaphragm which is spring loaded to control the gas pressure and in turn the amount of LPG delivered to achieve stoichiometric air-fuel ratio for combustion. Adjusting the spring pressure either higher or lower alters the control pressure and the air fuel ratio adjustment. This will result in higher or lower fuel flow rates which can result in rich or lean biased fuel supply and potentially rich or lean combustion if it is outside the range of the closed loop feedback control for fuel supply. It can also result in fuelling control switching from

closed loop feedback control to open loop control adding another variable element which further impacts the emissions and could produce a large variation in a set of test results.

Restricted main fuel line in vapouriser

Once the fuel has become a gas in the vapouriser it travels from there to the mixing valve on the throttlebody where it is metered into the intake manifold. Blockages can occur in the vapouriser and restrict the flow of fuel. To simulate this failure a line from the vapouriser to the mixing valve had an adjustable stop valve installed which could be used to restrict the fuel flow. When the fuel flow is restricted, the vehicle loses power under heavy acceleration and load.

Restricted idle fuel supply line

The idle fuel supply is also subject to blockages before it arrives at the idle injector in the throttlebody. Similar to the main fuel supply in the vapouriser, the idle supply can be restricted as well. The simulation of this failure was by an adjustable stop valve installed in the fuel line which was used to restrict fuel flow. When the fuel flow is restricted, the vehicle experiences rough idling conditions.

Faulty fuel cut solenoid value in vapouriser

The fuel cut solenoid valve (Figure 3.6 (b)) is used to stop the fuel flow from the vapouriser to the main mixture control valve and the idle control valves in the throttlebody. It opens when the fuel system primes before the engine starts and stays open while the engine is running. When the engine is turned off, it shuts off fuel supply to the vapouriser. The fault is simulated using a valve that is sticking when opening or closing. This results in the gas flow not stopping or starting when required and the engine operation not being controlled as needed.

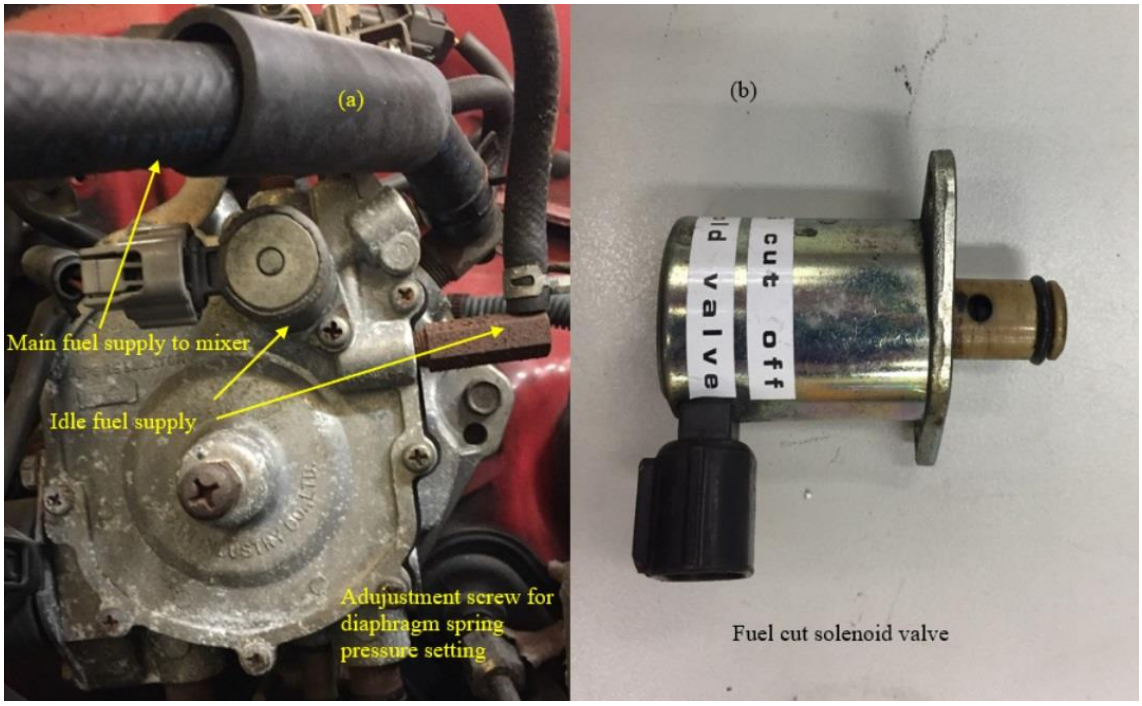

Figure 3.6: Modified Fuel system hardware for experimental testing (a – b).

3.1.4 Ignition system

Faulty spark plug

The spark plug is essential in a spark ignition engine to provide the ignition source for the air fuel mixture in the cylinder. The spark plugs used in the Toyota Crown Comfort LPG taxi have been selected to optimise performance under the combustion conditions of the Toyota 3Y-PE engine used in these vehicles. As spark plugs wear over time, i.e., electrode(s) deteriorating, spark gap increasing, deterioration of the insulator etc., the amount of energy required to form the spark increases, the duration of the spark and the quality of the ignition are impacted. These factors will impact the driving performance (fuel economy, misfire, rough idle, reduced acceleration power) and emissions of a vehicle. Worn spark plugs were utilised to simulate the malfunction.

Faulty distributor cap and rotor

The distributor functions to provide the required ignition timing to each cylinder at the correct time. The rotor is moving when the engine is running and touching the distributor cap contacts to provide the high voltage current from the coil to the spark plug to allow

ignition of the air fuel mixture in the cylinder. Over time the rotor and distributor cap can wear due to vibration, exposure to high temperature and voltage, cracking and carbon deposits building up. To simulate failure in the testing a distributor cap with worn contacts was used in conjunction with a worn rotor. The Faulty Distributor Cap and rotor are shown in Figure 3.7.

Figure 3.7: Worn Ignition system hardware for experimental testing.

3.2.5 Exhaust system

Worn /aged TWC

The TWC works to convert emissions of HC and CO by oxidation reactions to CO_2 and H_2O using the precious metals Platinum and Palladium. NO and NO_2 are converted by a reduction reaction using the precious metals Platinum and Rhodium to N_2 and H_2O (Chatterjee et al., 2001). The conversion reactions are represented by equations 3.5 – 3.7. A simulated malfunction has been produced by utilising a worn TWC which has reduced effective surface area of the catalyst materials within the substrate for effective pollutant reduction. To be able to demonstrate either a TWC in good condition and a simulated TWC malfunction or worn TWC, a specialised exhaust system with both TWCs installed was fitted to the vehicle. This dual catalyst system allowed either the good or worn TWC to be selected quickly for emissions testing to compare the performance of a good and

worn TWC. The exhaust system was modified so both catalysts could be installed under the vehicle floor at the same time (away from the manifold due to size limitations), with flow valves being used to select either the good or the worn/aged catalyst for a test. This dual catalyst installation is shown in Figure 3.8(a). The worn/aged TWC malfunction was the most commonly observed failure mode. Another failure mode also observed less frequently was blockage of the TWC. When this occurred the TWC substrate effectively acted as plug when under higher load and acceleration and the vehicle driveability was severely in impacted with loss of power, reduced top speed and engine stalling occurring in some instances.

$$CO + \frac{1}{2}O_2 \rightarrow CO_2 \tag{3.5}$$

$$C_nH_m + \left(n + \frac{m}{4}\right)O_2 \rightarrow nCO_2 + \frac{m}{2}H_2O \tag{3.6}$$

$$CO + NO \rightarrow CO_2 + \frac{1}{2}N_2 \tag{3.7}$$

Faulty oxygen sensor

The oxygen sensor (Figure 3.8 (c) monitors the oxygen content in the exhaust gas before it enters the TWC. The sensor installed in this vehicle provides a variable voltage signal. If the exhaust is rich (high THC or CO), the voltage is around 0.9 V; if lean (high NO_x) the voltage is 0.1 V or when the mixture is at stoichiometric (balanced) the voltage is 0.45 V. The signal is utilised by the ECU to modulate and trim the fuel supply to try to achieve stoichiometric combustion conditions. The ECU either supplies additional fuel when the signal is lean or reduces the supply when it is rich. To simulate failures in this study, a breakout box was installed so that a fixed voltage signal from a power supply could be sent to the ECU. Constant voltage signals of 0.1 V and 0.9 V were utilised to simulate a faulty oxygen sensor. Additionally, when the oxygen sensor maintains a voltage signal that is excessively high or low for an extended period, the ECU can switch from using this signal in closed loop control to open loop control where fuel is supplied at predetermined settings for a given acceleration or driving demand. This can increase emissions by impacting the rich or lean conditions that already exist in the engine and could also produce a possible large variation in a set of test results.

EGR valve jammed open/closed

The EGR valve (Figure 3.8 (b) is utilised to allow a metered amount of exhaust gases back into the intake manifold which in turn reduces or dilutes the amount of available oxygen in the intake air available for combustion and lowers the temperature of combustion to reduce NO_x formation. The EGR valve in this vehicle opens and closes utilising manifold vacuum and is controlled by an ECU controlled solenoid valve. To simulate a jammed open EGR valve, the vacuum line was disconnected and reconnected to a manually operated vacuum pump to keep the valve open. Conversely to simulate a jammed closed valve, the vacuum line was disconnected from the EGR valve so it would remain closed during testing.

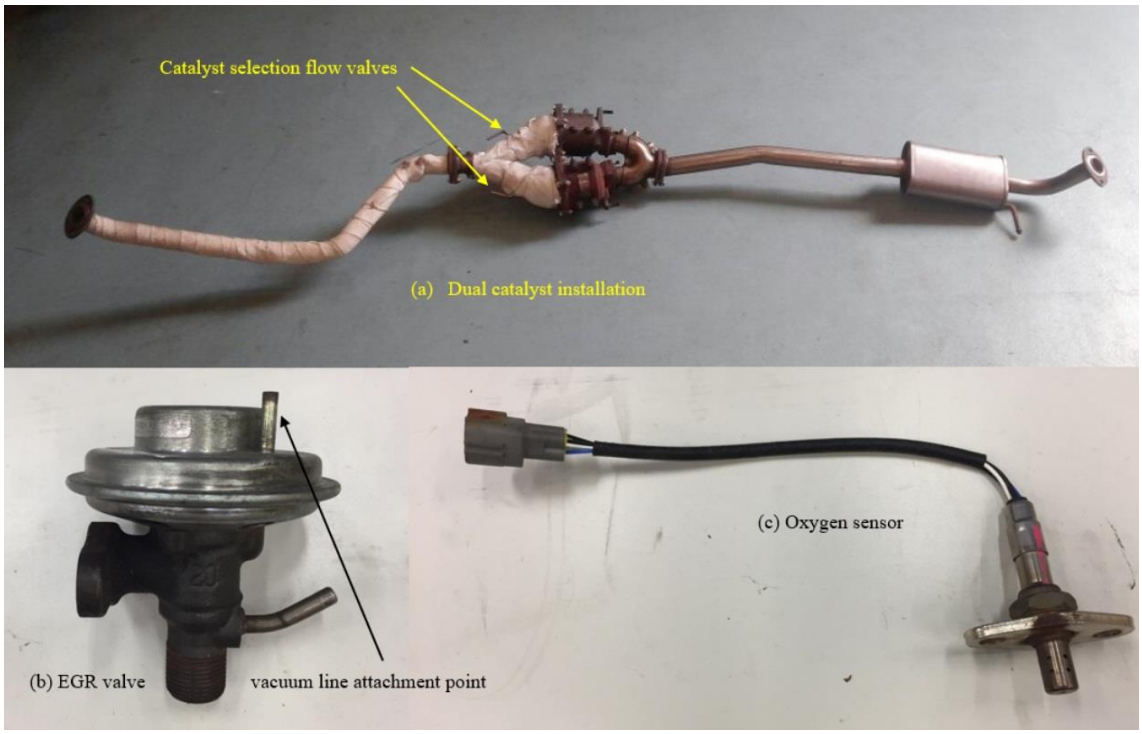

Figure 3.8: Modified Exhaust system hardware for experimental testing (a – c).

3.3 Factors affecting RS sensitivity

In conducting investigations to better identify factors which effect the sensitivity of RS measurements for gasoline and diesel engines, a series of study methodologies have been developed and applied. There are three main areas where testing methodologies were designed and developed, a new calibration device for baseline measurement of an RS device, developing a stable open air testing method for RS application and the experimental setup for measurement of vehicle exhaust temperature plumes on chassis dynamometer.

3.3.1 Calibration device for improved RS measurement

The development of a new calibration device began with consideration of normal checking or testing locations for RS equipment when being maintained or stored. The potential locations for this would be in either a factory, workshop or laboratory environment. The principal need for improvement was to achieve a calibration result which better approximates the usage of the RS equipment as the existing bench test methodology used by RS manufacturers and operators is not similar to the on-road test setup.

The following items are considered necessary for the development and operation of the calibration device.

- The calibration location should be within a covered environment protected from sunlight and inclement weather with good air circulation so test span gas or exhaust gases can dissipate without a localised concentration build-up which would affect potential RS or gas analyser measurements.
- There should be a chamber constructed with an area/volume into which a span or sample gas can flow into where it can start disperse from after short time similar to on-road exhaust emissions.
- The chamber should allow additional airflow rates to be simulated as needed to ensure/enable gas dispersion from within the chamber.

- The chamber shall have a sufficient width and height to allow an RS measurement beam to pass through and return without signal loss or other negative impacts.
- The temperature of exhaust gas flowing into the chamber shall be measured at multiple locations including gas entry points, central area of chamber, exit points.
- Control of flow of span gas injection or exhaust gas injection to be achieved with consistency of concentrations to be targeted.
- Monitoring of span of sample gas concentrations by conventional emissions gas analysers to be incorporated.

Fabrication of calibration devices was undertaken by HKEPD staff to support the RS research and investigations. An initial concept device was constructed and trialled to evaluate the performance and establish what further improvements might needed to be considered. A schematic for the initial trial device is shown in figure 3.9

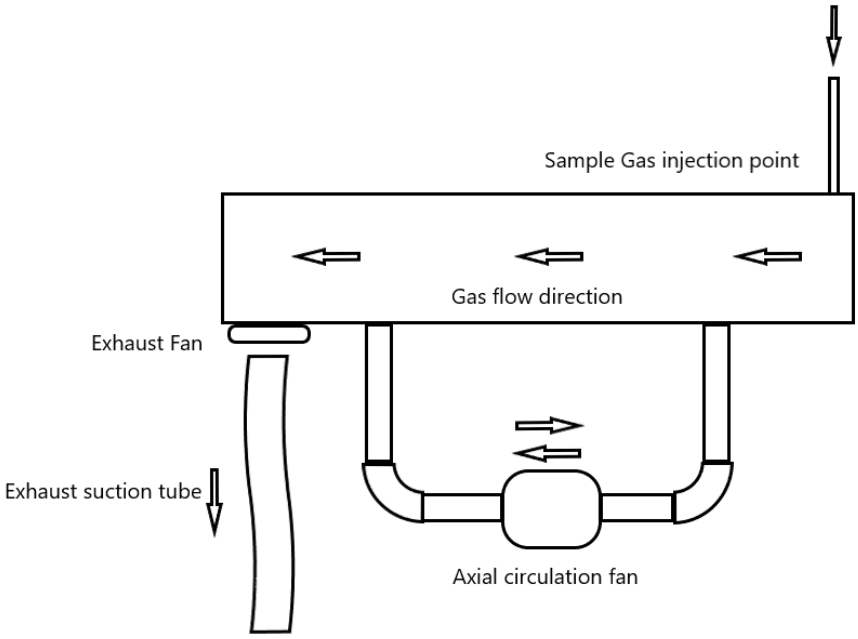

Figure 3.9: Initial trial calibration device schematic.

The initial trial device was setup to draw the span or exhaust gas from the injection point through the chamber and to an exhaust point attached to the building exhaust extraction system on the opposite end. The RS unit and reflector were able to be set up on either side of the device with a separation gap of up to 5m to simulate a typical on-road configuration. Sample gas from either a span gas bottle or the exhaust from generator could be connected to the injection point.

The axial flow circulation fan could be operated to create turbulence or increase/decrease time taken for gas to transit through. To simulate varying airflows through the chamber, a large instrument cooling fan was installed on the opposite side and end away from the gas injection point. This could be turned on or off and work in conjunction with the building exhaust extraction system.

Testing was conducted with the trial device and it was found to be able to measure the gas samples, but the consistency the RS data between measurements was lower than expected. Using the observations from the experiments conducted, a refined version of the calibration device was designed and constructed with some enhanced functionality.

To better manage the nature of the flow of sample gas from the injection point to the exit, the flow path was changed to a diverging cross flow arrangement where the gas flow was now perpendicular to the RS beams where previously it had been flowing in line with the beams. Improved control of the amount of suction from the injection point to the exit point was enabled by installing an array of five smaller cooling fans that could be individually operated to vary the amount of airflow/suction. The design of the chamber now incorporated a V section to draw the gas both left and right of the injection point to assist with dispersion of the sample.

Span gas would no longer be injected directly from a gas bottle as the injected plume takes a significant time to equalise its flow and pressure distribution and was not representative of on-road testing conditions. Span gas would now be loaded into a specially made plunger device for injection at ambient temperature and pressure. A generator set which would be used to provide exhaust gas needed to have improved load control so the emission gas sample being measured would be consistent.

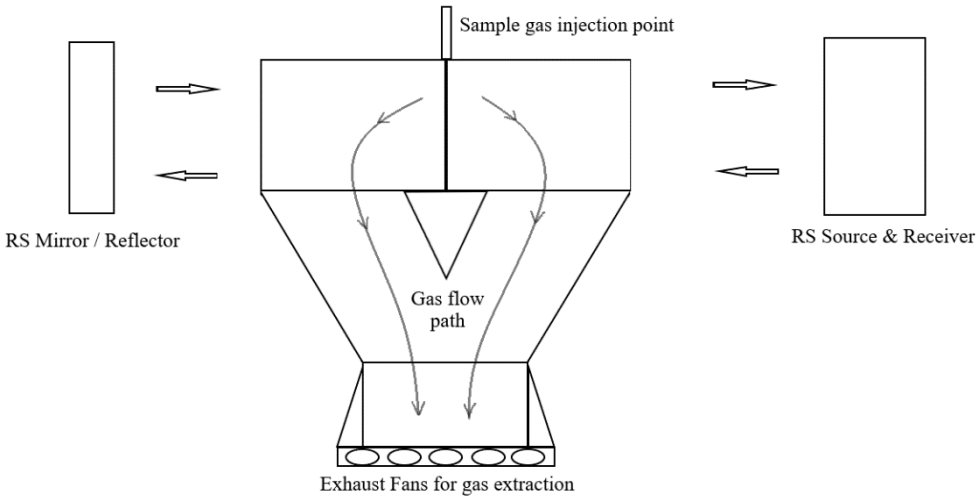

Figure 3.10: Concept for the refined calibration device for testing.

Figure 3.10 shows the schematic layout of the device. A new gas plunger concept was designed so it could be filled with a set amount of span gas at ambient temperature and pressure. The plunger was setup to be manually operated for a fixed duration so the sample gas was injected into the chamber and could dissipate without delay. Figure 3.11 shows the initial schematic for the plunger device assembly.

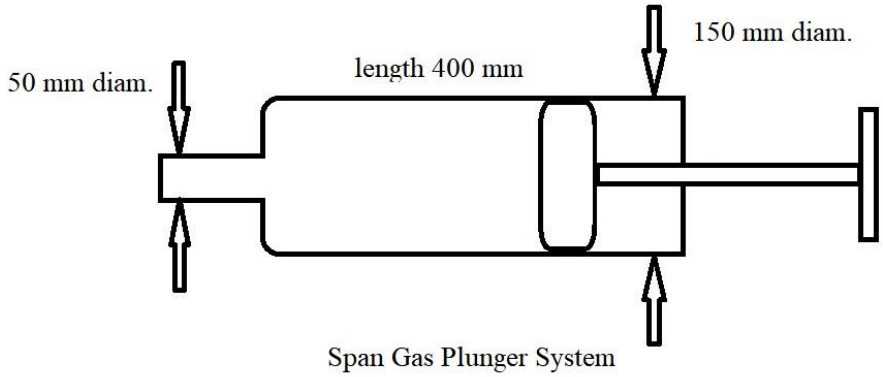

Figure 3.11: The concept of gas plunger system for calibration device

When assembled, it was filled with gas via a filling cap attached to the nozzle. When used for injecting span gas into the calibration device, the plunger was operated slowly over a few seconds to ensure a smooth flow of gas into the RS measurement area.

This device reduced the variability experienced when injecting span gas from a storage bottle to provide more consistency for RS span check measurements.

With these considerations and improvements being incorporated into the refined design, the HKEPD proceeded with construction of a new refined calibration device (Lee, 2019). See Figure 3.12 for device drawing. The setup of the refined calibration device followed the base layout used with the initial concept device in the test centre.

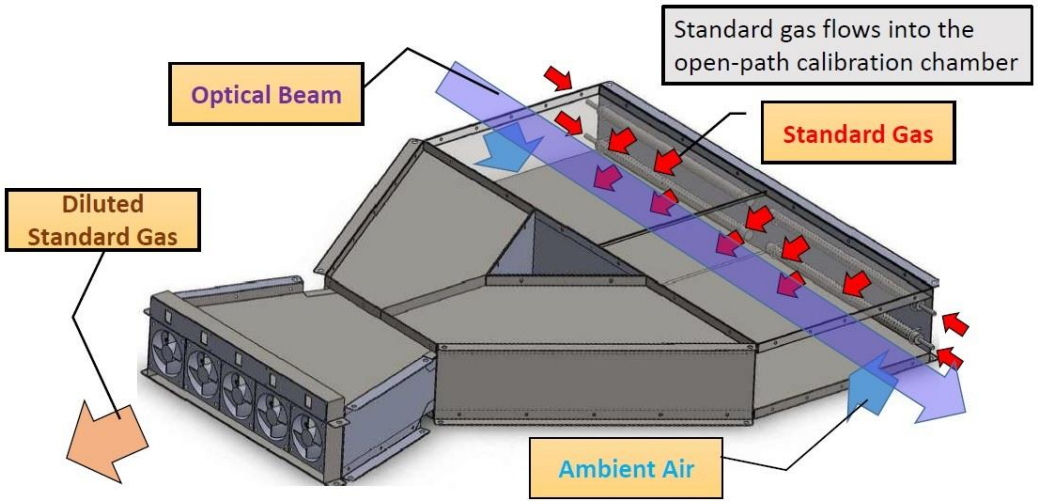

Figure 3.12: Refined calibration device drawing model

When the refined RS calibration device had been constructed, new experiments were conducted to collect RS and conventional emissions measurements for analysis.

The equipment and experiment setup were modified further from the initial tests.

- The gasoline generator was replaced by a diesel generator.
- An induction heater and an industrial vacuum cleaner were used to provide a consistent electrical load on the generator whilst testing.
- The RS equipment was setup to continuously measure 152 points per second.
- Exhaust gas temperature was measured at five locations from 300 mm before the injection point of the device to 100 mm before the injection point with 50 mm spacing in between. The temperature was measured using 0.2 mm K type thermocouples connected to a GRAPHTEC midi logger GL220, 10-channel data logger.

- To reduce heat losses, some sections of the exhaust were wrapped with exhaust insulation bandages to maintain the exhaust gas temperature.

The setup of the thermocouples is shown in Figure 3.13.

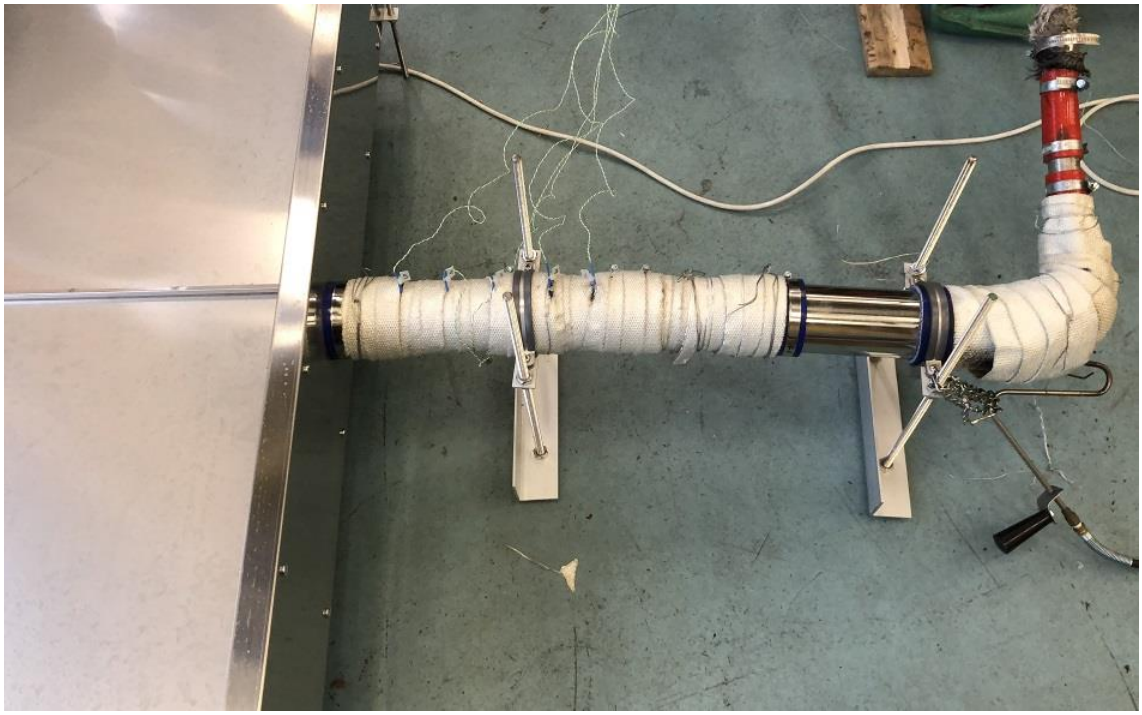

Figure 3.13: Thermocouple setup for exhaust gas monitoring

The equipment was set up and run with the operational configurations listed in Table 3.3. The different loading configurations were selected to evaluate which would provide the most suitable sets of data for RS evaluation when compared with conventional measurements.

Table 3.3: Experimental test setup and sequence.

Configuration	**1st Test**	**2nd Test**
Emissions source	Diesel generator	Diesel generator
Electrical load	Industrial vacuum	Induction heater
Suction/Cooling fans	All 5 fans turned on	All 5 fans turned on
Temperature logging	5 K type thermocouples	5 K type thermocouples
Test Sequence	Generator turned on, idling. Vacuum set to high speed. Vacuum off, generator idling. Vacuum set to high speed. Vacuum set to low speed. Turn off vacuum followed by generator after 10s.	Generator turned on, idling. Heater on, setting = 9 Heater off, generator idling. Heater on, setting = 7. Heater off, generator idling. Repeat sequence if needed. Turn off heater followed by generator after 10s.

To make further investigations in the temperature effect, it was necessary to improve the test setup and potential measurement capability. For this a more stable electrical loading system for the generator with discrete loading control was required. Initially single discrete resistance loads were considered. Obtaining suitably sized resistance loads for the generator set proved to be challenging. Most of the teaching and research loads available were designed for DC applications, up to 50 V with current rating between 2 to 4 amps. The diesel generator was rated to provide up to 13 Amps ay 220 V AC. After making many enquiries, a AC resistive load bank (a DeLorenzo DL2090) suitable for 220V AV and 3.6 kW of power absorption, was found to be available from the Electrical Engineering Department of Tsing Yi IVE. This was able to be borrowed and planning for a series of new experiments with the refined calibration device and RS system proceeded.

The load bank was used to replace the industrial vacuum cleaner as the load source for improving the consistency of emissions being measured through refined calibration device with the EMS and RS test equipment. To provide the maximum potential load for the generator the three load bank resistors were connected in parallel. To ensure consistency of the electrical load, a cooling fan was used to cool the resistor bank when connected to the generator. Figure 3.14 shows the schematic setup with the resistor load bank set up and connected.

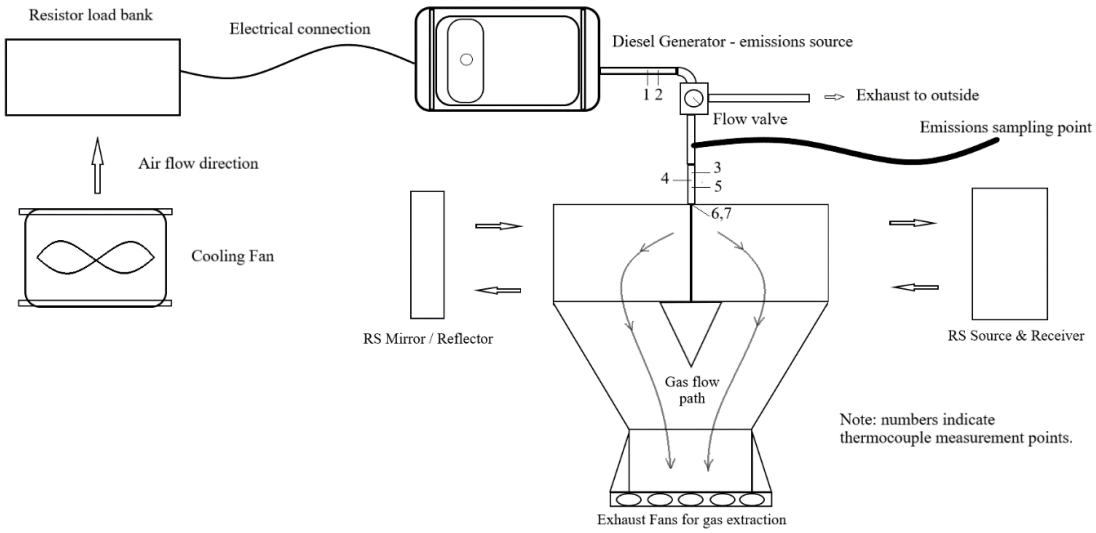

Figure 3.14: RS testing with resistance load bank connected

Testing was undertaken with a series of set loads applied and with varying exhaust flow volume into the device and suction from the exhaust fans. Resistance load settings utilised for testing and descriptions of thermocouple measuring locations are shown in Table 3.4. Testing with this equipment setup was conducted and results are shown in section 6.2.

3.3.2 Open path measurement technique for improved RS measurement.

The refined calibration device developed and utilised for experiments previously described in section 3.3.1, and with the results reviewed in chapter 6.2 has proved effective being used for determining measurement consistency. Whilst this will prove beneficial in future for conducting comparison measurements with RS equipment from different manufacturers. It also provided data indicating that the RS measurement is impacted by varying temperatures. i.e., the exhaust gas temperature and the temperature of the RS calibration device structure. To improve evaluation of the temperature impact on RS measurements it was necessary to setup a test method without the calibration device for evaluation. This method is described as an ‘open path’ measurement technique.

Table 3.4: Resistance load bank setting and thermocouple locations used for testing.

Setting	Current (A)	Power (kW)
0	0.0	0.000
1	2.3	0.506
2	5.0	1.100
3	7.6	1.672
4	10.2	2.244
5	11.1	2.442
6	12.6	2.772

No.	Thermocouple location
1	100 mm before end of pipe connecting to valve from generator exhaust
2	50 mm before end of pipe connecting to valve from generator exhaust
3	200 mm before calibration device
4	150 mm before calibration device
5	100 mm before calibration device
6	First thermocouple at entry to calibration device
7	Second thermocouple at entry to calibration device
8	Left Hand Side (LHS) of calibration device suction V
9	Right Hand Side (RHS) of calibration device suction V
10	Centre of calibration device V joint before exhaust fans

Development of the open path testing method was based on equipment utilised for the for the testing of the refined calibration device. The calibration device was no longer utilised so the exhaust gas could be emitted directly to ambient air. This way there would be no contained heating effect to influence the exhaust gas temperature. Furthermore, without the calibration device which was guiding the dispersion and funnelling the flow of exhaust gas another methodology would be need to be applied to assist/guide the exhaust plume to flow in the desired direction for consistent RS measurement.

The location for the experiment needed to be open to the outside to avoid potential build-up of pollutant gases in the test area where the experiment is conducted. This would impact the background concentration of pollutant gases if not managed sufficiently. Ideally the equipment such as the generator, resistor bank, heat exchanger, pressure damper/mixer, gas analyser(s), measurement equipment, cooling fans and other blowers required would be under shelter out of direct sunlight and protected from rain.

When considering placement of the exhaust point from the generator system, it would be into an outside area for the exhaust gas to disperse. The RS measurement system would be located in this area to capture the measurement. To ensure the flow of gas, a suction fan with a flow focusing cone would be placed in the external area, approximately one to two metres from the exhaust point to assist with drawing the plume towards the RS measurement zone.

Ideally, the area for the experimental testing should have limited exposure to wind so there is minimal impact to the RS measurement being conducted. The natural airflow through the area should be considered and a determination made if it affects the RS measurements. A proposed schematic for the open path test experiment is shown in Figure 3.15.

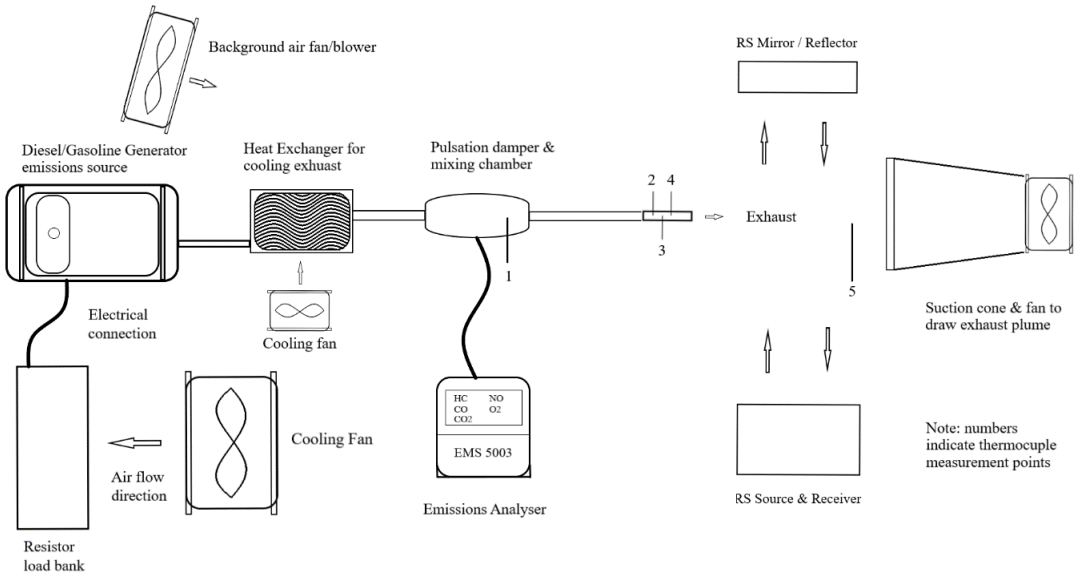

Figure 3.15: Proposed open path RS testing schematic

The setup is designed to allow testing to be conducted with the option to control factors such as the gas exhaust temperature by a combination of resistance loading of the generator or cooling the exhaust gas with a heat exchanger, variable background airflow around the system and changing the generator from a diesel fuelled device to gasoline fuelled.

Testing was undertaken over two days. The first day using a diesel generator as the emissions source and the second using a gasoline generator as the emissions source. For these experiments the original resistor load bank was not available. An alternate device,

a Cressall AC6 Load bank, rated at 6 kW at 230 Vac was utilised in its place. The configuration of the load bank resistances is as shown in Table 3.5

Table 3.5: Resistance load bank setting of gasoline open path RS experiment.

Setting	Current (A)	Power (kW)
0	0.0	0.000
1	1.4	0.308
2	2.7	0.594
3	4.1	0.902
4	5.4	1.188
5	6.7	1.474
6	7.3	1.606
7	8.1	1.782
8	9.9	2.178
9	11.3	2.489
10	12.6	2.772
11	13.9	3.058
12	15.3	3.366
13	16.6	3.652

Note: Thermocouple locations used for open path RS testing were located in the mid-point of the exhaust pulsation damper/mixing chamber, at 150, 100 and 50 mm before the exhaust pipe exit and at 50 mm before the suction cone inlet.

The diesel generator to be used in the testing (up to 3 kW) is noted to produce excessive smoke and can run with unstable engine speeds when loaded above 10 Amps. With this consideration the test loading targeted lower current loading when testing. For gasoline testing, two identical generators with their exhausts joining together at Y piece connector before the heat exchanger, were utilised that running together can deliver higher current loads and are targeted to assess these higher load conditions when testing.

The test procedure followed a similar application developed from the refined calibration device testing. Each test consisted of two repeated four step loadings finishing at a 0 Amps. The test conditions are tabulated and shown in the results section, 6.2.1.

3.3.3 Determination of vehicle exhaust plume temperature profile

With the identification of varying exhaust gas temperature impacting the RS measurement it was next necessary to determine the exhaust plume temperature profile of some sample test vehicles when being driven to determine at what distance after the gas plume exits the exhaust pipe an RS measurement could begin reduce variability in the data sample. The experiment was conducted using gasoline and diesel vehicles being driven on a chassis dynamometer.

A temperature recording array of exposed K type thermocouples with a fast response time of 0.6s was set up to record the temperature of the exhaust plume as it exits the exhaust pipe. Vehicles were setup to drive on the chassis dynamometer with inertia loading per the Euro 6 load setting tables of ECE Regulation 83 (UNECE, 2015). The experiment examined a range of steady state speeds for driving and resultant temperature profile of the exhaust plume.

The experiment utilised a National Instruments (NI) Compact Data Acquisition (C-DAQ) chassis with selected analogue, digital and thermocouple modules to allow recording of data for the temperature profile measurement. The data also included weather station information for the testing location, (barometric pressure, ambient temperature and relative humidity). This setup accommodated connection of between 12 to 14 thermocouples. The thermocouples were be placed on a slotted right angle steel strip and fastened in place at pre-determined measurement locations. Each thermocouple measurement point was located 100 mm distant from the right-angle strip the wire is fixed to so that only the thermocouple measurement point is centred in the exhaust plume and heat absorbed and radiated from the strip did not influence the temperature measurement. The ‘0’ cm thermocouple was located on a separate support arm so is maybe manoeuvred into a suitable location to support the measurement. To ensure the correct measurement location on the right-angle slotted strip a measuring tape was fixed in place on the top flat section of the strip.

As funding was not available for purchase of new measurement instruments or tools, all the measurement equipment and instrumentation were recycled from earlier testing projects conducted by JCEC at IVE in Hong Kong and rebuilt to support this experiment. This included rewiring and testing all thermocouples and the extension harnesses to ensure they were fully functional for the research. Assembling the NI CDAQ chassis with

data input modules and constructing a new measurement programme and recording array. Testing and debugging the array and software consumed numerous days before the beginning test. Further to this budget for vehicle hire was also not available, so vehicles were borrowed from those which had been used for testing at JCEC and were still available onsite at the time of testing. Testing was conducted between other projects and also utilised to train staff technicians to be able to better prepare and operate the chassis dynamometer. The testing layout is shown in Figure 3.16 and the setup of the thermocouple array spacing is as shown in Table 3.6. The data collected from using this test setup can then be assessed to provide suggested optimised distances at which RS measurement could start with the least exhaust gas temperature interference.

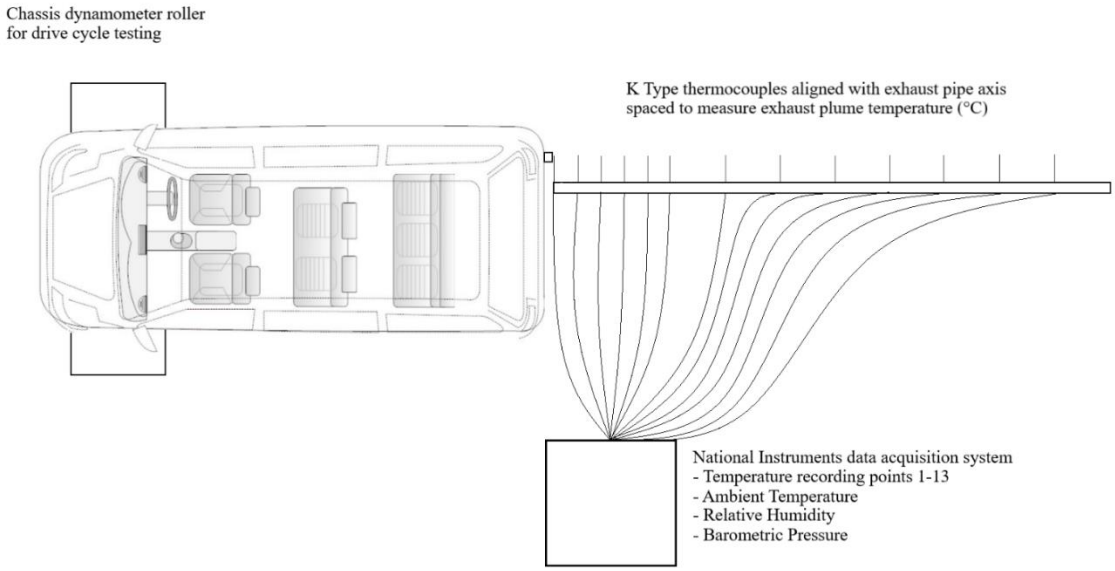

Figure 3.16: Vehicle exhaust plume temperature test experimental layout. Minivan art (SmartDraw, 2021)

Table 3.6: Thermocouple array configurations used for exhaust plume measurement.

No.	Thermocouple distance from exhaust pipe (cm)		
	Test 1 & 2	**Test 3 & 4**	**Test 4 higher resolution**
1	-	0	0
2	10	10t	5
3	20	20	10
4	30	30	15
5	40	40	20
6	50	50	25
7	75	75	30
8	100	100	40
9	125	125	50
10	-	150	75
11	-	175	100
12	-	200	125
13	-	225	225

Note: All thermocouples were aligned centrally with exhaust pipe and gas plume.

Initial driving tests followed a pattern controlled by the driver to maintain a vehicle speed for a minimum amount of time before accelerating to a new driving test speed. After the initial tests had been conducted a series of automated driving cycles for testing were developed and trialled for measurement. One of the drive cycles (Exhaust Emissions Temperature (EET) Drive Cycle 7) developed and used for testing is shown in Figure 3.17. Data points for each of the drive cycles developed for the all of the experimental testing are shown in Appendix C, Table C1.

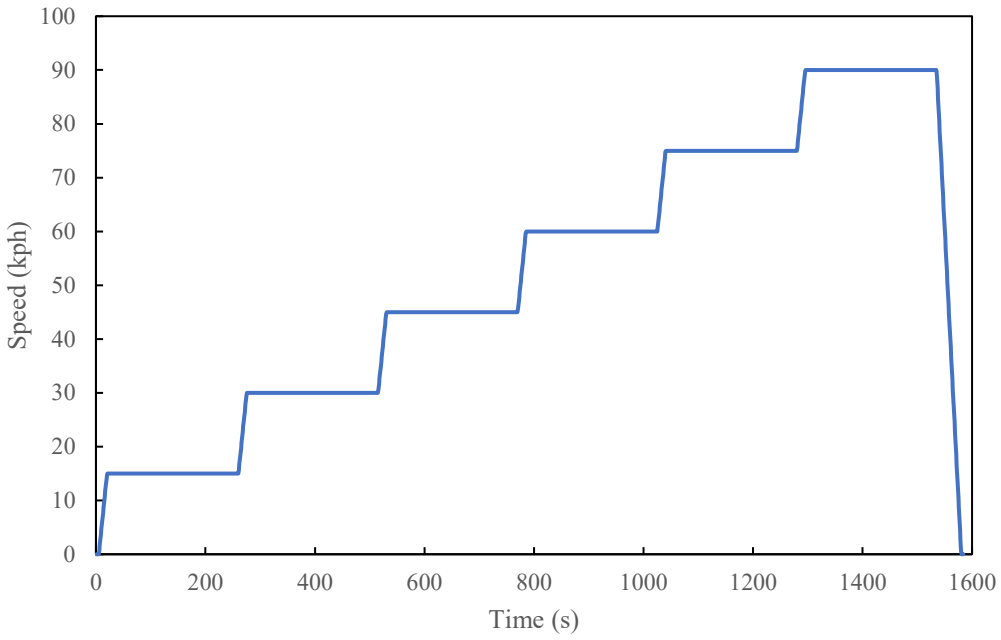

Figure 3.17: EET drive cycle 7 – 15 km/h steps.

After the first three vehicle tests were conducted, it was determined that a finer resolution of the exhaust gas plume temperature measurement should be attempted closer to the exhaust pipe. To facilitate this the thermocouple spacing was revised. The revised positions for the thermocouples are shown in Table 3.5. Testing undertaken with the revised thermocouple positions was conducted utilising EET drive cycle 7. Results for this experiment are shown in section 6.3.

Chapter Four

4. Analysis of RS emissions monitoring data

Many papers and studies have been published in recent years covering the use of RS programmes for the purpose of inventory data collection. However, no papers were available to outline the effectiveness of using RS for identifying high emitters and requiring them to have their vehicle repaired and pass emissions testing. A 'strengthened emissions control of gasoline and LPG vehicles' programme has been operating in Hong Kong since September 2014 utilising RS. This chapter reviews RS database information from HKEPD and evaluates the effectiveness of this globally unique RS monitoring programme.

A large RS dataset of 2,144,422 records was obtained covering the period from 6th January 2012 to 30th December 2016. Analysis of the data shows that the strengthened emissions control programme utilising RS has been very effective in identifying high emitting vehicles for repair so as to reduce the emissions from gasoline and LPG vehicles under real driving.

4.1 Introduction

Air pollution control measures for motor vehicles were first developed in the US in the 1950s (US Public Law, 1955) after motor vehicles were identified as major contributors to the problem of air quality (Giechaskiel et al., 2018b; Requia et al., 2016). Today the control of toxic vehicle emissions worldwide is by the following primary regulatory instruments. In Europe this is managed with the United Nations Economic Commission for Europe (UNECE) (Giechaskiel et al., 2018a; Suarez-Bertoa and Astorga, 2018) regulations for vehicles. In the US federal standards are established by the USEPA and further more stringent regulations are imposed by California Air Resources Board (CARB) (Perugu et al., 2018). The Ministry of Environment in Japan issues its motor vehicle exhaust emission standards. Many countries around the world follow the UNECE

regulations either directly or with some level of testing variation pending local conditions. The US and Japanese regulations may also be accepted in lieu of the UNECE regulations in some countries as well. In Asia, China has one of the largest and fastest growing vehicle fleets and Chinese regulations, denoted as CN followed the UNECE regulation level (number), currently CN5, but it is already starting to change with CN6 being implemented now in some cities and for the whole country in July 2020 (Tang et al., 2019). Locally in Hong Kong the vehicle regulations follow the UNECE regulations, currently Euro 6 except those for diesel private cars which are based on CARB's requirements, currently LEV 3.

Each of these regulatory instruments have reduced new vehicle emissions limits to achieve Air Quality Objectives (AQO) in respective countries and cities. In Hong Kong, the AQOs (Hong Kong Environment Protection Department, 2013) are based on the WHO guidelines (World Health Organisation, 2018). The latest published data for compliance to these targets in Hong Kong showed a significant number of exceedances for NO_2 at the roadside in 2017 (Hong Kong Environment Protection Department, 2018), although the NO_2 concentration had been reduced by 30% compared with that of 2013.

Vehicle emissions are a major source of roadside air pollution. Whilst the air quality issues vary between country, region or city, the systems for controlling and reducing vehicle emissions lie mainly with the vehicle design and hardware installed. The vehicle manufacturers are utilising a combination of the latest range of engine and exhaust/emissions control hardware (Huang et al., 2019a; Huang et al., 2019c; Zheng et al., 2018) combined with calibrated engine management software to alert drivers to check faulty emissions control systems. Such measures are essential in order to achieve compliance with the regulations of each market where vehicles are being sold. Once a vehicle has been sold and is in use on the road, factors which influence the emissions performance of each vehicle begin to vary significantly. Determining factors influencing long term emissions are individual vehicle usage patterns and loading, road and traffic conditions and vehicle maintenance (Fontaras et al., 2017; O'Driscoll et al., 2018). The capability of each vehicle to continue to meet their respective emissions regulation limits is not guaranteed if the required vehicle maintenance is not performed.

The reality of gasoline and LPG in-use vehicle emissions differs from the desired outcome of these successive regulatory steps. Each new regulation step has progressively lowered the allowable level of on-road vehicle emissions. If the vehicle fleet was properly

maintained, the emissions results with successive reducing regulatory emissions limits should be showing over time the impact of vehicle emissions on air quality is reducing. The improvements in emissions control technology and the increased durability requirements (Table 3.1) reflect this for all vehicles. For many vehicles which are maintained correctly this is the case, but there is a portion of the vehicle fleet which is either faulty from new or has little or no maintenance or have their emissions control systems tampered with (Borken-Kleefeld and Chen, 2015; He et al., 2019; Wenzel, 2001). It is these vehicles which have accumulated high mileage that show significant deterioration and in turn contribute a disproportionate amount of emissions that impacts local air quality (Bishop et al., 2016; Popp et al., 1999; Pujadas et al., 2017). In Hong Kong, the Environment Bureau issued 'A Clean Air Plan for Hong Kong' (Hong Kong Environment Bureau, 2013) that outlined the problems of local roadside pollution. It highlighted that a high mileage LPG vehicle with worn out emissions control hardware emitted ten times more NO_x, CO and VOC's than when these devices were in good condition. Identifying this problem, the Government allocated HK $150 million to provide a one-off subsidy to replace worn out catalytic converters and oxygen sensors in LPG/gasoline taxis and light buses to assist the transport sector to improve vehicle maintenance (Hong Kong Government, 2012). This ran between August 2013 to April 2014 and vehicle owners could on a voluntarily basis choose to have a new catalytic converter and oxygen sensor installed in their vehicle. A total of 13,942 taxis and 2,881 light buses received a replacement emissions catalyst and oxygen sensor (approximately 80% of the LPG vehicles). This was then followed by a strengthened emission control plan to identify high emitting vehicles which the owners would then need to repair and maintain.

The question that followed was how to implement a strengthened emissions control programme to determine if a vehicle's emissions control system is functioning correctly. Mechanisms for effectively checking and testing of vehicle hardware condition are short cycle transient dynamometer tests like the USEPA IM240 (Wenzel, 2001) or the utilisation of OBD systems. The dynamometer test is effective, but has the limitation that it can only be applied to a small number of vehicles. Whilst OBD is effective for determining serious vehicle failures, it became apparent that moderate and slow deterioration of catalytic converter systems was not being detected and aging vehicles were becoming high emitters and contributing significantly to roadside air quality

deterioration without being detected. It is also known that OBD systems can be prone to tampering so that malfunction alerts or reporting of emissions equipment failures are not reported or acted upon with the result of high emitting vehicles remaining on-road without proper maintenance (USEPA, 2014). Other monitoring and enforcement capabilities available to check the on-road vehicle fleet are roadside spot checks or time-consuming testing using tools such as portable emissions monitoring systems (PEMS), plume chasing (Borken-Kleefeld, 2013; Franco et al., 2013; Lau et al., 2015; Ning et al., 2012; Ropkins et al., 2009), and testing at vehicle inspection centres. Each of these options have not been able to keep pace with the growth of vehicle ownership and usage.

It was determined that RS could be used as a mechanism for effectively measuring emissions of passing vehicles. It has gained popularity as such a tool for the rapid detection of vehicle engine emissions (Huang *el al*., 2018b). It was selected for the purpose and has been used in the strengthened vehicle emissions control programme in Hong Kong since the 1st September 2014 (Hong Kong Government, 2014). By using the RS tool, the HKEPD has the means to identify individual gasoline and LPG vehicles which are high emitters. Emissions limit cut points have been determined for all gasoline and LPG vehicle classes (Table 4.1). When identified the vehicle owner is sent an Emissions Test Notice (ETN) which informs them their vehicle has been identified as having high emissions. They then have 12 working days to have the vehicle repaired and tested to prove it complies with its respective emissions limit. Otherwise, they will have their vehicle registration cancelled and it will be removed from the on-road vehicle fleet. There are no fines applied when an ETN is issued to a vehicle owner. However, the owner is responsible for all costs related to the necessary maintenance/repairs and the subsequent emissions test.

This strengthened emissions control programme in Hong Kong is pioneering in utilising RS in this manner. This research evaluates the effectiveness of using RS to identify high emitting vehicles for notification of repair and testing on vehicle emissions reductions in Hong Kong. A large dataset of 2,144,422 gasoline and LPG vehicle emissions records was collected in five years from 6th January 2012 to 30th December 2016. Analysis to select valid RS data and determine EFs was performed to assess the effect of the strengthened emissions control programme on the overall emissions trends of gasoline and LPG vehicles as well as for the dominant vehicle models.

Table 4.1: RS emissions limit cut points for identification of high emitting vehicles

Euro Type	Engine Type	Licence Class	Manufacture Year From	Manufacture Year To	HC (ppm)	CO (%)	NO_x (ppm)
Euro 1	Gasoline	LGV	1996	1998	1300	3	2000
Euro 2	Gasoline	LGV	1999	2001	1300	3	1500
Euro 3	Gasoline	LGV	2002	2006	700	3	750
Euro 4	Gasoline	LGV	2007	2012	700	3	750
Euro 5	Gasoline	LGV	2013	2016	700	3	750
Pre-Euro	Gasoline	PC	1975	1995	500	5	4000
Euro 1	Gasoline	PC	1996	1997	500	2	2000
Euro 2	Gasoline	PC	1998	2000	500	2	1500
Euro 3	Gasoline	PC	2001	2005	500	2	750
Euro 4	Gasoline	PC	2006	2012	500	2	750
Euro 5	Gasoline	PC	2013	2016	500	2	750
Euro II	LPG	PrivLB	1975	2003	700	5	2000
Euro III	LPG	PrivLB	2004	2006	700	5	2000
Euro IV	LPG	PrivLB	2007	2012	700	5	2000
Euro V	LPG	PrivLB	2013	2016	700	5	2000
Pre-Euro	Gasoline	PrivLB	1975	1995	700	5	2000
Euro I	Gasoline	PrivLB	1996	1998	700	5	2000
Euro II	Gasoline	PrivLB	1999	2001	700	5	2000
Euro III	Gasoline	PrivLB	2002	2006	700	5	2000
Euro IV	Gasoline	PrivLB	2007	2012	700	5	2000
Euro V	Gasoline	PrivLB	2013	2016	700	5	2000
Euro II	LPG	PLB	1975	2003	700	5	2000
Euro III	LPG	PLB	2004	2006	700	5	2000
Euro IV	LPG	PLB	2007	2012	700	5	2000
Euro V	LPG	PLB	2013	2016	700	5	2000
Pre-Euro	Gasoline	PLB	1975	1995	700	5	2000
Euro I	Gasoline	PLB	1996	1998	700	5	2000
Euro II	Gasoline	PLB	1999	2001	700	5	2000
Euro III	Gasoline	PLB	2002	2006	700	5	2000
Euro IV	Gasoline	PLB	2007	2012	700	5	2000
Euro V	Gasoline	PLB	2013	2016	700	5	2000
Euro 2	LPG	Taxi	1975	2003	500	2	1500
Euro 3	LPG	Taxi	2004	2005	500	2	750
Euro 4	LPG	Taxi	2006	2012	500	2	750
Euro 5	LPG	Taxi	2013	2016	500	2	750
Pre-Euro	Gasoline	Taxi	1975	1995	500	5	4000
Euro 1	Gasoline	Taxi	1996	1998	500	2	2000
Euro 2	Gasoline	Taxi	1999	2000	500	2	1500
Euro 3	Gasoline	Taxi	2001	2005	500	2	750
Euro 4	Gasoline	Taxi	2006	2012	500	2	750
Euro 5	Gasoline	Taxi	2013	2016	500	2	750

PC – Private Car LGV – Light Goods Vehicle PLB – Public Light Bus PrivLB – Private Light Bus

4.2 Results and discussion

4.2.1 Survey data characteristics

After filtering and selection criteria have been applied, the breakdown of the number of vehicles analysed for each survey year and fuel type are shown in Table 4.2. To ensure statistical validity of EFs for survey and model year assessment of results, there is a minimum of 100 records used for each point (Bernard et al., 2018; Chen and Borken-Kleefeld, 2016). The distribution of vehicle makes and models across each year of the survey period varies pending on the fuel type. For gasoline fuelled vehicles, there is a broad range of many makes and models making up the sample population. There are some 157 different vehicle makes alone recorded in the gasoline samples. Table 4.3 shows the sample distribution for the top 20 most dominant vehicles representing 52.3% of all the gasoline RS samples.

Table 4.2: Number of valid vehicle emission measurements by RS during 2012-2016.

Survey year	**Gasoline**	**LPG**	**Combined**
2012	40,188	39,666	79,854
2013	108,132	165,937	274,069
2014	148,052	100,454	248,506
2015	177,855	166,429	344,284
2016	169,065	90,984	260,049
Total	643,292	563,470	1,206,762

Table 4.3: Most frequently measured gasoline vehicles in the RS database.

Category	Vehicle make code*	Engine size (cc)	No. of samples	% of total samples	Manufacture year	European standard
1	1	3456	52,260	8.12%	2006-2016	Euro 4-5
2	1	2362	47,625	7.40%	1997-2016	Euro 2-5
3	2	3498	19,498	3.03%	2004-2015	Euro 3-5
4	1	1497	19,492	3.03%	1994-2016	Euro 1-5
5	2	1796	17,716	2.75%	2001-2014	Euro 3-5
6	1	2994	17,114	2.66%	1996-2008	Euro 1-4
7	1	1998	16,866	2.62%	1986-2015	Pre Euro to Euro 5
8	1	1987	15,105	2.35%	2008-2011	Euro 4-5
9	3	1997	15,001	2.33%	2004-2016	Euro 3-5
10	4	2979	12,939	2.01%	2000-2016	Euro 2-5
11	5	1984	11,098	1.72%	1994-2016	Euro 1-5
12	4	1997	11,088	1.72%	2011-2016	Euro 4-5
13	4	2497	11,087	1.72%	2004-2011	Euro 3-4
14	2	3199	10,828	1.68%	1992-2007	Pre Euro to Euro 4
15	6	2354	10,555	1.64%	2002-2015	Euro 3-5
16	5	1390	10,357	1.61%	2002-2016	Euro 3-5
17	6	1998	10,137	1.58%	1997-2011	Euro 2-4
18	3	3498	9,799	1.52%	2000-2016	Euro 3-5
19	6	1997	9,676	1.50%	1991-2015	Pre Euro to Euro 5
20	6	1339	8,704	1.35%	2001-2014	Euro 3-5

*Note: 'Vehicle make code' refers to a sequentially assigned number to identify makes in the data set provided by HKEPD

The distribution of vehicle makes and models for LPG is significantly different. The use of LPG fuel in Hong Kong is limited to taxis, Public Light Buses (PLB), Special Purpose Vehicles (SPV) and Private Light Buses (PrivLB). In this study the dominant vehicle model for taxis is the Toyota Crown Comfort Sedan and the dominant vehicle model for PLBs is the Toyota Coaster 16-seat minibus. They make up 72.2% and 27.6% respectively of the LPG RS sample population in the dataset. Table 4.4 shows the sample distribution for the major analysed LPG vehicles measured by RS. These distributions of

make and models for each fuel type present a significantly different picture for analysis of the subsequent EFs when compared to the gasoline RS sample data.

Table 4.4: Number of LPG vehicles and associated RS measurements

Vehicle ıake	Engine size (cc)	No. of records	% of total records	Manufacture year	European standard	Vehicle class
Toyota	1998	406,716	72.18%	1997-2016	Euro 2-5	Taxi
Toyota	4104	155,231	27.55%	2001-2016	Euro II-V	PLB, SPV
Nissan	1998	997	0.18%	1999-2001	Euro 2	Taxi
Nissan	1597	417	0.07%	2014-2015	Euro 5	Taxi
Ford	2488	106	0.02%	2014-2015	Euro 5	SPV

For the strengthened emissions control programme, the number of ETNs issued for vehicle classes, the pass rate for the HKTET and license cancellations are shown in Table 4.5. It should be noted that an ETN is issued only when a vehicle is measured and exceeded either CO, HC or NO cut points on both RS units.

Table 4.5: Statistics on number of ETNs issued (1/9/2014 to 31/12/2016)

Vehicle Type	Number of vehicles	%
Private Car	2168	28.6 %
Taxi	5005	65.9 %
Light Bus	398	5.2 %
Light Goods Vehicle	22	0.3 %
Total number of ETNs	7593	100%
Repaired and passed HKTET	7258	95.6 %
Vehicle license cancellations	335	4.4 %

4.2.2 Overall emissions trends

Figure 4.1 shows EFs for all gasoline and LPG vehicles by survey year for EF_{HC} (a), EF_{CO} (b) and EF_{NO} (c). For the combined dataset the general trend for EFs in 2012 and 2013 shows an increase of 24% EF_{HC} and 5% EF_{CO} (Figure 4.1a and b) and a decrease of 18% EF_{NO} (Figure 4.1c). From 2014 onwards there is an average decrease for all EFs which continues for EF_{HC} and EF_{NO} through to 2016. The EF_{CO} begins to increase in 2015 by 18% and then decreases again in 2016 by 23%. Overall EF magnitudes for all pollutant

gases have decreased from the beginning of the survey data period by 55.9%, 50.5% and 60.9% for HC, CO and NO respectively. Considering the fuel types separately, the gasoline EFs are noted to be significantly lower in most instances than the LPG EFs throughout the survey period. Early in the survey period the LPG EFs are in the range of 2.7 to 5.3 times higher than the gasoline EFs. As the survey period progresses the absolute EF values decrease and the magnitude of difference between the EFs changes to 2.9 to 3.7 times higher for LPG. The 2014 EF reductions can be directly linked to the government subsidised LPG emissions catalyst and oxygen sensor replacement scheme. Gasoline EFs are noted to be relatively stable or overall decreasing for each pollutant gas between the years from 2012 to 2015, with a reduction of 37% EF_{HC}, 52% EF_{CO} and 38% EF_{NO}, after which EF_{HC} continues to decrease by 5% whilst there is an increase of 14% EF_{CO} and 13% EF_{NO}. Overall EF magnitudes for all pollutant gases have decreased from the beginning of the survey data period by 40.5% HC, 45.3% CO and 29.6% NO for gasoline and by 48.4% HC, 41.1% CO and 58.7% NO for LPG. The government subsidised LPG catalyst and oxygen sensor replacement programme combined with the strengthened emissions control programme have reduced vehicle emissions and through the ETN process continue to reduce the number of high emitting vehicles on the road.

The RS data for LPG covers vehicles manufactured between 1997 and 2016. Figure 4.2 shows EFs for LPG vehicles breaking the data down further by survey and manufacture year for EF_{HC} (a), EF_{CO} (b) and EF_{NO} (c). It also shows EFs for taxis separately further by survey and manufacture year for EF_{HC} (d), EF_{CO} (e) and EF_{NO} (f). LPG EFs increase from the 2012 to 2013 survey years for EF_{HC} by 12% and EF_{CO} by 4% (Figure 4.2 a and b) whilst the EF_{NO} (Figure 4.2c) is decreasing by 28%. In 2014 all LPG EFs show dramatic improvement with significant decreases from 33% to 50% in EFs across all pollutant gases. The trend for EF_{HC} and EF_{NO} continues to decrease over the period by 18% and 15% respectively. The EF_{CO} on the other hand increases in 2015 by 21% and then decreases in 2016 by 18%.

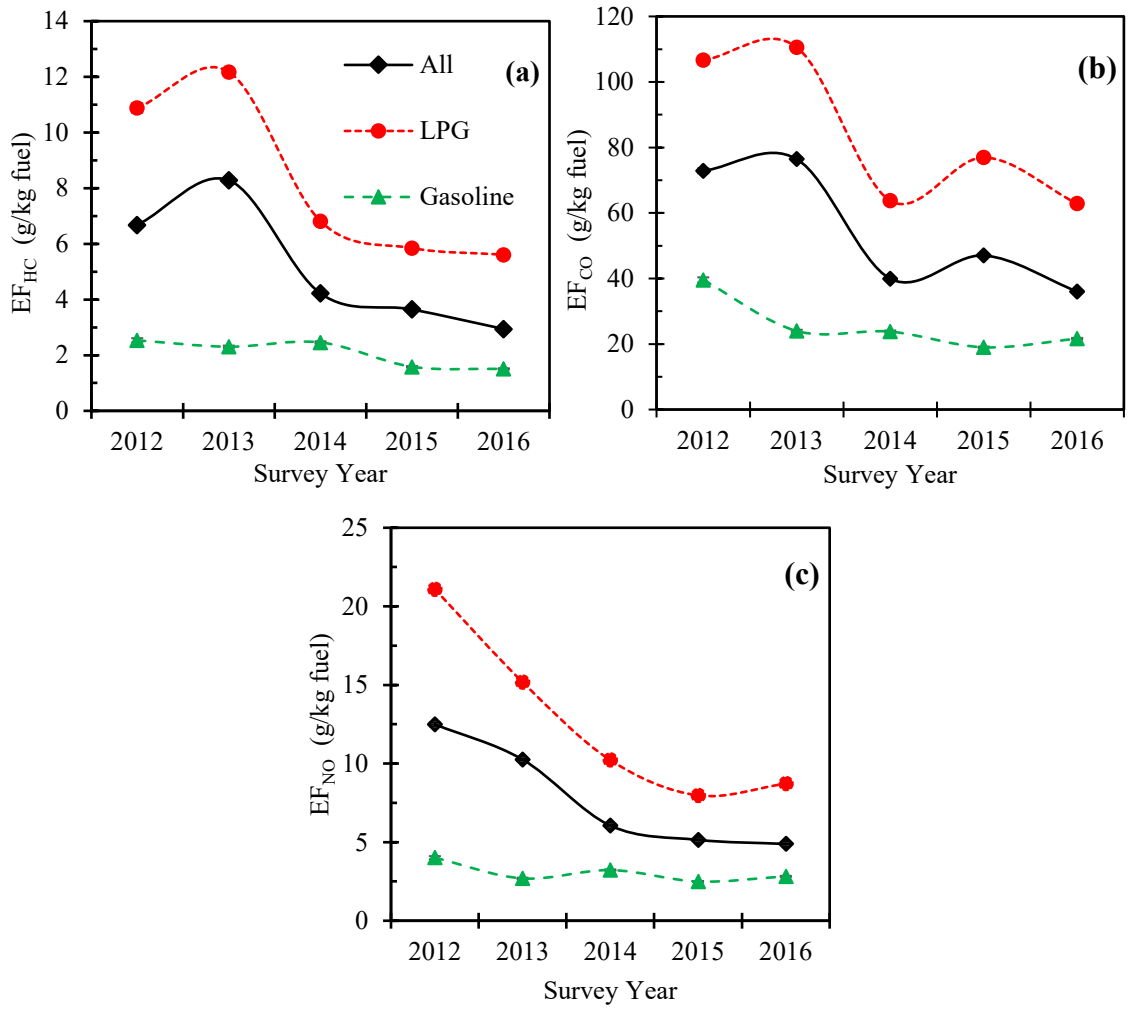

Figure 4.1: Emission factors of HC (a), CO (b) and NO (c) for gasoline and LPG vehicles during 2012-2016.

This significant drop in EF values from 2013 to 2014 for LPG vehicles can be directly linked to the government subsidised programme to provide a free replacement catalytic converter and oxygen sensor per registered taxi and PLB/minibus, as mentioned earlier. The 2013 to 2014 reductions for EF_{HC}, EF_{CO} and EF_{NO} were 44.0%, 42.4% and 32.7% respectively for the LPG vehicle fleet. This improvement in reduced emissions is in line with the effect of other catalytic converter replacement programmes (Brezny and Kubsh, 2013).

The EF results for LPG vehicles can be further investigated to determine the influence of the two dominant vehicle classes, i.e., taxis and PLBs in the results data. Comparing the combined LPG vehicle result against the taxi results (Figures 4.2d-4.2f), some distinct characteristics are observed. The survey years 2012 and 2013 show higher or increasing EFs for each pollutant. The 2014 EF data shows the impact of the catalytic and oxygen

sensor replacement programme as mentioned previously. As the survey years progress from 2015 to 2016 the EFs increase (Lau et al., 2012) as the taxis and PLBs accumulate mileage at a high rate with daily usage (up to 20 hours driving a day for a taxi and 17 hours driving a day for the PLBs). Mileage in excess of 100,000 km annually (Bishop et al., 2016; Lau et al., 2012) is not unexpected. It should be noted in the Figure 4.2 charts that the EF deterioration described for vehicles manufactured after 2008 is present, but it can be obscured by size of the EF scale for the charts. The findings indicate the crucial importance in maintaining the performance of exhaust control systems (Zachariadis et al., 2001). Within the EF chart curves (Figure 4.2), it can be observed that for individual vehicle classes (taxis or PLBs) or models particular vehicle emissions characteristics can be identified and investigated. The characteristics may relate to individual years of vehicle manufacture or relevant European emissions regulations for the vehicle class or model in question.

In the combined LPG EF_{HC} results (Figure 4.2a), there are some emission peaks in 2012 and 2013 survey years before the impact of the Government subsidised LPG catalytic converter and oxygen sensor replacement programme is observed. The results become more consistent (considering age and vehicle emissions standards) until 2016 when the EF_{HC} level begins to increase. Reviewing the taxi EF_{HC} data (Figure 4.2d), the magnitude of these characteristics is less pronounced in comparison to the combined chart (Figure 4.2a). This would suggest the peaks in the manufacture years 2003-2005 in 2012 and 2013 were from PLBs.

In the combined LPG EF_{CO} results (Figure 4.2b), there are two periods where the values are significantly higher, in the manufacturing years 2003 to 2005 range and in 2009 to 2010. The effect of the HKEPD replacement programme is variable for EF_{CO} across the years of manufacture for all LPG vehicles. The taxi EF_{CO} values (Figure 4.2e) show significant reductions from survey years 2013 to 2014 when compared to the combined LPG results. The taxi EF_{CO} did not show any significantly higher results until the survey year 2016 and it is especially pronounced for vehicles manufactured in 2009 and 2010. This suggests that a problem has arisen for vehicles built in these two model years which is impacting the emissions performance. These vehicles are of Euro 4 emissions standards, but not representative of all Euro 4 vehicles. This is potentially an indication of these Euro 4 model vehicles being driven higher mileages than older vehicles and the replacement TWC and oxygen sensors that were installed during the government

sponsored replacement programme have reached the effective end of their service life and need a further replacement.

The peaks in the 2003-2005 range are identified as coming from the PLBs are the source of the higher EFs, which can be traced to the Euro III standard vehicles. It would suggest that the Euro III PLBs have emissions problems with either the oxidation related emissions control or other engine issues which impact emissions, specifically CO.
The EF_{NO} (Figure 4.2 c and f) practically follow the same patterns for the combined and the taxi results. The EF_{NO} reduction in magnitude in 2014 can be linked to the Government subsidised LPG catalytic converter and oxygen sensor replacement programme. The subsequent survey years show EF_{NO} deterioration to be slowly increasing and at levels which are respective to the particular Euro emissions standards for the manufacture year of the vehicles. This indicates the higher EF_{NO} are from the taxis, not the PLBs. The PLB EF_{NO} are lower, but not significantly so that they affect the overall LPG results. Furthermore, it is observed from these results that RS data has been very effectively utilised in identifying high emitters so they can be issued an ETN to be repaired and in turn helping to maintaining significantly lower EF_{NO} for the older taxis manufactured before 2006.

What is evident from reviewing the charts in Figure 4.2 is how effective the combination of the Government subsidised LPG catalytic converter and oxygen sensor replacement programme (Lyu et al., 2016; Yao et al., 2019) and the introduction of the strengthened emissions control programme have been for improving the emissions performance of high mileage accumulating LPG vehicles. Furthermore, it is expected that as the vehicles which participated in the replacement programme continue to accumulate mileage at high rates, that the TWC and oxygen sensor would need replacement every one to two years to maintain emissions compliance or be detected by RS as a high emitting vehicle.

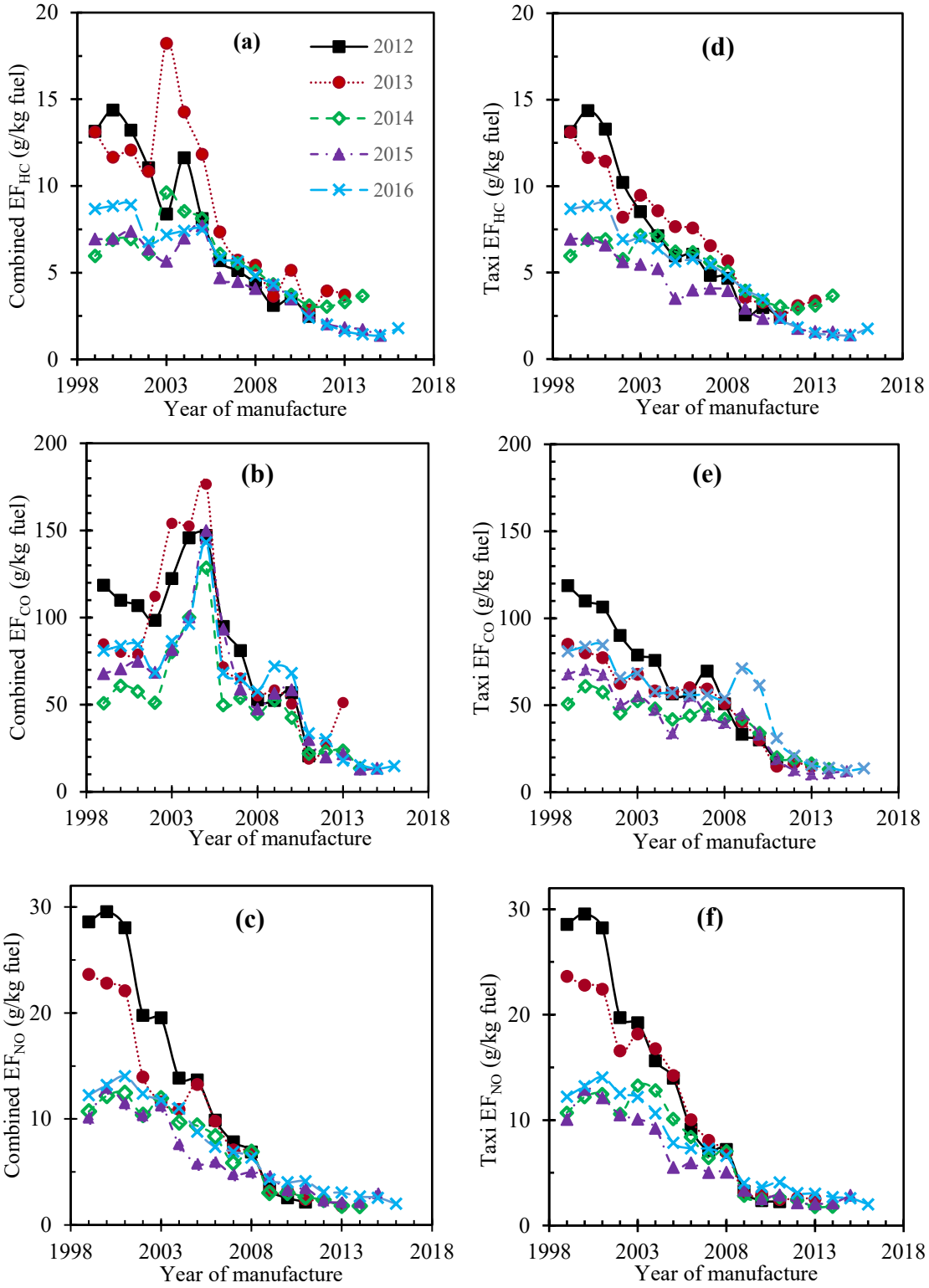

Figure 4.2: Emission factors for all LPG vehicle and taxi measurements.

Figure 4.3 shows EFs for gasoline vehicles by survey and manufacture year for HC (a), CO (b) and NO (c). The gasoline EF results present a summary of a diverse range of vehicles which are on the whole not accumulating mileage at the same rate as the LPG taxis and PLBs (Bishop et al., 2016; Lau et al., 2012) and in turn present lower EFs. The

RS data for gasoline covers vehicles manufactured from 1926 through to 2016. Vehicles with emissions controls were introduced from 1975 in Hong Kong. Reviewing the distribution of the RS data it shows that the majority of all results are for vehicles with a year of manufacture since the mid-1990s. The sample size of data before 1994 is small and presents a large variation in results. For effective analysis purposes detailed analysis has focussed on vehicles with a year of manufacture from 1994 to 2016. The trends of EFs for all of the gases show reducing values which reflect the progress of emissions standards and new technological innovations in emissions controls (Bishop and Haugen, 2018).

The EF_{HC} results (Figure 4.3a) show the highest values in the survey years 2012 to 2014. In 2015 there is an average decrease of 30.3% in EF_{HC} values for the survey year. This overall reduction shows the impact of the strengthened emissions control programme which began in 2014. The EF_{CO} results (Figure 4.3b) show that the 2012 survey year has the highest EF_{CO} values for the survey period, being 27% higher than in 2013 and 2016. The EF_{CO} values start decreasing in 2013 and continue to decrease through to 2015 when they are at their lowest. In the 2016 survey year the trend reverses indicating deterioration of EF_{CO} values, which is partly due to mileage accumulation/fleet aging. Further to this for later model vehicles (manufacture year 2007 and newer), the EF values are starting to returning to levels approaching those from the 2012 survey year. The trends of EF_{NO} values (Figure 4.3c) from survey years 2012-2014 show the values for vehicles manufactured before 2000 to be on average 3.4 times higher and with greater variability in comparison to post 2000 vehicles. In the 2015 survey year there is a 12% decrease in average EF_{NO} values. For vehicles manufactured before 2000 the EF_{NO} values on average have reduced by 22% in comparison to the 2014 survey year. These results show the effective impact of the strengthened emissions control programme after its first full year of operation. In the 2016 survey year, EF_{NO} values are observed to increase on average by 16%. These increases are noted for 86% of the years of manufacture for the vehicles.

The gasoline EF results show the strengthened emissions control programme to have positive impacts for all measured pollutant gases for all vehicle years of manufacture in the 2015 survey data. The reductions achieved in 2015 were 35.6% for HC, 20.16% for CO and 22.5% for NO. In 2016 some deterioration is noted, for HC the changes are minor and just noticeable. For CO and NO the deteriorations are more significant for older vehicles manufactured before 2000. This EF deterioration is affected by the effort made

for RS measurements and the resulting number of ETNs issued. It is noted that the HKEPD has stepped up the roadside RS measurement since 2018 after reviewing the programme data.

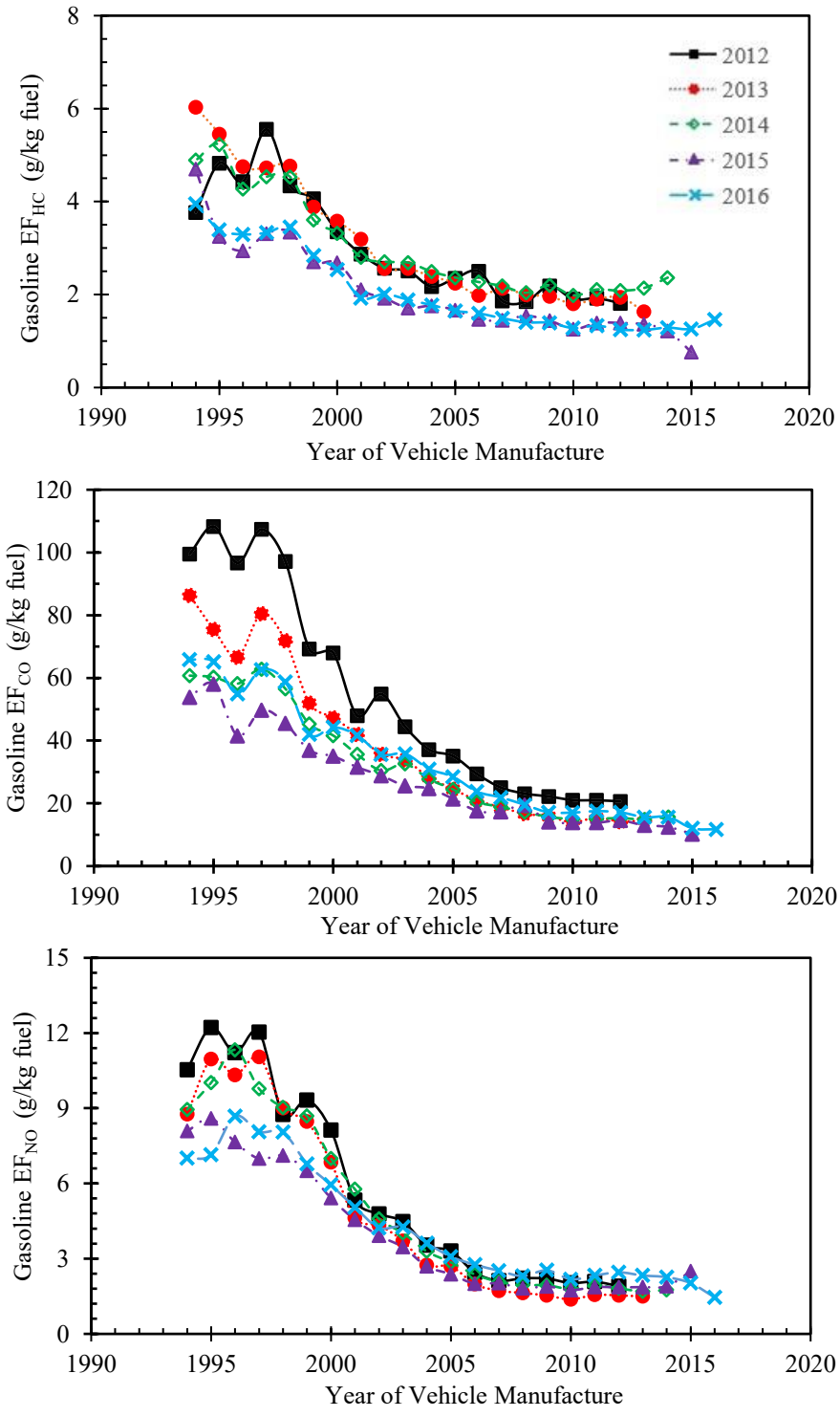

Figure 4.3: Gasoline emission factors by survey year and vehicle year of manufacture

4.2.3 Emissions trends of dominant gasoline vehicle models

The four most commonly measured gasoline vehicles in the survey period comprise 138,875 RS measurements or 21.6% of the results (refer table 4.3 for identification of these vehicles). Figure 4.4 shows EFs for the dominant gasoline vehicles breaking the data down by survey year for EF_{HC} (a), EF_{CO} (b) and EF_{NO} (c). In the survey period the results for all EFs show what could be model to model variation in the years 2012 and 2013 with values being both higher or lower than the average result for 'all gasoline' vehicles. The exception here is the no. 1 dominant vehicle which has lower EFs for all gases in all years of the survey than the average result and also each of the other dominant vehicles as well. For EF_{HC} (Figure 4.4a) the trend for the dominant vehicles shows vehicles 1, 2 and 4 having lower EFs than the average result in 2012 and 2013. This changes in the years from 2014 to 2015. For all of the dominant vehicles there is a noted decrease compared to the average result which is generally maintained in 2016. The EF_{CO} (Figure 4.4b) is decreasing in 2012 and 2013 in line with the average result. This continues in 2014 and 2015 except for vehicle no. 4 which increases above the average result before decreasing to a lower value in 2016. The lowest values for all of the EFs occurs in 2015. The average result and the results for vehicles 1, 2 and 3 then begin to increase in 2016. The EF_{NO} values (Figure 4.4c) are lower than the average result except for vehicle no. 3 from 2012 to 2014. In 2015 this is the only time all vehicles have a lower EF than the average result. From 2016 the EFs for each vehicle begin to increase whilst the average for the whole vehicle fleet result lowers.

The gasoline vehicles which have been measured by RS during the survey period are predominantly private vehicles. Some of them are used by businesses for company transport or commercial purposes such as limousine or private shuttle services, but this comprises only < one percent of the gasoline vehicle fleet (Hong Kong Government, 2018; Transport Department, 2017). For gasoline vehicles there have been no programmes such as the catalyst and oxygen sensor replacement that was undertaken in the LPG fleet which would influence reductions in the EF values. Influencing factors for improving emissions trends of gasoline vehicles would include regular vehicle maintenance, annual roadworthy inspection for vehicles older than six years, replacement of older vehicles by new ones (fleet renewal) and since September 2014 the introduction of the RS programme to strengthen emissions controls.

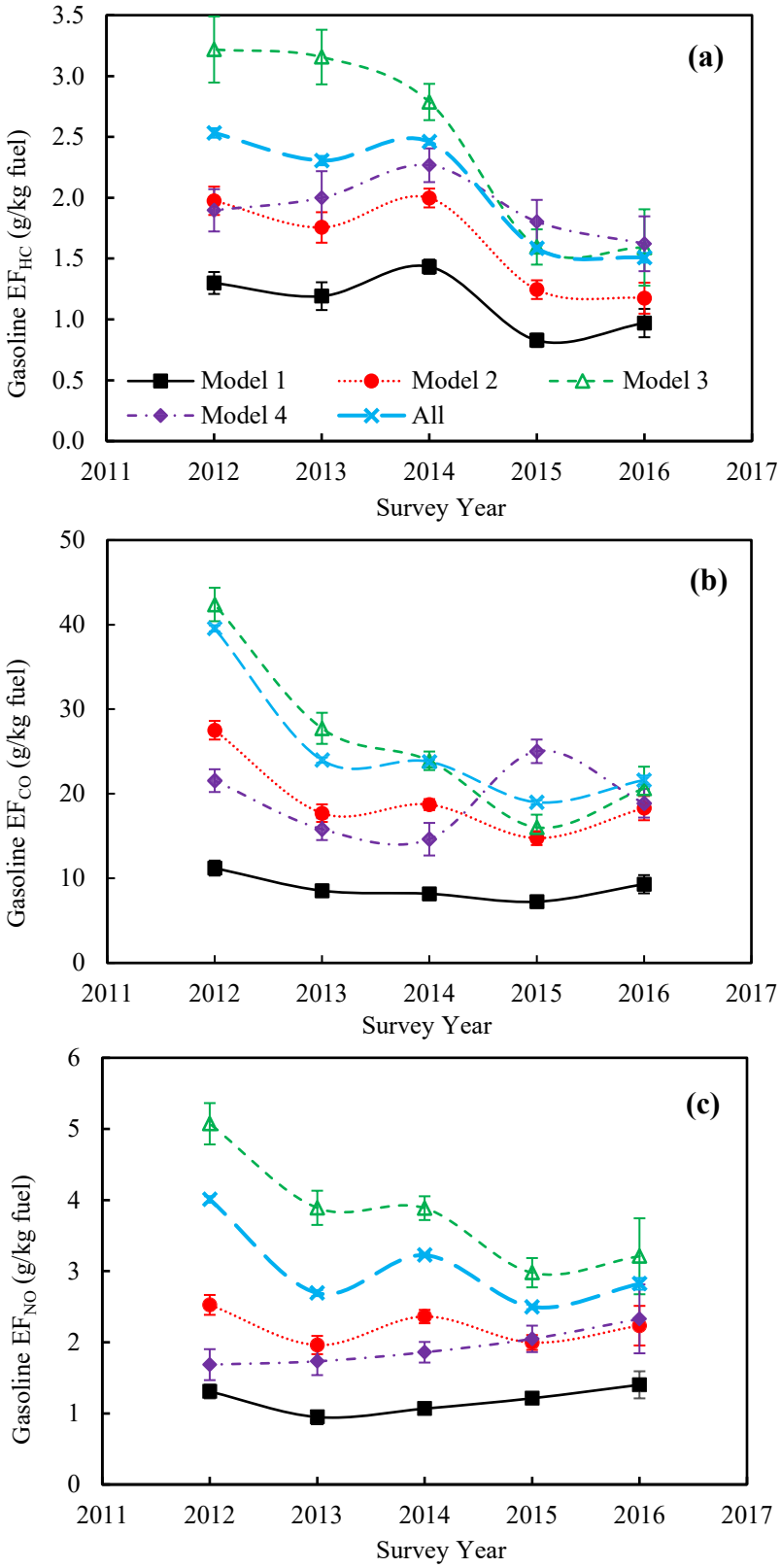

Figure 4.4: Gasoline emission factors for dominant measured vehicle models during 2012-2016. The error bars represent the 95% confidence interval over the mean.

Reviewing the dominant vehicle EF charts for each survey year, for EF_{HC} all dominant vehicle models show a decrease from 2014 to 2015. For $EF_{CO,}$ the trend is the same for all but one vehicle, model 4, which does not start to decrease until the 2015 to 2016 timeframe. EF_{NO} for model 2 and 3 decreases in 2014-2015, then in 2016 all models increase. It is safe to attribute these EF decreases to the introduction of the strengthened emissions control programme. The results for EF_{HC} (Figure 4.4a) show that there is a steep decrease from 2014 to 2015 when the initial impact of the programme would become measurable. EF_{HC} remains at values lower than before the programme began for each dominant vehicle model. The EF_{HC} results suggest all of the dominant vehicle models have responded to the identification of individual high emitting vehicles and the issuing of ETNs with the vehicles being repaired and pollutant emissions lowering in 2015. The EF_{CO} results (Figure 4.4b) show a steady decrease for each vehicle type with the lowest EF_{CO} values in 2015 except for vehicle model 4 which increases in 2015 after the programme has been put in place before having a delayed decrease in 2016 whilst the other vehicles EF values begin to increase in these years. These results suggest that vehicle model 1, 2 and 3 have responded to the influence of the programme in 2015 whilst vehicle model 4 did not until 2016. The EF_{NO} (Figure 4.4c) results differ from both EF_{HC} and EF_{CO}. For EF_{NO} vehicle 1 and 4 show no reduction after the programme begins. Whereas vehicle models 2 and 3 have lower EF_{NO} values in 2015. Further to this there is a steady increase in all vehicle models EF_{NO} values in 2016. This suggests there could be an apparent deterioration for all vehicles and/or especially those accumulating high mileage similar to that of taxis as the fleet is observed to age. These results suggest that for vehicle model 1 and 4 the average NO levels are generally low and on the whole lower than cut point limits for detection of high emitters. Vehicle models 2 and 3 have higher NO levels and with the implementation of the strengthened emissions control programme and the issuing of ETNs the high emitting vehicles of these models are repaired the NO values are reducing in their values from 2014 to 2015.

The overall results indicate that the gasoline vehicle fleet has some high emitting vehicles which are effectively being detected (Lau et al., 2012) and having their emissions related defects repaired or they are removed from the on-road fleet. The overall gasoline vehicle fleet EFs are much lower to begin with than the LPG fleet and as such the reductions appear incremental in comparison to the reductions being achieved with the LPG vehicle fleet.

The gasoline vehicle fleet differs considerably in size, composition and how it is utilised. The percentage of vehicles that are detected as high emitters is much lower than that for LPG vehicles, but the effect of ETNs being issued, repairs made and vehicles returning to the road with lower emissions is measurable as the progressive EF results show from RS data.

A review of the gasoline dominant model's information suggests that for any of these particular vehicle models, the percentage of vehicles needing to be identified as high emitters to be repaired before the EF average for the model decreases is around 5% of the valid RS measurements for that model. Verification of this would require confirmation of data from the HKEPD ETN process. This not possible due to confidentiality and privacy restrictions.

Table 4.6: Average vehicle age (years) for main LPG and dominant gasoline models during RS survey

	Average vehicle age (years)				
LPG	**2012**	**2013**	**2014**	**2015**	**2016**
Toyota Crown Comfort Taxi	**9.6**	**10.4**	**10.8**	**10.2**	**9.7**
Toyota Coaster Minibus	6.5	7.5	8.3	8.9	9.4
Gasoline					
Model 1	**2.6**	3.3	4.1	4.2	4.4
Model 2	5.1	5.9	7	7.3	8
Model 3	6.2	6.9	7.2	7.4	8
Model 4	3.8	4.4	5.2	5.7	6.5

A factor mentioned earlier that can affect the EFs for the vehicle fleet is fleet renewal. To determine if the influence of this has changed during the survey period, the average vehicle ages of the main LPG and dominant gasoline models for the survey period has been checked (Table 4.6).

For LPG vehicles, the average age of taxis was 9.6 years at the beginning of the survey period, it rose to a high of 10.8 years in 2014 before beginning to reduce to 9.7 years by 2016. This data shows for taxis the strengthened emission control programme has been successful in accelerating the fleet renewal of LPG taxis, reducing the average fleet age and helping to reduce emissions. Further to support this observation, it is noted that for LPG taxis in 2012 before the government sponsored catalytic converter and oxygen sensor replacement programme and then the strengthened emissions control programme

implementation began, there were 300 new taxi registrations. By the end of 2015, after 16 months of the strengthened emissions control programme began, there were 2,340 new taxi registrations. This is a change from 1.6% per annum to 12.9% per annum fleet renewal (Transport Department, 2013; Transport Department, 2016).

For the LPG minibuses/PLBs the average age has increased from 6.5 to 9.4 years over the survey period. Whilst the average has not reduced, its rate of increase is noted to be slowing after the beginning of the strengthened emission control programme which suggests that the rate renewal has also increased.

For the Gasoline dominant models, the average age for each model has been noted to be increasing over the survey period, none have reversed the trend. It is noted that for model 1, the increase of the average age has slowed down since 2015. For the other models it has been noted to decrease in 2015 but then increase in 2016. This suggests for Model 1 there is increased fleet renewal in in 2015 and 2016. For the other 3 models the rate of renewal has not consistently increased. It should also be considered that gasoline vehicle renewal rates will not show the same improvement as the LPG vehicles as these vehicles are predominantly private cars and utilised in a different manner, often with much lower mileage when compared to vehicles used for commercial operation.

Overall, these results clearly show that the strengthened emissions control programme is providing non-invasive on-road monitoring data which is able to cover a significant proportion of the vehicle fleet. The ability to measure hundreds to thousands of vehicles at each measurement site on any day provides an amount of emissions data many times greater than any other individual vehicle measurement programme that has been utilised previously. The results over the five-year period show that since September 2014, RS data has been successfully utilised to identify high emitting vehicles providing a new mechanism for the HKEPD to ensure the high emitting vehicles are repaired and pass the proscribed emissions test or be removed from the vehicle fleet.

4.3 Conclusions

This chapter analysed the effectiveness of a unique strengthened emissions control programme using RS technology. The large size of the unique dataset has allowed for analysis that shows there are high confidence levels in the resultant EFs calculated for each element of assessment undertaken. The following conclusions can be derived from the results of the data analysis.

- Due to poor maintenance practices where failed catalytic converters and oxygen sensors were not regularly replaced, the LPG vehicle fleet was shown to be emitting significantly higher amounts of regulated pollutants than the gasoline vehicle fleet. From 2013 to 2014, a government sponsored catalytic converter and oxygen sensor replacement programme for taxis and PLBs proved to be highly effective in reducing the EF_{HC}, EF_{CO} and EF_{NO} by 44.0%, 42.4% and 32.7% respectively for the LPG vehicle fleet. For the whole survey period (2012-2016), overall LPG EF reductions of 48.4% EF_{HC}, 41.1% EF_{CO} and 58.7% EF_{NO} have been achieved.
- Gasoline vehicles had the lowest EFs throughout the survey period with the implementation of the strengthened emissions control programme. During 2014-2015, reductions of 35.6% HC, 20.16% CO and 22.5% NO were achieved. For the whole period (2012-2016), there were overall gasoline EF reductions of 40.5% HC, 45.3% CO and 29.6% NO.
- From January 2012 to December 2016, the overall EF reductions of 55.9%, 55.6% and 60.9% were achieved for HC, CO and NO, respectively.
- The results confirm that the combination of the government sponsored catalytic converter and oxygen sensor replacement programme then followed by the strengthened emissions control programme was effective in reducing emissions levels and identifying high gasoline and LPG emitters, allowing HKEPD to issue ETNs so these vehicles were able to be repaired and pass the proscribed emissions test or be removed from the vehicle fleet. The RS survey data was also effective in highlighting particular manufacture years and Euro emissions standards of taxis and PLBs which were the high emitters needing urgent maintenance.

Chapter Five

5 Analysis of simulated engine faults and their impact

From the literature review, one of the items identified as needed to assist with improving the success of an enhanced emissions control programme using RS was information on what engine and emissions system faults will produce the highest levels of pollutant emissions. This crucial information is key to improving the education and training available to the repair industry on the specialities of emissions repairs, but it was found to be mostly absent from the published literature. Some studies (listed within this chapter) had focussed on selected parts or failure modes, but nowhere was there a comprehensive study which could deliver this information. The following outlines the background of the faults and the summary of results for each of the selected systems in respect of pollutant emissions, fuel economy impact and resultant CO_2 emissions. In all it shows the real difference that can be made when individual high emitting vehicles are repaired and maintained as required.

5.1 Introduction

The performance of vehicles being driven on-road has long been a major focus of manufacturers, regulators and users (De Simone et al., 2019). Characteristics such as reliability, speed, handling and fuel consumption were often the focus of manufacturers and users as these impacted sales, user satisfaction and operating costs (Grigoratos et al., 2019). As vehicle fleet sizes increased and road traffic density intensified, the negative environmental emissions impact of vehicles became evident (Haagen-Smit, 1962; Requia et al., 2016; Weber et al., 2019). The identification of the pollutants and the mechanisms that created them lead to a progressive development of increasingly stringent regulations to address the problems at the source. In turn validation of emissions performance/compliance was necessary and the evolution of laboratory emissions testing of vehicles developed and became the standard for regulatory type approval. Testing

technology has progressed to improve measurement capabilities in the years since regulations were established and more recently the introduction of real driving emissions (RDE) to measure on-road emissions have enabled regulators and manufacturers to reduce the gap between real-world and laboratory performance (Bishop et al., 2019; Huang et al., 2019c; Kumar Pathak et al., 2016). The goal of these testing mechanisms is to support the target of reducing emissions from vehicles to meet Clean Air Plan targets or AQOs that have been established in various regions and cities around the globe.

On the vehicle side to achieve this continuous drive for lower emissions, numerous technological advancements have evolved to address the various aspects of pollution control and mitigation (Chandra and Camal, 2016). The majority of vehicles being manufactured and in use currently utilise engines based on the Otto cycle. For these engines, developments in emissions control, fuel injection, engine management and hardware have improved their emissions performance and fuel economy. Developments and innovations such as Exhaust Gas Recirculation (EGR), the progression from carburettor to mechanical then electronic fuel injection (EFI), pressurised fuel systems, manifold absolute pressure (MAP) sensors, manifold airflow (MAF) meters, electronic throttle control (ETC), spark plug development, TWC and oxygen sensors all of which are connected and controlled by an engine control unit (ECU). All of these systems have been studied extensively by manufacturers to investigate the effectiveness of each of the individual systems and how they improve vehicle performance and reduce emissions throughout a vehicle's lifecycle (Zhang et al., 2018). When vehicles utilising these technologies are new or on the road with low mileage the systems will still be in good condition and performing effectively to meet regulatory requirements. As mileage increases, the maintenance of each of these systems is crucial in ensuring the overall driving and emissions performance of vehicles (Austin and Ross, 2001; Hickman, 1994). Since the usage of each vehicle on-road varies, deterioration of these systems whether by tampering, lack of or infrequent maintenance or failure as mileage accumulates begins to impact the capability of vehicle to maintain their compliance to performance standards/regulations (He et al., 2019).

This brings the focus of this part of my research to the technical training for mechanics and technicians. Training standards vary in each country around the globe and overall training for students requires them to learn and assimilate knowledge on all the various systems present in vehicles. As such the focus regarding exhaust emissions compliance

is just one of the many aspects of the overall vehicle knowledge which students will need to learn during their training. What is identified from this is that mechanics and technicians working in the automotive repair industry could have a lack of detailed knowledge or experience when it comes to the overall emissions performance impact of malfunctions and failures of one or more of these technologies. It should also be noted that the primary focus for maintenance/repairs and vehicle performance had been to make sure that faults which impact driveability, safety and fuel economy are repaired promptly to ensure costs are minimised. Furthermore, consideration of costs and these elements were regularly put before vehicle emissions. As deteriorating or poor air quality in major cities like Hong Kong continued to be an on-going issue, it was evident that without a process or mechanism to push vehicle owners to keep vehicles in good condition and the automotive repair industry to improve the effectiveness of maintenance to reduce emissions. This issue would likely see the continuation of deteriorating air quality.

This highlighted the need to identify individual high emitting vehicles and then require them to be successfully repaired by the local vehicle repair industry. It was determined that a real-time monitoring tool capable of passively measuring hundreds of passing vehicles per hour should be utilised to identify high emitting vehicles. The tool selected to be most effective for this task was RS (Huang et al., 2018b; Organ et al., 2019). With RS to use as an effective tool, the HKEPD worked to develop a new strengthened emissions control program to identify high emitting gasoline and liquified petroleum gas (LPG) vehicles (Hong Kong Government, 2014) and have them repaired. The vehicle repair industry reaction to the introduction of the RS programme was of concern as it was identified that detailed knowledge for repairing emissions failures had not been a major industry focus previously and there was concern vehicle owners or operators could be unfairly impacted financially if vehicles failed to pass testing after repairs with the possibility of vehicles being deregistered. To address this situation, the HKEPD begun an engagement exercise supporting a series of testing and evaluation programmes to engage with transport operators, repair industry associations and other stakeholders to identify which hardware failures impacted the transport industry and its performance. The most frequent and worst-case failures were determined from the programmes and the information shared with all stakeholders. With a list of hardware failures identified, planning was undertaken to manage industry concerns and deliver an acceptable outcome which would improve the emissions performance of the on-road vehicle fleet. This

outcome was that a programme would be established to support improving the required emissions testing outcomes for high emitting vehicles identified by the RS enforcement programme. I was able to undertake this task and worked to build up a test vehicle which could be used to simulate a comprehensive range of commonly observed engine and exhaust component failures as worst-case scenarios. A list of failures was compiled from the earlier consultation exercise was used to plan the simulated emissions faults for study. Demonstration of these failures were then performed under repeatable test conditions using a chassis dynamometer where the automotive repair industry members/audience were able to learn firsthand about the impact of different failed components and which repairs were needed to ensure vehicles would be compliant with their respective emissions regulations.

Reviewing studies conducted on failure simulations shows they have focused on specific elements of vehicles. Toma et al. (2019) tested fault simulations created by disconnecting the electrical connector from either the MAP sensor, a fuel injector or the oxygen sensor. The testing was performed on four Dacia Logan cars at low and high idle and 50 km/h steady state speed. They observed significant increases of THC and CO for the MAP sensor and higher again for the oxygen sensor fault. Each of these observed results are a product of the ECU using open loop operation when sensor signals are not available. Nevius et al. (2012) conducted emissions measurements using PEMS and FTIR recording the outcome of EGR valve failure. The effectiveness of the EGR valve when working correctly to reduce THC, CO and all NO_x gas species to the vehicles Euro 4 emissions limits was shown. Lee et al. (2002) studied the impact of variations to engine ignition such as ignition retard, ignition timing, excess air or fuel and misfire on close coupled TWC at various engine loads from 1,500 to 4,000 rpm. They identified the damage that can occur to TWC from misfire, too much retard and excess air ratio all of which lead to higher temperatures above 1050°C which will damage the precious metals in the TWC wash coat. Zheng et al. (2018) conducted testing on taxis with deactivated TWCs showing the significant emissions difference between these vehicles and ‘China 4’ regulation taxis with active catalysts. Comprehensive studies generally have not been conducted to cover a complete range of common failures to determine their emissions impact, except for a recent study on a diesel Euro VI medium goods vehicle (Huang et al., 2019a). As the combustion and emissions aftertreatment technologies between diesel and spark ignition engines differ considerably, so the outcomes of that study vary from the results of this

study. The value and novelty of this study cannot be understated as it unique in demonstrating a broad range of emissions failures for spark ignition engines and can help professionals in the automotive repair industry quickly and effectively identify emissions faults for repair.

The aim of this research was to simulate commonly identified engine faults and their impacts on vehicle emissions, fuel consumption and drivability. In total 15 different malfunctions (targeting worst case conditions) were simulated using a chassis dynamometer, which were grouped into the following functional areas: air intake, fuel delivery, ignition and exhaust after treatment systems. It provided essential knowledge for the automotive repair and maintenance industry to effectively identify and repair emission-related faults of LPG and gasoline vehicles. It also established a higher and more comprehensive level of research undertaken to address improving knowledge and its delivery to industry, which was a necessary support for improving the results of the HKEPD RS enforcement program. In addition, it provides further value in outlining a proven research and training framework that could be utilised in other cities and regions to characterise and address failures producing high emissions from their vehicle fleets regardless vehicle type, age or emissions standards.

5.2 Results and discussion

The results analysis and discussion are separated into the following sub-sections. Sub-section 5.2.1 covers the effect of malfunctions on regulated gaseous emissions. Sub-section 5.2.2 covers the effect of the malfunctions on CO_2 emissions and fuel consumption. Sub-section 5.2.3 discusses which malfunctions impact the driveability performance of the vehicle. Sub-section 5.2.4 outlines how the industry training programme was organised utilising the results of the study for improving the knowledge and experience of the repair industry.

5.2.1 Regulated gaseous emissions

The European emissions regulations for light duty (< 3.5 t) positive (spark) ignition engine vehicles have emissions factor limits specified in g/km. The Toyota Crown Comfort Taxi tested in this study was built to the Euro 2 standard. The UNECE Regulation 83 Euro 2, type 1 test emissions limits for these vehicles were 0.5 g/km for THC+NO_x and 2.2 g/km for CO (Australian Government, 2018). Figures 5.1 and 5.2 show the effect of the simulated engine malfunctions on THC and CO, respectively. For reference, the Euro 3 emissions limits have been included in these tables as the Euro 3 standard vehicle was similar in construction to the test vehicle used in the study. The differences for the Euro 3 model are a larger TWC, upgraded mixture control valve, throttlebody venturi and ECU software to improve cold start and hot emissions performance. A summary showing the comparison of the relative changes of emissions factors for each simulated malfunction and the baseline test is presented in Table 5.1.

Table 5.1: Summary of relative change from baseline test of emissions factors of simulated malfunctions.

System	Fault Description	(g/km)			
		THC	CO	NO_x	NO_x + THC
Exhaust system	Worn/Aged TWC	131%	211%	178%	161%
	Faulty O2 sensor - 0.1V	249%	150%	33%	109%
	Faulty O2 sensor - 0.9V	317%	410%	61%	152%
	EGR valve open	169%	34%	3%	62%
	EGR valve closed	-45%	-39%	72%	31%
Fuel system	Overly rich Air-fuel ratio	17%	276%	-5%	3%
	Overly lean Air-fuel ratio	-32%	-38%	-41%	-38%
	Restricted main fuel	49%	-5%	352%	245%
	Restricted idle fuel	30%	294%	-6%	6%
	Faulty fuel cut valve	-39%	-43%	-50%	-46%
Intake system	Worn Throttlebody	31%	218%	-40%	-15%
	Sticky mixture control valve	168%	782%	-86%	4%
	Sticky idle control valve	-28%	-51%	151%	88%
Ignition system	Faulty spark plug	0%	60%	-40%	-26%
	Faulty distributor cap and rotor	-13%	-29%	-20%	-17%

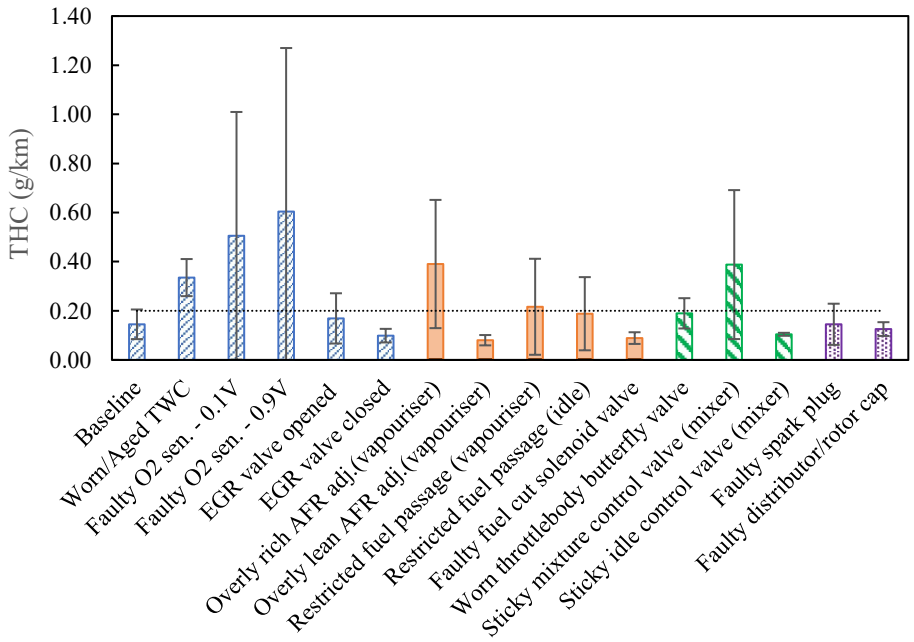

Figure 5.1: THC emissions results for malfunctions. Error bars indicate standard deviations and the dotted black line indicates Euro 3 THC emissions limit. (For Euro 2 standard, THC emissions are combined with NO_x)

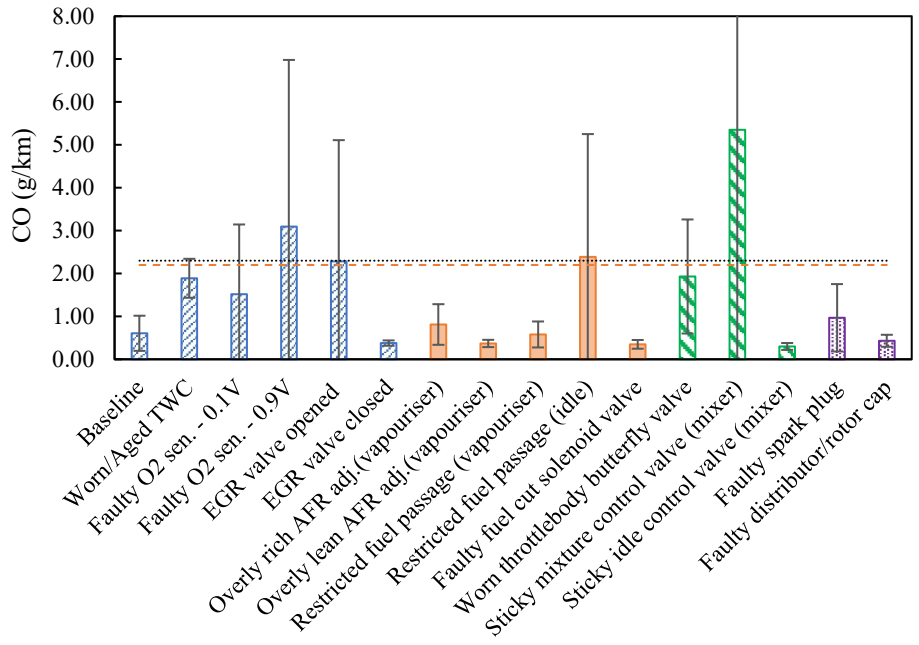

Figure 5.2: CO emissions results for malfunctions. Error bars indicate standard deviations and the dashed orange line indicates Euro 2 CO emissions limit. Dotted black line indicates Euro 3 CO emissions limit.

Reviewing the results for the simulated malfunctions, the majority of the THC and CO emission factors are lower than both the Euro 2 and 3 emissions limits. The impact of the simulations shows for many of the failures there is little effect on the emissions or there are slight reductions from the baseline result. The THC results, Figure 5.1, show that for six out of the 15 simulated malfunctions the emissions factors are similar to or lower than that of the baseline result. The CO results (Figure 5.2) show a similar pattern as the THC for these six simulated malfunctions, five are the same as THC, having similar or lower emissions factors as the baseline result. This consistency is not unexpected as THC and CO emissions often have similar trends in spark ignition vehicles. When these results are compared to the THC+NO_x and NO_x results (Figures 5.3 and 5.4), it can be seen in some instances the simulated malfunctions have trends that are opposite to the results observed for THC and CO. This also is expected when the balance of fuelling has been biased either rich or lean by the simulations. These results provide support to the different/conflicting emission formation mechanisms of THC/CO vs NO: THC and CO are results of unburnt and partial combustion respectively (mainly rich fuel combustion) while NO is formed in high temperature rich-oxygen condition (slightly lean fuel combustion) (SAE, 2015).

The baseline test result with the new catalyst and all systems functioning properly shows this high mileage vehicle (odometer mileage of > 436,000 km when tested) to be in good condition and repair to have relatively low emissions for each individual pollutant gas or combination of gases when tested using the HKTET transient emissions test.

The highest increase in the THC emissions factor is the result of a simulated faulty oxygen sensor signal which produces increases of 4.2 times for THC (206% of the THC+NO_x limit) and 5.1 times for CO. This has occurred when the oxygen sensor signal voltage has been replaced by a constant input voltage (0.9 V). In this instance the ECU has trimmed/reduced the fuel supply as the supplied voltage simulating the sensor signal indicates the combustion is rich. When this reduction in fuelling has occurred, it produced misfire events and has resulted in high THC and CO levels being produced. The highest increases in the CO emissions factors are the result of a sticky mixture control valve which produces increases of 8.8 times for CO (243% of the CO limit) and 2.7 times for THC. This has occurred when the mixture control valve sticks when operating. In this instance there has been excess fuel resulting in rich combustion. Further faults producing significant increases are the low oxygen sensor supply voltage malfunction (0.1 V) with THC and CO being 3.5 and 2.5 times higher. In this instance when the fuel trim has added more fuel, the combustion becomes rich and delivers unburnt THC as well as CO. The restricted idle fuel delivery fault simulation has also produced CO emissions 3.9 times higher (109% of the limit) when the fuel supply is unstable at idle, this produced rough idle and impacted the completeness of combustion. The other fault simulations which produced higher THC and CO emissions than the baseline was either just greater than the Euro 2 emissions limits or just below them. The faulty/aged TWC produced THC and CO emissions that are 2.3 and 3.1 times higher than the baseline. In this instance only when THC+NO_x results, Figure 5.3, are combined does the result exceed the Euro 2 emissions limit (214% of the limit). Further noticeable increases that occurred are the overly rich Air Fuel ratio adjustment producing THC and CO emissions 1.2 and 3.8 times the baseline result (104% of CO limit). Other increases greater than the baseline result but lower than the emissions limits were from the EGR valve jammed open, restricted fuel passages for main and idle fuel supply and the worn throttlebody valve.

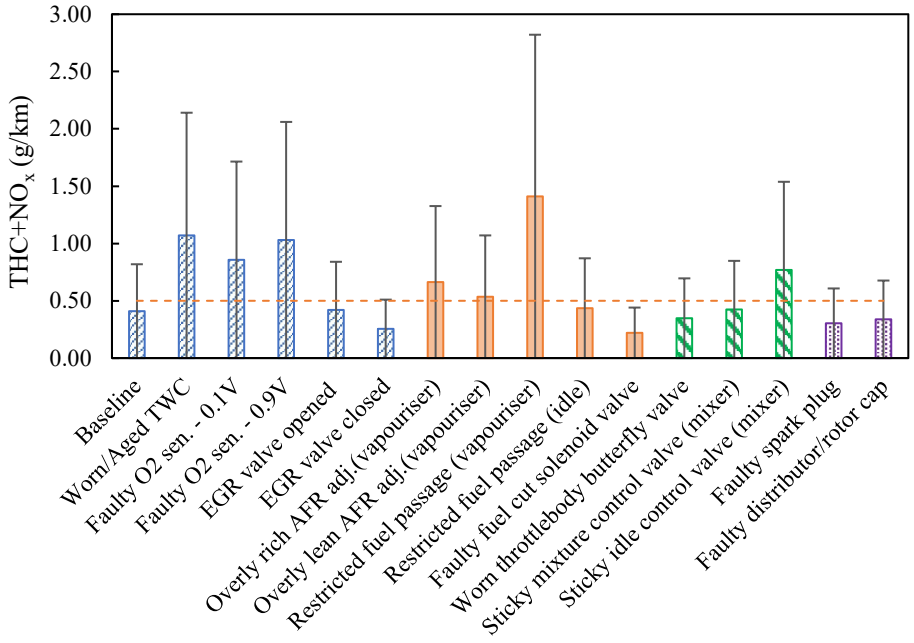

Figure 5.3: THC+NO_x emissions results for malfunctions. Error bars indicate standard deviations, and the dashed orange line indicates Euro 2 THC+NO_x emissions standard.

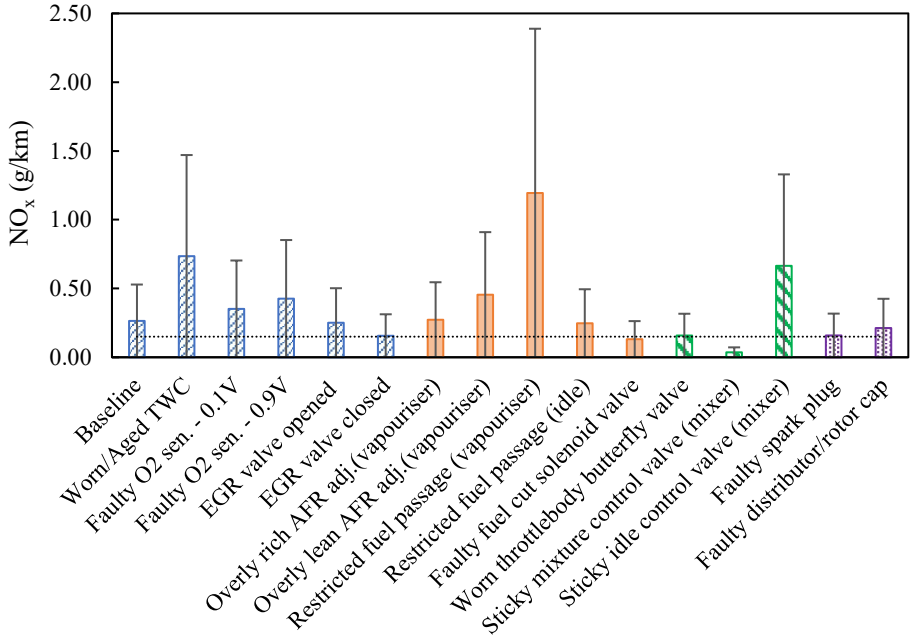

Figure 5.4: NO_x emissions results for malfunctions. Error bars indicate standard deviations and the dotted black line indicates Euro 3 NO_x emissions limit.

The highest increase of NO_x emissions, Figure 5.4, resulted from the restricted fuel supply passage in the vapouriser malfunction producing significantly lean conditions with NO_x emissions 4.5 times higher than baseline result (282% of THC+NO_x limit). The

worn/aged catalyst follows with NO_x emissions 2.8 times higher than the baseline (214% of THC+NO_x limit, as mentioned previously). The faulty oxygen sensor high voltage 0.9 V NO_x emissions were 1.6 times higher and when combined with THC exceeded the limit (206% of THC+NO_x limit). The sticky idle control valve produces 2.5 times higher NO_x emissions above the baseline (154% of THC+NO_x limit). When the EGR valve was jammed open (maximum EGR), NO_x emissions were similar to the baseline, but when considering the combined emissions of THC+NO_x the result exceeds the limit (133% of THC+NO_x limit).

Of these increased emissions results, the ones that attracted the most interest from government representatives, the trade and industry were the impact of the worn/aged TWC and the faulty oxygen sensor. The worn/aged TWC produced significant increases for each pollutant and with the results exceeding the respective reference emissions limit. The oxygen sensor results were more significant for THC and CO with the increased emissions of both of these pollutants with the results exceeding the respective emissions limits. The assessment of these particular malfunction simulation results reinforced support for the effectiveness a programme the HKEPD had undertaken from August 2013 to April 2014 to provide a one-off subsidised replacement catalyst and oxygen sensor for taxis and light buses (Hong Kong Government, 2012; Yao et al., 2019). This was significant as the impact of worn/aged catalysts and faulty oxygen sensors were not apparent to all owners, vehicle operators and repairers as these faults were not impacting driveability, downtime and operating costs for vehicles.

What is clearly observable from the malfunction simulation results is that there are a number of failures which produce unacceptably high results for all of the emissions gases in the roadside environment. In numerous cities worldwide the concentration of NO_x at the roadside is major problem. Whilst a significant portion of this can be traced to diesel vehicles (Grange et al., 2017), it should not be ignored that gasoline and LPG fuelled vehicles can also contribute to this problem as well (if their catalyst is not working properly for instance), being that they are the major portion of vehicles on-road. Being able to quantify the impact and magnitude of failures for each individual part of these vehicle engine systems, the critical focus can then be moved to ensuring these parts are properly understood and maintained by the repair industry and vehicle owners/operators. It further provides evidence to support the quantifiable benefit of having an RS monitoring programme capable of scanning the majority of a city or regional vehicle fleet

on a regular basis. Providing regulatory bodies with the ability to identify high emitters and also to provide feedback to the repair industry and associations on the most likely failures on a regular basis can ensure on road vehicle fleets will run at the lowest emissions levels possible.

5.2.2 Fuel consumption and CO_2 emissions

The fuel consumption of any vehicle is constantly being assessed by owners and fleet operators as it impacts the economic cost of operation. Likewise, the CO_2 emissions from vehicles are directly representative of fuel consumption and additionally they impact our environment by contributing to ambient CO_2 levels rising and which adds to greenhouse effects in the environment. The results for fuel consumption (l/100km) and CO_2 emission factor (g/km) are shown in Figures 5.5 and 5.6 respectively. Table 5.2 shows the relative change from the baseline result for fuel consumption and CO_2.

Table 5.2: Summary of relative change from baseline test of CO_2 emissions factors and fuel economy (l/100km) of simulated malfunctions

System	Fault Description	CO_2 (g/km)	Fuel Economy (l/100 km)
Exhaust system	Worn/Aged TWC	5.9%	7.3%
	Faulty O2 sensor - 0.1V	9.5%	10.8%
	Faulty O2 sensor - 0.9V	6.0%	8.9%
	EGR valve open	10.9%	11.4%
	EGR valve closed	5.0%	4.6%
Fuel system	Overly rich Air-fuel ratio	3.4%	4.8%
	Overly lean Air-fuel ratio	5.0%	4.7%
	Restricted main fuel	7.7%	7.7%
	Restricted idle fuel	4.4%	6.0%
	Faulty fuel cut valve	10.5%	10.1%
Intake system	Worn Throttlebody	14.4%	15.5%
	Sticky mixture control valve	-1.3%	3.3%
	Sticky idle control valve	11.2%	10.8%
Ignition system	Faulty spark plug	5.6%	5.8%
	Faulty distributor cap & rotor	6.2%	5.9%

The emissions factor results show that the majority of the fuel has been burnt in the engine and converted to CO_2. The fuel economy and CO_2 follow the same pattern and magnitude in almost all of the fault simulations. Where there are variances in the pattern it can be traced to higher emissions of CO produced as a result of the fault simulations. Malfunctions producing higher CO emissions were the sticky mixture control valve and the high oxygen sensor voltage as discussed in reviewing Figure 5.2.

Overall increases in fuel consumption figures compared to the baseline result were moderate with the highest increase of 15.5% from the worn throttlebody valve. This was followed by 11.4% for the EGR valve jammed open, 10.8% for the sticky idle control valve and low oxygen sensor voltage. The next highest increases were 10.1% from the faulty fuel cut solenoid and 8.9% for the high oxygen sensor voltage. The remainder of the increases ranged between 3.3% to 7.7% higher than the baseline. These results show the impact of malfunctions in normal operations will consume additional fuel. There were no results better than the baseline fuel economy. It was the lowest fuel consumption result of the study. The closest was a 3.3% increase for the sticky mixture control valve. This result could be considered representative of normal testing variation.

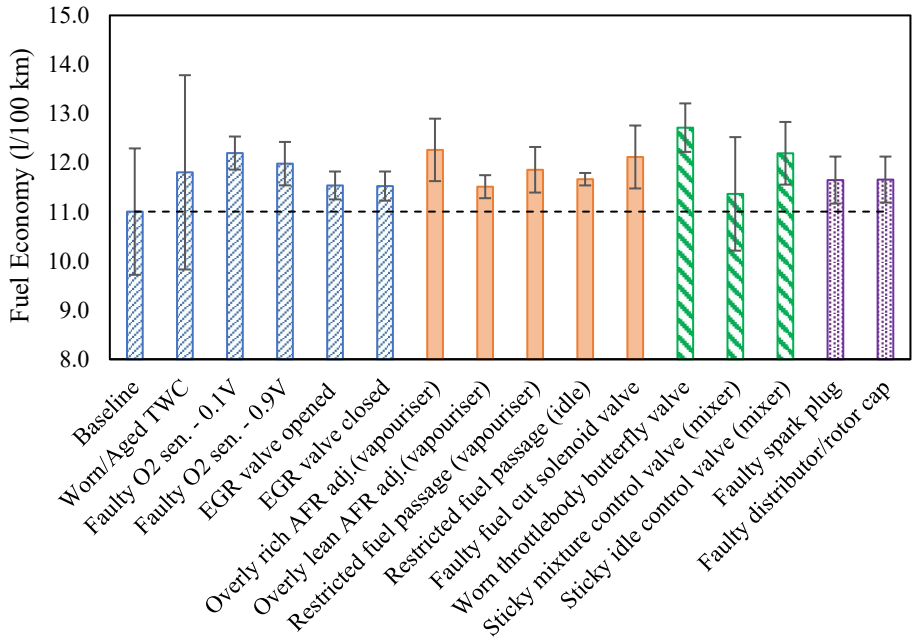

Figure 5.5: Fuel economy results for malfunctions. Error bars indicate standard deviations and the black dashed line represents the baseline fuel economy.

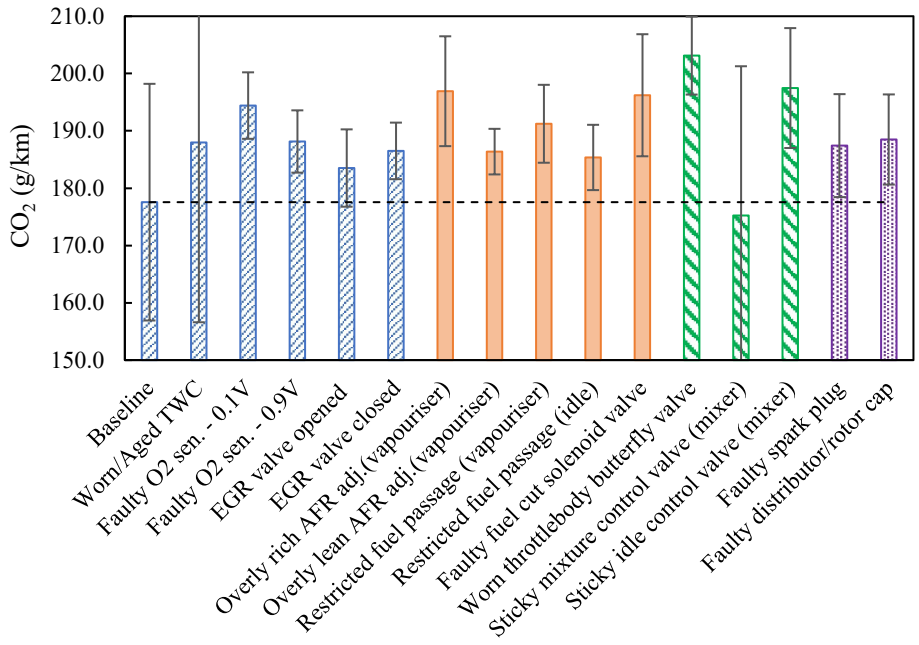

Figure 5.6: CO_2 emissions results for malfunctions.

Error bars indicate standard deviations and the black dashed line represents the baseline CO_2 emissions.

5.2.3 Impact on drivability

The impact on drivability of these malfunctions was variable. If the emissions increased as a result of the malfunction simulation, the drivability was not necessarily affected in a negative fashion.

From the exhaust system malfunctions, the impact on driveability was not noticeable for the worn/aged TWC, oxygen sensor faults and the EGR valve jammed closed. The vehicle responded as expected and drove in the manner anticipated for a vehicle running normally. When the EGR valve was jammed open the performance of the vehicle at idle was impacted. Idle stability was poor and acceleration from a standing start was rough.

The fuel system malfunctions which impacted the emissions also had an impact on the drivability. The restricted main fuel supply in the vapouriser produced increased NO_x emissions as well as having an impact on the performance. There was a speed response lag when the vehicle accelerated. The restricted fuel to the idle control valve in the mixer

produced rough idle with misfire occurring when insufficient fuel was available for ignition. The resultant poor idling reduced the quality of the driving experience.

Two of the intake malfunctions impacted drivability. The worn bushings on the throttle body butterfly valve resulted in the valve not moving smoothly and sticking at points when accelerating and decelerating. This impacted the drivers' ability to maintain smooth accelerations, decelerations and maintaining the desired/stable test speeds. The sticky mixture idle control valve produced rough idle as the valve opening time was longer than normal when activated. Both of these malfunctions reduced the quality of the driving experience. The sticky idle control valve also produced increased NO_x emissions which exceeded the regulation emissions limit.

The ignition system spark plug malfunction produced misfire events, whilst these were noticeable, the impact to the driving performance was limited to reduced driving quality. This malfunction produced increased CO emissions by 5.3 times.

For the malfunction simulations tested in which the driveability is affected there can be significant variations in results which can be attributed to rough and or unstable engine idle and running. This significant variability leads to large error bars for the results.

5.2.4 Impact on industry training and knowledge

The results of the fault simulations from this study provided compelling evidence to show which failures would impact roadside emissions and air quality in faulty gasoline and LPG fuelled vehicles (Organ et al., 2020). It highlights the need to identify and deal with maintenance and repairs of malfunctioning vehicle engine and emissions control hardware. In Hong Kong utilisation of RS has provided the mechanism to identify significant numbers of high emitting vehicles. A vehicle is identified as a high emitter when emissions exceed two times the emissions limit for its respective European regulation. Being able to effectively repair these vehicles is the required outcome to reduce emissions and improve air quality. To deliver this outcome after vehicles are identified as high emitters, it is necessary to ensure vehicle mechanics have the requisite knowledge to effectively identify and repair emissions related faults. Developing a

training/education programme to do this is a necessary prerequisite for delivering a successful I/M programme.

The organisation of the technical training sessions began by advertisements being placed in popular local newspapers, information was circulated to all automotive industry groups, repair associations, by email and letter and it was advertised online on the HKEPD website. The advertised programme of free training sessions (funded by the HKEPD) were listed and interested automotive industry staff, repair industry staff or members of the public could enrol to attend (first priority was allocated to industry staff before members of the public). The training programme provided sessions broken into specialised half day sessions (a half-day session being chosen so as to minimise the impact on businesses when staff attended) which were conducted at various locations in the different regions around Hong Kong. The demonstration taxi was taken to each training location so that it could be used for testing demonstration and explanations during the sessions. The sessions were led by HKEPD technical staff with support from a mechanic with suitable knowledge and experience in emissions diagnosis and repair and support technicians to run HKTET emissions tests.

The utilisation of the emissions testing and fuel economy results of these simulated malfunctions along with the demonstration taxi provided a solid foundation for the local Hong Kong automotive and repair industries to develop their emission related knowledge for vehicles. Training sessions were able to highlight which malfunctions had the greatest potential to produce high emissions. There were two types of training sessions organised for the attendees to choose from. The first was a ‘Mechanic Service Session’ where the HKEPD technical staff worked with a mechanic who had been trained in emission repairs and was familiar with the vehicle and the components. They would display the hardware in question and demonstrate its function. The second consisted of a ‘Workshop Service Session’ where the taxi would be tested on a chassis dynamometer to demonstrate the simulated malfunctions which produced high emissions. Following this the support mechanic would then demonstrate the ways to reduce the emissions from the taxi by undertaking the necessary/proper maintenance to return a vehicle to normal/low emissions and fuel consumption ensuring that drivability and performance were achieved as well.

5.3 Conclusions

The aim of this chapter was to conduct a broad range of 15 simulated malfunctions on a Toyota Crown Comfort LPG taxi to determine their impact. The simulated hardware malfunctions from a range of various engine systems known to fail or breakdown were thoroughly investigated to determine their effect on gaseous emissions, fuel economy and performance when tested on Euro 5 compliant chassis dynamometer and emissions measuring system. The test results were compared against a baseline result for the taxi in good mechanical order with the engine and all hardware functioning properly. The results of the study clearly show that when engine hardware and emissions control systems are working together properly, they are clearly capable of achieving emissions pollution control and vehicle driving performance targets. The main points are summarised as follows:

- For six of the malfunctions, there were insignificant changes or lower results for THC and CO emissions factors. There were however increases for the high voltage faulty oxygen sensor signal of 317% (0.604 g/km) for THC and for the sticky mixture control valve of 782% (5.351 g/km) for CO. Other malfunctions which produced high THC emissions were the low voltage oxygen sensor signal of 247% (0.506 g/km) and the EGR valve jammed open of 169% (0.369 g/km). High CO emissions were produced by high voltage oxygen sensor 410% (3.09 g/km), the restricted idle fuel supply of 293% (2.388 g/km) and the worn/aged TWC of 211% (1.89 g/km).
- The most significant NO_x increase was for the restricted main fuel supply in the vapouriser of 352% (1.41 g/km). Other simulated malfunctions producing high NO_x emissions were the worn/aged TWC 178% (0.735 g/km) and the sticky idle control valve of 151% (0.665 g/km).
- The fuel economy and CO_2 emissions produced moderate increases with the largest increase in fuel consumption being 15.5% for the worn throttlebody. Likewise, it had the highest CO_2 emissions increase of 14.4%. Eight of the malfunctions had fuel consumption and CO_2 emissions variations 5% higher which would noticeably impact the fuel economy and operation cost of the vehicle.

- Negative driveability impacts were not necessarily related to increases in emissions from malfunctions. The EGR open malfunction impacted the smoothness of the drivability under idle and acceleration conditions. Fuel system malfunctions in the main fuel and idle fuel delivery plus the worn throttlebody and sticky mixture idle control valve in the intake system impacted acceleration smoothness, driving stability and idle control which reduced the quality of the driving experience.
- An effective training programme was able to be implemented by the HKEPD using the demonstration taxi and the fault simulation results. The training utilised evidence supported testing with tailored sessions for the automotive and repair industry to learn which malfunctions have the greatest impact on emissions, fuel consumption and drivability. The training provided essential knowledge to the industry with positive progress being noted after the first half year to successfully repair vehicles identified as high emitters to pass required emissions test standards.

Chapter Six

6. Factors affecting RS sensitivity

A significant portion of the literature published regarding RS is devoted to outlining the results obtained by individual surveys undertaken to determine the emission profiles in various locations around the world. In some cases, it has been instrumental in identifying failures of emissions regulations to reduce specific emission types (Borken-Kleefeld and Chen, 2015; Carslaw and Rhys-Tyler, 2013). What was not published is material outlining the functional aspects of RS and what variables or characteristics of the technique impact the accuracy and usability of the results. This type of information is needed to deliver improvements to the performance of RS and to potentially expand its applicability in successfully being able to identify high emitting vehicles using any the various fuels commonly available on the market currently.

One of the interesting results from chapter 4 shows that the current RS technology being applied is effective in identifying high/gross emitters from vehicles built to the Pre Euro to Euro 4 emissions standards. For vehicles built to Euro 5 and 6 emissions standards, the results from these are being measured at values which are frequently at or lower than the rated accuracy tolerances for the current RS equipment. In this situation, the RS system is not able to effectively be used to detect an emissions limit lower than that for a Euro 4 vehicle. Hence, the current RS system effectively allows Euro 5 and 6 vehicles to potentially have significantly higher emissions which exceeds an ideal reasonable level for these emissions standards due to the capability limitations of the equipment when measuring HC, CO and NO.

Experimental work undertaken during my research into RS reviewed various aspects of measurements and testing that could be undertaken in laboratory conditions to test various aspects of vehicle testing. This was needed to further characterise and understand the nature of the RS measurement process and data being collected. Initial experimentation utilised a combination of an RS system in the laboratory in conjunction with laboratory emissions analysers or PEMS to characterise the emissions from a vehicle or engine source with known/consistent operating conditions. To provide steady state emissions,

vehicles were set up on chassis dynamometers and driven under a range of operating speeds.

To investigate and potentially improve the equipment capability, a local RS contractor, Green Environmental Emission Consultants Ltd. (GEEC) who provides monitoring services to HKEPD has been working to develop an RS system which can reduce the uncertainty of measurement. Whilst investigating the characterisation of RS, I engaged GEEC with the goal to try to obtain the stream of individual data points making up the sets of data used to produce the final emissions concentrations and ratios, with testing setups as shown in Chapter 4. As the planning and discussions progressed a significant difficulty became apparent. Generally, the equipment manufacturers and suppliers who produce RS equipment are reluctant to provide the detailed information used to determine the final RS figures utilised as they want to protect their Intellectual Property and methodologies used in design, manufacture and operation of the equipment from other manufacturers. After significant discussions and negotiations, it was agreed they would provide unprocessed sensor data which could be used to compared the system performance between various testing configurations/setups for my experiments. To provide a reference baseline, other conventional emissions measurement equipment was used to determine actual emissions levels. This data collected from experiments was utilised for assessment of the RS instrument performance.

6.1 RS instrumentation calibration

The calibration of RS instrumentation is an area in which key factors controlling the measurement are checked and confirmed to be within performance specifications. For RS, calibration has been a potential source of measurement variability. Since RS has been in use, there have been different calibration procedures used in a laboratory or workshop setup and onsite measurement. In a laboratory or workshop setting the calibration measurement has utilised a static measurement device setup in the RS beam between the light source and the detector into which a regulated amount of a reference span gas is injected (Bishop et al., 1989). The duration of this measurement can be set up to simulate the on-road duration, say 0.5s, or modified per individual equipment manufacturers specifications. This, combined with a zero-reference measurement, allows instrument

verification in a closed environment. When onsite, the RS instrument is calibrated in an open environment. When the equipment has been set up, a puff of a reference span gas from a pressurised gas bottle, BAR-97 High Range calibration gas, is injected into the light beam to again check the performance. The onsite calibration check must be successful before the RS instruments can be used for data collection (Bishop et al., 1989; Huang et al., 2018b; Organ et al., 2018). Furthermore, routine checking of the data to ensure stability and drift are within acceptable parameters for the RS system in use is conducted after each hour of testing.

These types of calibration checks have been utilised since roadside RS measurements were introduced and reported in 1989. As manufacturers of RS equipment have developed their own unique equipment/systems, they have also further developed their own parallel calibration methods. One common method in bench testing of RS equipment has been to use a variable volume chamber that the RS beam can pass through in which a known concentration of gas is contained. The size/length of the chamber can be varied and excess gas is moved from or into a side storage compartment. This allowed for a consistent bench test result to be achieved, but it was not a dynamic measurement that could compare well with the puff gas test or the with on-road real-world testing conditions.

When vehicle fleet raw emissions levels were higher in the 1990s and early 2000s, the impact of differences between variable bench testing practices and real-world RS testing was very low. But as the Euro and USEPA regulations have progressed, the impact of the differences of measurement techniques has become significant due to the much lower emissions standards and now requires a standardised approach to be developed and taken so effective comparisons of different equipment manufacturers products and their respective instrument calibrations can be established.

The HKEPD had noted this issue when they compared RS equipment and measurements from various manufacturers and found a range variability when comparing various RS suppliers' measurement data for late and current model emission regulation vehicles. HKEPD needed to ensure each RS system could be checked to ensure each could meet a standardised calibration check. To do so, they started to design a new calibration testing system and I worked with them providing some design suggestions, a vehicle testing laboratory with potential emissions sources and emissions measurement equipment to conduct experiments to help setup and investigate the results and in turn develop the technique.

6.1.1 Initial version of calibration device

The proposed initial concept for a standardised calibration device uses the premise that the sample of gas measured by an RS system will initially hold constant ratios of target gases. To take advantage of this, the target measurement gas is injected into an open-ended rectangular box structure or chamber which would contain the gases for a few seconds before they spread out the ends and dissipated from the controlled volume of the device.

To try to achieve this, an initial device was built to allow the introduction of a sample of reference gas into one end of a large rectangular chamber which was open at each end so the RS light beam could pass through it. The measurement sample was released from a gas cylinder and drawn from its injection point through the chamber by an exhaust fan installed at the far end of the device chamber on the opposite side to the injection point and into an exhaust suction hose. Whilst being drawn through the chamber, the gas inside was subject to induced turbulence and mixing. To facilitate this, two holes had been added to the chamber, also on the side opposite the gas injection point. These were connected by pipes to an axial circulation fan installed to assist with circulation of the air within the chamber and to assist its dispersion as an exhaust plume would in a real-world on-site RS measurement situation.

Initial testing was performed utilising reference span gases discharged in short bursts from a low pressure prefilled storage cylinder. Trial test gases utilised were BAR-97 High range calibration gas (3200 ppm HC, 8.0% CO, 12.0% CO_2 and 3000 ppm NO), high concentration, CO (9%), CO_2 (9.4%) and N_2 as zero gas. Additionally, a 2kVA gasoline fuelled generator was used to provide a raw exhaust gas sample during the testing as well.

The trial calibration device was able to draw the injected reference gas samples through the chamber. Whilst RS measurements were successfully recorded, they varied pending a number of factors as explained below:

- The amount of suction applied to the exit either by the exhaust fan and/or with the exhaust suction pipe applied.

- The additional mixing and via the axial fan introduced the target dispersion, but the magnitude varied pending the speed and the air flow direction of the fan.
- Injecting gas from a pressurised storage vessel produced a concentrated injection plume which did not begin dissipate until it equalised in pressure
- When the exhaust gas from the gasoline fuelled generator was utilised the RS measurements showed there was significant range of variation measured as the loading control was not stable.

Overall, whilst a number of the tests with the trial device produced greater measurement variability than desired some aspects of the trial device showed that it had the potential for producing a suitable device for checking the performance of any subject RS system. The features of most interest were the chambers size, shape, its ability to draw in sample gas or exhaust gas and being able to facilitate a moderate amount of dispersion. Another lesson learnt was from the injection of pressurised reference gases (from low pressure storage cylinders), the gas remains concentrated and at a different temperature momentarily to ambient in the injection plume before equalising and beginning to dissipate. This can produce offsets in the results when data measurements are taken before the plume velocity reduces, the temperature equalises and the gas begins to mix and dilute into the ambient air in the measurement chamber.

6.2 Refined RS calibration device

From the experience gained in using the initial calibration device, a new calibration device was designed and fabricated for further testing. The initial device consisted of a wooden box structure with an injection tube, suction fan and mixing/dispersion pipes attached. The refined concept was designed and fabricated from sheet metal. To promote improved dispersion of the target gas sample the refined device had finally been made with the standard or reference sample gas injection point centrally positioned to provide an even dispersion for the gas into the chamber. The size of chamber had been widened and two symmetrical ducts had been installed to draw the gas sample from the injection points along the opposite wall to the sides and the rear of the device. In lieu of one large circulation or suction fan, five smaller individually selectable fans were installed to

provide a range of potential suction rates. Figure 6.1a shows the schematic and 6.1b the setup utilised for experimental tests.

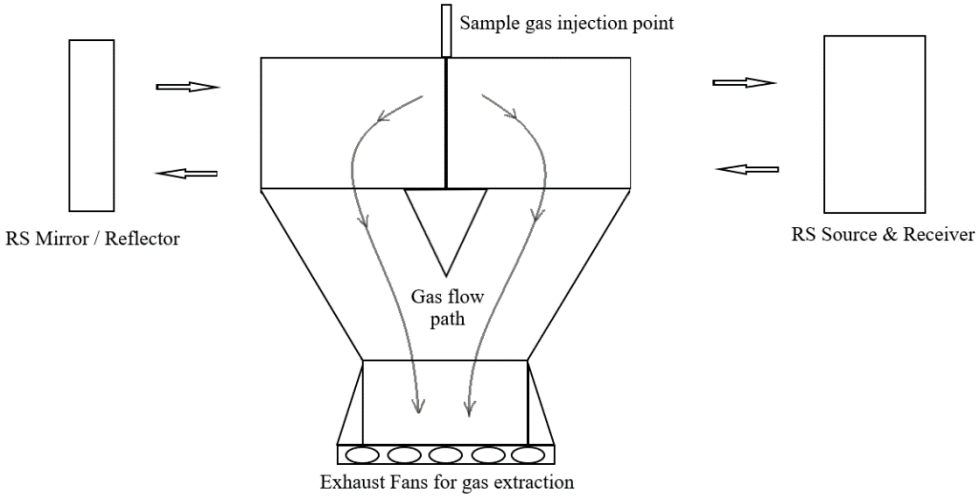

(a)

(b)

Figure 6.1: Refined RS calibration device – schematic (a) and test equipment setup (b).

Testing was undertaken with the refined RS calibration device using a diesel generator as the emissions source connected to either an industrial vacuum cleaner or an induction heater for the electrical loads. Initial testing utilised the industrial vacuum cleaner to provide a series of loads upon the generator. The generator, temperature logging, EMS gas analyser and load were set up and data collected, as shown in Figure 6.2.

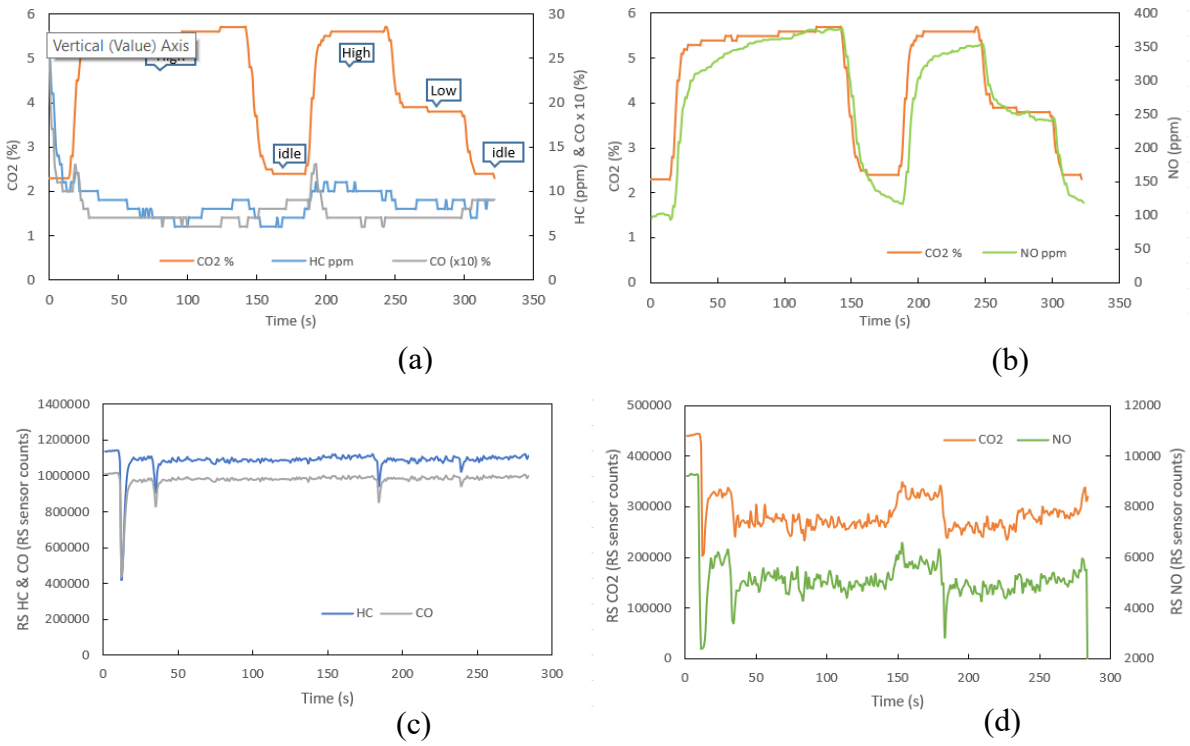

Figure 6.2: Refined calibration device emissions measurements from EMS 5003 gas analyser (a and b) and from RS device (c and d).

The EMS gas analyser measurements show the emissions response of load increases and decreases to the electrical load of the industrial vacuum cleaner connected to the diesel generator. The CO_2 emissions (Figure 6.3 a and b) reflect the respective fuel consumption changes, for high load, low load and idle. The output data from the RS measurements (Figure 6.3 c and d) taken using the calibration device show the target wavelength absorption responses to the exhaust gas emissions.

Each set of traces (EMS 5003 and RS) show the similar, but inverse response patterns (i.e., the RS sensor count value will reduce as the gas concentration increases) when comparing the CO_2 and NO data and likewise the HC and CO data from the conventional gas analyser and the RS measurement system. When comparing the emissions traces from the two systems with the exhaust gas temperature, a significant measurement difference is noted in the RS data for measurements at the same load condition, which is not present in the EMS data. Figure 6.3 shows the comparison of emissions and exhaust gas temperature.

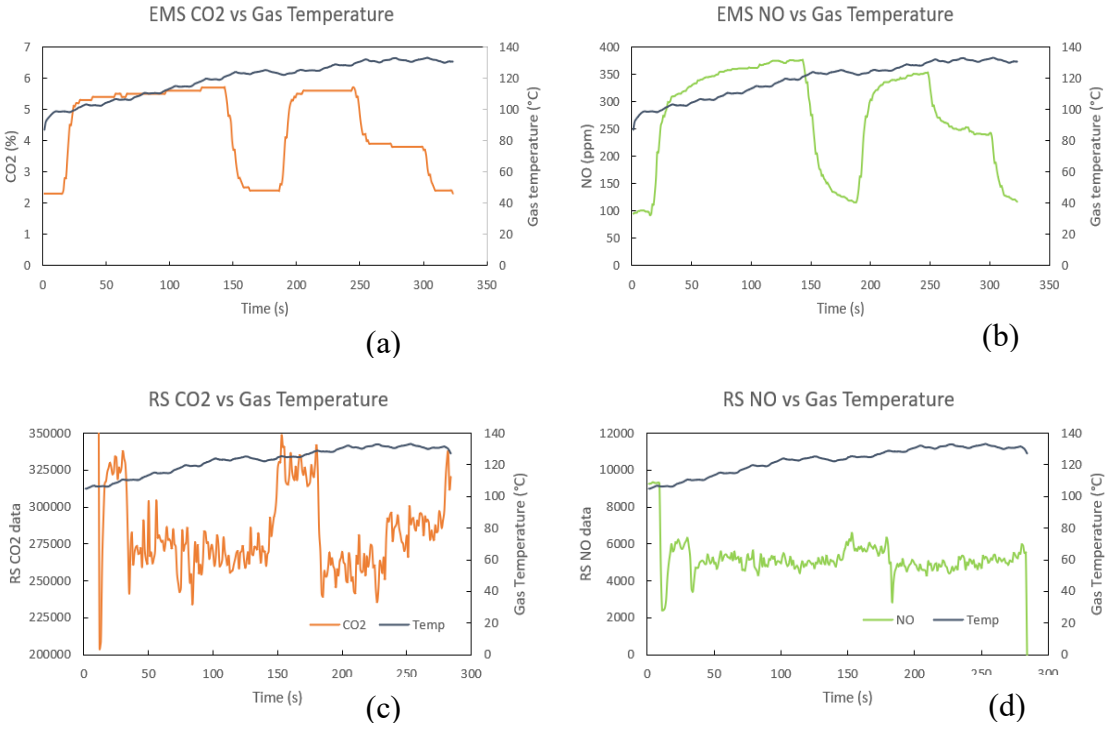

Figure 6.3: Comparison of EMS 5003 gas analyser (a and b) and RS (c and d) data with exhaust gas temperatures.

From the review of the CO_2 data for the high load condition, the EMS chart shows consistent average concentrations of 5.56-5.60% independent of exhaust gas temperature. The CO_2 RS shows differing average data outputs of 270,095 units @ 112.7°C and 258,757 units @ 127.3°C. The NO data from the UV channel shows some similar RS characteristics at the high load conditions (Table 6.1). Ideally a further comparison of the measured gas concentration of the gas from the RS instrument would be desirable to complete the comparison, but it was not available from the RS instrument setup in these experiments. Whilst not available in this case, the signal was able to be compared to a conventional emissions analyser using a traceable calibration gas and is comparable to other RS data outputs recorded in these experiments.

A second test setup trialling the use of an induction heater in place of the industrial vacuum cleaner was utilised to collect a further dataset. The induction heater loading on the generator was cyclical (digital on/off cycle) and did not provide a stable dataset from either EMS or RS measurement systems.

Table 6.1: RS and temperature data comparison

	RS average unit output	Temperature (°C)	Diff from CO_2 ref
CO_2 ref	442,750	90	
High load no.1	270,095	112.7	61.0%
High load no.2	258,757	127.3	58.4%
Δ	11,338	14.6	2.6%

	RS average unit output	Temperature (°C)	Diff from NO ref
NO ref	9259.5	90	-
High load no.1	5072.7	112.7	54.8%
High load no.2	4760.81	127.3	51.4%
Δ	312	14.6	3.4%

The experimental data identified there is an impact of variable gas temperatures on the RS output signal for CO_2 and NO measurements. As CO_2 molecules can absorb and emit energy from IR radiation, the motion of CO_2 molecules increases at higher temperatures and the amount of emitted radiation energy can increase or decrease with temperature variation (UCAR, 2022; Wei et al., 2018). To further investigate the magnitude of the effect of varying gas temperature changes on the RS signals, improvements to the experimental setup were required. The variable with the greatest potential to improve measurement stability was the loading method of the generator. The industrial vacuum had provided two stable loads, but more load control was required. The induction heater had 10 variable heat settings for loading, but it was not suitable due to its cyclical loading pattern.

A new solution was required to achieve an improved result. A revised setup was established utilising a DL2090 (220Vac and up to 3.6kW) variable resistor load bank as the electrical load for the generator. Utilizing this, an assessment of the system performance with the resistor load bank was undertaken with a series of four measurements divided into two sets of tests being conducted.

The first and second tests applied basic step loading patterns to the generator. Test 1 stepped from low to high loading, (0 - 2.3 – 7.6 - 11.1- 0 Amps) and Test 2 stepped from high to low loading (0 – 12.6 – 7.6 – 0 Amps). The test duration was 600s with loading steps on average of 120s.

Test 1 followed a steady load ramp from low to high loads with exhaust temperature 1 and 2 (measured after generator exhaust) steadily increasing throughout the test. The remaining temperatures do not vary noticeably until a loading of 11.1 A is applied towards the end of the test cycle. CO_2 measurements from the AVL PEMS gas analyser and RS appear relatively consistent. The monitored exhaust temperatures at the RS measurement point do not vary significantly through the duration of the test.

Test 2 followed a reverse pattern with an immediate step from an idle after start up to high loading, 12.6 A. In this instance the initial high transient loading has resulted in a short duration unstable generator operating condition producing smoke and in turn the CO_2 measurements do not show a smooth/steady step change after the load increased. When comparing the difference test 1 steps are between 10 to 15s in duration before stabilising whereas in test 2 it can take at least 45s or three times longer. Test 2 overall shows there is a lasting impact to the CO_2 emission measurements when high loading occurs and subsequently steady state running of the equipment takes much longer to achieve. Analytically the exhaust gas temperatures are seen to rise faster in Test 2.

The second set of tests, 3 and 4, were modified and used a revised loading pattern based on test 2 as it could deliver higher gas temperatures for RS measurement. The peak loading step on the generator was reduced to minimise issues of combustion instability and reduce smoke production. Furthermore, to investigate the potential of temperature effects impacting the RS measurements the exhaust pipe from the generator to the flow valve was insulated to reduce heat losses and the tube length between the valve and thermocouples 3, 4 and 5 was shortened. Also, to simulate a vehicles exhaust system the shortened tube was pre heated before the test began to around 80-85 °C (standard diesel vehicle engine coolant temperature) before the measurement begins. The test pattern load cycle was setup (0 – 10.2 – 5 – 2.3 – 0 Amps) and repeated to complete two load cycles with a duration of 1200s or greater. On the revised calibration device three of the five exhaust fans were turned on and the flow valve was set to 50% open to allow half the exhaust gas to enter the calibration device. Results from test 3 and 4 are shown in Figure 6.4.

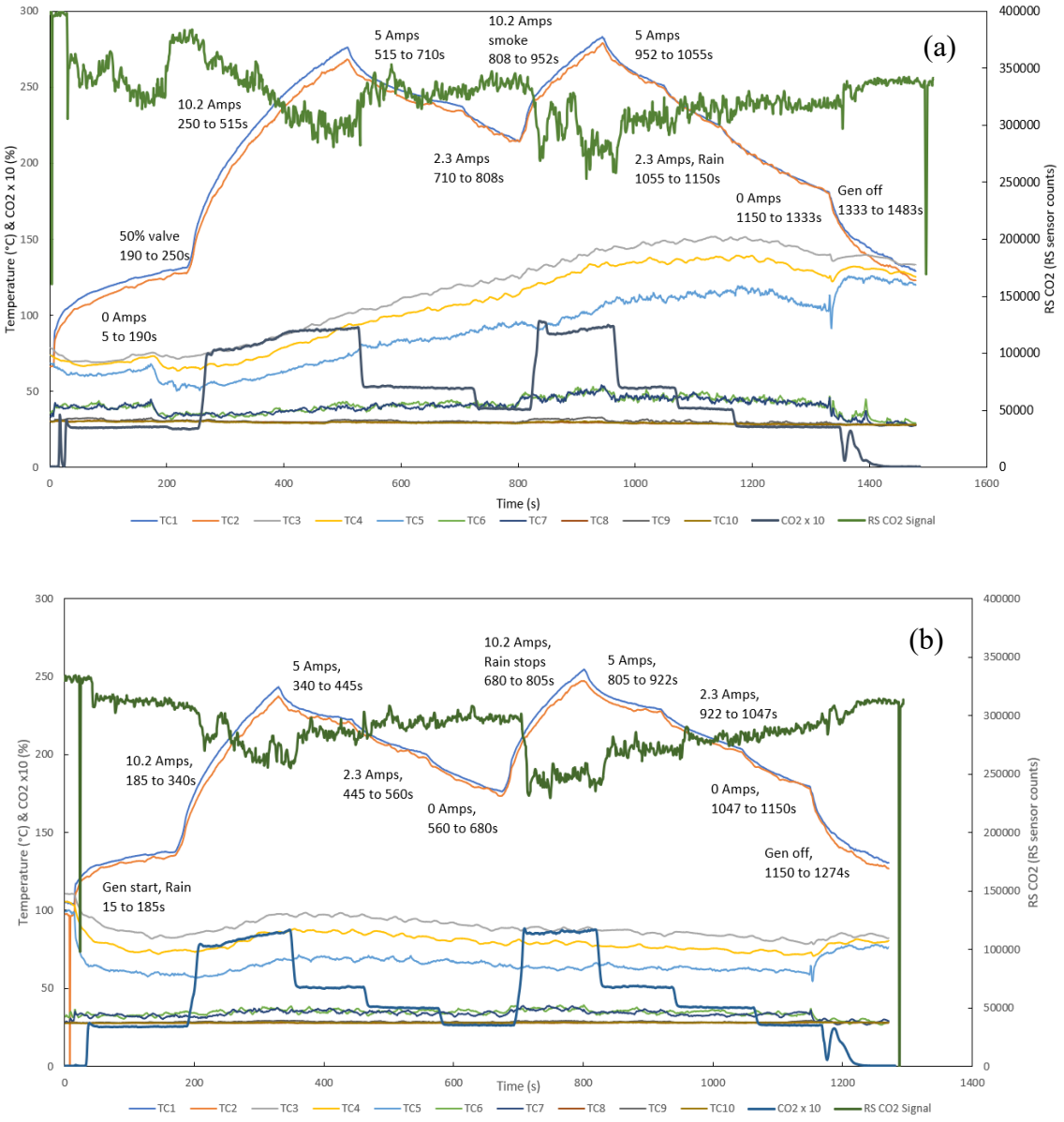

Figure 6.4: Resistor load bank test for revised calibration device.

Test 3 (Figure 6.4 a) proceeded with a steady response of the diesel generator to the applied loading. After starting and a short idle period with zero load, the step to 10.2 A was selected and immediately the combustion was more stable with no visible smoke being produced. CO_2 measurements from the AVL shows a range from 7.4% to 9.0 % CO_2 first 120 s at 10.2 before stabilising. The RS CO_2 signal data shows a similar response. It is noted that when changing from the idle condition to the 10.2 A the temperatures measured at thermocouples 3 through to 7 all drop initially by around 10 degrees suggesting a short transient cooling effect as a result of the higher mass flow rate from the generator before returning to increasing temperatures after 30s.

The response of the system to the decreasing step loads from 10.2 to 5 to 2.3 A shows temperatures at thermocouples 1 and 2 decreasing while temperatures at thermocouples 3 to 7 keep increasing. This data shows a reasonable system response, whilst the combustion temperatures were decreasing, they were still high enough to continue heating the exhaust system further away from the engine.

As the loading pattern repeats and continues through to the end of the cycle, thermocouples 1 and 2 recorded a similar pattern of temperature responses and 3 through to 7 continued increasing until the load applied became zero. Whilst the emissions analyser CO_2 measurement values remain similar or the same, the RS CO_2 signal is noted to vary more comparing the magnitude of the signal values during the first load steps compared to the second set of load steps. The RS CO_2 values noted during the second set of steps vary from 15,000 to 20,000 units lower than those from the first set. As the operation of the generator and its loading has remained consistent during the test, this suggests that gas temperature has been a significant variable delivering the variation in the RS CO_2 signal measurement. Between the first and second loading sets the temperature at thermocouples 6 and 7 were 35 – 40°C and 38-50°C respectively.

Test 4 (Figure 6.4 b) followed a similar pattern to test 3 with an additional step in the first set from 2.3 to 0 A so both of the load sets matched. It was missed in the first set load steps of test 3. The measured temperatures for the engine exhaust at thermocouples 1and 2 were consistent with each other, and so to were the AVL CO_2 measurements. It was noted the maximum temperatures were in the range of 20 to 30°C lower than in test 3. In this test the measured temperatures from thermocouples 3 to 7 were both lower and showed less range variation than in test 3. This suggested the RS CO_2 measurements might be of similar magnitude to each other. This was not the case; it was noted during the second loading set the RS measurements showed a magnitude difference of around 10,000 units lower to those from the first set.

Investigating this result further, it noted that it was raining outside the undercover area where the test was run. This factor could have assisted to reduce the maximum measured temperatures. Furthermore, it was determined that the refined calibration device itself was also heating up as the testing progressed. It was nominally close to ambient temperature or the preheated temperature when a test began and then as a test proceeded the body of the device was maintaining its temperature or was progressively heated up by the exhaust gas, focussed in the area around the gas entry point. The impact of this factor previously

not included in the experimental design needed to be accounted for or a test method established where it would not impact the measured results.

The refined calibration device was able to be setup and utilised to provide repeatable experimental results for calibration checks using a real-life emissions source. It was also able to be utilised to demonstrate that the RS signal, primarily the CO_2 measurement, is impacted by varying temperature of the gas and also the surrounding environment. Whilst the experimental results derived from using the device demonstrated the temperature effect on the RS signal, it would be necessary to further develop the measurement techniques to ascertain the potential range of impact this had on measurements. This factor of RS measurement was further developed and measured in section 6.2.1.

6.2.1. Identification of temperature influence in open path RS measurements

To negate the potential temperature influence of the calibration device when taking RS measurements, a new set of experiments were planned to take measurements that did not use the calibration device. These tests were called open path measurements as there was no containment of gas samples after they exited the exhaust pipe.

The open path experiments undertaken were grouped primarily by the fuel type used by the generator in the test setup, either diesel or gasoline. The testing was setup and then conducted over two days, the first day using a diesel generator. Each test was setup with the same type of equipment with new operating variables being used to develop control and repeatability. These consisted of the use of different cooling fans to apply a range of potential temperature reduction factors to the experiment and also the use of different lengths of stainless-steel piping between the pressure pulsation damper and the thermocouple instrumented exhaust pipe.

A series of seven tests were conducted with the diesel generator setup with five of the seven being completed successfully without failures. The 2nd and 7th tests had incomplete datasets due to RS measurement dropout or failures. The operating loading and subsequent setup of each test is show in Table 6.2. The test setup for the open path experiment testing is shown in Figure 6.5.

Table 6.2: Diesel open path testing operational loading and individual test variables

Step no.	**1**	**2**	**3**	**4**	**5**	**6**
	Start	7.3A	4.1A	1.4A	0A	7.3A
Step no.	**7**	**8**	**9**	**10**	**11**	
	4.1A	1.4A	0A	Off	End	

Test	**Suction flow(m/s)**	**Background Fan flow (m/s)**	**RS Position from exhaust (cm)**	**Pipe length to exhaust (cm)**	**Heat exchanger fan**
1	4.5	0	40	40	No Cooler
2	-	-	-	-	-
3	4.5	4	40	40	No Cooler
4	4.5	4.5	40	40	No Cooler
5	4.5	0	40	120	No Cooler
6	4.5	4	40	120	No Cooler
7	4.5	0	40	120	S,M fans

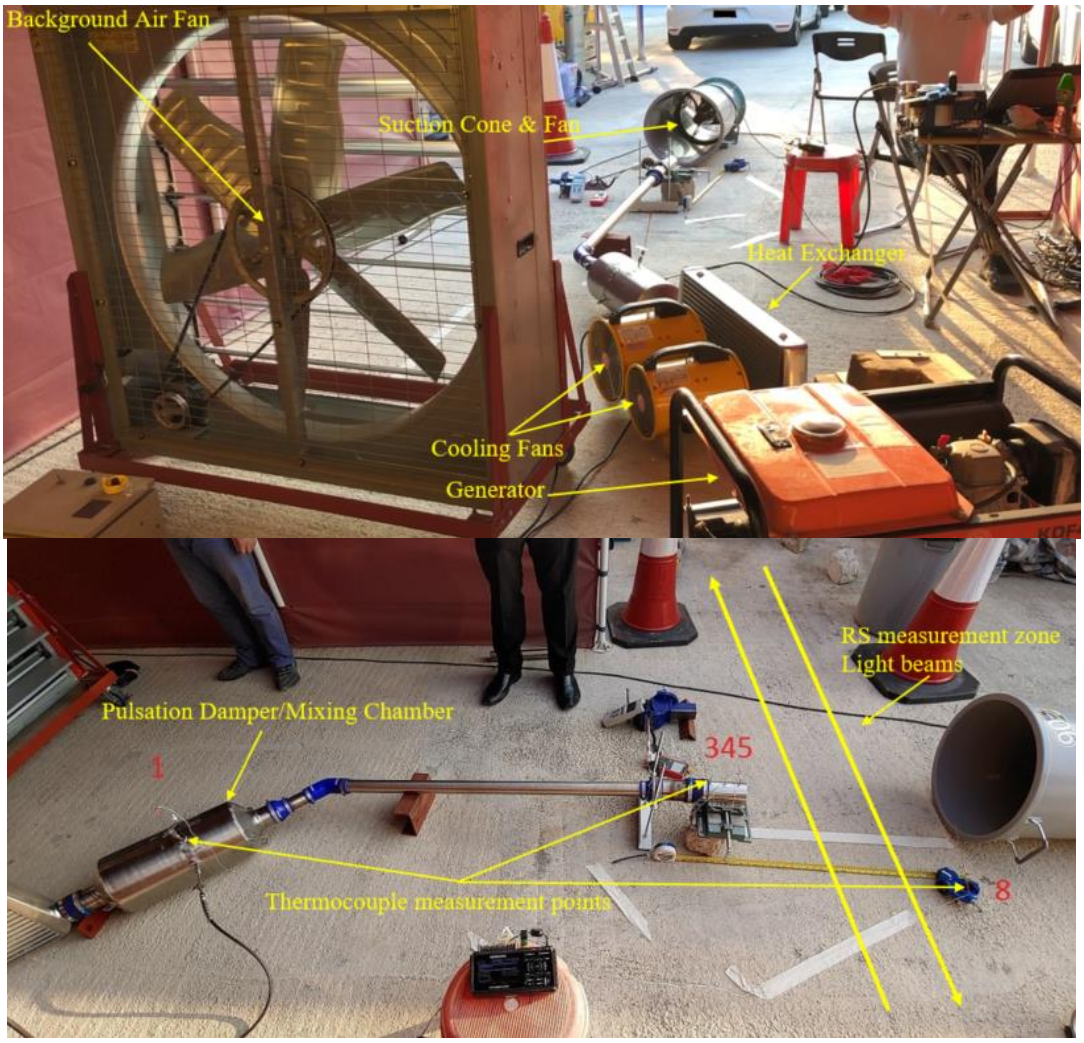

Figure 6.5: Equipment layout for open path experiment testing.

The RS measurement position and the suction flow fan were setup and operated consistently for each test. Only the background airflow fan and the pipe length to the

exhaust were varied in the diesel generator experiment. From the results of these tests a comparison of the CO_2 measurements from an EMS 5003 conventional gas analyser and the RS CO_2 unit signal have been plotted against the exhaust gas temperature and are shown in Figure 6.6.

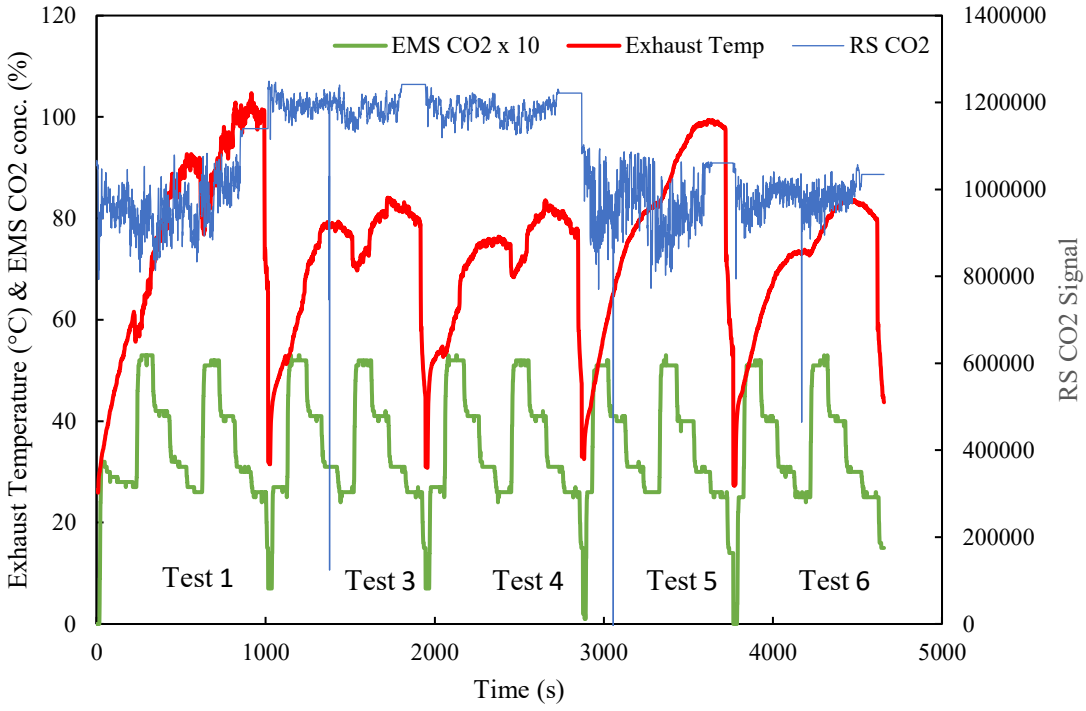

Figure 6.6: Diesel open path experiment test results.

From the results the consistency of the test CO_2 emissions measurement can be seen from the data taken by the EMS 5003 gas analyser with data ranging between 2.7 to 5.3% CO_2 concentration during the test cycles. Following the same loading pattern for each of the tests consistent and repeatable emissions are produced in each test. These conventional CO_2 measurements serve as the baseline reference of each test cycle.

Reviewing the exhaust gas temperature, it can be seen there are varying higher and lower measurements across the individual test cycles. In the case of the lower test temperatures each of these can be correlated to the inclusion of adding a background airflow that provides cooling for test cycles 3, 4 and 6. Tests 1 and 5 have no additional background airflow and in turn show exhaust gas temperatures in the range of 20° C higher that the other tests. Furthermore, tests 3 and 4 are almost the same in their setup and have produced very similar temperature profiles which allows for a repeatable comparison.

When reviewing exhaust gas temperature with the RS CO_2 signal, we are able to see the response of the RS in each test case with respect to the temperature. Tests 1 and 5 show the with the higher temperatures the average RS signal value is around 1,000,000 range. Whereas for tests 3 and 4 which have practically the same measurement results, the RS signal value is around 1,200,000 range. The additional setup variable for consideration is the connecting pipe length to the exhaust point. In tests 1, 3, and 4 it was 40 cm, for tests 5 and 6 it was 120 cm. When comparing the tests with higher exhaust gas temperatures the length appears to have an impact on the consistency of the gas temperature. The longer pipe in these tests show the exhaust temperature to have smoother transitions/less variability as it increases and decreases. What is curious is the RS CO_2 signal between tests 5 and 6. In this case it had been anticipated that the RS signal value would higher similar to tests 3 and 4, but it is not the case. The RS CO_2 signal for test 6 shows less signal variation which is consistent with RS measurement at lower temperatures. This is an item that warrants further investigation at a later date to determine what additional factor can influence the RS signal to produce this level of result.

Overall, the diesel open path RS experiment shows there is a positive identification that the exhaust gas temperature is impacting the measured RS CO_2 signal. It also shows that the RS signal measurement at higher temperatures shows consistently higher variation when compared to testing conducted at lower temperatures. The RS CO_2 average values, standard deviations and temperature ranges for each Diesel test outlining this are shown in Table 6.3:

Table 6.3: Diesel CO_2 RS and temperature values

	Test 1	**Test 3**	**Test 4**	**Test 5**	**Test 6**
RS CO2 Average	987,969.3	1,196,204.0	1,187,333.6	981,869.6	988,110.0
RS CO2 Std Dev	82,504.3	47,224.6	24,437.6	80,375.7	39,971.5
Temperature (°C)					
Minimum	25.9	31.5	30.8	32.5	27.2
Maximum	104.7	84.1	83.5	99.4	84.2
Average	77.2	70.9	70.5	78.4	70
Range	78.8	52.6	52.7	66.9	57

The second set of tests performed in the open path experiment utilised two identical gasoline fuelled generators. As the power supply capacity of the two gasoline generators was higher than that of the single diesel generator so the approach to testing allowed for

a greater range of loads to be considered and applied to produce the exhaust emissions and range of gas temperatures. Furthermore, as the combustion temperature of the gasoline engine is higher than that of the diesel engine, longer connection pipes were utilised between the pulsation damper/mixing chamber and the exhaust pipe exit to ensure gas temperatures were not too high as to potentially burn or damage equipment or harm testing personnel.

A series of six tests were conducted with the gasoline generator setup with five of the six being completed successfully without failures. The 1st test failed due to incomplete temperature datasets due to thermocouple connection failures. The operating loading and subsequent setup of each complete test is shown in Table 6.4:

Table 6.4: Gasoline open path testing operational loading and individual test variables

Step / Test	1	2	3	4	5	6	7	8	9	10	11
2	Start	4.1A	2.7A	1.4A	0A	4.1A	2.7A	1.4A	0A	Off	End
3	Start	4.1A	2.7A	1.4A	0A	8.1A	6.7A	5.4A	0A	Off	End
4	Start	12.6A	11.3A	9.9A	0A	12.6A	11.3A	9.9A	0A	Off	End
5	Start	16.6A	15.3A	13.9A	0A	16.6A	15.3A	13.9A	0A	Off	End
6	Start	16.6A	15.3A	13.9A	0A	4.1A	2.7A	1.4A	0A	Off	End

Test	Suction flow(m/s)	Background Fan flow (m/s)	RS Position from exhaust (cm)	Pipe length to exhaust (cm)	Heat exchanger fan
2	4.5	0	40	40	No Cooler
3	4.5	0	40	40	No Cooler
4	4.5	0	40	40	No Cooler
5	4.5	0	40	40	No Cooler
6	4.5	0	40	40	No Cooler

As per the diesel testing, for the gasoline testing the RS measurement position and the suction flow fan were setup and operated consistently for each test. The background airflow fan and the pipe length to the exhaust were kept the same in the experiment as in these tests the electrical loading was being used to vary the system performance. From the results of these gasoline tests a comparison of the CO_2 measurements from the EMS 5003 conventional gas analyser and the RS CO_2 unit signal have been plotted again the exhaust gas temperature and are shown in Figure 6.7.

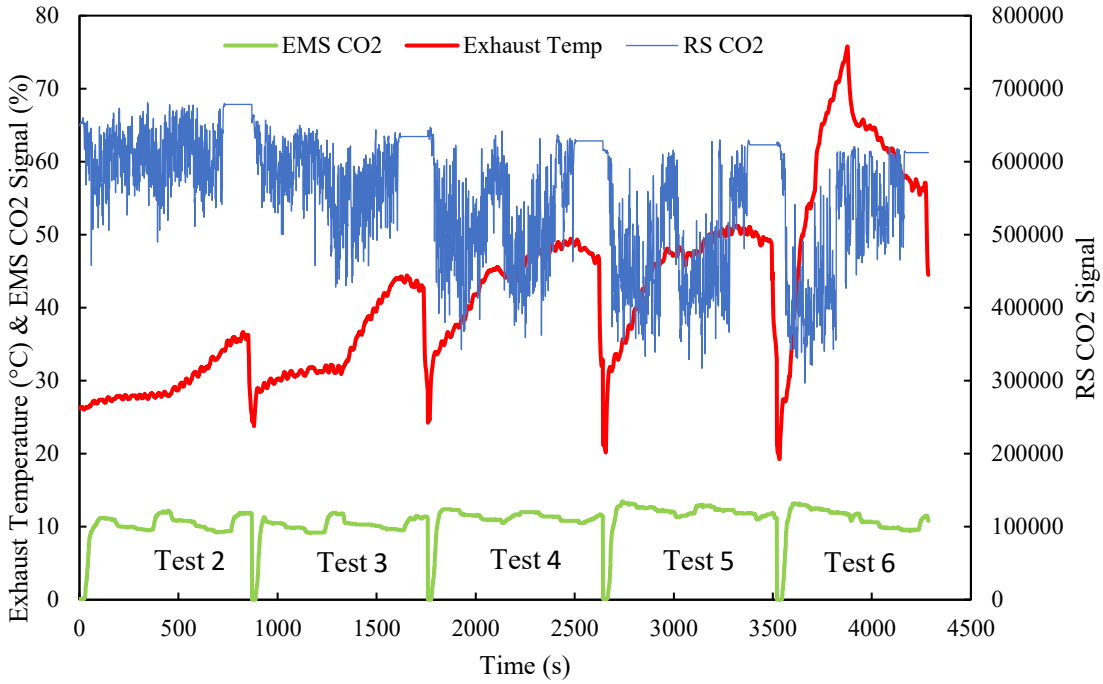

Figure 6.7: Gasoline open path experiment test results.

Review of the gasoline test data shows characteristic differences between the combustion processes. The nature of gasoline combustion (using an Otto cycle) produces significantly higher CO_2 concentrations in the range of 10 to 14% measured by the EMS 5003 gas analyser. Also, the greater electrical load which could be applied to the gasoline generators allowing for it to be slowly ramped up (utilising a step loading pattern) between each test. The CO_2 emissions curve/patterns remain almost the same with some small differences that are expected with the load variations. This resultant CO_2 concentration curve shows there is a baseline with repeatable characteristics to compare to the RS CO_2 and exhaust temperature measurements, similar to that of the diesel testing.

Following the gradual electrical load step increases made, per the test schedule data in Table 6.4, there are some slight increases in measured maximum CO_2 emission concentrations ranging from 12% to 13.2%. In line with these CO_2 increases the exhaust gas temperature is also increasing as the tests progress. Maximum temperatures within each cycle step up from 36°C in test 2 to 75°C in test 6. It is noted that the corresponding magnitude of the RS CO_2 signal drops in line with the progressive increase in exhaust gas temperature. The average figures for the RS CO_2 signal begin around 600,000 and drop

to around 400,000 to 450,000 units in the final cycle after running at the maximum loading point.

In this series of tests for the measurement of gasoline emissions, the magnitude of the RS CO_2 signal decrease is similar to that seen in the diesel testing. What is evident in this series of tests is that there is a relationship between the temperature increase and the decreasing magnitude of the RS CO_2 signal.

The initial observation when comparing gasoline test 2 and test 3 is the loading patterns are initially similar and show repeatability in the curve pattern formed by the RS CO_2 signal. This changes quickly in the second half of test 3 as the load and the gas temperature increases with the measured RS CO_2 signal value dropping. This pattern continues as the tests progress with each subsequent temperature increase resulting in further decreases in the magnitude of the measured RS CO_2 signal. The RS CO_2 average values, standard deviations and temperature ranges for each Gasoline test outlining this are shown in Table 6.5:

Table 6.5: Gasoline CO_2 RS and temperature values

	Test 2	**Test 3**	**Test 4**	**Test 5**	**Test 6**
RS CO2 Average	620,674.9	588,303.1	537,391.8	504,189.6	517,142.2
RS CO2 Std Dev	43,058.1	47,965.6	75,270.5	88,304.2	91,868.6
Temperature (°C)					
Minimum	25.4	23.8	24.2	20.2	19.2
Maximum	36.7	44.4	49.4	51.2	75.8
Average	29.8	35	43.4	44.9	57.4
Range	11.3	20.6	25.2	31	56.6

Considering now the results from both the diesel and gasoline testing, the magnitude of the changes to the RS CO_2 signal observed in both test series shows a steady and quantifiable decrease when the exhaust gas temperature increases. This has been possible to identify in these experiments as there has been a series of tests undertaken with stable conditions that have provided a significantly longer sequential dataset for analysis. Without which there would only be an indication from some of the earlier experimental measurements that there was a potential temperature impact. Developing a new testing methodology, open path measurement, combined with designing experiments to collect the series of measurements has allowed for identification of the relationship.

Considering the above that the temperature of the emissions gases needs be taken into consideration when examining at the measurement sensitivity and accuracy of RS systems. An area of significant importance where this should be applied is in the RS measurement application method. In discussions with HKEPD staff and RS equipment manufacturers and suppliers, it is apparent the methodology undertaken with some system designs is to begin the RS measurement of the exhaust plume as close to the exhaust pipe exit as possible so it has little time to disperse and measurement of the highest concentrations gases in the exhaust plume is possible before is begins to substantially disperse. This idea would appear to be a sensible or reasonable approach, but considering the implication that increased exhaust gas temperatures have on RS measurements the application of the measurement method needs to be critically reviewed. Review of this aspect of measurement has been undertaken and experiments designed and conducted to propose application suggestions to reduce the impact of temperature variations on RS measurements. This discussed and outlined in section 6.3.

6.3 Exhaust plume temperature measurements

The identification that increases in exhaust gas temperatures results in RS CO_2 signals having lower measured system values requires a review of the measurement methodology used with RS systems. As mentioned in section 6.2, systems which begin RS data measurement of exhaust gases as soon as the plume exits the exhaust pipe have been developed by some RS suppliers. This concept appeared to be a sensible approach to data collection, but considering that temperature of the exhaust gas significantly influences the measurement result. It needs to be assessed what the temperature profile of exhaust plumes are like, so suggestions can be made about what distance an RS measurement could start from to minimise variations from gas temperatures. This following section covers the development of the measurement experiment and the outcomes from the measurements undertaken.

6.3.1 Design of experimental measurements

The development of the measurement process was undertaken with the plan that a chassis dynamometer test cell capable of testing vehicles would be utilised for the experiments so consistency of measurements and repeatability could be maximised.

The experimental setup used the light duty Euro 6 emissions testing 4x4 chassis dynamometer at JCEC with a thermocouple array assembled for the task arranged with initial spacing of 10 cm per measurement point from the tailpipe to 50 cm, then 25 cm spacing thereafter. The measurement array covered a distance of 225cm in length. To ensure emissions gases did not build up and impact testing, an exhaust extraction hose was located around 1 m behind the last thermocouple point to draw gases away without applying suction too close to the exhaust or the array measurement points. To further assist with dispersion of exhaust gases the test area access roller door was partly open as well to allow natural airflow.

For the initial testing, the thermocouple measurement array was assembled and setup in the chassis dynamometer and was able to display the temperatures, but the recording/data logging array was not initially operational. In lieu of datalogging a video was taken to record the real-time temperature display effectively logging the temperature changes during testing. This initial experimental setup was used for the first and second vehicle tests.

These first tests consisted of taking temperature measurements for the vehicles exhaust plumes initially in ‘Park’ gear, first idling and followed by then increasing the engine speed to 2000 rpm for 300s respectively for each condition. Next each vehicle was placed into the ‘Drive’ gear and driven from 20 to 40 km/h with 5 km/h speed steps for the first vehicle test and similarly 20 to 45 km/h for the second vehicle test. Step duration varied between 2 to 5 minutes during the first test. The second test utilised 3-minute step durations.

Changes introduced with the third vehicle tests were the use of programmed drive cycles specifically created for the exhaust plume temperature measurement. These were setup and programmed into the dynamometer drivers aid system so the driver could follow the programmed driving routines. This removed the element of depending on the driver to follow timing sequences manually and provided an accurate speed target to follow.

Initially 6 drive cycles had been created for testing. From the 6, 4 of these were selected for testing. From testing these drive cycles, a new 7th cycle with a slightly longer duration created for use with all further tests. This improved duration and reduced variability. The data acquisition system recording had also been enabled and was working for all the tests beginning with the third vehicle going forward. The progressive development of this experiment allowed for improved measurement conditions and testing cycles.

Further changes which were made during the testing of the fourth vehicle which focussed on increasing the resolution of temperature measurement with a thermocouple spacing of 5cm from the tailpipe to 30 cm, then 10 cm spacing to 50 cm followed by 25cm spacing until the last thermocouple which remained at 225 cm from the tailpipe.

6.3.2 Vehicle testing

The first vehicle utilised was a gasoline fuelled 2010 BMW 320i sedan. It was setup and driven on the JCEC 4x4 chassis dynamometer with the thermocouple array arranged with initial thermocouple spacing as described in section 6.3.1. As the test temperatures were recorded by video and not a data acquisition, results analysis was conducted manually by extracting the temperature data at 10 second intervals in these initial test cycles. The experimental setup for the first vehicle is shown below in Figure 6.8.

The alignment of the thermocouple measurement points was in line with the centreline of the tailpipe in the direction where the exhaust plume flowed. A tape measure was attached to the slotted steel right-angle piece which the thermocouples were fixed too. The tape measure provided an accurate reference check that the thermocouple placement was correct or if not, it provided easy reference for position adjustment when needed as testing was undertaken. The data collected from the first vehicle test is shown in Figure 6.9.

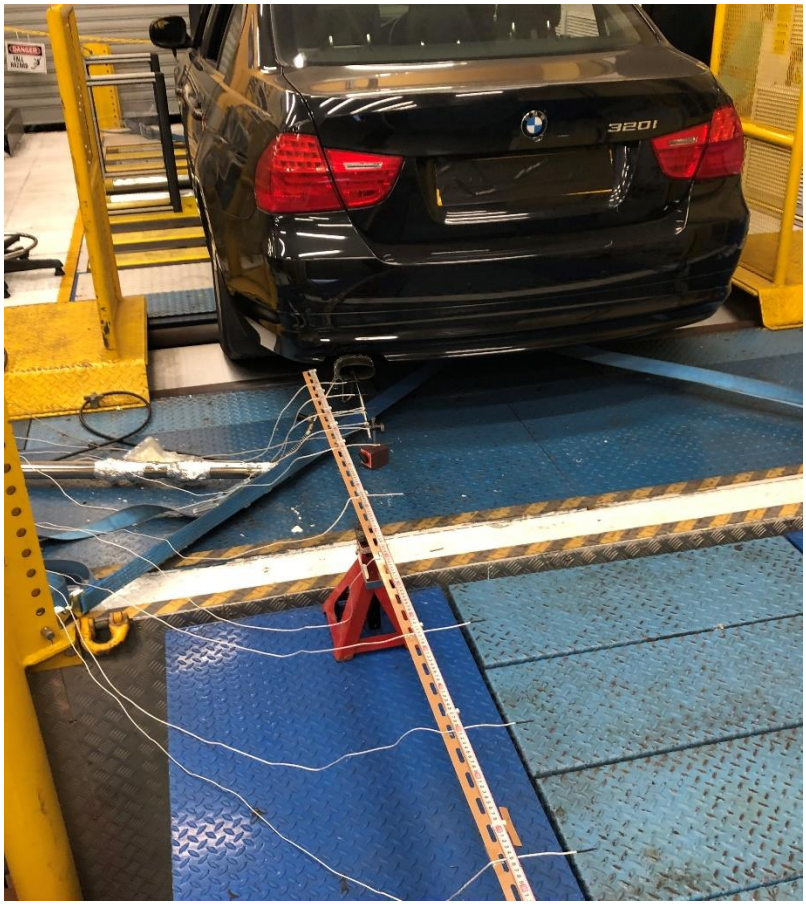

Figure 6.8: Experimental setup of vehicle and thermocouples for exhaust plume temperature logging.

The data collected from the first vehicle tests of the experiment shows distinct temperature profiles under the various loading conditions selected for testing of the vehicle. The Figure 6.9 a, shows the temperature profile measured when the vehicle is stationary and park gear is selected. At idle, 750 rpm, the measured temperature across the measurement array range over five minutes was between 21 and 25°C.

The next step shows the measurement response after the engine speed is increased to 2000 rpm. Within 10 to 20 seconds the temperatures have all taken a noticeable step increase. Within 50cm from the tailpipe the range is between 10 to 20°C higher, whilst from 75cm and further the increase is of 5 °C or less. Over the five minutes of measurement three areas of temperature behaviour can be identified.

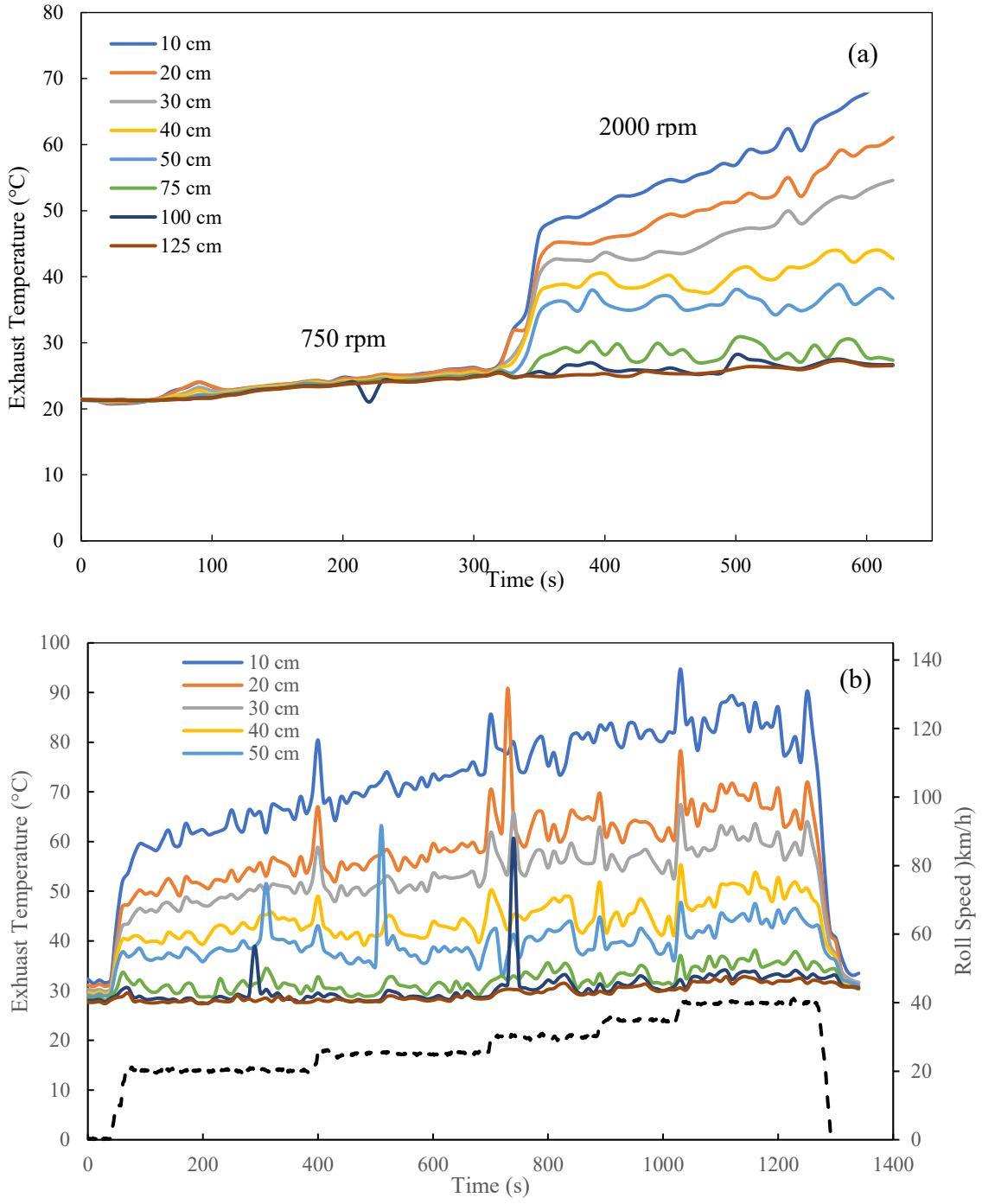

Figure 6.9: First vehicle exhaust plume temperatures at discrete measurement points from tailpipe.

The range from 10 to 30 cm shows the greatest increases, as would be expected, with each measurement point showing the temperatures increasing at a similar rate with traces displaying a similar gradient. The 40 and 50 cm range shows the initial step increase of between 10 to 15°C and then afterwards the temperatures appear to oscillate with a range 3 to 4°C with some minor of up to increases 3°C for the 40cm point. The 50 cm and

further range has initial increases of up to 5°C and oscillate with a magnitude of 2 to 3°C for the remainder of the measurement.

The results from the driving test for this vehicle are shown in Figure 6.9 b. Before the driving begins all temperatures are within a range of 27 to 31°C. Within 10 to 20 seconds of the start of driving from 0 to 20 km/h, temperatures in the 10 to 50 cm range from the tailpipe all raise quickly by 10 to 22°C. Within 60 seconds of the start temperatures within 10 to 30 cm continued to increase by 15 to 30°C after which the rate of increase reduces and each begins to follow a relatively linear rate of increase. As in the park test the 40 to 50 cm range has a much slower temperature increase which oscillates as it increases. Also similar to the park test at 75 cm and beyond these points do not show further significant temperature increases and temperature oscillate within a 2 to 4 degrees range of the previous measurement.

When the speed increases by 5 km/h, each of the measurement points shows a significant high/increased transient temperature response before falling to lower temperatures closer to the value prior to the acceleration. For each area identified the temperatures follow the similar patterns of continuous increase, a step and then minor increases or a step only followed by minor temperature oscillations.

For the remaining duration of the driving test these patterns repeat for the 25 and 30 km/h sections, for the 35 and 40 km/h sections the rate temperature increases slow down and may plateau for some periods.

An important observation from the data collected for this first test vehicle is the temperature of the exhaust plume can be significantly influenced by step increases in speed or speed instability. Most of the high temperature transients measured show this behaviour.

The second vehicle tested was a 2002 diesel fuelled Toyota Grand HiAce people carrier/multi-purpose vehicle (MPV). It was setup with the same measurement equipment as the 1st vehicle test and repeated the testing procedure. Changes made in the 2nd test were improving the consistency of the test timing and speed control. One additional measurement point available was for 0cm/the exit of the exhaust pipe. In the first test this test point failed to measure correctly and was unusable. Temperatures were again recorded by a video file. The data collected from these tests is shown in Figure 6.10.

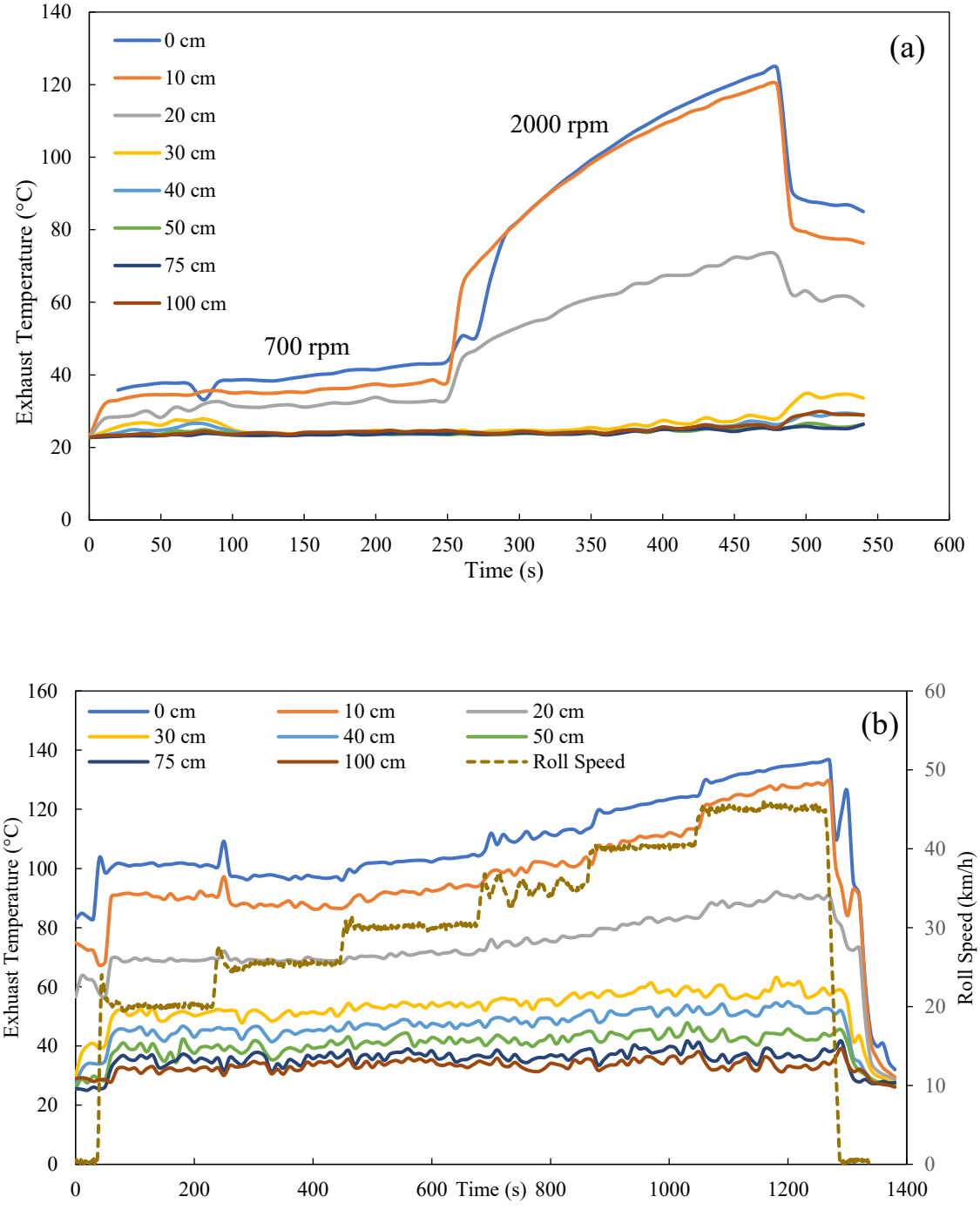

Figure 6.10: Second vehicle - exhaust plume temperatures at discrete measurement points from tailpipe.

The second vehicle data set differs from the first vehicle temperature profile in a number of areas. In Figure 6.10 a, overall, the line charts are smoother showing much less transient variation compared to the first test. In the park test, the 0 and 10 cm from the tailpipe positions are similarly grouped and show the highest temperature increase responses. The 20 cm position is similar to the 10 cm for the idle/750 rpm section and

then has a much lower/moderate increase response after the step up to 2000 rpm. The remaining measurement points from 30 to 100 cm show only small responses to changes with some small temperature oscillations for the park testing. The 125 cm measuring point did not record correctly in this test and was unable to be used in the data set.

Figure 6.10 b shows the driving test. This test was conducted with only a short time between the park test ending and the drive test beginning during which the engine continued to run. This allowed the exhaust temperatures to remain higher so any potential transient steps that occurred when the driving started would be less severe. The groupings of temperatures in the drive test were similar to those of the park test. The positions at 0 and 10 cm from the tailpipe rose to 90 and 100°C quickly after the driving started. For 20 and 25 km/h test speeds both maintained relatively stable temperatures of 101 and 96°C at 0cm then 90 and 87°C at 10cm for the respective speeds. From 30 through to 45 km/h temperatures has transient step increases followed by further linear increases thereafter. The position 20cm from the tailpipe had a moderate increase in comparison to 0 and 10 cm, but then followed similar patterns with stable temperature at 20 and 25 km/h, then followed by linear increases in temperature between 30 to 45 km/h. The remaining positions from 30 to 100cm from the tailpipe measured between 33 to 55°C for the duration of the testing and were seen to oscillate within a small range. The 30 and 40 cm positions showed some further increases at 40 and 45 km/h. It should also be noted the vehicle speed was unstable at the 35 km/h position. This introduced some further variability, but the impact did not change the overall results. It effectively added a noise or uncertainty element to the temperature measurement.

Overall, the second test results showed improved vehicle speed control along with each speed step having a 3-minute period before the next step increase. Many transient increases observed in the first vehicle test did not occur. With the improved data set, a 3D exhaust plume temperature profile or surface map was created showing in clearer detail temperature increases at each point over the drive cycle. See Figure 6.11. This presentation allows easier data interpretation in comparison to a 2D temperature chart.

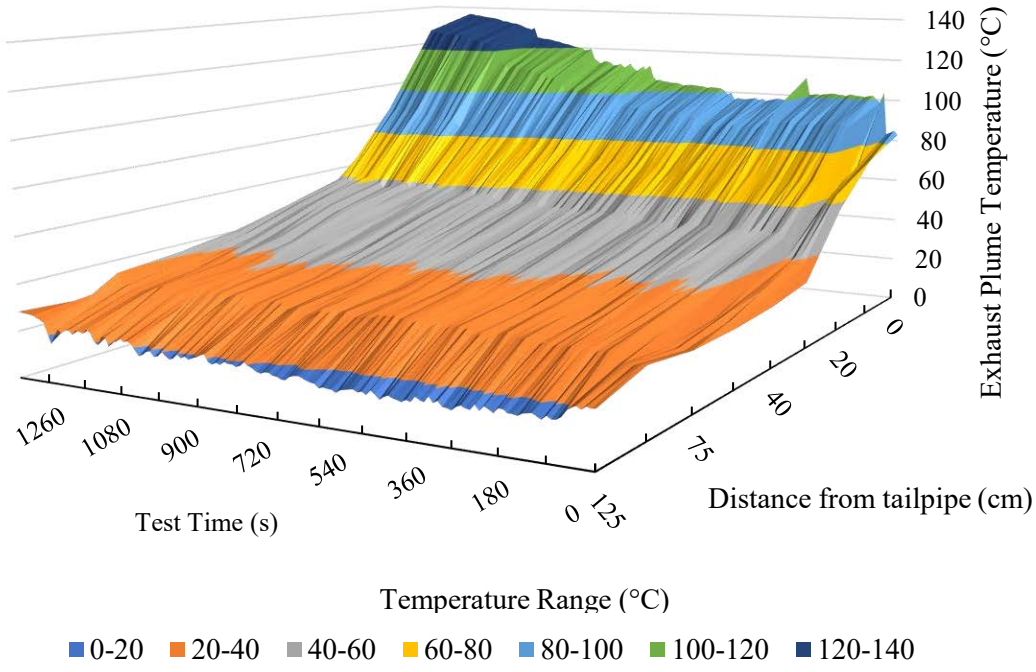

Figure 6.11: Second vehicle exhaust plume temperature profile.

The chart is read as follows:

- The horizontal axis displays the test time from right to left in seconds.
- The vertical axis indicates the measured temperature of the exhaust plume in °C.
- The depth axis indicates the distance of the thermocouple measurement point from the tailpipe.
- The vertical and depth axes zero points are co-located.
- The horizontal axis is shown with its zero point at the maximum depth location so it is not hidden by the 3D surface temperature profile created from the test data.

The development of the 3D surface temperature profile or exhaust plume temperature profile allows fast identification of which regions are hottest as the driving test progresses and where the temperatures have the least change when driving.

From the beginning of the 3rd vehicle measurements more temperature points were able to be measured and datalogging/recording was functioning so a finer time resolution of temperature measurement was able to be achieved. With the creation of new specialised Exhaust Emission Temperature (EET) drive cycles programmed into the chassis dynamometer more test cycles could be run sequentially.

The third vehicle tested was gasoline 2005 Nissan Lafesta. With this vehicle setup on the chassis dynamometer and with the improvements made to the data logging. Testing of the new EET drive cycle programmes was able to proceed. A summary of the EET drive cycles is shown in Table 6.6.

Table 6.6: EET drive cycle description and parameters

Drive Cycle	Speed (km/h)		Step duration (s)
	Step size	Range	
Original	5	20 - 45	180
1	15	15 - 90	100
2	15	15 - 90	60
3	5	15 - 90	60
4	10	10 - 90	60
5	5	10 - 90	60
6	15	15 - 90	200
7	15	15 - 90	240

A further benefit of the improved automation was multiple tests could now be conducted in a shorter period of time. Figure 6.12 shows the exhaust plume temperature profile results from EET drive cycle 6.

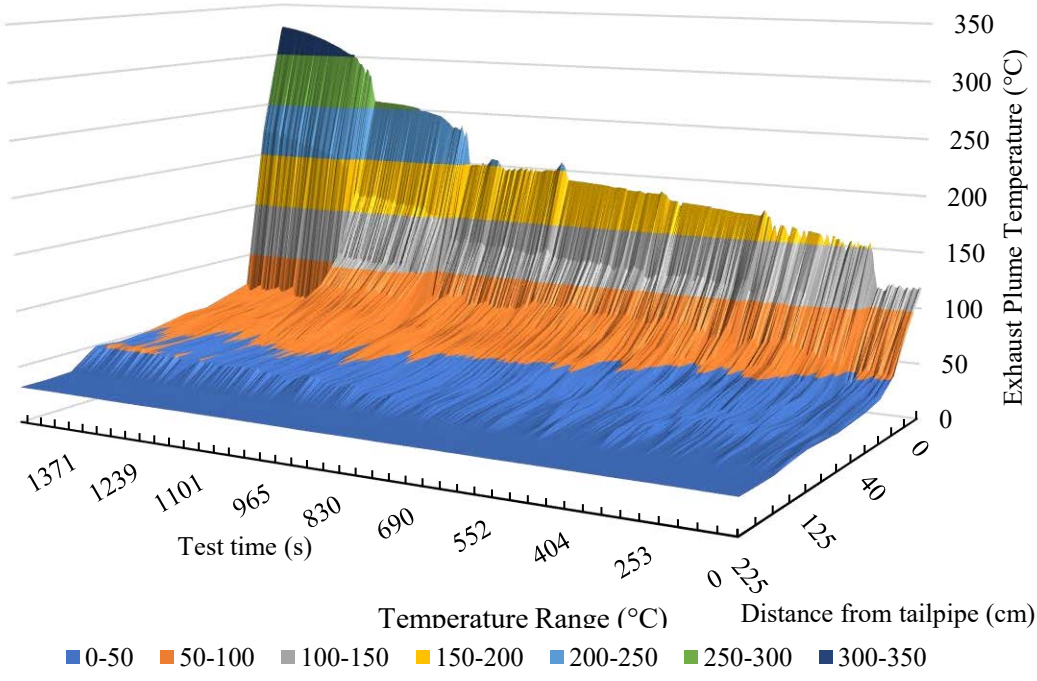

Figure 6.12: EET drive cycle 6 exhaust plume temperature profile from Nissan Lafesta testing.

Testing with EET drive cycles 1, 2, 4, and 6 provided feedback that helped to determine that shorter duration steps could be subject to more variation in settling of the driving speed and in turn the exhaust plume temperature. This could lead to not having as stable a measurement if the step duration is shorter, i.e., around 60 to 100s. When these shorter time periods are combined with more speed steps for finer resolution of speed measurement, then there will be more transient steps and a resultant shorter stable speed and temperature measurement period. Considering this it was decided that EET drive cycles 1,2 and 4 would not be utilised further. EET drive cycle 6 was selected for further use, but an additional modification was made. The duration of the speed steps was increased from 200 to 240s. This became EET drive cycle 7.

The EET drive cycle 7 was next utilised to perform a series of three exhaust plume temperature tests for the third test vehicle. A sample of the data collected from the first of these tests is shown in Figure 6.13.

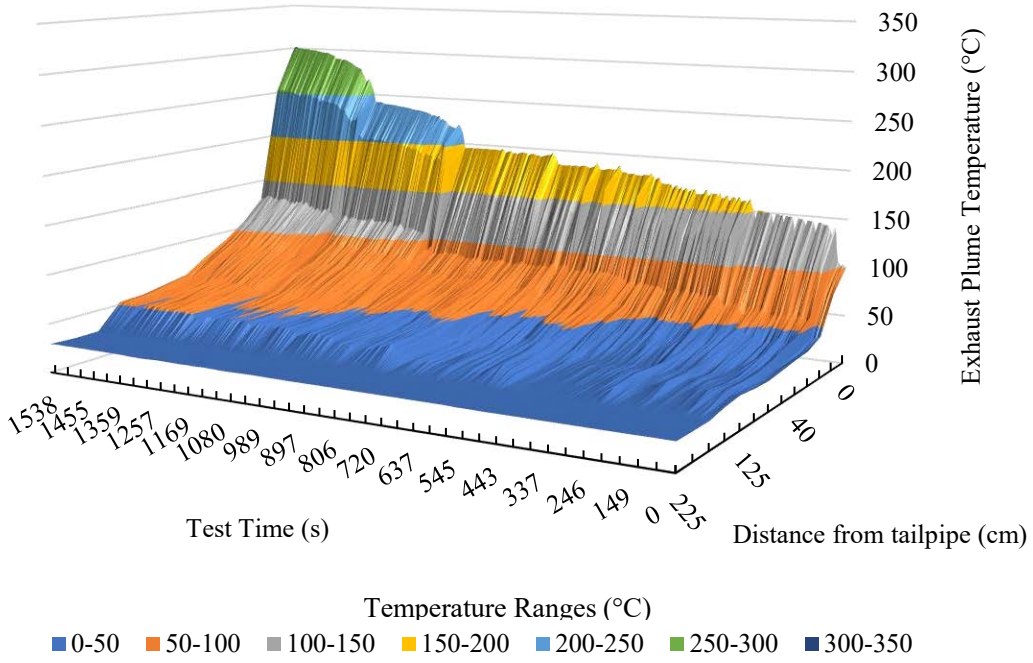

Figure 6.13: Third vehicle exhaust plume temperature profile - test 1.

The test result shown in Figure 6.14 is from the first of the three tests with EET drive cycle 7 and is representative of each of the tests. The results show that with the EET drive cycle 7 a repeatable pattern of temperature measurement results can be obtained from tests conducted over a short period such as an afternoon. In these tests the vehicle engine

and emissions catalyst systems were able to cool down as there was a significant break between tests and there was not any major offsets of the measured exhaust gas temperatures noted at the start or throughout each of the tests.

Similar to earlier test results there three main areas of temperature response in the measurements. The first being at the points 0 and 10 cm from the tailpipe where the temperatures are the highest measured with significant step increases when the vehicle speeds up by 15 k m/h followed by a gradual/relatively linear increase thereafter. The second area in these tests are the points 20 to 50 cm from the tailpipe. These points show a reduced magnitude step increase of temperature when speeds increase and then either remain at the new higher temperature point and oscillate within a few degrees of these points. The third section is from 50cm from the tailpipe onwards, at these points the temperature increases when the vehicle accelerates, but then drops down afterwards when the new speed target is reached. This occurs for the speeds from 15 to 45 km/h. For the speeds from 60 to 90 km/h the temperature stays around the higher level that it attains when the vehicle reaches the next target speed. In this area the temperatures remain generally stable once the speed settles.

The fourth vehicle tests utilised the 2002 diesel Toyota Grand HiAce again with the same experimental set up as per the last tests of the 3rd vehicle. A series of five tests were successfully completed, A representative result from these tests is shown in Figure 6.14.

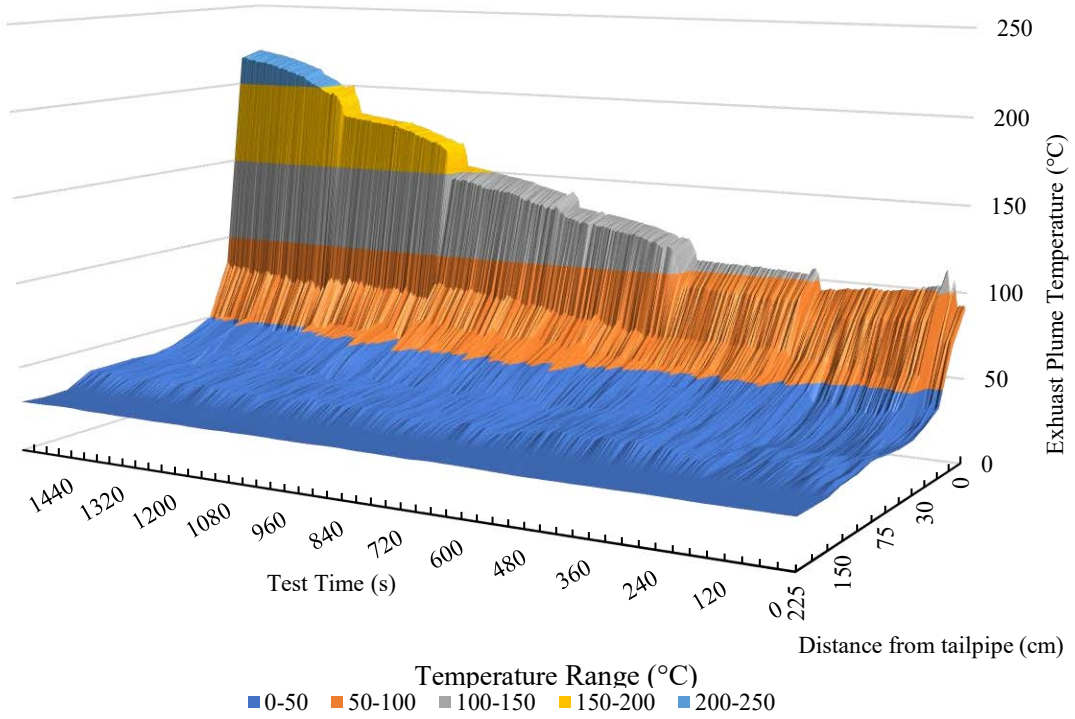

Figure 6.14: Fourth vehicle - sample result from first set of exhaust plume temperature tests.

The measurement results showed improved consistency as each successive test was conducted. The temperatures from show consistent grouping of the temperatures in each characteristic area of the temperature measurement. The groupings noted are 0 and 10 cm, 20 to 50 cm and 50 cm from the tailpipe onwards. This is similar to the results grouping observed from the gasoline vehicle measurements in the third series of tests.

In these results the resolution of data appears to show some significant temperature differences in the measurement range between 10 and 20 cm from the tailpipe. The exhaust plume temperature profile shows a sharp drop off in temperature values from 10 to 20 cm which suggests a possible lack of data resolution in this region. To check and potentially improve the measurement resolution of the plume temperatures in this area the measurement array was adjusted from having 10 cm spacings between each thermocouple up to 50 cm from the tailpipe to 5 cm spacings between thermocouples up to 30 cm, then followed by 10cm spacings to 50 cm. A series of 3 exhaust plume temperature tests were conducted using the new array spacing in conjunction with the equipment setup otherwise unchanged. The result from the 3rd of these tests is shown in Figure 6.15.

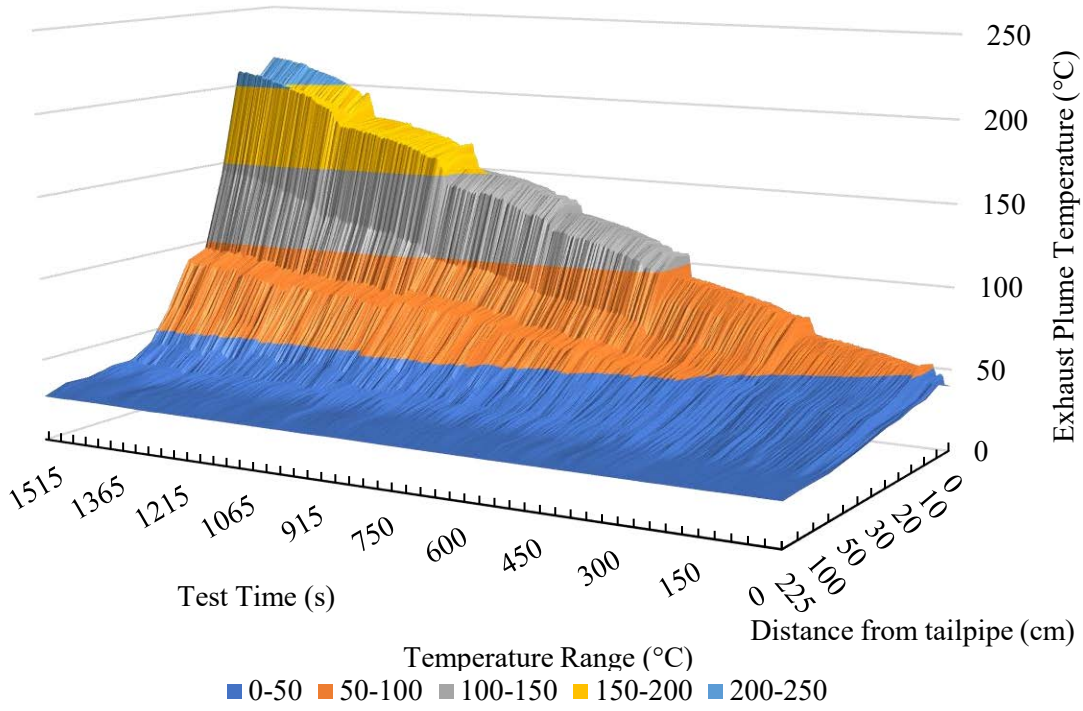

Figure 6.15: Fourth vehicle - sample result for revised thermocouple array spacing for exhaust plume temperature test.

The refined resolution from these tests shows some further details. It be seen in Figure 6.15 that in the area 0 to 15 cm from the tailpipe there is the largest temperature changes after each step speed change. The area 20 to 25 cm from the tailpipe is now showing more temperature response to vehicle speed and the third area 30 cm and greater from the tailpipe is mostly stable except when a step speed change occurs for the temperature to increase. Whilst it could be still be suggested that there appear to be some measurement gaps remaining in the experimental study area, this is not the case. The temperature of the exhaust plume is reducing rapidly and this adjustment to the measuring array has provided a clearer resolution of the temperature profiles close to the exhaust pipe as was desired.

To consolidate the testing results a further set of measurement data was taken with the fourth vehicle to ensure completeness of the data set. There was one more additional adjustment made lowering the height on the measurement array from 25 to 22 cm. The 3rd result from the final 4 measurements for the vehicle is shown in Figure 6.16.

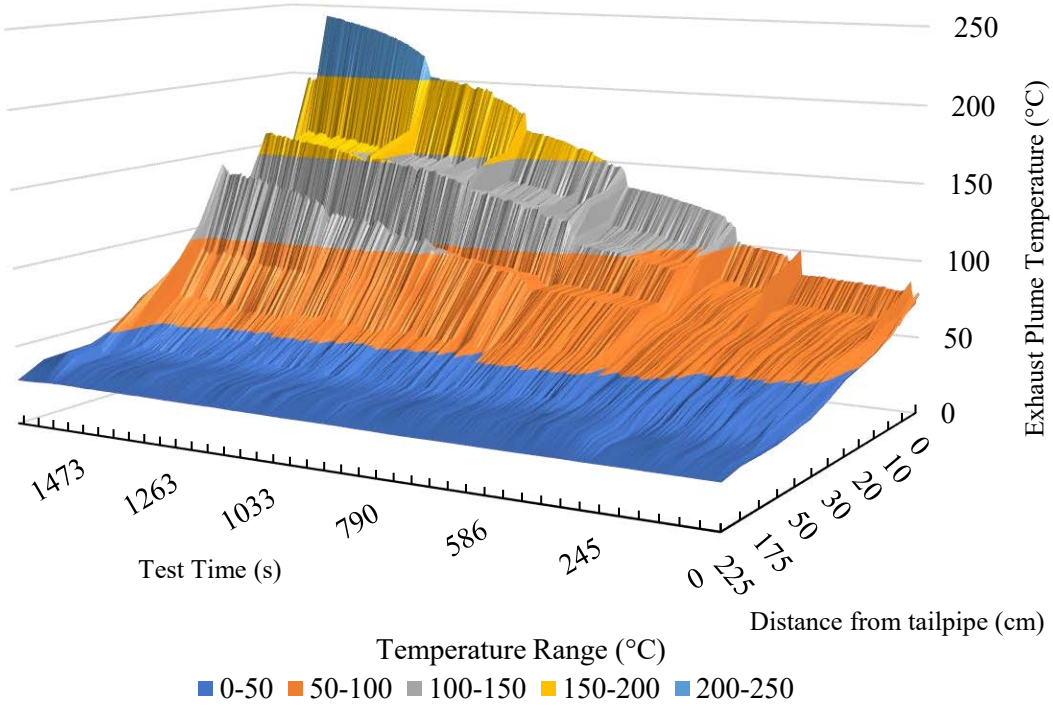

Figure 6.16: Fourth vehicle final consolidation measurements with revised thermocouple array spacing for exhaust plume temperature tests.

The general nature of the measurements taken appear reasonable and representative of anticipated results for the tests. What was unexpected in the 1st and 2nd tests was the temperature at 5 cm from the exhaust pipe was measured to be lower than that at 10 and 15cm from the exhaust pipe. Whilst unexpected the magnitude of the measurement data is close to what was anticipated at this measurement point. For the 3rd and 4th tests the observation follows with the temperature at 5 cm from the tailpipe being between the 0 and 10 cm points (which is the anticipated outcome and shown in Figure 6.17). Another unexpected observation was with the 20 and 25cm points. Midway thought the measurement at 25 cm temperature became hotter than the 20 cm measurement and remained this way until the final speed at 90 km/h step was completed.

Even though these observations are noted, these results still show three to four distinct areas of the exhaust plume which can be characterised between those with high temperature changes and continuous increase throughout to the measurements showing either no change or to slow rises in temperature to step responses and steady state driving. Assessment of the noted outcomes and how it will impact RS measurement is discussed in the next section.

6.3.3 Assessment of Exhaust Plume measurements

Through the experimental series of vehicle tests conducted on a chassis dynamometer to investigate and characterise the temperature profile of vehicle exhaust plumes, a new visualisation of the plume and its temperature spread has been developed.

The 3D 'exhaust plume temperature profile' allows examination of temperatures as a test progresses over time and through a range of vehicle speeds. Sections of profile data can be examined with respect to time, temperature or speed. It has allowed effective visualisation of the sections of an exhaust plume to identify areas that will affect RS measurements and areas where the temperature will not.

Further to this a number unique characteristics are identifiable. From the profiles and the data measurements. The exhaust plumes have areas or perhaps zones where temperatures will increase or remain stable with similar characteristics. These can be classified into 4 distinct areas or zones and are described as follows:

1st – High Temperature Response Area/Zone.

This zone is closest to the tailpipe exit where exhaust gases are potentially at the hottest temperatures of emission. In the experiment the measurement points that were identified are at 0, 5,10 and 15 cm from the tailpipe exit. Characteristics of temperatures in this zone are:

- Rapid and high magnitude temperature increases to step changes in test speed.
- Step changes may produce significant transient temperature spikes which can last for 5 to 10 seconds.
- At high loads temperatures can vary by up 80°C between points (i.e., 0 to 15 cm from exhaust pipe).
- The temperatures in this area are the most sensitive to speed and load changes and rapidly reflect any minor variations.
- After the vehicle test speed stabilises, these gas temperatures will continue to increase at a steady/almost linear rate.

2nd – Middle Temperature Response Area/Zone.

This zone is where the exhaust gas plume velocities from the tailpipe begin to reduce and the initial dispersion of the plume starts. The gas temperatures are high and significantly greater than ambient temperature. In the experiment the measurement points that were identified are at 20 and 25 cm from the tailpipe, and occasionally at 30 cm. Characteristics of temperatures in this zone are:

- Moderate to low magnitude temperature increases to step changes in test speed.
- Transient load or speed changes have a noticeable, but lower effect on gas temperature and the rate of change of temperature slows down.
- After the vehicle test speed stabilises, gas temperatures will continue to increase at a steady/almost linear rate.

3rd – Moderate Temperature Response Area/Zone.

This zone is further from the tailpipe exit where the exhaust plume velocities have slowed considerably and gas dispersion/diffusion is increasing, but there is still a noticeable/measurable flow. The gas temperatures are now moderate and in the range of 20 to 40°C higher than ambient temperature. In the experiment the measurement points that were identified are at 30, 40 and sometimes 50 cm from the tailpipe exit. Characteristics of temperatures in this zone are:

- Low magnitude temperature increases to step changes in test speed.
- Transient load or speed changes have a low/minor effect on gas temperature and the rate of change of temperature is very slow.
- After the vehicle test speed stabilises, gas temperatures may or may not continue to increase at a low rate.

4th – Low Temperature Response Area/Zone.

This zone is furthest from the exhaust pipe exit where the exhaust plume velocities have begun to match that of the ambient airflow with flow momentum decreasing and the plume is dispersing. The gas temperatures are now lower and mostly within the range of 20°C higher than ambient temperature. In the experiment the measurement points that were identified are at 50, 75, 100, 125, 150, 175, 200 and 225 cm (pending the points measured in the various tests) from the tailpipe exit. Characteristics of temperatures in this zone are:

- Minor or negligible temperature increases to step changes in test speed.
- Transient load or speed changes have a very minor effect on gas temperature and the temperatures tend to oscillate in a range without increasing.
- After the vehicle test speed stabilises, gas temperatures are not seen to be increasing.

It was considered that a model to represent these temperature profiles could be developed and implemented, but the need identified in the earlier experimental section 6.2 was to determine how to minimise the impact of temperature variations on the RS signal being measured from a vehicle.

From the experimental measurements conducted the data collected has allowed us to identify the target area or zone after the exhaust pipe. Temperature measurements of the exhaust plume from both gasoline and diesel show that at a distance of 50 cm from the exhaust pipe the variations in the exhaust gas temperatures are minimising and likely to have a low impact on the RS measurement signal at speeds of up to 60 km/h which covers the majority of RS measurements, over 95%, taken on-road (Huang et al., 2020b). Figure 6.17 provides an indication of the where the suggested low temperature area begins (at 50 cm from the exhaust pipe exit) on a gasoline exhaust plume temperature profile chart.

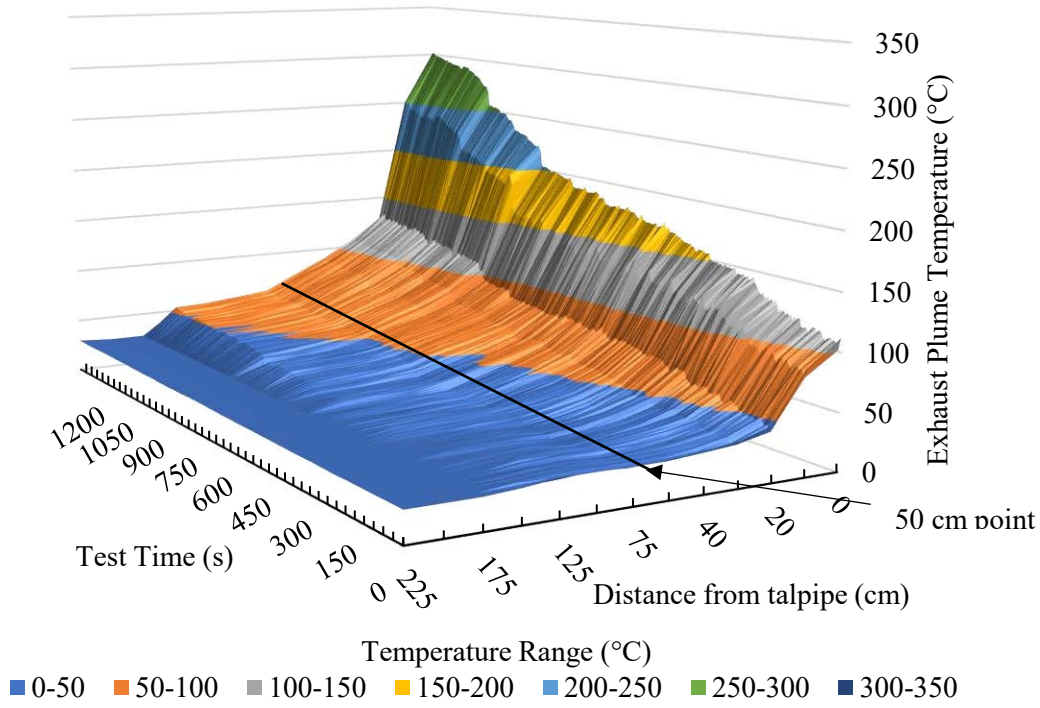

Figure 6.17: Combined gasoline exhaust plume temperature profile measurements with 50 cm cut point indication.

The benefit of starting the analysis RS measurement data collection from this distance after the exhaust pipe will be reduced variation from measurement to measurement due to temperature which can in future allow for more accurate measurement of newer Euro standard vehicles such as Euro 5 or 6. It will provide a much needed step in being able identify more vehicles which are high emitters from the latest vehicles on-road and potentially allow emissions cut points, refer Table 5.1, utilised for RS enforcement processes to be reduced.

It may be questioned if this step will be beneficial as using RS data collected from the exhaust plume once the gases are 50 cm away from the exhaust pipe is subject to the degree of dispersion of the plume and could result in the concentrations being too low to be consistently measured.

Previous studies on the modelling of exhaust plume behaviour and dispersion from a Toyota HiAce vehicle (Huang et al., 2020a) indicate that for CO_2, the RS measurable length of the exhaust plume is 2.7m ± 1.1 m in the vertical plane and 1.5m ± 0.2 m in the horizontal plane at 30 km/h. It is also noted that for NO the measurable plume lengths are shorter being 1.4 ± 0.2 m in the vertical plane and 1.1 ± 0.3 in the horizontal plane at 30

km/h. Considering this information the RS measurement speed, which can be 200 Hz or higher could allow for sufficient data to be collected for analysis.

Considering each of the measurement steps that lead to the development of the exhaust plume temperature profile to assess the gas temperature at various distances from the exhaust pipe under different loading conditions. Some relationship observations can be made.

From the data collected in the open path testing its noted that changes in the temperature of the exhaust plume delivered significant variations in the raw CO_2 measurement values being collected by the RS detector unit. As the temperature increased the RS measured values of the target gas, CO_2, showed significant decreases compared to measurements at lower temperatures. These results were compared against sample gas measurement taken by a conventional gas analyser from the exhaust. The conventional analyser CO_2 measurement results were consistent without significant variation. This indicates for an RS system which is not measuring the instantaneous temperature variations and compensating for them (which most of the RS systems I've been able to review have not incorporated), the results will be offset from the actual value. Which in turn increases the uncertainty of measurement and will reduce measurement accuracy at low concentration levels. The relationship can be described as inversely proportional.

$$T_{Exhpl} \propto \frac{1}{RS_{CO2\ value}} \tag{6.1}$$

where T_{Exhpl} and RS_{CO2} are the Temperature of the exhaust plume (°C) and the RS CO_2 measurement value of the exhaust plume gas.

To achieve the best RS measurement accuracy from the exhaust plume the ideal measurement temperature would be at an ambient temperature around 25 to 30°C. This in practice is not realistic as by the time the gas temperature reaches the ambient it will have dispersed too much and not be measurable. Instead, it is important to identify where the optimum measurements can begin, both considering the distance from the exhaust and temperature of the exhaust plume.

With regard to the optimum temperature for measurement, this should be below 50°C as RS measurement variability is minimal at temperature level. When combining this factor with measurement distance from the exhaust pipe, it is noted that this variable is proportional to the driving speed of the vehicle. As the vehicle speeds increased, the

distance from the tailpipe that the 50°C and below temperature zone exists moves further away from the exhaust pipe. Considering that 95% of RS measurements are at speeds of 60 km/h or less, we can consider this as the boundary condition for simplicity of measurement setup. At 60 km/h the RS measurement of the exhaust plume will need to start at a distance of 50 cm after it leaves the exhaust pipe. For practical purposes 50 cm can be the set point utilised for beginning the RS data measurement analysis.

It should be noted that setting up a variable distance measurement with respect to speed vehicle would be possible, but this would need undertaken as part of a future measurement project for further improving RS measurements and reducing the uncertainty of measurement for new RS systems.

6.4 Conclusions

The aim of this chapter was to develop, setup and conduct experiments to investigate aspects of RS systems and their performance with the potential to identify areas in where the measurement technique could be revised to deliver improvements to the results and potentially reduce uncertainties currently being experienced by users. A series of calibration devices and new open path testing methods were created, tested and the data assessed to identity benefits and potential areas of improvement for RS measurement The main conclusion points are summarised as follows:

Development of a new refined calibration device for assessing performance and allowing an unbiased comparison of RS systems from different manufacturers opened up the potential for checking and verification of instrument performance against a reference test method. This was previously not available for those looking to purchase RS systems and it can help them with making a better-informed choice when selecting measurement equipment. The calibration device provided more stable measurement conditions and assessment of the data identified that high or increasing exhaust gas temperatures above ambient have an effect of the measurement accuracy. A measured ΔT of 14.6°C resulted in 2.6 % variation in the RS data for the same concentration. As varying gas temperatures across a plume could be significantly higher the RS % variation would increase in proportion to the temperature. Furthermore, this information was important in identifying that for comparison purposes the new calibration device would need to be used with gases

at ambient or low exhaust temperatures. This is necessary as the device can absorb heat from exhaust gases, become hotter and in turn influence RS measurements if this is not controlled.

Development of a new testing method followed development of the calibration device. This was called Open Path RS measurement. Without the calibration device to contain and absorb the heat, this removed a variable that could negatively influence RS measurements. The process was developed with a number of control variables that could managed during the testing and provide measurement repeatability. Utilising a generator, an electrical load bank and working in a relatively open environment not subject to wind gusts, a range of varying load cycles were used to assess exhaust gas samples over a range of test temperatures. With development this technique showed that there was a reduction in the RS CO_2 signal values for steady CO_2 emissions as gas temperatures increased.

Utilising this information, a new experiment was devised to measure the temperature of exhaust gas plumes. A vehicle chassis dynamometer, gasoline and diesel test vehicles, and temperature measurement array were assembled and used to collect temperature measurements over a range of loads and speeds. This information was used to create 3D exhaust plume measurements showing different temperature zones, 4 in all and could also to identify which measurement distance and test speeds were impacting the consistency of the RS measurement result. The relationship was used to identify that after a distance of 50 cm from the exhaust pipe the impact of temperature variations could be minimised.

Further to this, RS experimental studies now being undertaken are using a measurement distance of 50cm or greater from the exhaust pipe. It is also possible to implement this in RS field measurements in future if modifications to post processing of measurement data uses vehicle speed measurements at the RS measurement point to determine the required time offset to be applied when selecting the data to be used for determination of the RS emissions results.

Chapter Seven

7. Conclusions and future work

7.1 Conclusions

The objectives of this thesis were to analytically determine the effectiveness of RS systems today and gain an understanding of the greater areas of uncertainty for the purpose of improving accuracy and precision. This was undertaken by studying RS data from the HKEPD, assessing it and the outcomes, developing testing under controlled conditions to research aspects of RS variability and then investigating selected aspects identified to verify potential measurement and technique improvements.

The assessment of the actual performance of the HKEPD RS based strengthened emissions control programme was conducted utilising 5 years of RS emissions measurement data covering 2,144,422 records. The major conclusions of the review and assessment are as follows:

1. Analysis of the emissions performance of the Hong Kong vehicle fleet showed significantly high EFs being produced for the LPG fuelled vehicle fleet primarily consisting of high mileage taxis and PLB's when compared to the gasoline fleet at the beginning of RS monitoring. Further analysis was able to determine the effectiveness of a one-off government sponsored catalytic converter and oxygen sensor replacement programme for LPG vehicles reducing the fleet EF_{HC}, EF_{CO} and EF_{NO} by 44.0%, 42.4% and 32.7% respectively for the LPG vehicle fleet. This level of emissions improvement across a fleet is almost unheard of and represents a unique kind of result in renewing an entire vehicle fleet emissions compliance condition.
2. In the case of the gasoline vehicle fleet which was only subject to annual roadworthy requirements and user maintenance, the strengthened RS emissions control programme can also make improvement in the EFs for the entire fleet. For the whole period (2012–2016), there were overall reductions of 40.5% for EF_{HC}, 45.3% for EF_{CO} and 29.6% for EF_{NO}.

3. New details were able to be extracted identifying individual problem vehicle models that were high emitters, along with identification the problematic model years too. In particular, this study has confirmed the strength of RS through analytical techniques to allow focus on individual vehicles or differing fleet segments that contribute the highest emissions so the identified vehicles are repaired to manufacturer standard or removed from the road to reduce the amount of high emitting vehicles in use.

To enhance and further contribute to the body of knowledge for RS, the study of common engine faults has been conducted to understand the impact of various emissions failures RS potentially identifies. To educate the automotive industry and government of the impact of these vehicle engine and emissions system malfunctions/faults which are also applicable to the broader gasoline vehicle fleet, a Toyota Crown Comfort LPG Taxi was used to simulate a range of emissions malfunctions/faults and also to show correct gaseous emissions behaviours. The vehicle was rebuilt to manufacturer specifications to obtain the regulation emissions compliance. Following this additional engine components and emissions system hardware were obtained which were either worn out or they were modified to simulate faults. There were 15 simulated malfunctions/faults which could be achieved by installing and using the worn or faulty hardware. The major conclusions of this fault simulation experiment are as follows:

1. The impact of simulated faults produced emissions increases of up to 317% for THC, 782% for CO and 352% for NO_x. Other significant increases were identified and this data was incorporated into a package of materials made available to inform and educate what hardware malfunctions/faults created the highest emissions levels.
2. It was determined that negative emissions impacts and deterioration of driving performance did not directly correlate for each major emissions malfunction/fault. Likewise, the same as found the poor driving performance did not correlate with poor emissions performance. Subsequently automotive repairers could not rely on a vehicle driving well to ensure both emissions compliance and desired driving performance.
3. The information learnt from this was utilised to design and deliver training with emissions equipment and diagnostic techniques to educate the local automotive industry and government on the magnitude and source of emissions related failures. Development and implementation of this type of industry training scheme tailored

to address emissions problems was able to support the vehicle maintenance/repair industry cope with the introduction of RS enforcement by the HKEPD and make transition to a higher level of regulation sustainable.

Studying the performance of new RS calibration devices provided the opportunity to determine effectiveness of measurement techniques and to contribute to the development process. Conducting these studies identified that RS measurement is sensitive to varying exhaust gas temperature and that it could affect measurements. Further experiments were conducted to determine how it does impact measurements so improvements to the technique could be identified. The major conclusions drawn from this study are:

1. Development of a new/refined RS calibration device has allowed for effective independent comparison of RS equipment performance from different manufacturers which was not possible previously. During the development process for this device, it identified that high or increasing exhaust gas temperatures have an effect on the measurement accuracy. A measured ΔT of 14.6°C resulted in 2.6 % variation in the RS data for the same CO_2 concentration. As varying gas temperatures across a plume could be significantly higher the RS % variation would increase in proportion to the temperature. CO_2 was the subject of the study being the bulk gas from a vehicle and subject to lower measurement variability compared to the other pollutant gases. The outcome of this was the new RS calibration device would primarily be used to measure gases at ambient or low temperatures as it can otherwise contain the heat and influence the RS measurement if allowed to heat up. It is planned that future trials conducted with new RS equipment will implement these test controls.
2. To negate the impact of temperature on RS calibration checks, a new test which did not use a calibration device was developed. This was called ‘Open Path’ RS testing. With this, it was necessary to develop strong variable controls to achieve good measurement repeatability. The key aspects of this were to utilise a generator set with resistance load bank, conduct testing in a semi open environment where emissions dispersion is consistent. Furthermore, it was determined that the measurement process needs to follow a varying loading cycle that could provide a range of steady state conditions for measurement. The resultant measurement setup could draw a selected/set temperature gas sample from an exhaust tailpipe across an open area for consistent RS measurements. The open path system provided data

to show a progressive reduction in the RS CO_2 signal for steady CO_2 emissions as the gas temperatures increased.

3. To determine the impact of temperature increases, an experiment was conducted to drive test vehicles on a chassis dynamometer and to accurately measure the temperature of the exhaust gas plumes exiting the tailpipe. The measurements were used to construct a 3D exhaust plume temperature profile which showed these testing profiles, 4 areas or temperature response zones (High, Middle, Moderate and Low) of temperature increases were identified. The higher zones experience greater temperature variations, turbulence and instability characteristics which would produce greater uncertainty in any RS measurement results. It has been determined that in the Low temperature response zone (50 cm from tailpipe), the temperature is most stable and suitable for RS measurement. RS measurement at this distance from the exhaust pipe should reduce the impact of temperature variation without the need for significant redesign or rebuilding existing RS measurement systems.

7.2 Suggestions for future work

With consideration of the conclusions and challenges facing RS applications, future study should be considered.

Following on from the identification of the exhaust plume temperature zones, it is suggested that new experimental work be undertaken to determine the magnitude of RS measurement improvements that can be achieved by minimising the impact of high exhaust gas temperature on RS and changing the measurement techniques to improve accuracy and reduce measurement uncertainty.

Further to this, it is suggested that investigations could be conducted on how to apply gas plume temperature measurements in conjunction with RS at measurement sites. This could allow either measurement of exhaust plumes closer to the exit from the exhaust pipe or further identify improvements to the accuracy of the technique.

If temperature measurement of plumes is incorporated into measurement systems it may also assist in further expanding the measurement capability of RS from single lane applications to potentially multilane measurements. It can further help to know if the

plume gas temperatures in a given traffic lane will impact the one next to it. Also applying the exhaust plume temperature profiles with data on plume dispersion could help with allowing longer distance multilane measurements of traffic flows (two or three lanes) or perhaps help refine RS signal measurements for vehicle being driven roads at higher speeds.

As temperature of the exhaust plume has been identified to be important, we also need to consider the measurement of the background gases that are often taken of the air from in front of a vehicle before it passes the RS sensors. If this measurement is also too close to the vehicle, the heat from the vehicle (either radiant or in a boundary layer) could also impact the background air measurements. This could impact any potential background correction calculations being performed. Identifying suggested guidelines for this aspect of RS measurements could help with improving accuracy.

It is suggested to further investigate the impact of airflow turbulence on RS measurements. Turbulence can likely reduce the quality of RS measurements and in turn the capability of an RS system to identify high emitting vehicles. Being able to quantify the impact that intense gusts have on RS data at measurement sites or being able to determine the impact that design/layout of an exhaust system has on the exhaust plume could improve RS measurement.

The open path measurement technique that has been developed also presents an opportunity to utilise this methodology to investigate emissions characteristics which currently present problems for determining high emitters. It is suggested that studying the nature of diesel vehicle emissions with the open path measurement technique may allow new analyses to be undertaken which could help with development and validation of effective use of RS for a strengthened emissions control programme that includes diesel vehicles of all sizes to be able to be identified as high emitters and be repaired to manufacturer standard or removed from the on-road fleet.

References

Abshire JB, Riris H, Allan GR, Weaver CJ, Mao J, Sun X, et al. Pulsed airborne lidar measurements of atmospheric CO2 column absorption. Tellus B: Chemical and Physical Meteorology 2010; 62: 770-783.

Ångström AJ. Optiska undersökningar [Optical investigations]. ongliga Vetenskaps-Akademiens Handlingar [Proceedings of the Royal Academy of Science] (in Swedish) 1853; 40: 333-360.

Ashbaugh LL, Lawson DR, Bishop GA, Guenther PL, Stedman DH, Stephens RD, et al. On-Road Remote Sensing of Carbon Monoxide and Hydrocarbon Emissions During Several Vehicle Operating Conditions. AWMA/EPA Conference on "PM10 Standards and Nontraditional Particulate source controls", Phoenix AZ, 1992, pp. 15.

Austin S, Ross M. History of Emissions Reduction: Normal Emitters in FTP-type Driving. SAE International, 2001.

Australian Government. Vehicle Standard (Australian Design Rule 79/00 — Emission Control for Light Vehicles) 2005. Federal Register of Legislative Instruments F2005L04079. 79/00, 2018.

Barrass S, Gérard Y, Holdsworth RJ, Martin PA. Near-infrared tunable diode laser spectrometer for the remote sensing of vehicle emissions. Spectrochimica Acta Part A: Molecular and Biomolecular Spectroscopy 2004; 60: 3353-3360.

Bay Area Air District. History of the Bay Area Air District. 2021, 2021.

Beaton SP, Bishop GA, Stedman DH. Emission Characteristics of Mexico City Vehicles. J. Air Waste Manage. Assoc. 1992; 42: 1424-1429.

Beaton SP, Bishop GA, Zhang Y, Ashbaugh LL, Lawson DR, Stedman DH. On-road vehicle emissions: Regulations, costs, and benefits. Science 1995; 268: 991.

Beevers SD, Westmoreland E, de Jong MC, Williams ML, Carslaw DC. Trends in NOx and NO2 emissions from road traffic in Great Britain. Atmospheric Environment 2012; 54: 107-116.

Bernard Y, Tietge U, German J, Muncrief R. Determination of real-world emissions from passenger vehicle using remote sensing data. International Council on Clean Transportation, 2018.

Bishop GA, Haugen MJ. The Story of Ever Diminishing Vehicle Tailpipe Emissions as Observed in the Chicago, Illinois Area. Environmental Science & Technology 2018: 7.

Bishop GA, Starkey JR, Ihlenfeldt A, Williams WJ, Stedman DH. IR Long-Path Photometry: A Remote Sensing Tool for Automobile Emissions. Analytical Chemistry 1989; 61: 671A-677A.

Bishop GA, Stedman DH. Measuring the Emissions of Passing Cars. Accounts of Chemical Research 1996; 29: 489-495.

Bishop GA, Stedman DH. FEAT Equations for CO, HC and NO. Denver University, 2014.

Bishop GA, Stedman DH, Burgard DA, Atkinson O. High-Mileage Light-Duty Fleet Vehicle Emissions: Their Potentially Overlooked Importance. Environmental Science & Technology 2016; 50: 5405-5411.

Bishop GA, Stedman DH, Jessop T. Infrared Emission and Remote Sensing. Air and Waste Managament Association 1992; 42: 3.

Bishop JDK, Molden N, Boies AM. Using portable emissions measurement systems (PEMS) to derive more accurate estimates of fuel use and nitrogen oxides

emissions from modern Euro 6 passenger cars under real-world driving conditions. Applied Energy 2019; 242: 942-973.
Borken-Kleefeld J. Guidance note about on-road vehicle emissions remote sensing. San Francisco/USA: The International Council on Clean Transportation (ICCT). Available at: http://theicct.org/road-vehicleemissions-remote-sensing [Accessed October 13, 2013], 2013.
Borken-Kleefeld J, Chen Y. New emission deterioration rates for gasoline cars – Results from long-term measurements. Atmospheric Environment 2015; 101: 58-64.
Borken-Kleefeld J, Dallmann T. REMOTE SENSING OF MOTOR VEHICLE EXHAUST EMISSIONS. International Council on Clean Transportation, 2018.
Breuer MA, Burgard DA. Bridge-based remote sensing of NOx emissions from locomotives. Atmospheric Environment 2019; 198: 77-82.
Brezny R, Kubsh J. Emission Performance of California and Federal Aftermarket TWC Converters. SAE International, 2013.
Britannica TEoE. U-2 Reconnaissance aircraft. In: Britannica E, editor, 2021.
Burgard DA, Bishop GA, Stadtmuller RS, Dalton TR, Stedman DH. Spectroscopy Applied to On-Road Mobile Source Emissions. Applied Spectroscopy 2006a; 60: 135A-148A.
Burgard DA, Bria CRM. Bridge-based sensing of NOx and SO2 emissions from ocean-going ships. Atmospheric Environment 2016; 136: 54-60.
Burgard DA, Bria CRM, Berenbeim JA. Remote Sensing of Emissions from In-Use Small Engine Marine Vessels. Environmental Science & Technology 2011; 45: 2894-2901.
Burgard DA, Dalton TR, Bishop GA, Starkey JR, Stedman DH. Nitrogen dioxide, sulfur dioxide, and ammonia detector for remote sensing of vehicle emissions. Review of Scientific Instruments 2006b; 77: 014101.
California Air Resources Board. History of the California Air Resources Board. 2021, 2021.
Carslaw DC, Beevers SD, Tate JE, Westmoreland EJ, Williams ML. Recent evidence concerning higher NOx emissions from passenger cars and light duty vehicles. Atmospheric Environment 2011; 45: 7053-7063.
Carslaw DC, Rhys-Tyler G. New insights from comprehensive on-road measurements of NOx, NO2 and NH3 from vehicle emission remote sensing in London, UK. Atmospheric Environment 2013; 81: 339-347.
Chan T, Ning Z. On-road remote sensing of diesel vehicle emissions measurement and emission factors estimation in Hong Kong. Atmospheric Environment 2005; 39: 6843-6856.
Chan TL, Ning Z, Leung CW, Cheung CS, Hung WT, Dong G. On-road remote sensing of petrol vehicle emissions measurement and emission factors estimation in Hong Kong. Atmospheric Environment 2004; 38: 2055-2066.
Chandra S, Camal F. A Simulation-based Evaluation of Connected Vehicle Technology for Emissions and Fuel Consumption. Procedia Engineering 2016; 145: 296-303.
Chaney LW. Ambient Air Carbon Monoxide Measurements. Environmental Protection Technology. Univserity of Michigan, 1979a, pp. 35.
Chaney LW. Microscale variations in ambient concentrations of pollutants in St. Louis Air. Environmental Protection Technology. Univserity of Michigan, 1979b, pp. 65.
Chaney LW. The Remote Measurement of Traffic Generated Carbon Monoxide. Journal of the Air Pollution Control Association 1983; 33: 220-222.

Chatterjee D, Deutschmann O, Warnatz J. Detailed surface reaction mechanism in a three-way catalyst. Faraday Discussions 2001; 119: 371-384.
Chen G, Prochnau TJ, Hofeldt DL. Feasibility of Remote Sensing of Particulate Emissions from Heavy-Duty Vehicles. SAE International, 1996.
Chen Y, Borken-Kleefeld J. Real-driving emissions from cars and light commercial vehicles – Results from 13 years remote sensing at Zurich/CH. Atmospheric Environment 2014; 88: 157-164.
Chen Y, Borken-Kleefeld J. NOx Emissions from Diesel Passenger Cars Worsen with Age. Environmental Science & Technology 2016; 50: 3327-3332.
Chiang H-L, Tsai J-H, Yao Y-C, Ho W-Y. Deterioration of gasoline vehicle emissions and effectiveness of tune-up for high-polluted vehicles. Transportation Research Part D: Transport and Environment 2008; 13: 47-53.
Collins K. Virginia's Inspection and Maintenance (I/M) Program: Air Check Virginia. In: Quality VDoE, editor, Richmond Virginia, 2018, pp. 6.
Commissioner for Transport. Code of Practice for Designated Vehicle Emission Testing Centres. In: Transport Department, editor. 3, Hong Kong, 2012, pp. 1-93.
Corbin WL, Imprimerie d AReC, Imprimerie de C, Imprimerie de Louis G, Société Philomathique de P. Extraits des procès-verbaux des séances / Société philomathique de Paris. Vol t.13-15 (1848-1850). Paris :: A. René, 1848.
Dallmann T. Use of remote-sensing technology for vehicle emissions monitoring and control. The International Council on Clean Transport, 2018, pp. 7.
De Simone E, D'Uva M, Ercolano S. Don't save lemons! The impact of older technology vehicles on environmental expenditure at regional level in Italy. Ecological Indicators 2019; 106: 105540.
EKT Interactive. History of Oil. 2022. EKT Interactive, 2022.
European Economic Community. COUNCIL DIRECTIVE of 20 March 1970 on the approximation of the laws of the Member States relating to measures to be taken against air pollution by gases from positive-ignition engines of motor vehicles (70/220/EEC). No L 76/1. 70/220/EEC. UNECE, 1970, pp. 21.
European Economic Community. COUNCIL DIRECTIVE of 26 June 1991 amending Directive 70/220/EEC on the approximation of the laws of the Member States relating to measures to be taken against air pollution by emissions from motor vehicles (91 /441 /EEC). In: Union E, editor. No L 242/ 1. 91 /441 /EEC. UNECE, 1991, pp. 106.
European Economic Community. REGULATION (EC) No 715/2007 OF THE EUROPEAN PARLIAMENT AND OF THE COUNCIL of 20 June 2007 on type approval of motor vehicles with respect to emissions from light passenger and commercial vehicles (Euro 5 and Euro 6) and on access to vehicle repair and maintenance information. In: Union E, editor. 715/2007, 2007, pp. 16.
European Economic Community. COMMISSION REGULATION (EC) No 692/2008 of 18 July 2008 implementing and amending Regulation (EC) No 715/2007 of the European Parliament and of the Council on type-approval of motor vehicles with respect to emissions from light passenger and commercial vehicles (Euro 5 and Euro 6) and on access to vehicle repair and maintenance information. In: Union E, editor. 692/2008. UNECE, 2008, pp. 136.
Fontaras G, Zacharof N-G, Ciuffo B. Fuel consumption and CO2 emissions from passenger cars in Europe – Laboratory versus real-world emissions. Progress in Energy and Combustion Science 2017; 60: 97-131.

Franco V, Kousoulidou M, Muntean M, Ntziachristos L, Hausberger S, Dilara P. Road vehicle emission factors development: A review. Atmospheric Environment 2013; 70: 84-97.
Franco V, Sánchez FP, German J, Mock P. REAL-WORLD EXHAUST EMISSIONS FROM MODERN DIESEL CARS. ICCT, 2014.
Fraunhofer J. Bestimmung des Brechungs‐ und des Farbenzerstreungs‐Vermögens verschiedener Glasarten, in Bezug auf die Vervollkommnung achromatischer Fernröhre/Determination of the refractive and color-dispersing power of different types of glass, in relation to the improvement of achromatic telescopes). Denkschriften_der_Königlichen_Akademie 1814-1815 1815; 5: 220-221.
Fraunhofer J. Reprint - Bestimmung des Brechungs‐ und des Farbenzerstreungs‐Vermögens verschiedener Glasarten, in Bezug auf die Vervollkommnung achromatischer Fernröhre/Determination of the refractive and color-dispersing power of different types of glass, in relation to the improvement of achromatic telescopes). Denkschriften der Königlichen Akademie der Wissenschaften zu München/Memoirs of the Royal Academy of Sciences in Munich 1817; 56: 264-313.
Frey HC, Unal A, Rouphail NM, Colyar JD. On-road measurement of vehicle tailpipe emissions using a portable instrument. Journal of the Air & Waste Management Association 2003; 53: 992-1002.
Ghaffarpasand O, Beddows DCS, Ropkins K, Pope FD. Real-world assessment of vehicle air pollutant emissions subset by vehicle type, fuel and EURO class: New findings from the recent UK EDAR field campaigns, and implications for emissions restricted zones. Science of The Total Environment 2020; 734: 139416.
Giechaskiel B, Clairotte M, Valverde-Morales V, Bonnel P, Kregar Z, Franco V, et al. Framework for the assessment of PEMS (Portable Emissions Measurement Systems) uncertainty. Environmental Research 2018a; 166: 251-260.
Giechaskiel B, Melas A, Martini G, Dilara P. Overview of Vehicle Exhaust Particle Number Regulations. Processes 2021; 9: 2216.
Giechaskiel B, Suarez-Bertoa R, Lähde T, Clairotte M, Carriero M, Bonnel P, et al. Evaluation of NOx emissions of a retrofitted Euro 5 passenger car for the Horizon prize “Engine retrofit”. Environmental Research 2018b; 166: 298-309.
Grange SK, Lewis AC, Moller SJ, Carslaw DC. Lower vehicular primary emissions of NO2 in Europe than assumed in policy projections. Nature Geoscience 2017; 10: 914-918.
Gregory K, Webster C, Durk S. Estimates of damage to forests in Europe due to emissions of acidifying pollutants. Energy Policy 1996; 24: 655-664.
Grennfelt P, Engleryd A, Forsius M, Hov Ø, Rodhe H, Cowling E. Acid rain and air pollution: 50 years of progress in environmental science and policy. Ambio 2020; 49: 849-864.
Grigoratos T, Fontaras G, Giechaskiel B, Zacharof N. Real world emissions performance of heavy-duty Euro VI diesel vehicles. Atmospheric Environment 2019; 201: 348-359.
Guenther PL, Stedman DH, Bishop GA, Hannigan JW, Bean JH, Quine RW. Remote Sensing of Automobile Exhuast, 1991, pp. 43.
Guo H, Zhang Q, Shi Y, Wang D. On-road remote sensing measurements and fuel-based motor vehicle emission inventory in Hangzhou, China. Atmospheric Environment 2007; 41: 3095-3107.

Haagen-Smit AJ. Chemistry and Physiology of Los Angeles Smog. Industrial and Engineering Chemistry 1952.
Haagen-Smit AJ. Smog control - is it just around the corner. Engineering and Science 1962; 26: 9-14.
Hager JS. EDAR North American and European case studies. 2021. HEAT LLC, 2021.
Hass GC, Brubache ML. A Test Procedure for Motor Vehicle Exhaust Emissions. Journal of the Air Pollution Control Association 1962; 12: 505-543.
He L, Hu J, Yang L, Li Z, Zheng X, Xie S, et al. Real-world gaseous emissions of high-mileage taxi fleets in China. Science of The Total Environment 2019; 659: 267-274.
Herschel J, Fredrick W. On the absorption of light by coloured media, and on the colours of the prismatic spectrum exhibited by certain flames; with an account of a ready mode of determining the absolute dispersive power of any medium, by direct experiment. Transactions of the Royal Society of Edinburgh 1823: 445-460.
Hickman AJ. Vehicle maintenance and exhaust emissions. Science of The Total Environment 1994; 146-147: 235-243.
Hong Kong Environment Bureau. A Clean Air Plan for Hong Kong. In: Bureau HKE, editor, Hong Kong, 2013.
Hong Kong Environment Protection Department. Air Quality Objectives for Hong Kong, 2013.
Hong Kong Environment Protection Department. Air Quality Compppliance Status 2017, 2018.
Hong Kong Government. One-off subsidy to assist vehicle owners to replace the catalytic converters and oxygen sensors of their petrol and liquefied petroleum gas taxis and light buses. In: Finance Committee, editor. HEAD 44 – ENVIRONMENTAL PROTECTION DEPARTMENT Subhead 700 General non-recurrent New Item, Hong Kong, 2012.
Hong Kong Government. EPD to strengthen emission control of petrol and LPG vehicles in September. Article 3743, Hong Kong, 2014, pp. 1.
Hong Kong Government. Hire Car Permits (Limitation on Numbers) Notice, 2018, pp. 1.
Hong Kong Observatory. Table 4. Monthly means of daily maximum, mean and minimum temperature recorded at the Observatory between 1981-2010. 2019, 2019a.
Hong Kong Observatory. Table 7. Monthly means of prevailing wind direction and mean wind speed recorded at the Observatory and Waglan Island between 1981-2010. 2019, 2019b.
Hounshell DA. From the American System to Mass Production 1800-1932 - The Development of Manufacturig Technology in the United States: The John Hopkins University Press, 1984.
Huang Y, Ng ECY, Surawski NC, Yam Y-S, Mok W-C, Liu C-H, et al. Large eddy simulation of vehicle emissions dispersion: Implications for on-road remote sensing measurements. Environmental Pollution 2020a; 259: 113974.
Huang Y, Ng ECY, Yam Y-s, Lee CKC, Surawski NC, Mok W-c, et al. Impact of potential engine malfunctions on fuel consumption and gaseous emissions of a Euro VI diesel truck. Energy Conversion and Management 2019a; 184: 521-529.
Huang Y, Organ B, Zhou JL, Surawski NC, Hong G, Chan EFC, et al. Emission measurement of diesel vehicles in Hong Kong through on-road remote sensing:

Performance review and identification of high-emitters. Environmental Pollution 2018a; 237: 133-142.
Huang Y, Organ B, Zhou JL, Surawski NC, Hong G, Chan EFC, et al. Remote sensing of on-road vehicle emissions: Mechanism, applications and a case study from Hong Kong. Atmospheric Environment 2018b; 182: 58-74.
Huang Y, Organ B, Zhou JL, Surawski NC, Yam Y-s, Chan EFC. Characterisation of diesel vehicle emissions and determination of remote sensing cutpoints for diesel high-emitters. Environmental Pollution 2019b; 252: 31-38.
Huang Y, Surawski NC, Organ B, Zhou JL, Tang OHH, Chan EFC. Fuel consumption and emissions performance under real driving: Comparison between hybrid and conventional vehicles. Science of The Total Environment 2019c; 659: 275-282.
Huang Y, Yam YS, Lee CKC, Organ B, Zhou JL, Surawski NC, et al. Tackling nitric oxide emissions from dominant diesel vehicle models using on-road remote sensing technology. Environmental Pollution 2018c; 243: 1177-1185.
Huang Y, Yu Y, Yam Y-s, Zhou JL, Lei C, Organ B, et al. Statistical evaluation of on-road vehicle emissions measurement using a dual remote sensing technique. Environmental Pollution 2020b; 267: 115456.
Huddle FP. Automobiles in the postwar economy. Editorial research reports 1945 (Vol. II), 1945.
Johnson D. Description of the Real-time On-road Vehicle Emissions Reporter. MSTRS Meeting. USEPA, 2002, pp. 17.
Kašpar J, Fornasiero P, Hickey N. Automotive catalytic converters: current status and some perspectives. Catalysis Today 2003; 77: 419-449.
Kassel R, Couch P, Conolly M, Hammer-Barulich A. Ultrafine Particulate Matter and the Benefits of Reducing Particle Numbers in the United States. Ultrafine Particulate Matter White Paper, 2013, pp. 74.
Kirchhoff G, Bunsen R. IX. Chemical analysis by spectrum-observations. The London, Edinburgh, and Dublin Philosophical Magazine and Journal of Science 1860; 20: 88-109.
Kirchhoff GR. Ueber die Fraunhofers'chen Linien / On Fraunhofers lines. Monatsbericht der Königlichen Preussische Akademie der Wissenschaften zu Berlin (Monthly report of the Royal Prussian Academy of Sciences in Berlin) 1859: 4.
Kittelson DB. Engines and nanoparticles: a review. Journal of Aerosol Science 1998; 29: 575-588.
Klier T, Linn J. Comparing US and EU Approaches to Regulating Automotive Emissions and Fuel Economy. Resources for the Future 2016; 16: 9.
Kumar Pathak S, Sood V, Singh Y, Channiwala SA. Real world vehicle emissions: Their correlation with driving parameters. Transportation Research Part D: Transport and Environment 2016; 44: 157-176.
La Rocca A, Bonatesta F, Fay MW, Campanella F. Characterisation of soot in oil from a gasoline direct injection engine using Transmission Electron Microscopy. Tribology International 2015; 86: 77-84.
Landrigan PJ, Fuller R, Acosta NJR, Adeyi O, Arnold R, Basu N, et al. The Lancet Commission on pollution and health. The Lancet 2018; 391: 462-512.
Lau CF, Rakowska A, Townsend T, Brimblecombe P, Chan TL, Yam YS, et al. Evaluation of diesel fleet emissions and control policies from plume chasing measurements of on-road vehicles. Atmospheric Environment 2015; 122: 171-182.

Lau J, Hung WT, Cheung CS. Observation of increases in emission from modern vehicles over time in Hong Kong using remote sensing. Environmental Pollution 2012; 163: 14-23.
Lee CKC. Refined RS Calibration device, 2019, pp. Remote Sesning calibration checking/testing device.
Lee S, Bae C, Lee Y, Han T. Effects of Engine Operating Conditions on Catalytic Converter Temperature in an SI Engine. SAE International, 2002.
Li Z, Ming T, Shi T, Zhang H, Wen C-Y, Lu X, et al. Review on pollutant dispersion in urban areas-part B: Local mitigation strategies, optimization framework, and evaluation theory. Building and Environment 2021; 198: 107890.
Liu T, Zhou L, Liu Q, Lee BP, Yao D, Lu H, et al. Secondary Organic Aerosol Formation from Urban Roadside Air in Hong Kong. Environmental Science & Technology 2019; 53: 3001-3009.
Lockheed Martin. History of SR71 Blackbird. Lockhead Martin, 2021.
Lyu X, Guo H, Simpson IJ, Meinardi S, Louie PKK, Ling Z, et al. Effectiveness of replacing catalytic converters in LPG-fueled vehicles in Hong Kong. Atmospheric Chemistry and Physics 2016; 16: 6609-6626.
Maga JA, Hass GC. The Development of Motor Vehicle Exhaust Emission Standards in California. Journal of the Air Pollution Control Association 1960; 10: 393-414.
Mazzoleni C, Kuhns HD, Moosmüller H. Monitoring Automotive Particulate Matter Emissions with LiDAR: A Review. Remote Sensing 2010; 2: 1077-1119.
Mazzoleni C, Moosmüller H, Kuhns HD, Keislar RE, Barber PW, Nikolic D, et al. Correlation between automotive CO, HC, NO, and PM emission factors from on-road remote sensing: implications for inspection and maintenance programs. Transportation Research Part D: Transport and Environment 2004; 9: 477-496.
McClintock PM. 2007 High Emitter Remote Sensing Project. Southeast Michigan Council of Governments, 2007.
Melvill T. Observation on light and colours. "Observations on light and colours". Essays and Observations, Physical and Literary. Read before a Society in Edinburgh 1752; Philosophical Society of Edinburgh.Philosophical Society of Edinburgh.
Miller D. The Democratization of Vehicle Emissions Testing. PEMS Workshop 2018, Riverside, CA, 2018, pp. 36.
Nevius T, Rooney R, Zummer R. Speciation of Nitrogen Oxides in a Light Duty Diesel Engine During an EGR System Failure. SAE International, 2012.
Newton I. Some Experiments Propos'd in Relation to Mr. Newtons Theory of Light. Philosophical Transactions (1665-1678) 1672; 7: 4.
Nikolao K, Stedman DH. Remote Sensing of Vehicle Emissions, Case Study: Thessaloniki, Greece,. 4th International Conference on Advances in Communication and Control, Rhodes, Greece,, 1993.
Ning Z, Chan TL. On-road remote sensing of liquefied petroleum gas (LPG) vehicle emissions measurement and emission factors estimation. Atmospheric Environment 2007; 41: 9099-9110.
Ning Z, Wubulihairen M, Yang F. PM, NOx and butane emissions from on-road vehicle fleets in Hong Kong and their implications on emission control policy. Atmospheric Environment 2012; 61: 265-274.
O'Driscoll R, Stettler MEJ, Molden N, Oxley T, ApSimon HM. Real world CO2 and NOx emissions from 149 Euro 5 and 6 diesel, gasoline and hybrid passenger cars. Science of The Total Environment 2018; 621: 282-290.

Organ B, Huang Y, Zhou JL, Hong G, Yam YS, Chan EFC. Emission Performance of LPG Vehicles by Remote Sensing Technique in Hong Kong. SAE, Heidelberg, Germany, 2018, pp. 6.
Organ B, Huang Y, Zhou JL, Surawski NC, Yam Y-S, Mok W-C, et al. A remote sensing emissions monitoring programme reduces emissions of gasoline and LPG vehicles. Environmental Research 2019; 177: 108614.
Organ B, Huang Y, Zhou JL, Yam Y-S, Mok W-C, Chan EFC. Simulation of engine faults and their impact on emissions and vehicle performance for a liquefied petroleum gas taxi. Science of The Total Environment 2020; 716: 137066.
Pall Life Sciences. Info Sheet: Filtration Products for Air Monitoring and Sampling, 2021.
PAPA International PAPAI. Histroy of Aerial Photography. 2021. Professional Aerial Photographers Association, 2021.
Perugu H, Ramirez L, DaMassa J. Incorporating temperature effects in California's on-road emission gridding process for air quality model inputs. Environmental Pollution 2018; 239: 1-12.
Peterson JE, Stedman DH, Bishop GA. Remote Sensing of Automotive Emissions in Toronto,. Air & Waste Management Association. AWMA - Ontario Section Currents, 1991, pp. 4.
Pokharel SS, Bishop GA, Stedman DH. Fuel-Based On-Road Motor Vehicle Emissions Inventory for the Denver Metropolitan Area, 2001.
Popp PJ, Bishop GA, Stedman DH. Development of a High-Speed Ultraviolet Spectrometer for Remote Sensing of Mobile Source Nitric Oxide Emissions. Journal of the Air & Waste Management Association 1999; 49: 1463-1468.
Pujadas M, Domínguez-Sáez A, De la Fuente J. Real-driving emissions of circulating Spanish car fleet in 2015 using RSD Technology. Science of The Total Environment 2017; 576: 193-209.
Rakowska A, Wong KC, Townsend T, Chan KL, Westerdahl D, Ng S, et al. Impact of traffic volume and composition on the air quality and pedestrian exposure in urban street canyon. Atmospheric Environment 2014; 98: 260-270.
Requia WJ, Koutrakis P, Roig HL, Adams MD, Santos CM. Association between vehicular emissions and cardiorespiratory disease risk in Brazil and its variation by spatial clustering of socio-economic factors. Environmental Research 2016; 150: 452-460.
Ristovski ZD, Miljevic B, Surawski NC, Morawska L, Fong KM, Goh F, et al. Respiratory health effects of diesel particulate matter. Respirology 2012; 17: 201-212.
Ropkins K, Beebe J, Li H, Daham B, Tate J, Bell M, et al. Real-World Vehicle Exhaust Emissions Monitoring: Review and Critical Discussion. Critical Reviews in Environmental Science and Technology 2009; 39: 79-152.
Ropkins K, DeFries TH, Pope F, Green DC, Kemper J, Kishan S, et al. Evaluation of EDAR vehicle emissions remote sensing technology. Science of The Total Environment 2017; 609: 1464-1474.
Saari S, Karjalainen P, Ntziachristos L, Pirjola L, Matilainen P, Keskinen J, et al. Exhaust particle and NOx emission performance of an SCR heavy duty truck operating in real-world conditions. Atmospheric Environment 2016; 126: 136-144.
Sadler L, Jenkins N, Legassick W, Sokhi RS. Remote sensing of vehicle emissions on British urban roads. Science of The Total Environment 1996; 189-190: 155-160.

SAE. Stoichiometric Air-Fuel Ratios of Automotive Fuels J1829_201503. SAE International, 2015, pp. 10.
Samaras Z, Kitsopanidis I. Methodology and results of the evaluation of alternative short tests applied in inspection and maintenance programmes. Transportation Research Part D: Transport and Environment 2001; 6: 111-122.
Samaras Z, Zachariadis T, Joumard R, Hassel D, Weber F-J, Rijkeboer R. An Outline of the 1994-1998 European Inspection and Maintenance Study: Part I—Design, Tests, and Results of Experimental Methods. Journal of the Air & Waste Management Association 2001; 51: 913-938.
Shimoda H. Remote Sensing Data Applications. In: Pelton JN, Madry S, Camacho-Lara S, editors. Handbook of Satellite Applications. Springer New York, New York, NY, 2013, pp. 865-933.
Simonetti D, Preatoni D, Simonetti E. Phenology-based land cover classification using Landsat 8 time series. Publications Office of the EU 2014.
SmartDraw. Minivan 1. SmartDraw, LLC, 2021.
Smith A, Davies H. A review of the history of emission legislation, urban and national transport trends and their impact on transport emissions. Transactions on the Built Environment 1996; vol 23: 10.
Stedman DH, Bishop GA. Automobile Carbon Monoxide (CO) Emission Inventory Using Remote Sensing. Proceedings of the 28th Liege International Astrophysical Colloquium, Liege, Belgium, 1989.
Stedman DH, Bishop GA. Evaluation of A Remote Sensor for Mobile Source CO Emissions. United States Environmental Protection Department, USA, 1991, pp. 90.
Stedman DH, Bishop GA. Opacity Enhancement of the On-Road Remote Sensor for HC, CO and NO. University of Denver, Denver, 2002, pp. 17.
Stedman DH, Bishop GA, Aldrete P. On-road CO, HC, NO & Opacity Measurements. 7th CRC ON-Road Vehicle Emissions Workshop, San Diego California, 1997, pp. 7.
Stedman DH, Bishop GA, Peterson JE, Guenther PL. On-Road Remote Sensing of CO Emissions in the Los Angeles Basin. Final report to the California Air Resources Board under Contract No. A932-189, 1991. California Air Resources Board, 1991a, pp. 71.
Stedman DH, Bishop GA, Peterson JE, Guenther PL, McVey IE, Beaton SP. On-Road Carbon Monoxide and Hydrocarbon Remote Sensing in The Chicago Area. Final Report to the Illinois Dept. of Energy and Natural Resources, ILENR/RE-AQ-91/14, 1991. Illinois Department of Energy and Natural Resources, 1991b, pp. 83.
Stephens RD, Cadle SH. Remote Sensing Measurements of Carbon Monoxide Emissions from On-Road Vehicles. Journal of the Air & Waste Management Association 1991; 41: 39-46.
Suarez-Bertoa R, Astorga C. Impact of cold temperature on Euro 6 passenger car emissions. Environmental Pollution 2018; 234: 318-329.
Talbot W, Fox H. Experiments on Coloured Flames. The Edinburgh Journal of Science 1826; V: 77-80.
Tang W, Siani A, Chen F, Chen B. On Developing Advanced Catalysts Systems to Meet China New Regulations. SAE International, 2019.
The Health Effects Institute. AIR POLLUTION, THE AUTOMOBILE, AND PUBLIC HEALTH. Washington, D.C.: NATIONAL ACADEMY PRESS, 1988.

Toma M, Micu D, Andreescu C. Influences of engine faults on pollutant emission. Procedia Manufacturing 2019; 32: 529-536.
Transport Department. Table 4.1a - Registration and Licensing of Vehicles by Class of Vehicles - Jan 2013. In: Department T, editor. 2013-1, Hong Kong, 2013.
Transport Department. Table 4.1a - Registration and Licensing of Vehicles by Class of Vehicles - Jan 2016. In: Department T, editor, Hong Kong, 2016.
Transport Department. Table 4.1a - Registration and Licensing of Vehicles by Class of Vehicles - Apr 2017. In: Department T, editor, 2017.
Turner KC. Automobile Catalytic Converters. Vol Science and Technology. Berlin, Heidelberg,: Springer, , 1984.
UCAR. Carbon Dioxide Absorbs and Re-emits Infrared Radiation. In: Education CfS, editor. 2022. UCAR - University Corporation for Atmospheric Research, 2022.
UNECE UNECfE-. Regulation 101 - Uniform provisions concerning the approval of passenger cars powered by an internal combustion engine only, or powered by a hybrid electric power train with regard to the measurement of the emission of carbon dioxide and fuel consumption and/or the measurement of electric energy consumption and electric range, and of categories M1 and N1 vehicles powered by an electric power train only with regard to the measurement of electric energy consumption and electric range. In: UNECE, editor. 101 R3, 2013.
UNECE UNECfE-. Regulation 83 - Uniform provisions concerning the approval of vehicles with regard to the emission of pollutants according to engine fuel requirements, 2015.
United Nations Economic Commission for Europe. Global technical regulation No. 15 Worldwide harmonized Light vehicles Test Procedure. In: UNECE, editor. ECE/TRANS/180/Add.15, 2014, pp. 234.
US Government. Subpart J - Field Testing and Portable Emission Measurement Systems. US Government, United States of America, 2005.
US Public Law. Air Pollution Control Act. Government Publishing Office [US],, United States of Amerca, 1955, pp. 2.
US Public Law. Clean Air Act. Government Publishing Office [US],, United States of America, 1963.
US Public Law. Motor Vehicle Air Pollution Control Act. Government Publishing Office [US],, United States of America, 1965.
USEPA. EPA Vehicle Chassis Dynamometer Driving Schedules - Urban Dynamometer Driving Schedule. Enviromental Protection Agency of the United States,, 1972.
USEPA. EPA Vehicle Chassis Dynamometer Driving Schedules (DDS) - Federal Test Procedure. Environmental Protection Agency of the United States, 1975.
USEPA. Summary of Criminal Prosecutions - Clean Air Act - OBD Tampering, 2014.
USEPA. Evolution of the Clean Air Act. 2022, 2022.
Vescio N. Three Decades of Real World Driving Emissions (Remote Sensing). Scottish Air Quality Database and Website Annual Seminar, 2019, pp. 48.
Weber C, Sundvor I, Figenbaum E. Comparison of regulated emission factors of Euro 6 LDV in Nordic temperatures and cold start conditions: Diesel- and gasoline direct-injection. Atmospheric Environment 2019; 206: 208-217.
Wei P-S, Hsieh Y-C, Chiu H-H, Yen D-L, Lee C, Tsai Y-C, et al. Absorption coefficient of carbon dioxide across atmospheric troposphere layer. Heliyon 2018; 4: e00785-e00785.
Wenzel T. Reducing emissions from in-use vehicles: an evaluation of the Phoenix inspection and maintenance program using test results and independent emissions measurements. Environmental Science & Policy 2001; 4: 359-376.

Wheatstone C. On the prismatic decomposition of electrical light. Notices and Abstracts of Communications to the British Association for the Advancement of Science, at the Dublin Meeting 1835.
Wollaston WH. A method of examining refractive and dispersive powers, by prismatic reflection. Phil. Trans. R. Soc. 1802; 92: 365–380.
World Health Organisation. Ambient (outdoor) air quality and health. 2019, 2018.
Wright W, Wright O. Wilbur Wright und seine Flugmaschine, 1909, pp. 3:28.
Xie S, Bluett J, Fisher G, Kuschel G, Stedman D. On-Road Remote Sensing of Vehicle Exhaust Emissions in Auckland, New Zealand. Clean Air and Environmental Quality 2005; Vol. 39,: 37-42.
Yao D, Lyu X, Murray F, Morawska L, Yu W, Wang J, et al. Continuous effectiveness of replacing catalytic converters on liquified petroleum gas-fueled vehicles in Hong Kong. Science of the Total Environment 2019; 648: 830-838.
Zachariadis T, Ntziachristos L, Samaras Z. The effect of age and technological change on motor vehicle emissions. Transportation Research Part D: Transport and Environment 2001; 6: 221-227.
Zhang Q, Fan J, Yang W, Ying F, Bao Z, Sheng Y, et al. Influences of accumulated mileage and technological changes on emissions of regulated pollutants from gasoline passenger vehicles. Journal of Environmental Sciences 2018; 71: 197-206.
Zhang Y, Stedman DH, Bishop GA, Beaton SP, Guenther PL, McVey IF. Enhancement of remote sensing for mobile source nitric oxide. Journal of the Air & Waste Management Association 1996a; 46: 25-29.
Zhang Y, Stedman DH, Bishop GA, Beaton SP, Guenther PL, McVey IF. Enhancement of remote sensing for mobile source nitric oxide. Air Waste 1996b; 46: 29.
Zhang Y, Stedman DH, Bishop GA, Guenther PL, Beaton SP. Worldwide On-Road Vehicle Exhaust Emissions Study by Remote Sensing. Environmental Science & Technology 1995; 29: 2286-2294.
Zhang Y, Stedman DH, Bishop GA, Guenther PL, Beaton SP, Peterson JE. On-road hydrocarbon remote sensing in the Denver area. Environmental Science & Technology 1993; 27: 1885-1891.
Zheng X, Wu Y, Zhang S, He L, Hao J. Evaluating real-world emissions of light-duty gasoline vehicles with deactivated three-way catalyst converters. Atmospheric Pollution Research 2018; 9: 126-132.
Zhou Y, Fu L, Cheng L. Characterization of In-Use Light-Duty Gasoline Vehicle Emissions by Remote Sensing in Beijing: Impact of Recent Control Measures. Journal of the Air & Waste Management Association 2007; 57: 1071-1077.

Appendix A – RS measurement locations

Table A1. RS measurement location data

Measurement location	Average Speed (km/h)	Average Acceleration (km/h.s)	No. of visits to site	No. of valid RS records	Average No. of valid records per site visit	% of Gasoline vehicles	% of LPG vehicles
H0001	27.93	0.028	43	119041	2768.3	61.4%	38.6%
H0002	58.18	-0.809	4	504	126	81.5%	18.5%
H0003	43.4	-1.125	1	365	365	61.4%	38.6%
H0004	52.77	-0.5	15	5617	374.4	64.2%	35.8%
H0005	47.22	0.114	12	7367	613.9	55.0%	45.0%
H0006	42.74	-0.096	8	3416	427	73.2%	26.8%
H0008	27.6	0.376	45	81381	1808.4	51.5%	48.5%
H0009	37.72	0.393	8	6708	838.5	65.4%	34.6%
H0010	33.92	-0.479	13	19697	1515.1	56.5%	43.5%
H0011	27.57	0.521	5	3850	770	44.7%	55.3%
H0014	60.12	-0.239	1	382	382	61.5%	38.5%
H0015	28.48	0.249	27	33540	1242.2	69.1%	30.9%
H0016	42.7	-0.647	8	2013	251.6	51.5%	48.5%
H0018	44.91	-0.298	5	681	136.2	50.4%	49.6%
H0019	43.99	0.135	25	31079	1243.1	50.5%	49.5%
H0020	44.65	-0.007	4	2416	604	55.0%	45.0%
H0021	35.45	0.37	13	7543	580.2	50.4%	49.6%
H0022	25.79	0.365	7	2345	335	57.3%	42.7%
H0023	34.56	-0.153	7	2693	384.7	63.4%	36.6%
H0024	31.58	0.269	1	2270	2270	41.5%	58.5%
H0025	15.3	0.321	1	2686	2686	47.2%	52.8%
H0026	32.22	0.299	4	3116	779	46.0%	54.0%
H0028	39.37	0.034	23	18056	785	67.9%	32.1%
H0029	31.99	0.46	4	1923	480.7	50.2%	49.8%
H0031	54.39	-0.526	4	1687	421.7	70.2%	29.8%
H0032	28.35	-0.274	8	9116	1139.5	17.7%	82.3%
H0033	28.47	0.188	4	3064	766	50.5%	49.5%
H0034	29.6	0.017	3	2760	920	60.3%	39.7%
H0035	28.79	0.207	5	3166	633.2	46.4%	53.6%
H0036	31.22	-0.127	5	8333	1666.6	7.2%	92.8%
H0037	25.92	-0.024	6	4663	777.1	65.7%	34.3%
H0038	23.93	-0.294	1	3921	3921	17.5%	82.5%
H0039	23.07	-0.04	10	23113	2311.3	13.0%	87.0%
H0040	41.04	-0.516	4	1978	494.5	73.7%	26.3%
H0041	35.52	-0.23	4	5579	1394.7	73.3%	26.7%
H0042	42.28	0.849	3	1564	521.3	38.8%	61.2%
HD008	27.24	0.276	1	413	413	52.3%	47.7%
HD015	32.04	-0.038	2	733	366.5	66.3%	33.7%
HD019	42.9	-0.584	1	344	344	62.5%	37.5%

HD021	36.11	0.988	1	42	42	69.0%	31.0%
HD028	39.08	0.687	3	563	187.6	68.9%	31.1%
HD039	21.91	0.077	1	102	102	31.4%	68.6%
I0001	40.03	0.102	5	678	135.6	79.4%	20.6%
I0002	42.48	0.272	3	294	98	81.0%	19.0%
I0004	50.05	-0.72	8	2880	360	43.4%	56.6%
K0001	47.61	-0.398	21	13400	638	60.6%	39.4%
K0002	31.66	0.413	41	60841	1483.9	45.5%	54.5%
K0004	34.41	0.174	12	10073	839.4	30.2%	69.8%
K0005	50.75	-0.226	41	58708	1431.9	48.0%	52.0%
K0006	58.82	-0.837	22	11067	503	58.4%	41.6%
K0007	47.53	0.038	21	20682	984.8	70.0%	30.0%
K0008	54.22	0.147	17	10989	646.4	82.8%	17.2%
K0009	43.18	0.235	15	7574	504.9	78.6%	21.4%
K0011	49.31	-0.866	13	2252	173.2	69.8%	30.2%
K0012	45.8	-0.326	7	2118	302.5	72.6%	27.4%
K0013	57.32	-0.229	10	1605	160.5	76.7%	23.3%
K0014	35.12	0.252	25	33207	1328.2	66.2%	33.8%
K0015	44.1	0.157	8	4870	608.7	50.1%	49.9%
K0016	45.34	-1.173	2	655	327.5	60.8%	39.2%
K0018	42.7	-0.365	27	24441	905.2	14.1%	85.9%
K0019	36.33	0.052	9	4872	541.3	37.2%	62.8%
K0023	38.04	0.315	8	4071	508.8	35.5%	64.5%
K0024	10.65	-0.086	1	245	245	83.3%	16.7%
K0025	19.75	-0.378	2	656	328	82.8%	17.2%
K0026	68.49	-1.408	3	536	178.6	56.5%	43.5%
K0027	49.33	0.484	4	1120	280	64.0%	36.0%
K0028	48.7	-0.218	5	3652	730.4	50.6%	49.4%
K0029	59.72	-0.886	5	235	47	70.6%	29.4%
K0030	27.92	-0.246	5	4618	923.6	40.4%	59.6%
K0031	34.52	-0.327	5	5055	1011	17.2%	82.8%
K0032	33.7	0.129	5	3831	766.2	57.9%	42.1%
K0034	40.41	-0.657	5	1681	336.2	63.2%	36.8%
K0035	32.05	-0.084	8	2412	301.5	33.4%	66.6%
K0036	34.08	0.336	3	1388	462.6	33.9%	66.1%
K0037	31.93	0.191	5	4669	933.8	59.9%	40.1%
K0038	25.25	-0.104	19	11120	585.2	61.4%	38.6%
K0039	35.24	0.161	11	10188	926.1	28.1%	71.9%
K0040	50.98	-0.861	3	1486	495.3	27.3%	72.7%
K0041	42.94	-0.892	3	1359	453	33.0%	67.0%
KD001	43.49	-0.508	3	746	248.6	63.3%	36.7%
KD002	31.63	0.236	2	574	287	57.8%	42.2%
KD005	41.97	-0.06	4	859	214.7	64.7%	35.3%
KD006	56.43	-1.339	3	276	92	61.6%	38.4%
KD007	40	0.427	2	194	97	70.6%	29.4%
KD008	54.46	0.61	5	1184	236.8	83.9%	16.1%
KD009	45.21	1.43	1	98	98	81.6%	18.4%
KD014	32.73	-0.083	4	2667	666.7	71.4%	28.6%

KD038	17.03	-0.106	1	16	16	81.3%	18.8%
KD039	38.6	0.671	1	25	25	36.0%	64.0%
N0001	58.4	-0.261	9	2543	282.5	66.5%	33.5%
N0002	47.59	-0.402	11	4304	391.2	79.3%	20.7%
N0003	42.18	-0.491	4	1251	312.7	82.5%	17.5%
N0004	38.62	-0.069	18	30944	1719.1	82.6%	17.4%
N0005	51.09	-0.19	25	20851	834	55.5%	44.5%
N0006	41.78	-0.026	20	8523	426.1	58.8%	41.2%
N0007	39.26	0.146	24	9867	411.1	71.5%	28.5%
N0008	55.18	-1.236	11	8056	732.3	83.3%	16.7%
N0011	38.23	0.276	1	251	251	72.5%	27.5%
N0012	44.11	-0.283	6	3069	511.5	64.8%	35.2%
N0013	41.47	-0.099	7	4164	594.8	67.5%	32.5%
N0014	45.23	-0.385	7	3863	551.8	90.5%	9.5%
N0015	50.21	-0.649	5	1190	238	71.9%	28.1%
N0016	32.82	-0.609	1	254	254	78.0%	22.0%
N0017	47.42	-0.39	10	3395	339.5	64.4%	35.6%
N0018	37.04	0.14	14	3778	269.8	85.3%	14.7%
N0019	51.86	-1.76	11	517	47	64.0%	36.0%
N0020	41.68	-0.057	5	2281	456.2	78.9%	21.1%
N0021	45.02	-0.483	17	7457	438.6	55.4%	44.6%
N0022	38.51	-0.055	16	7600	475	15.7%	84.3%
N0023	52.44	-0.285	9	1229	136.5	26.5%	73.5%
N0025	27.58	0.064	15	15695	1046.3	64.8%	35.2%
N0029	46.21	-0.975	5	2697	539.4	91.8%	8.2%
N0030	63.46	-1.087	5	216	43.2	57.9%	42.1%
N0031	45.89	-0.719	5	887	177.4	79.1%	20.9%
N0032	35.91	0.126	12	4398	366.5	58.5%	41.5%
N0037	30.7	-0.187	6	1729	288.1	67.5%	32.5%
N0038	46.86	-0.054	5	1507	301.4	58.7%	41.3%
N0040	44.7	-0.675	9	2019	224.3	67.8%	32.2%
N0041	49.38	-0.616	9	4714	523.7	67.5%	32.5%
N0042	39.38	-0.334	7	1097	156.7	68.4%	31.6%
N0043	56.51	-1.582	4	274	68.5	51.1%	48.9%
N0044	61.72	-0.626	5	1059	211.8	69.9%	30.1%
N0045	43.75	0.545	4	1912	478	52.8%	47.2%
N0047	29.43	-0.108	7	569	81.2	62.0%	38.0%
N0048	27.22	-0.282	6	4149	691.5	14.9%	85.1%
N0049	37.98	0.566	7	3300	471.4	29.4%	70.6%
N0050	36.46	-0.849	1	424	424	70.8%	29.2%
N0051	46.01	-0.751	2	96	48	83.3%	16.7%
N0052	28.87	-0.043	3	769	256.3	64.0%	36.0%
N0053	32.62	0.021	1	147	147	96.6%	3.4%
N0054	43.39	0.36	18	9960	553.3	7.3%	92.7%
N0055	27.84	0.099	5	1072	214.4	74.5%	25.5%
N0056	28.66	0.067	18	20395	1133	53.2%	46.8%
N0057	26.7	-0.448	6	587	97.8	79.4%	20.6%
N0058	33.53	-0.728	6	880	146.6	85.2%	14.8%

N0059	36.19	0.147	5	5662	1132.4	60.7%	39.3%
N0060	39.66	0.095	8	6129	766.1	63.7%	36.3%
N0061	26.38	-0.41	1	516	516	14.9%	85.1%
N0062	27.14	0.036	17	23381	1375.3	55.7%	44.3%
N0063	39.85	-0.424	7	1622	231.7	34.4%	65.6%
N0064	41.95	0.225	2	1062	531	30.1%	69.9%
N0065	29.91	0.399	19	34950	1839.4	32.5%	67.5%
N0066	33.65	-0.068	4	611	152.7	90.5%	9.5%
N0068	49.92	-0.143	16	6800	425	58.2%	41.8%
N0069	48.55	-0.739	4	1502	375.5	61.4%	38.6%
N0070	32.17	0.041	16	14431	901.9	25.7%	74.3%
N0071	31.3	0.395	17	30497	1793.9	26.4%	73.6%
N0072	45.23	0.026	1	351	351	57.3%	42.7%
N0073	39.29	0.032	22	24910	1132.2	70.1%	29.9%
N0074	36.52	0.096	15	21700	1446.6	65.9%	34.1%
N0075	46.42	-0.383	16	29952	1872	60.9%	39.1%
N0076	53.06	-0.324	6	879	146.5	74.9%	25.1%
N0077	57.86	-1.499	2	1625	812.5	43.4%	56.6%
N0078	45.74	0.155	2	284	142	60.6%	39.4%
N0079	27.03	0.341	11	5629	511.7	56.8%	43.2%
N0080	43.37	-0.351	10	5983	598.3	30.8%	69.2%
N0081	23.78	-0.111	5	1131	226.2	50.0%	50.0%
N0082	28.17	0.46	3	1005	335	47.9%	52.1%
N0083	40.83	-0.307	10	445	44.5	93.5%	6.5%
N0084	43.63	-0.076	6	1873	312.1	70.0%	30.0%
N0087	46.22	-1.095	8	369	46.1	74.3%	25.7%
N0088	43.12	-0.157	5	253	50.6	57.7%	42.3%
N0089	46.15	-0.381	3	110	36.6	53.6%	46.4%
N0091	28.07	-0.431	2	4057	2028.5	35.8%	64.2%
ND007	36.73	0.535	2	559	279.5	66.9%	33.1%
ND018	30.8	0.587	1	16	16	75.0%	25.0%
ND022	38.42	0.074	2	194	97	43.3%	56.7%
ND073	40.78	-0.188	4	962	240.5	76.2%	23.8%
ND074	38.95	0.768	1	975	975	75.9%	24.1%
ND075	44.08	-0.1	1	3903	3903	55.0%	45.0%
ND080	40.35	0.691	1	37	37	29.7%	70.3%
ND084	37.35	-0.066	1	459	459	67.3%	32.7%
ND089	46.8	0.3	1	2	2	100.0%	0.0%

There are 148 measurement locations. The orange highlighted sites listed with HDxxx, KDxxx or NDxxx are the same location as the number without D but have been specifically identified for the purpose of focused diesel vehicle RS survey measurement.

Appendix B – Signal emissions analyser

Table B1. Signal Maxsys900 emissions analyser system accuracy

Gas	Principle	Model	Accuracy
THC	FID	3000HM	Better than ±1 % range or ±0.2 ppm whichever is greater
NO_x	CLA	4000VM	Better than ±1 % range or ±0.2 ppm whichever is greater
CO	NDIR	7100FM	Better than ±1 % of range or ±0.5 ppm whichever is greater
CO_2	NDIR	7200FM	Better than ±1 % of range or ±0.5 ppm whichever is greater

Appendix C – Exhaust emission temperature - drive cycles

For the experimental testing conducted in section 6.3, a series of test 'drive cycles' were developed for trial to facilitate repeatable and consistent testing measurements. Table C1 shows the numerical values for the test time, the target vehicle speed and the overall duration.

Figures C1 to C8 show the graphical representation for each of the driver cycle speed curves with respect to time in seconds.

Table C1. EET drive cycles numerical data tables

Exhaust Emissions Temperature Drive Cycles for Testing							
Original Drive Cycle		**Drive Cycle 1**		**Drive Cycle 2**		**Drive Cycle 3**	
Duration (s)	**1190**	**800**		**560**		**1155**	
Time (s)	**Speed (kph)**	**Time**	**Speed (kph)**	**Time**	**Speed (kph)**	**Time**	**Speed (kph)**
0	0	0	0	0	0	0	0
10	0	10	0	10	0	10	0
30	20	25	15	25	15	25	15
210	20	125	15	85	15	85	15
215	25	140	30	100	30	90	20
395	25	240	30	160	30	145	20
400	30	255	45	175	45	150	25
580	30	355	45	235	45	210	25
585	35	370	60	250	60	215	30
765	35	470	60	310	60	275	30
770	40	485	75	325	75	280	35
950	40	585	75	385	75	340	35
955	45	600	90	400	90	345	40
1135	45	700	90	460	90	405	40
1180	0	790	0	550	0	410	45
1190	0	800	0	560	0	470	45
						475	50
						535	50
						540	55
						600	55
						605	60
						665	60
						670	65
						730	65
						735	70
						795	70
						800	75
						860	75
						865	80
						925	80
						930	85
						990	85
						995	90
						1055	90
						1145	0
						1155	0

Exhaust Emissions Temperature Drive Cycles for Testing							
Drive Cycle 4		Drive Cycle 5		Drive Cycle 6		Drive Cycle 7	
740		1220		1390		1630	
Time	Speed (kph)	Time	Speed (kph)	Time	Speed (kph)	Time	Speed (kph)
0	0	0	0	0	0	0	0
10	0	10	0	5	0	5	0
20	10	20	10	20	15	20	15
80	10	80	10	220	15	260	15
90	20	85	15	235	30	275	30
150	20	145	15	435	30	515	30
160	30	150	20	450	45	530	45
220	30	210	20	650	45	770	45
230	40	215	25	665	60	785	60
290	40	275	25	865	60	1025	60
300	50	280	30	880	75	1040	75
360	50	340	30	1080	75	1280	75
370	60	345	35	1095	90	1295	90
430	60	405	35	1295	90	1535	90
440	70	410	40	1385	0	1625	0
500	70	470	40	1390	0	1630	0
510	80	475	45				
570	80	535	45				
580	90	540	50				
640	90	600	50				
730	0	605	55				
740	0	665	55				
		670	60				
		730	60				
		735	65				
		795	65				
		800	70				
		860	70				
		865	75				
		925	75				
		930	80				
		990	80				
		995	85				
		1055	85				
		1060	90				
		1120	90				
		1210	0				
		1220	0				

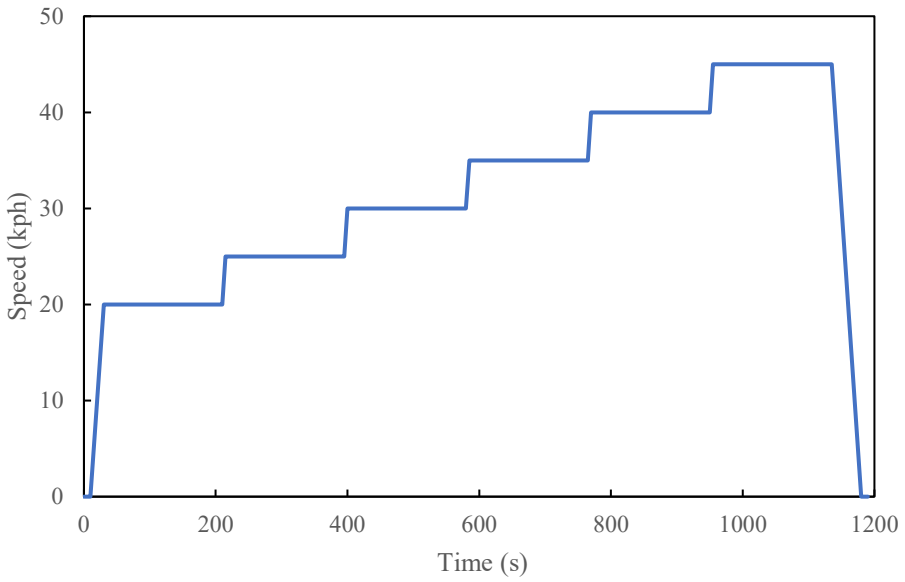

Figure C1: Original drive cycle - 5 kph steps, 20 - 45 kph, 180s duration

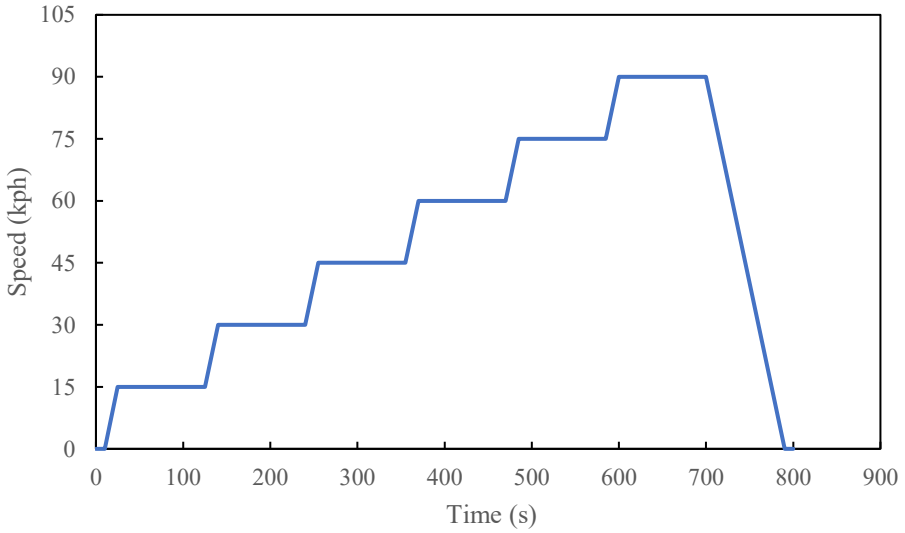

Figure C2: Drive cycle 1 - 15 kph steps, 15 - 90 kph, 100s duration

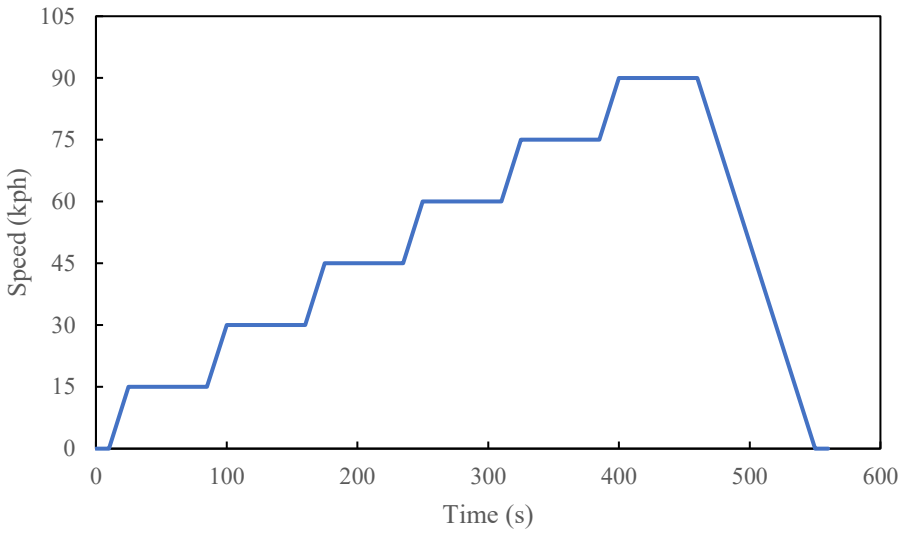

Figure C3: Drive cycle 2 - 15 kph steps, 15 - 90 kph, 60s duration

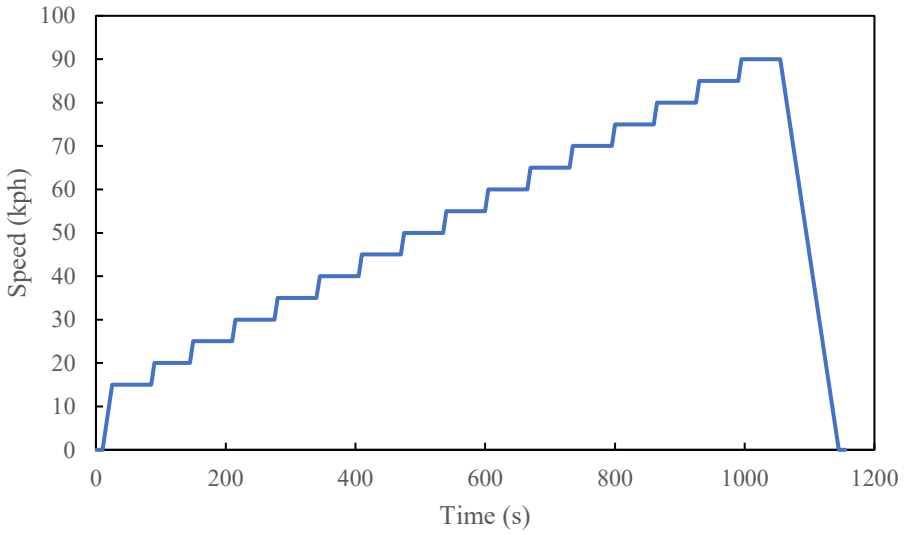

Figure C4: Drive cycle 3 – 5 kph steps, 15 - 90 kph, 60s duration

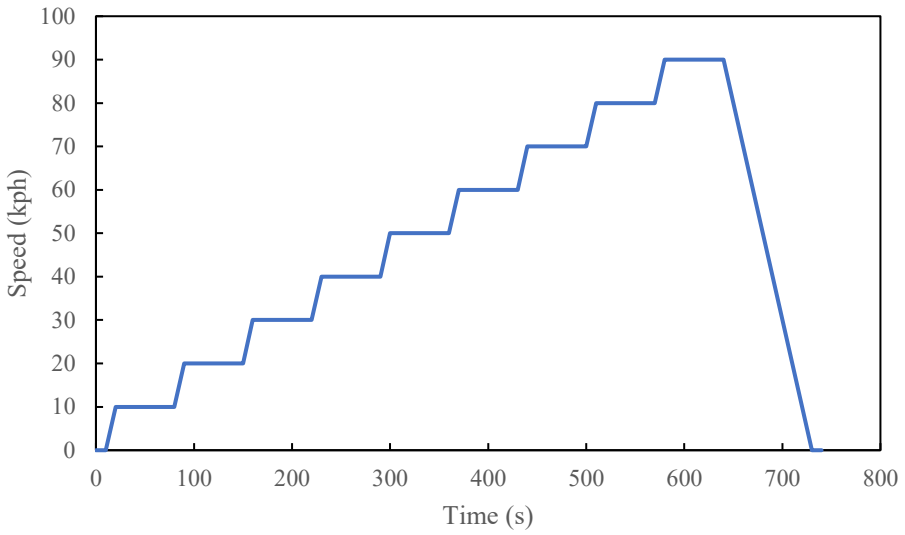

Figure C5: Drive cycle 4 – 10 kph steps, 10 - 90 kph, 60s duration

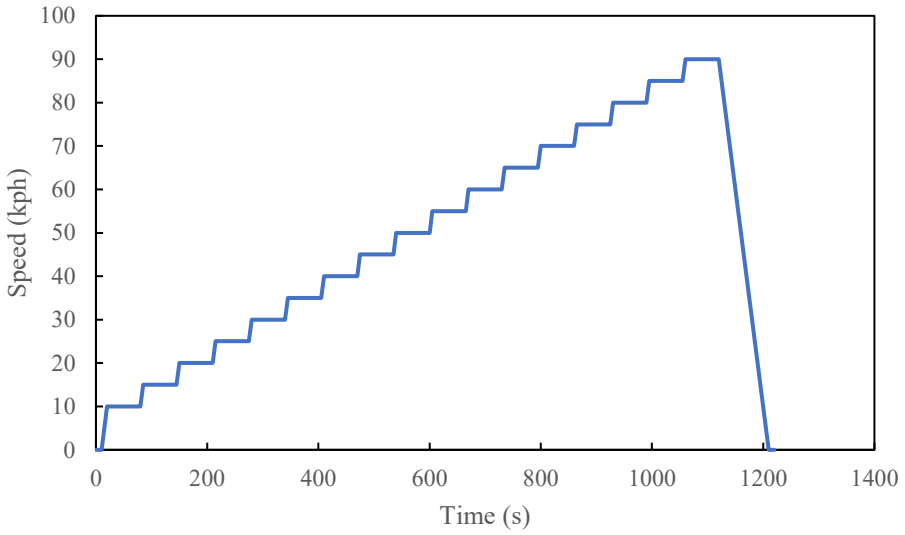

Figure C6: Drive cycle 5 – 5 kph steps, 10 - 90 kph, 60s duration

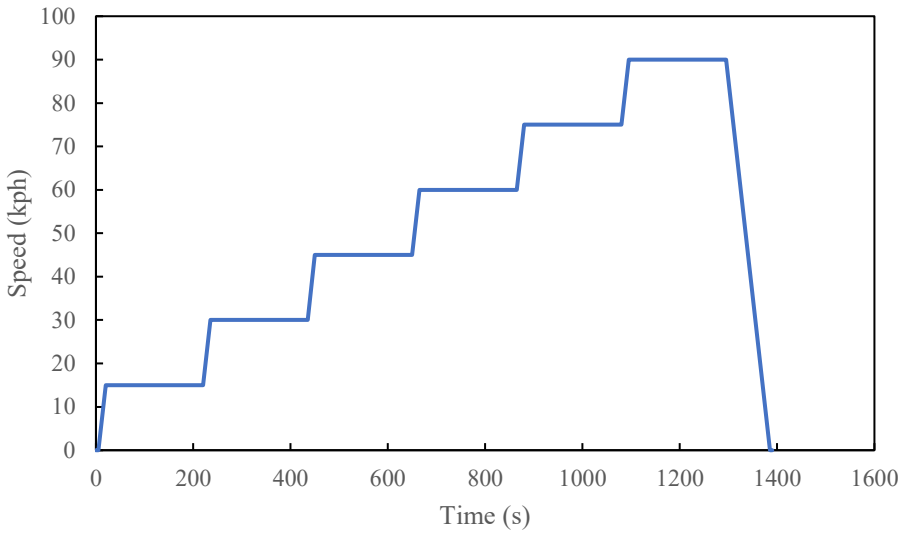

Figure C7: Drive cycle 6 – 15 kph steps, 15 - 90 kph, 200s duration

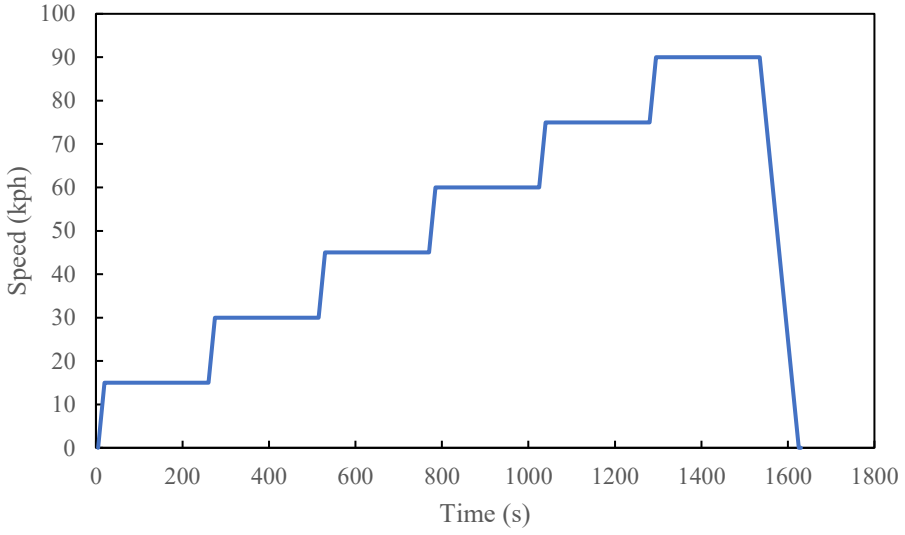

Figure C8: Drive cycle 7 – 15 kph steps, 15 - 90 kph, 240s duration